SETTLEMENT REDUCTION AND STRESS CONCENTRATION FACTORS IN RAMMED AGGREGATE PIERS DETERMINED FROM FULL SCALE LOAD TESTS

A THESIS SUBMITTED TO
THE GRADUATE SCHOOL OF NATURAL AND APPLIED SCIENCES
OF
MIDDLE EAST TECHNICAL UNIVERSITY

BY

ASLI ÖZKESKİN

IN PARTIAL FULFILLMENT OF THE REQUIREMENTS
FOR
THE DEGREE OF DOCTOR OF PHILOSOPHY
IN
CIVIL ENGINEERING

JULY 2004

ABSTRACT

SETTLEMENT REDUCTION AND STRESS CONCENTRATION FACTORS IN RAMMED AGGREGATE PIERS DETERMINED FROM FULL- SCALE GROUP LOAD TESTS

Özkeskin, Aslı
Ph.D., Department of Civil Engineering
Supervisor: Prof. Dr. Orhan Erol

July 2004, 230 pages

Despite the developments in the last decades, field performance information for short aggregate pier improved ground is needed for future design and to develop a better understanding of the performance of the short (floating) aggregate piers.

A full-scale field study was performed to investigate the floating aggregate pier behavior in a soft clayey soil. Site investigations included five boreholes and sampling, four CPT soundings, and SPT and laboratory testing. The soil profile consisted of 8m thick compressible clay overlying weathered rock.

Four large plate load test stations were prepared. A rigid steel footing having plan dimensions of 3.0m by 3.5m were used for loading. Four 65cm diameter reaction piles and steel cross beams were used to load the soil in each station.

First test comprised of loading the untreated soil up to 250 kPa with increments, and monitoring the surface settlements. Moreover, distribution of settlements with depth is recorded by means of deep settlement gages installed prior to loading.

Other three tests were conducted on clay soil improved by rammed aggregate piers. In each station, seven stone columns were installed, having a diameter of 65cm, area ratio of 0.25, placed in a triangular pattern with a center to center spacing of 1.25m. The length of the columns were 3m, 5m in the two station resembling floating columns, and 8m in the last station to simulate end bearing columns to observe the level of the improvement in the floating columns. Field instrumentations included surface and deep settlement gages, and load cell placed on a aggregate pier to determine distribution of the applied vertical stress between the column and the natural soil , thus to find magnitude of the stress concentration factor, n , in end bearing and floating aggregate piers.

It has been found that, the presence of floating aggregate piers reduce settlements, revealing that major improvement in the settlements takes place at relatively short column lengths.

It has been also found that the stress concentration factor is not constant, but varies depending on the magnitude of the applied stress. The magnitude of stress concentration factor varies over a range from 2.1 to 5.6 showing a decreasing trend with increasing vertical stress.

Key Words: Ground Improvement, Floating, Rammed Aggregate Pier, Settlement Reduction Factor, Stone Column, Stress Concentration Factor

ÖZ

TOKMAKLANMIŞ TAŞ KOLONLARDA OTURMA AZALTMA VE GERİLME YOĞUNLUĞU FAKTÖRLERİNİN ARAZİDE GRUP YÜKLEME DENEYLERİ İLE BELİRLENMESİ

Özkeskin, Aslı
Doktora., İnşaat Mühendisliği Bölümü
Tez Yöneticisi: Prof. Dr. Orhan Erol

Temmuz 2004, 230 sayfa

Son yıllarda kaydedilen gelişmelere rağmen, kısa (yüzer) taş kolonların davranışlarının daha iyi anlaşılabilmesi için hala kısa taş kolonlarla güçlendirilmiş zeminler üzerinde arazi performans deneylerine gereksinim duyulmaktadır.

Kısa taş kolonların, yumuşak zeminlerdeki davranışlarını incelemek üzere arazide birebir yükleme deneyleri yapılmıştır. Sondaj, örnek alımı, CPT , SPT ve laboratuar deneylerini kapsayan zemin etüdü gerçekleştirilmiştir. Zemin profili yüzeyde 8m kalınlığında yumuşak kohesive yapıdaki sıkışabilir tabaka ve altında ayrışmış kayadan oluşmaktadır.

Dört adet büyük plaka yükleme deney düzeneği hazırlanmıştır. Yüklemelerde, 3mx3.5m boyutlarında rijit çelik yükleme plakası, 65cm çapında reaksiyon kazıkları ve çelik kirişler kullanılmıştır.

İlk yükleme deneyi güçlendirilmemiş zeminde, en fazla 250 kPa yüke kademelerle çıkılarak yapılmış ve yüzey oturmalarına ek olarak, oturmaların zemin profili boyunca zamana bağlı olarak dağılımları derin oturma ölçerler ile kaydedilmiştir.

Diğer üç yükleme deneyi, tokmaklanmış taş kolonlar ile güçlendirilmiş zeminlerde yapılmıştır. Her yükleme istasyonunda 65cm çapında, alan oranı 0.25, ve merkezden merkeze uzaklıkları 1.25m olarak üçgensel düzenekte 7 adet taş kolon imal edilmiştir. İki yükleme istasyonundaki taş kolon boyları yüzer taş kolonları temsilen 3m ve 5m olarak planlanmıştır. Son istasyonda ise taş kolon boyları uç kazığı olacak şekilde 8.0m olarak imal edilmiştir. Arazide ölçüm düzeneği, yüzey ve derin oturma ölçerler ve taş kolon üzerine, kolon ve zemin arasındaki yük paylaşımını ve gerilme yoğunluğu faktörünü belirlemek için yerleştirilmiş basınç ölçerden oluşmaktadır.

Yüzer taş kolonların oturmaları, güçlendirilmemiş zemine kıyasla azalttığı ve oturma azaltma oranının büyük kısmının kısa kolonlarla güçlendirilmiş zeminde olduğu gözlenmiştir.

Gerilme yoğunluğu faktörünün sabit olmadığı, uygulanan yüzey basıncının artması ile artış gösterdiği ve değerlerinin 2.1 ile 5.6 arasında değiştiği belirlenmiştir.

Anahtar Kelimeler : Gerilme Yoğunluğu Faktörü, Oturma Azaltma Faktörü, Taş Kolon, Tokmaklanmış Taş Kolon, Zemin İyileştirmesi

CANIM BABAM'A

Did you ever know that you are my hero?
You are everything I wish I could be
I could fly higher than en eagle
For you are the wind beneath my wings,
Cause you are the wind beneath my wings

ACKNOWLEDGMENTS

My greatest gratitude goes to *Professor ORHAN EROL* without whom the completion of this dissertation would be unattainable. You never gave up providing your moral and material support and I found your endless knowledge and experience at my disposal every time I needed, even at those moments when I was ready to suspend or quit. I am GRATEFUL to you deeply from my heart.

My next appreciation goes to *Muzaffer ÇEVİK* and all the members of the "*SONAR Drilling and Geological Research Center*" society. The book you are about to read would not be complete without the continuous moral and financial support, labor contribution and deep consideration of these great people working in *SONAR* especially during months long and tedious ground productions and after and, preparation of loading experiments. Thank you all.

I am also grateful to *Toker Drilling and Construction Co.* for taking in the first trial investigation, to *Zemar Lt*d for carrying the CPT soundings and to METU for providing the experiment field.

The remarkable assistance provided by the people in Soil Mechanics Laboratory of METU also deserves my sincere appreciation.

Last but not least, I am GRATEFUL to my family for their eternal faith and patience until the end.

TABLE OF CONTENTS

LIST OF TABLES

TABLE

LIST OF FIGURES

FIGURE

CHAPTER I

INTRODUCTION

1.1 General

Stone columns are one method of ground improvement that offers, under certain conditions, an alternative to conventional support methods in both weak cohesive soils and also loose silty sands. The stone column technique of ground treatment has proven successful in (1) improving slope stability of both embankments and natural slopes, (2) increasing bearing capacity, (3) reducing total and differential settlements, (4) reducing the liquefaction potential of sands and (5) increasing the time rate of settlement.

Stone columns have been used for site improvement in Europe since the 1950's and in the U.S. since 1972. Stone columns have a wide range of potential applications which include a) improvement of both cohesive soils and slightly silty sands, b) embankment support over soft cohesive soils, c) bridge abutments, d) landslide stabilization and liquefaction problems, e) support of bridge bent foundations and similar structures.

Stone columns are usually constructed using a vibrating probe often called a vibroflot. In the wet process, the vibroflot opens a hole by jetting using large quantities of water under high pressure. In the dry process, which may utilize air, the probe displaces the native soil laterally as it is advanced into the ground. The dry process is used primarily for environmental reasons and has

been used in both Europe and Canada. Rammed stone columns are also sometimes used primarily in Belgium and India.

Subsurface investigation and evaluation of geotechnical properties are essential for the design of stone columns and the selection of the most suitable design alternative.

Stone columns can be constructed by the vibro-replacement technique in a variety of soils varying from gravels and sands to silty sands, silts, and clays. For embankment construction, the soils are generally soft to very soft, water deposited silts and clays. For bridge bent foundation support, silty sands having silts contents greater than about 15 percent and stiff clays are candidates for improvement with stone columns.

Stone columns should not be considered for use in soils having shear strengths less than 7 kN/m^2. Also stone columns in general should not be used in soils having sensitivities greater than about 5; experience is limited to this value of sensitivity (Baumann and Bauer, 1974). Caution should be exercised in constructing stone columns in soils having average shear strengths less than about 19 kN/m^2 as originally proposed by Thornburn (1975).

For sites having shear strengths less than 17 to 19 kN/m^2, use of sand for stability applications should be given in consideration. Use of sand piles, however, generally results in more settlement than for stone columns (Barksdale and Bachus, 1983).

Peat lenses are frequently encountered in soft compressible clay and silt deposits. Conventional stone columns should not be used at sites having peat layers greater in thickness than one stone column diameter. Where peat is encountered, two or more vibrators can be attached together to give large diameter stone columns. If peat lenses are encountered thicker than one pile

diameter, it may be feasible to use a rigid column (concrete) column within the peat layer, and a stone column through the reminder of the strata.

For economic reasons, the thickness of the strata to be improved should in general be no greater than 9.0m and preferably about 6.0m. Usually, the weak layer should be underlain by a competent bearing stratum to realize optimum utility and economy (Barksdale and Bachus, 1983)

The stone column gradation selected for design should follow a gradation that can be economically and readily supplied and be coarse enough to settle out rapidly. Each specialty contractor prefers a different gradation, and has differing philosophies on handling special problems encountered during construction, which will be discussed in Chapter II.

Design loads applied to each stone column typically vary depending on site conditions from about 15 to about 60 tons. The theories which will be presented in Chapter II can be used as a general guide in estimating the ultimate capacity of stone columns.

Area replacement ratios used vary from 0.15 to 0.35 for most applications. Stone columns are usually constructed using the compact equilateral triangular pattern as compared to a square pattern. Equilateral spacing used for stone columns varies from about 1.8 to 2.7m, with typical values being 2.0 to 2.4m.

The diameter of the constructed stone column depends primarily upon the type of soil present. It also varies to a lesser extend upon the quantity and velocity of water used in advancing the hole and the number of times the hole is flushed out by raising and dropping the vibroflot a short distance. Stone columns generally have diameters varying from 0.6m to 2.0m.

Stone columns act as drains and under favorable conditions can significantly decrease the time for primary consolidation to occur. Because of rapid

consolidation settlement secondary settlement becomes more important consideration when stone columns are used. Finally, the columns reduce the built-up in pore pressure in granular layers during an earthquake, and hence decrease liquefaction potential.

1.2 Aim of the Study

This full scale study on the settlement and stress distribution behaviors of rammed aggregate piers was planned to contribute to the foregoing arguments:

- the settlement reduction ratios within and under the rammed aggregate piers due to the presence of both floating and end-bearing piers
- the stress concentration factor, n in rammed aggregate piers

In this study, four large plate load tests were conducted. First load test was on untreated soil, which is soft clay. Second load test was Group A loading on improved ground with floating aggregate piers of 3.0m length, third load test was Group B loading on improved ground with floating aggregate piers of 5.0m length and finally fourth load test was Group C loading on improved ground with end-bearing aggregate piers of 8.0m length. During these tests, the settlement of the large loading plate and the settlements in the different levels of soil profile were measured. In addition, in Group A, B and C loadings, stresses on the center pier were measured.

A comprehensive literature survey on stone columns is given in Chapter II. A brief explanation of field works is given in Chapter III. The geological and site conditions were summarized in Chapter IV. The test results are presented in Chapter V. A detailed study of the test results are discussed in Chapter VI. Finally, Chapter VII concludes the study by highlighting the findings.

CHAPTER II

LITERATURE REVIEW ON STONE COLUMNS

2.1 Introduction

The increased cost of conventional foundations and numerous environmental constraints greatly encourage the in-situ improvement of weak soil deposits. To economically develop marginal sites a number of new ground improvement techniques have been recently developed (Greenwood and Kirsch, 1983; Mitchell, 1981). Some of these techniques are feasible for present use, but many require considerable additional research.

Stone columns are one method of ground improvement. They are ideally suited for improving soft clays and silts and also for loose silty sands. Apparently, the concept was first applied in France in 1830 to improve native soil. Stone columns have been in somewhat limited use in the U.S. since 1972. However, this method has been used extensively in Europe for site improvement since the late 1950's.

The stone column technique of ground treatment has proven successful in (1) improving slope stability of both embankments and natural slopes, (2) increasing bearing capacity, (3) reducing total and differential settlements, (4) reducing the liquefaction potential of sands and (5) increasing the time rate of settlement.

2.2 Present Status of Stone Columns

2.2.1 Feasibility and Applications of Stone Columns

A generalized summary of the factors affecting the feasibility of stabilizing soft ground with stone columns is as follows:

i. One of the best applications of stone columns is for stabilizing large area loads such as embankments, tank farms, and fills for overall stability and the control of total and differential settlements. Stone columns work most effectively when used for area stabilization rather than as a structural foundation alternative (Bachus and Barksdale, 1994).

ii. The design loading on the stone column should be relatively uniform and limited to between 20 and 50 tons per column. Table 2.1 gives typical design loads for foundation support where settlement is of concern (Barksdale and Bachus, 1983).

iii. The most improvement is likely to be obtained in compressible silts and clays occurring near the surface and ranging in shear strength from 15 to 50 kN/m^2. Stone columns should not be considered for use in soils having shear strengths less than 7 kN/m^2 (Bauman and Bauer, 1974). Caution should be exercised in constructing stone columns in soils having average shear strengths less than about 19 kN/m^2 as originally proposed by Thornburn (1975).

iv. The greatest economic advantage is generally realized if the depth to the bearing strata is between about 6 and 10m. End bearing is generally specified.

v. When the settlement of the foundation system with stone columns is well within the limit of tolerance of the structural settlement, the stone column system can be significantly cheaper then sand drains with preload fills. Settlements can be reduced to 40% of the settlement of untreated area or even less (Datye, 1982)

vi. A further advantage of the stone columns system is that the foundation can withstand large drag forces without collapse, and therefore in areas where pile foundations are subjected to negative skin friction, the stone column would score over piles (Datye, 1982).

vii. Stone columns can be constructed by the vibro-replacement technique in a variety of soils varying from gravels and sands to silty sands, silts, and clays (Figure 2.1). Special care must be taken when using stone columns in sensitive soils and in soils containing organics and peat lenses or layers. Because of the high compressibility of peat and organic soils, little lateral support may be developed and large vertical deflections of the columns may result. Stone columns in general should not be used in soils having sensitivities greater than about 5; experience is limited to this value of sensitivity (Bauman and Bauer, 1974).

Table 2.1 Approximate range in design loads used in practice for stone columns (Barksdale and Bachus, 1983)

Soil Type	Approximate Design Load (tons)	
	Foundation Design	Stability
1. Cohesive Soil		
19kPa<c<30kPa	15-30	20-45
30kPa<c<50kPa	25-45	30-60
c>50kPa	35-60	40-70
2. Cohesionless Soil	20-180	-

When used under the ideal conditions previously described, stone columns for certain conditions may be more economical than conventional alternatives such as complete replacement, and bored or driven piles (Barksdale and Bachus,

1983). By replacing/displacing a portion of the soft soils with a compacted granular backfill, a composite material is formed which is both stiffer and stronger than the unimproved native soil. Also the subsurface soils, when improved with stone columns, have more uniform strength and compressibility properties prior to improvement.

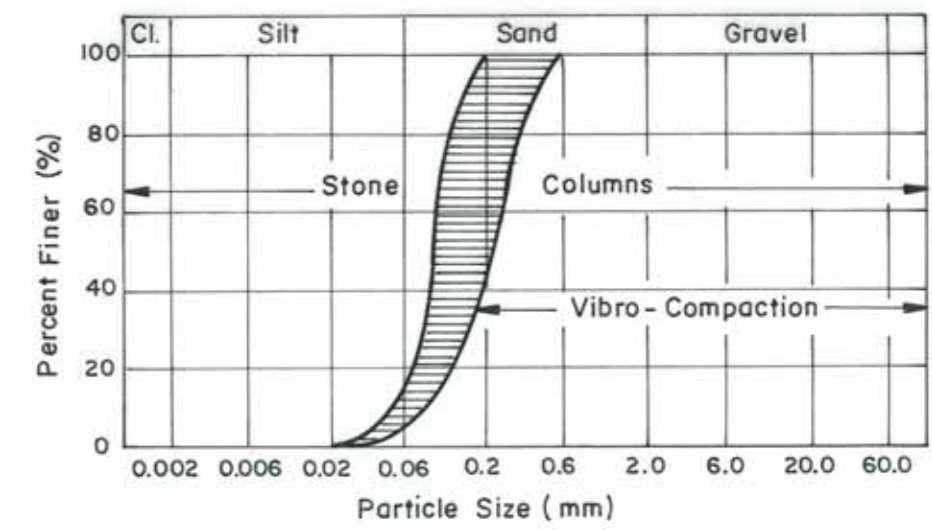

Figure 2.1 Application ranges of vibro-compaction and vibro-replacement (Priebe, 1993)

2.2.2 Construction of Stone Columns

As early as 1938 methods and equipment were developed which enabled the compaction of non-cohesive soils to practically any depth. This original process is now referred as *vibro-compaction*. The compactibility of soil depends mainly on its grain size distribution. Figure 2.1 shows a diagram with a hatched zone. Soils with grain distribution curves lying entirely on the coarse side of the hatched zone are generally well compactable with depth vibrators. If the grain size distribution curve falls in the hatched zone, it is advisable to backfill with coarser material during the compaction process to improve the contact between vibrator and treated soil. The many other soils with grain size

distribution curves on the fine side of the hatched zone are scarcely compactable by depth vibrators. For these soils some twenty years later the procedure of installing stone columns by depth vibrators was developed, now referred to as *vibro-replacement* (Priebe, 1993).

The improvement by vibro-replacement is based on completely different principles. Since its effect cannot be compared with compaction and vibro-compaction is generally suitable for non-cohesive materials, this method thought to be out of the scope and did not be described.

The principal construction methods of stone columns and typical site conditions where the techniques are used are as follows:

- Vibro-replacement method
- Vibro-displacement method
- Vibro-compozer method (sand compaction piles)
- Cased-borehole method (rammed stone columns)

Vibro-Replacement (wet) Method: In the vibro-replacement (wet) method, a hole is formed in the ground by jetting a probe with water down to the desired depth. The uncased hole is flushed out and then stone is added in 0.3 to 1.2m increments and densified by means of an electrically or hydraulically actuated vibrator located near the bottom of the probe. The wet process is generally used where borehole stability is questionable. Therefore, it is suited for sites underlain by very soft to firm soils (Cu = 15 to 50 kN/m^2) with more than 18% passing no. 200 U.S. standard sieve and a high ground water table (Baumann and Bauer, 1974; Engelhardt and Kirsch, 1977; Bergado et.al., 1991 and 1994).

This method is the fastest method; it typically results in the largest diameter stone columns (typically 0.7 to 1.1m in diameter); capable of supporting the highest design load per column and allows the use of the widest range of stone/gravel material gradations (Stark and Yacyshyn, 1990)

Vibro-Displacement (dry) Method: The main difference between vibro-displacement and vibro-replacement is the absence of jetting water during initial formation of the hole in the vibro-displacement method. To be able to use the vibro-displacement method the vibrated hole must be able to stand open upon extraction of the probe. Therefore, for vibro-displacement to be possible soils must exhibit undrained shear strengths in excess of about 30 to 60 kN/m^2, with a relatively low ground water table being present at the site (Munfakh et.al., 1987 and Stark and Yacyshyn, 1990). Stabilization of sites underlain by soft soils and high ground water using the dry process is made possible by using a "bottom feed" type vibrator. It serves as a casing that prevents collapse of the hole.

Due to the absence of a jetting fluid, the resulting stone columns have diameters that are approximately 15 to 25% smaller than the vibro-replacement method (Stark and Yacyshyn, 1990).

Cased-Borehole Method (Rammed stone columns): Rammed stone columns are constructed by either driving an open or closed end pipe in the ground or boring a hole. A mixture of sand and stone is placed in the hole in increments, and rammed using a heavy, falling weight (usually of 15 to 20 kN) from a height of 1.0 to 1.5m (Datye and Nagarju, 1981; Bergado et.al., 1984) Since a casing is initially placed into the subsurface soils, potential hole collapse is eliminated. Therefore, the technique has application in most soils treatable by the vibro-techniques. Disturbance and subsequent remolding of sensitive soils by the ramming operation, however, may limit its utility in these soils. The method is useful in developing countries utilizing only indigenous equipment in contrast to the other methods, which require special equipment and trained personnel (Ranjan and Rao, 1983)

Nayak, (1982) stated that capacity of the rammed stone columns was about 70% higher than the stone columns formed by vibroflot. Probable reasons same could be that contamination of granular backfill will be less than in vibro-

replacement method and even the compaction achieved could be better than with vibro-flot.

Vibro-Compozer Method (Sand Compaction Piles): Sand compaction piles and several modifications to this technique are used extensively in Japan. Sand compaction piles are constructed by driving a steel casing down to the desired elevation using a heavy, vertical vibratory hammer located at the top of the pile. As the pile is being driven the casing is filled with sand. The casing is than repeatedly extracted and partially redriven using the vibratory hammer. By the time the sand compaction pile has been completed the casing has been completely removed from the ground. The compacted sand pile, both in land and on the seabed is usually 70-700cm in diameter, depending on the diameter on the casing pipe, which is from 40 to 150 cm in diameter (Murayama and Ichimoto, 1982). Sand compaction piles are used for stabilizing soft clays in the presence of high ground water (Aboshi et.al., 1979).

The primary advantages of sand compaction piles compared to conventionally constructed stone columns are: 1) Construction of the sand column is extremely fast 2) Sand is usually cheaper than stone 3) The hole is fully supported by a casing during construction that eliminates the possibility of hole collapse. The primary disadvantages of sand compaction piles are: 1) Because of the use of sand, the column has a lower angle of internal friction; hence a larger percentage replacement of weak soil is required 2) Driving the casing through a clay layer causes “smear” along the boundary of the column that reduces lateral permeability and hence its effectiveness as a drain (Barksdale and Takefumi, 1990)

Other Methods: There are some recently developed special methods of installing stone columns. These will not be described in detailed here.

The recently developed ROTOCOLUMN ™ method of installing stone column is a promising alternative to conventional systems for stone column installation

in soft soils. Equipment and procedures for constructing stone columns by this method are described by Goughnour, (1997).

Rammed Aggregate Pier ™ systems have been successfully installed on numerous major project sites within the United States within a variety of soil conditions exclusive of peat soils, over time span over ten years (Edil et.al, 2000; Fox and Edil, 2000). Generalized construction and design methods for Rammed Aggregate Pier ™ systems are described by Lawton et.al, 1994.

2.2.3 Special Considerations

2.2.3.1 Stone/Gravel /Sand Requirements

Gradation of stone used varies greatly depending upon the available sources of aggregate, subsurface conditions and the contractor. A range of successfully used gradation for the vibro-replacement process is given in Table 2.2 in the guide specifications. For cohesive soils having strengths less than about 12 kN/m^2, the finer side of alternate gradations No.2, 3, or 4 or an even finer gradation such as sand should be used. For soils having shear strengths greater than about 12 kN/m^2, gradations similar to alternate No.1 or 3 are recommended.

In general a coarse, open-graded stone is used, varying from about 12 to 75mm in size. Bauman and Bauer (1974) accepted sizes up to 155mm if the material is well graded. Crushed stone is preferred although natural gravel is used. A small amount of fines in the vibro-replacement stone presents no problems since it is flushed to the surface by the upward flowing water.

For the dry method, a large stone up to 100 mm in size may be used t help insure it reaches the bottom. Stone specifications for the bottom feed units

include round to angular sand or gravel up to about 40 mm in diameter (Greenwood and Kirsch, 1983).

Table 2.2 A range of used gradation for the vibro-replacement process (Barksdale and Bachus, 1983)

Sieve Size (ins.)	Alternate 2 Percent Passing	Alternate 3 Percent Passing	Alternate 4 Percent Passing	Alternate 5 Percent Passing
4	-	-	100	-
3.5	-	-	90-100	-
3.0	90-100	-	-	-
2.5	-	-	25-100	100
2.0	40-90	100	-	65-100
1.5	-	-	0-60	-
1.0	-	2	-	20-100
0.75	0-10	-	0-10	10-55
0.50	0-5	-	0-5	0-5

Typical sand gradation specifications for sand compaction piles require a well-graded fine to medium sand with D_{10} between about 0.2 to 0.8mm and D_{60} between about 0.7 and 4mm (Barksdale and Takefumi, 1990).

The angle of internal friction of the stone column depends on the size and shape of the stone, the installation process and the infiltration of the native soil between stone particles (Munfakh et.al., 1987)

In order to obtain the internal friction angles of the granular materials, strain controlled laboratory direct shear test may be performed on samples prepared at the same water content and densities.

The test results presented by Bergado and Lam (1987) and Bergado et. al. (1984) show that internal friction angle of sand varies from 35^0 to 42^0; of gravel

varies from 40^0 to 44^0 and for gravel mixed with sand around 38^0. The gravel material yields the highest angle of internal friction.

Values of the internal friction angle of the stone measured by large-scale triaxial compression and shear box tests on stone columns, range from 50^0 to 55^0 for crushed, sound, well-compacted stone. Since the friction angle of stone decreases with increased confining stress, these values require correction for depth and confining stress on the column (Goughnour et. al. 1990)

2.2.3.2 Construction Control

Because of lateral displacement of the stone during vibration or ramming, the completed diameter of the hole is always greater than its initial diameter. Typical hole diameters vary from about 0.8 m to 1.2 m depending upon the type of soil, its undrained shear strength, stone size, characteristics of the vibrating probe and the construction method. The diameter of the finished column is usually estimated using the stone take and by assuming a compacted density. Datye and Nagaraju (1981) discussed that an important parameter governing the performance of granular piles is the consumption of materials in the granular piles and the gravel consumption varies progressively with depth.

Measurements should be made to obtain a reasonable estimate of the diameter of the compacted stone column. The cross-sectional areas of granular piles were computed from the compacted volume. Volumes of granular fill material consumption were measured in a bucket of standard size. The in-situ compacted volume can be taken as 0.80 of the volume measured by the bucket (Datye and Nagaraju, 1981; Bergado and Lam, 1987).

The degree of compaction can be measured by a “set” criterion, i.e. penetration of hammer in the field material for a given number of blows. Control on consumption of stone with a specific energy input for ramming as measured by

“set” will ensure a uniform quality of construction (Datye and Nagaraju, 1981; Bergado and Lam, 1987).

Slocombe and Mosoley (1991) give information on instrumentation systems use in Europe where measurement of vibrator depth, power consumption and weight of stone used can be recorded against time to give an accurate record of each stone column installed.

2.2.3.3 Performance Evaluation

The final condition of the treated soil is extremely important for the stability and long term behavior of the structure and it is essential that testing of the ground is performed.

For ground improvement by construction of stone columns using the vibro-replacement process, load testing of the treated ground to support the design loads within tolerable settlement limits. Full scale loading tests can, however prove uneconomic on small sites, and a variety of loading and in-situ tests have been used (Mosoley and Priebe, 1993). Table 2.3 sets out a suitability rating for these tests, based on predominant soil type. Short duration tests on metal plates of 600mm diameter (small plates in Table 2.3) are the most common form of testing stone columns in Britain, due to their speed and low cost. However, such test can only stress the soils to shallow depths (Slocombe and Mosoley, 1990).

To overcome these limitations and to provide more realistic simulation of applied building loads, zone loading or dummy footing tests are occasionally performed. Here, loading of up to 3 times the design bearing pressure are applied over a group of stone columns, typically of 4 to 9 in number.

Table 2.3 Suitability for Testing Stone Columns (Slocombe and Mosoley, 1990)

Test	Granular	Cohesive	Comments
McIntosh Probe	*	*	Before/after essential Can locate obstructions prior to treatment
Dynamic cone	**	*	Too insensitive to reveal clay fraction Can locate dense layers and buried features.
Mechanical cone	***	*	Rarely used
Electric cone	****	**	Particle size important Can be affected by lateral earth pressures generated by treatment Best test for seismic liquefaction evaluation
Boreholes + SPT	***	**	Efficiency of test important. Recovers samples
Dilatometer	***	*	Rarely used
Pressuremeter	***	*	Rarely used
Small plate	*	*	Does not adequately confine stone column Affected by pore water pressures
Large plate	**	**	Better confining action
Skip	**	**	Can maintain for extended period
Zone loading	****	****	Best test for realistic comparison with foundations
Full-scale	*****	*****	Rare

* least suitable
***** most suitable

2.3 Theory

2.3.1 Introduction

To economically utilize stone columns to the fullest extend, theories must be available for considering bearing capacity, settlement and general stability for problems involving both single stone columns and stone column groups. In this part the failure mechanisms of both a single stone column and a stone column

group are first described based on available information. Selected methods are then presented for predicting bearing capacity, settlement and slope stability.

2.3.2 Failure Mechanisms

Granular piles may be constructed as either end bearing on a firm stratum underlying soft soil, or as floating piles with their tips embedded within the soft clay layer. In practice, however, end bearing stone columns have almost always been used in the past. Granular piles may fail individually or as a group.

2.3.2.1 Single Stone Columns

The failure mechanisms for a single pile, loaded by its top only are illustrated in Figure 2.2a, b, c respectively, indicating the possible failures as: a) bulging (most probable failure mechanism for single isolated granular piles), b) general shear, and c) punching.

Either end bearing or free floating stone columns greater than about 2-3 diameters in length fail in bulging as illustrated in Figure 2.2a (Barksdale and Bachus, 1983). Similarly, Hughes and Withers (1974) states that the considerable vertical and lateral distortion which occurs at the top of the column rapidly diminishes with depth and at failure, about 4 diameters length of the column is being significantly strained.

Full-scale load test on granular piles (Hughes et.al, 1975; Bergado and Lam, 1987) have shown that maximum bulge occurs near the top of the pile at a depth approximately equal to one-half to one pile diameter.

A very short column bearing on a firm support will undergo either a general or local bearing capacity type failure at the surface (Barksdale and Bachus, 1983, Figure 2.2b.).

The general shear failure is prevented if a foundation pad or footing surcharge is provided.

Finally, a floating stone column less than about 2 to 3 diameters in length may fail in end bearing in the weak underlying layer before a bulging failure can develop (Fig. 2.2c) Hughes and Withers (1974) similarly clarified that if the length/diameter ratio is less than 4 then the columns would fail in end bearing before bulging.

Critical length is defined by Hughes et. al. (1975) as the minimum length at which both bulging and end bearing failure occur simultaneously .The pile failure criterion generally will not occur if the pile length exceeds the critical length (Bergado et.al. 1984). 4.1D was given as critical length by Hughes and Withers (1974).

Madhav (1982) states that equating the load carrying capacity of granular pile based on bulging and pile type failures, a critical pile length, L_{cr}, can be determined. If pile length, L_p, is less than critical pile length, $L_{cr,}$ there is pile type failure. If pile length, L_p, is greater than critical pile length, L_{cr}, there is bulging failure. However, Madhav and Miura (1994) noted that bulging and pile failure are not mutually exclusive. While the tendency for bulging is predominant, it occurs in conjunction with the pile action since the applied loads are transmitted through resistances mobilized around the perimeter and the base of the stone column. If the total in-situ radial stress is calculated at a depth of D/2 (diameter of pile/2), the values of L_{cr}/D can be obtained from Figure 2.3 (Madhav, 1982).

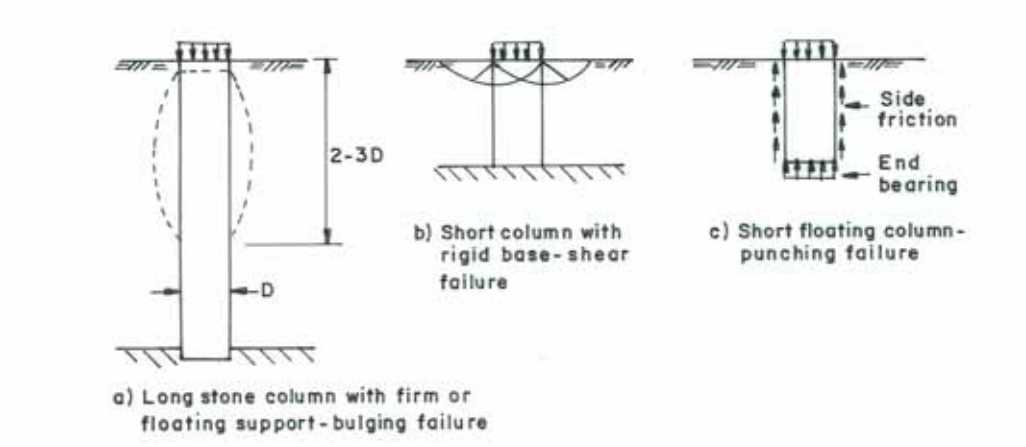

Figure 2.2 Failure mechanisms of a single stone column in a homogeneous soft layer (Barksdale and Bachus, 1983)

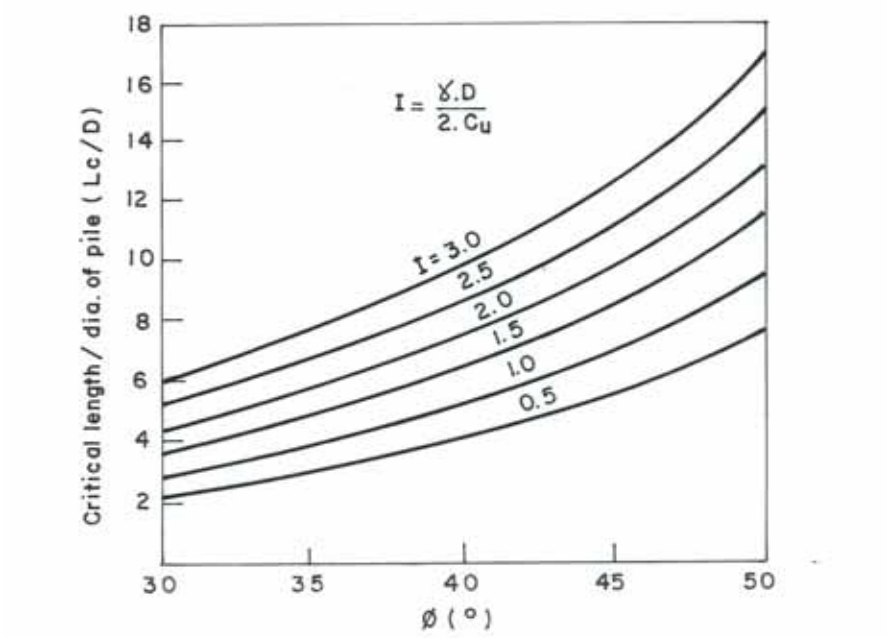

Figure 2.3 Critical length of granular pile (Madhav, 1982)

Small scale model studies (Hughes and Withers, 1974; Kaffezakis, 1983; Bachus and Barksdale, 1984) have shown that the bearing capacity and settlement behavior of a single stone column is significantly influenced by the method of applying load as shown in Figure 2.4. Applying the load through a

rigid foundation over an area greater than the stone column (Figure 2.4a) increases the vertical and lateral stress in the surrounding soft soil. The larger bearing area together with the additional support of the stone column results in less bulging and a greater ultimate load capacity.

Model tests indicate the total ultimate capacity of a square foundation having a total area 4 times that of the stone column beneath it is about 1.7 times greater than if just the area of the stone column is loaded. For a given load, a stone column loaded by a large rigid plate settles less than if just the stone column is loaded since a portion of the load is carried by both the stone column and the soft clay (Barksdale and Bachus, 1983).

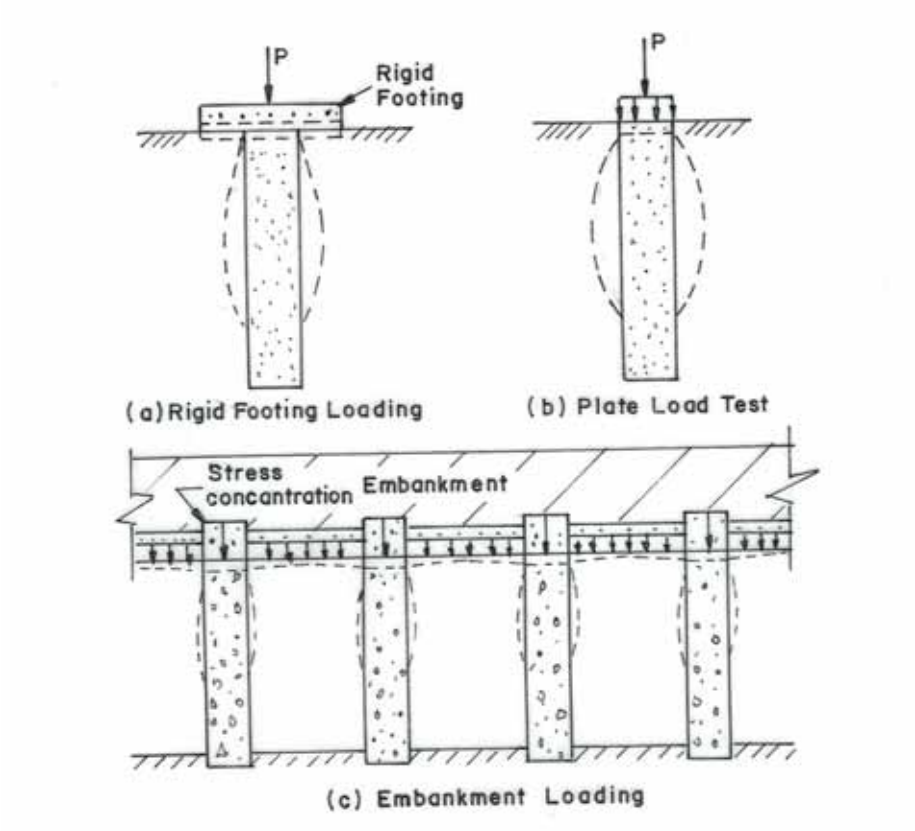

Figure 2.4 Different types of loadings applied to stone columns
(Barksdale and Bachus, 1983)

2.3.2.2 Stone Column Groups

An isolated single stone column compared to a stone column group has a slightly smaller ultimate load capacity per column than in the group. As surrounding columns are added to form a group, the interior columns are confined and hence somewhat stiffened by the surrounding columns. This results in a slight increase in the ultimate load capacity per column. Small-scale model studies show, for groups having 1 and 2 rows of stone columns that only a small increase in capacity per column occurs with increasing number of columns (Figure 2.5). A rigid foundation loading was used in these tests (Bachus and Barksdale, 1983).

For a wide flexible loading such as an embankment constructed over a stone column improved ground as illustrated in Figure 2.4c and 2.5a. It has been found that the settlement of the compressible soil and stone column to be approximately equal beneath an embankment. Due to the construction of an embankment over the weak foundation, the soil beneath and to the sides of the foundation move laterally outward as illustrated in Figure 2.5a and 2.5b. This phenomenon is called “spreading” (Tavenas et.al., 1979 and Poulos, 1972). Experience and finite element analysis have shown that settlement are greater when spreading occurs than if spreading is prevented. Compared to the restrained condition, spreading reduces the lateral support given to the stone column and surrounding soil. Lateral spreading also slightly increases the amount of bulging the stone column undergoes compared to the condition of no spreading (Barksdale and Bachus, 1983).

A group of stone columns in a soft soil probably undergoes a combined bulging and local bearing type of failure as illustrated in Figure 2.5c. A local bearing failure is the punching of a relatively rigid stone column (or group) in to the surrounding soft soil. Stone column groups having short column lengths can fail in end-bearing (Fig.2.5c) or perhaps undergo a bearing capacity failure

of individual stone columns similar to the failure mode of short, single stone columns.

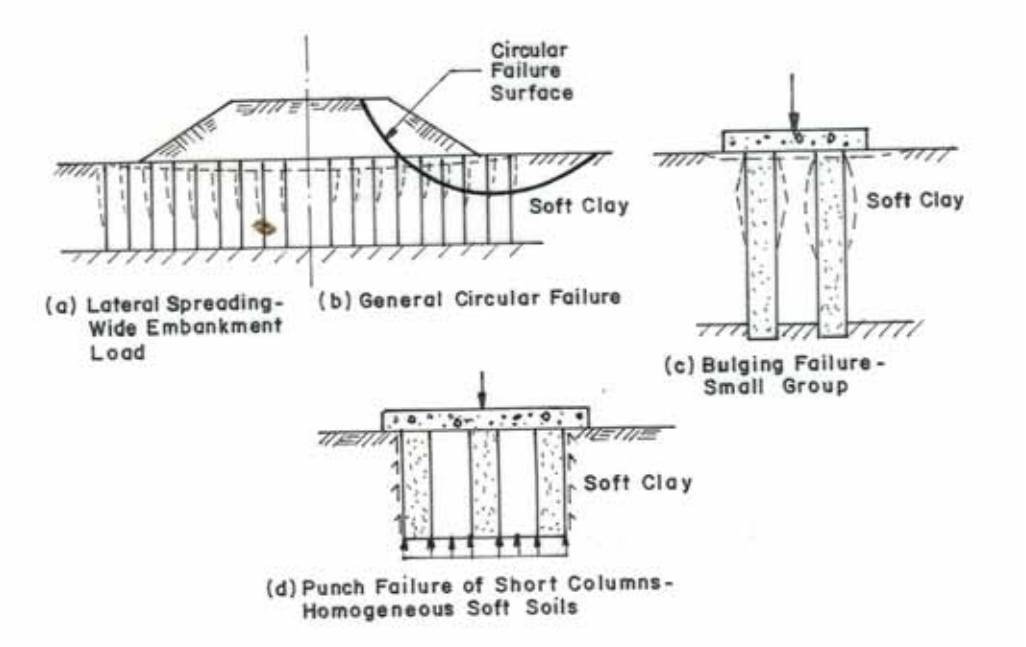

Figure 2.5 Failure modes of stone column groups
(Barksdale and Bachus, 1983)

The failure mechanisms described above are idealized, assuming uniform soil properties, which of course seldom, if ever, are found in nature. Experience indicates that isolated zones of very soft cohesive soils can result in significant bulging at both shallow and deep depths as illustrated in Figure 2.6. A very soft zone at the surface, 1 to 3m thick, has a dominating influence on the failure mechanism of either stone column groups or single columns (Fig.2.6a) Further, field experience indicates the presence of a very weak layer such as peat greater than about one column diameter in thickness can also seriously affect stone column performance (Figure 2.6b and 2.6c) (Barksdale and Bachus, 1983)

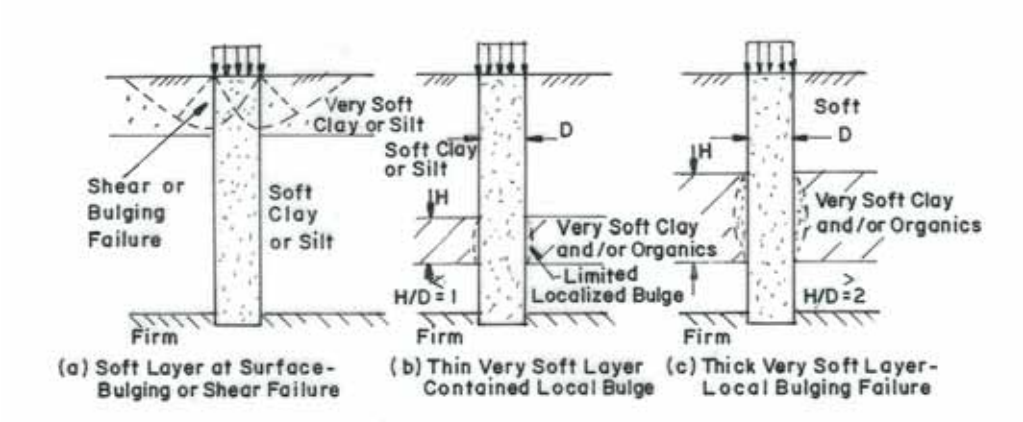

Figure 2.6 Stone column failure mechanisms in nonhomogeneous cohesive soil (Barksdale and Bachus, 1983)

2.3.3 Basic Relationships

Stone columns are constructed in an equilateral triangular pattern although a square pattern is sometimes used. The equilateral triangle pattern gives the densest packing of stone columns in a given area. A typical layout of stone columns in equilateral triangular and square patterns is shown in Figure 2.7.

2.3.3.1 Unit Cell Concept

For purposes of settlement and stability analysis, it is convenient to associate the tributary area of soil surrounding each stone column as illustrated in Figures 2.7 and 2.8. The tributary area can be closely approximated as an equivalent circle having the same total area.

For an equilateral triangular pattern of stone columns, the equivalent circle has an effective diameter of:

$$D_e = 1.05s \qquad (2.1)$$

while for a square pattern ,

$$D_e = 1.13s \qquad (2.2)$$

where s is the spacing of stone columns. The resulting equivalent cylinder of material having a diameter D_e enclosing the tributary soil and one stone column is known as the *unit cell*. The stone column is concentric to the exterior boundary of the unit cell (Fig.2.8a).

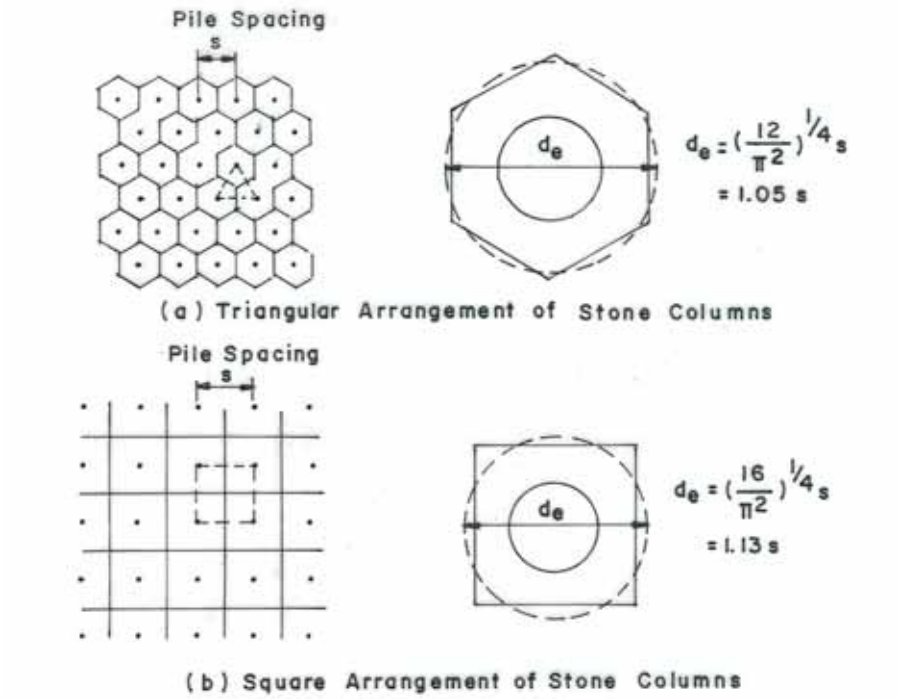

Figure 2.7 A typical layout of stone columns a) triangular arrangement b) square arrangement (Balaam and Booker, 1981)

For an infinitely large group of stone columns subjected to a uniform loading applied over the area; each interior column may be considered as a unit cell as shown in Figure 2.8b. Because of symmetry of load and geometry, lateral deformations cannot occur across the boundaries of the unit cell. Also from symmetry of load and geometry the shear stresses on the outside boundaries of

the unit cell must be zero. Following these assumptions a uniform loading applied over the top of the unit cell must remain within the unit cell. The distribution of stress within the unit cell between the stone and soil could, however, change with depth. As discussed later, several settlement theories assume this idealized extension of the unit cell concept to be valid. The unit cell can be physically modeled as a cylindrical-shaped container having frictionless, rigid exterior wall symmetrically located around the stone column (Fig.2.8c).

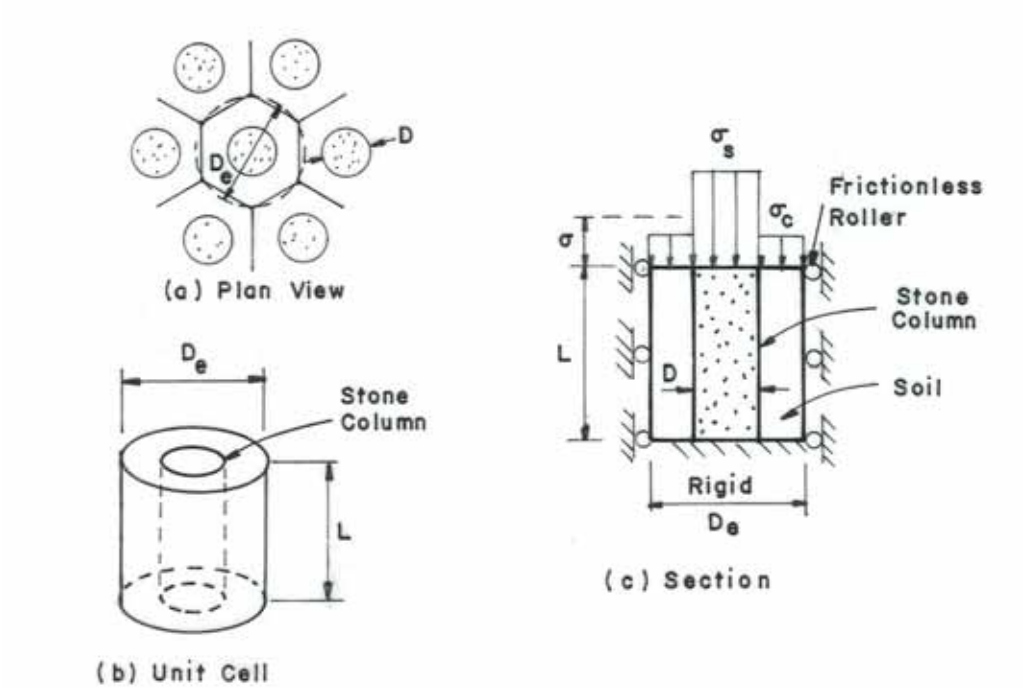

Figure 2.8 Unit cell idealizations (Bachus and Barksdale, 1989)

2.3.3.2 Area Replacement Ratio

To quantify the amount of soil replaced by the stone, the *area replacement ratio* is introduced and defined as the ratio of the granular pile area over the whole area of the equivalent cylindrical unit within the unit cell and expressed as:

$$a_s = \frac{A_s}{A} \qquad (2.3)$$

where a_s is the area replacement ratio, A_s is the area of the stone column and A is the total area within the unit cell. The area replacement ratio can be expressed in terms of the diameter and spacing of the stone columns as follows:

$$a_s = c_1\left(\frac{D}{s}\right)^2 \qquad (2.4)$$

where : D = diameter of the compacted stone column

s = center to center spacing of the stone columns

c_1 = a constant dependent upon the pattern of stone columns used; for a square pattern $c_1 = \pi/4$ and for an equilateral triangular pattern $c_1 = \pi/(2/\sqrt{3})$.

2.3.3.3 Stress Concentration

After placing a uniform stress with an embankment or foundation load over stone columns and allowing consolidation, an important concentration of stress occurs in the stone column and an accompanying reduction in stress occurs in the surrounding less stiff soil (Aboshi et.al, 1979; Balaam et.al, 1977; Goughnour and Bayuk, 1979). Since the vertical settlement of the stone column and surrounding soil is approximately the same, stress concentration occurs in the stone column since it is stiffer than a cohesive or a loose cohesionless soil.

When a composite foundation is loaded for which the unit cell concept is valid such as a reasonably wide, relatively uniform loading applied to a group of stone columns having either a square or equilateral triangular pattern, the

distribution of vertical stress within the unit cell (Fig.2.8c) can be expressed by a *stress concentration factor n* defined as:

$$n = \frac{\sigma_s}{\sigma_c} \qquad (2.5)$$

where σ_s = stress in the stone column

σ_c = stress in the surrounding cohesive soil

The average stress σ which must exist over the unit cell area at a given depth must, for equilibrium of vertical forces to exist within the unit cell, equal for a given area replacement ratio, a_s:

$$\sigma = \sigma_s a_s + \sigma_c (1 - a_s) \qquad (2.6)$$

where all the terms have been previously defined. Solving Equation (2.6) for the stress in the clay and stone using the stress concentration factor n gives (Aboshi et.al., 1979):

$$\sigma_c = \sigma / [1 + (n-1)a_s] = \mu_c \sigma \qquad (2.7a)$$

and

$$\sigma_s = n\sigma [1 + (n-1)a_s] = \mu_s \sigma \qquad (2.7b)$$

where μ_c and μ_s are the ratio of stresses in the clay and stone, respectively, to the average stress σ over the tributary area. For a given set of field conditions, the stress in the stone and the clay can be readily determined using Equations (2.7a) and (2.7b) if a reasonable value of the stress concentration factor is assumed based on previous measurements. The above σ, σ_c and σ_s stresses are

due to applied loading. In addition, the initial effective (and total) overburden and initial lateral stress at a given depth are also important quantities.

The above two equations, which give the stress due to the applied loading in the stone column and surrounding soil, are extremely useful in both settlement and stability analysis. Even where the extended unit cell concept is obviously not valid, use of Equations (2.7a) and (2.7b) in settlement calculations appears to give satisfactory results, probably because the average change in vertical stress with horizontal distance is not too great. As the number of stone columns in the group decreases, the accuracy of this approach would be expected to also decrease (Barksdale and Bachus, 1983).

The stress concentration factor n is dependent on a number of variables including the relative stiffness between the two materials, length of the stone column, area ratio and the characteristics of the granular blanket placed over the stone column. Values of stress concentration measure in field and laboratory studies are summarized in Table 2.4. Measured values of stress concentration have generally been between 2.5 and 5.0. The stress concentration factor measured in 4 of the five studies was either approximately constant or increased with time as consolidation occurred. Theory indicates the concentration factor should increase with time (Balaam, 1978). Since secondary settlement in reinforced cohesive soils is greater than in the stone column, the long-term stress concentration in the stone column should be no less than at the end of primary settlement (Barksdale and Bachus, 1983). Field measurements for sand compaction piles at four sites in Japan (Aboshi et.al. 1979) indicated stress concentration probably decreased with depth, but remained greater than 3.0 at the sites studied.

Stress concentration is a very important concept, which accounts for much of the beneficial effect of improving marginal ground with stone columns. For comparative purposes the influence of stress concentration factor on the stress

in the soil and stone can be easily determined using Figure 2.9 given by Bachus and Barksdale (1989).

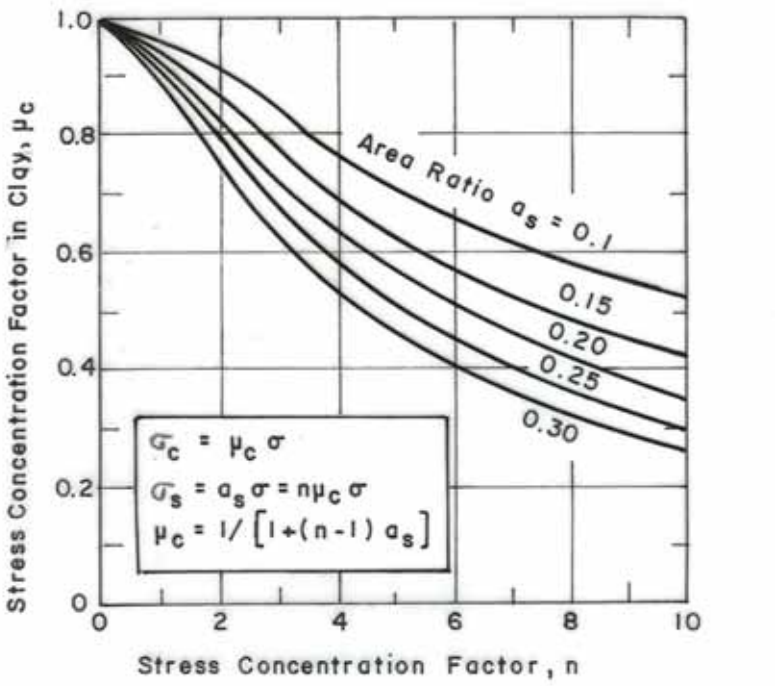

Figure 2.9 Variation of stress concentration factor
(Bachus and Barksdale 1989)

2.3.4 Ultimate Bearing Capacity of Stone Columns

In determining the ultimate bearing capacity of a stone column or a stone column group, the possible modes of failure should be considered as illustrated in Figures 2.2, 2.5 and 2.6.

Table 2.4 Observed stress concentration factors in stone columns (Barksdale and Bachus, 1983)*

Type Test	Design	Location	Stress Concentration n	Time variation of n	Stone column length (m)	Subsurface Conditions
Embankment	Square grid, s=1.7m,D=0.9m a_s=0.25	Rouen,France Vautrain, 1977	2.8 (avg)	Approx. Constant	6.6-7.8	Soft clay C=19-29 kN/m^2
Load Test; 45 stone columns (91cmx127cm)	Triangular grid s=1.74m,D=1.2m a_s=0.43	Hampton,Virginia Goughnour and Bayuk (1979)	3.0 (initial) 2.6 (final)	Decreasing	6.15	Very soft and soft silt and clay with sand C=9.6-38 kN/m^2
Test Fill 14 stone columns	Triangular grid s=2.1m,D=1.125m a_s=0.26	Jourdan Road Terminal, New Orleans,	2.6-2.4 (initial) 4.0-4.5 (final)	Increasing	19.5	Very soft clay with organics, silt and sand lenses, soft sandy clay
Embankments	a_s = 0.1-0.3	Japanese Studies-Sand compaction piles Aboshi et.al.(1979)	2.5-8.5 4.9 (average)	Increases	Variable	Very soft and soft sediments
Model Test	a_s = 0.07-0.4 D=2.9cm	GaTech Model Test Unit cell Sand column	1.5-5.0	Constant to slightly increasing	Variable	Soft clay, n appears to increase with a_s

*Vertical stress measured just below load except where indicated otherwise

2.3.4.1 Ultimate Bearing Capacity of Single Isolated Stone Column

Since most constructed stone columns have length to diameter ratios equal to or greater than 4 to 6, a bulging failure usually develops (Fig.2.4a) whether the tip of the column is floating in soft soil or resting on a firm-bearing layer. Figure 2.10 illustrates the bulging failure of a single model stone column floating in soft clay observed by Hughes and Withers (1974). The bulge that developed occurred over a depth of 2 to 3 diameters beneath the surface. These small-scale model tests were performed using 12.5 to 38mm diameter sand columns, which were 150mm in length. Soft kaolin clay was used having shear strength of 19 kN/m^2. Strains were determined in the composite soil mass from displacements obtained using radiographs taken of lead markers.

The load applied to a single stone column is transferred to the surrounding soft soil was verified in the small-scale experiments of Hughes and Withers (1974). As the column simultaneously bulges and moves downward, the granular material press into surrounding soft soil and transfers stress to the soil through shear.

A number of theories have been presented for predicting the ultimate capacity of an isolated, single stone column surrounded by a soft soil (Hughes and Withers, 1974; Wong, 1975; Bauman and Bauer, 1974; Thornburn, 1975; Aboshi et.al., 1979; Hughes et.al. 1975; Goughnour and Bayuk, 1979; Madhav et.al., 1979; Datye and Nagaraju, 1981; Balaam and Booker, 1985). Most of the analytical solutions assume a triaxial state of stress exists in the stone column, and both the column and surrounding soil are at failure. Table 2.5 tabulates the different methods, which will be discussed in detail at the following sections, to estimate the ultimate bearing capacity corresponding to bulging, general shear and sliding modes of failure.

The lateral confining stress σ_3 that supports the stone column is usually taken in these methods as the ultimate passive resistance that the surrounding soil can

mobilize as the stone column bulges outward against the soil. Since the column is assumed to be in a state of failure, the ultimate vertical stress, σ_1, which the column can take is equal to the coefficient of the passive pressure of the stone column, K_p, times the lateral confining stress, σ_3, which from classical plasticity theory can be expressed as:

$$\frac{\sigma_1}{\sigma_3} = \frac{1+\sin\phi_s}{1-\sin\phi_s} \tag{2.8}$$

where ϕ_s = angle of internal friction angle of the stone column

$\frac{\sigma_1}{\sigma_3}$ = coefficient of passive earth pressure K_p for the stone column.

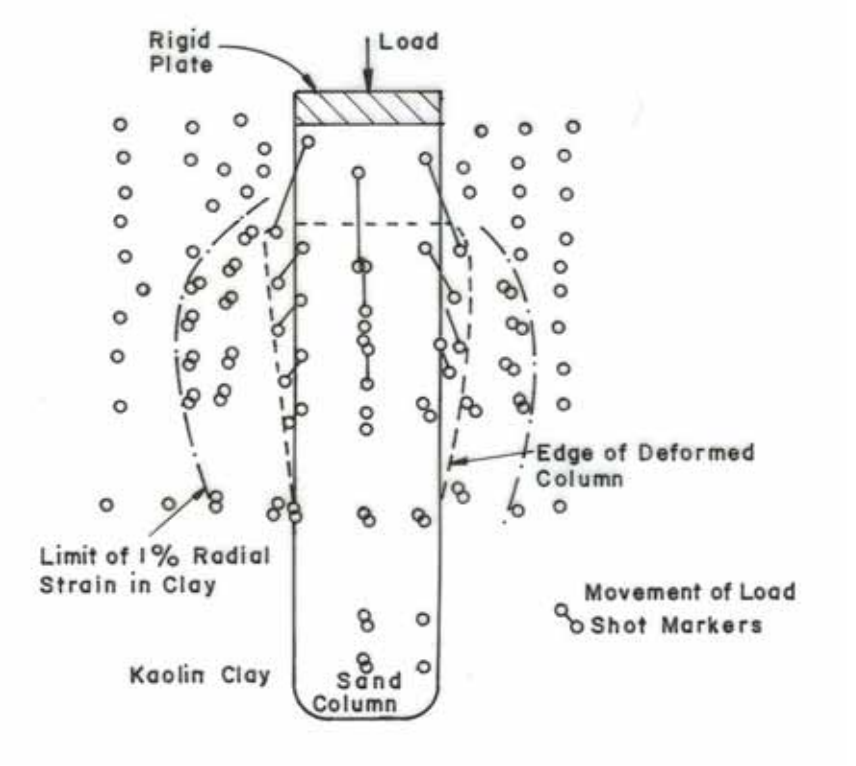

Figure 2.10 Bulging failure mode observed in model tests for a single stone column loaded with a rigid plate over the column (Hughes and Withers, 1974)

Table 2.5 Estimation of ultimate bearing capacity (Bergado et.al. 1994)

Mode of Failure	Derived formula	References
Bulging	$q_{ult} = \left(\gamma_c z K_p + 2c_u \sqrt{K_{pc}}\right)\frac{1+\sin\phi_s}{1-\sin\phi_s}$	Greenwood (1970)
	$q_{ult} = \left(F_c' c + F_q' q\right)\frac{1+\sin\phi_s}{1-\sin\phi_s}$	Vesic (1972), Datye and Nagaraju (1975)
	$q_{ult} = \left(\sigma_{ro} + 4c_u\right)\frac{1+\sin\phi_s}{1-\sin\phi_s}$	Hughes and Withers (1974)
	$q_{ult} = \frac{1+\sin\phi_s}{1-\sin\phi_s}\left(4c_u + \sigma_{ro} + K_0 q_s\right)(w/B)^2 + \left[1-(w/B)^2\right]q_s$	Madhav et. al. (1979)
General shear	$q_{ult} = \frac{1}{2}\gamma_c B N_\gamma + c_u N_c + \gamma_c D_f N_q$	Madhav and Vitkar (1978)
	$q_{ult} = 2A_s\left(K_p q_0 + 2c_u\sqrt{K_p}\right) + \left(1/K_{as}\right)\left[3d_s K_{pc}\gamma_c\left\{1-\left(3d_s/2L\right)\right\}\right]$	Wong (1975)
	$q_{ult} = \frac{1}{2}\gamma_c B\tan^3\beta + 2c_u\tan^2\beta + 2(1-a_s)c_u\tan\beta$ $\beta = 45^0 + \frac{\tan^{-1}\left(\mu_s a_s\tan\phi_s\right)}{2}$	Barksdale and Bachus (1983)
	$\tau = (1-a_s)c_u + \left(\gamma_s z + \mu_s\sigma_z\right)a_s\tan\phi_s\cos^2\theta$ $\mu_s = \frac{n}{1+(n-1)a_s}$	Aboshi et.al. (1979)

* Refer to appendix (A1) for notations

Greenwood (1970) and later Wong (1975) have assumed for preliminary analysis that the lateral resistance the surrounding soil can develop is equal to the passive resistance mobilized behind a long retaining wall which is laterally translated into the soil. Such an approach assumes a plane strain loading condition and hence does not realistically consider the 3-D geometry of a single column. The design approach of Wong (1975) in its final form does; however, appear to give reasonably good correlation with the measured response of stone column groups.

2.3.4.1.1 Cavity Expansion Theory

The passive resistance developed by the surrounding soil, as a first approximation can be better modeled as an infinitely long cylinder, which expands about the axis of symmetry until the ultimate passive resistance of the surrounding soil is developed. The expanding cylindrical cavity approximately simulates the lateral bulging of the column into the surrounding soil. Hughes and Withers (1974), Datye (1982), Datye and Nagaraju (1981) have evaluated the confining pressure on the stone column using this approach. Even though the stone column bulges outward along a distance of only 2 to 3 diameters, the model of an infinitely long expanding cylinder appears to give reasonably good results (Hughes and Withers, 1974; Datye and Nagaraju, 1977).

Hughes and Withers (1974) considered the bulging type failure of a single stone column to be similar to the cavity developed during a pressuremeter test. In their approach the elastic-plastic theory for a frictionless material and an infinitely long expanding cylindrical cavity was used for predicting undrained, ultimate lateral stress σ_3 of the soil surrounding the stone column:

$$\sigma_3 = \sigma_{ro} + c_u \left[1 + \ln_e \frac{E_c}{2c_u(1+\mu)} \right] \qquad (2.9)$$

where σ_3 = the total ultimate undrained lateral stress

σ_{ro} = total in-situ lateral stress (initial)

E_c = elastic modulus of the soil

c_u = undrained shear strength

μ = poisson's ratio

From a detailed examination of many field records of quick expansion pressuremeter tests it appears that Equation (2.9) can be approximated by:

$$\sigma_3 = \sigma'_{ro} + 4c_u + u \qquad (2.10)$$

where u is the pore pressure.

Substituting Equation (2.9) which gives the confining pressure on the stone column into (2.8) and letting q_{ult} equal σ_1 gives:

$$q_{ult} = \left\{ \sigma_{ro} + c_u \left[1 + \log_e \frac{E}{2c_u(1+\mu)} \right] \right\} \left(\frac{1+\sin\phi_s}{1-\sin\phi_s} \right) \qquad (2.11)$$

or

$$q_{ult} = (\sigma_{ro} + 4c_u - u) \frac{1+\sin\phi_s}{1-\sin\phi_s} \qquad (2.12)$$

where q_{ult} is the ultimate stress that can be applied to the stone column.

Hughes and Withers (1974) substituted measured values of cohesion, in situ lateral stress, the pore pressure and the angle of internal friction angle of the sand, they obtained in their model test, in to this equation and gave the ultimate stress that model column could support as:

$$q_{ult} = 25.2c_u \qquad (2.13)$$

2.3.4.1.2 Vesic Cavity Expansion Theory

Vesic (1972) has developed a general cylindrical cavity expansion solution extending earlier work to include soils with both friction and cohesion. Once again the cylinder is assumed to be infinitely long and the soil either elastic or plastic. The ultimate lateral resistance s_3 developed by the surrounding soil can be expressed as:

$$\sigma_3 = cF_c^{'} + qF_q^{'} \qquad (2.14)$$

where c = cohesion

q = mean stress $(s_1+s_2+s_3)/3$ at the equivalent failure depth

$F^{'}_c, F^{'}_q$ = cavity expansion factors

The cavity expansion factors $F^{'}_c, F^{'}_q$ shown in Figure 2.11 are a function of the angle of internal friction angle of the surrounding soil and the Rigidity Index, I_r. The Rigidity Index is expressed as:

$$I_r = \frac{E}{2(1+\mu)(c + q\tan\phi_c)} \qquad (2.15)$$

where E = modulus of elasticity of the surrounding soil in which cavity expansion is occurring

c = cohesion of the surrounding soil

μ = Poisson's ratio

q = mean stress within the zone of failure

Upon substituting Equation (2.14) into Equation (2.8) and letting q_{ult} equal σ_1, the ultimate stress that can be applied to the stone column becomes:

$$q_{ult} = \left[cF_c^{'} + qF_q^{'}\right]\left(\frac{1+\sin\phi_s}{1-\sin\phi_s}\right) \qquad (2.16)$$

where all the terms have been previously defined.

The mean stress q used in the above analysis should be taken as the stress occurring at the average depth of the bulge. The mean stress q is the sum of both initial stresses existing in the ground and the change in stress due to the externally applied load. Due to stress concentration in the stone column, however, the stress increase in the soil due to external loading will usually be only a portion of q. Both the short and long term ultimate capacity of a stone column can be estimated using cavity expansion theory.

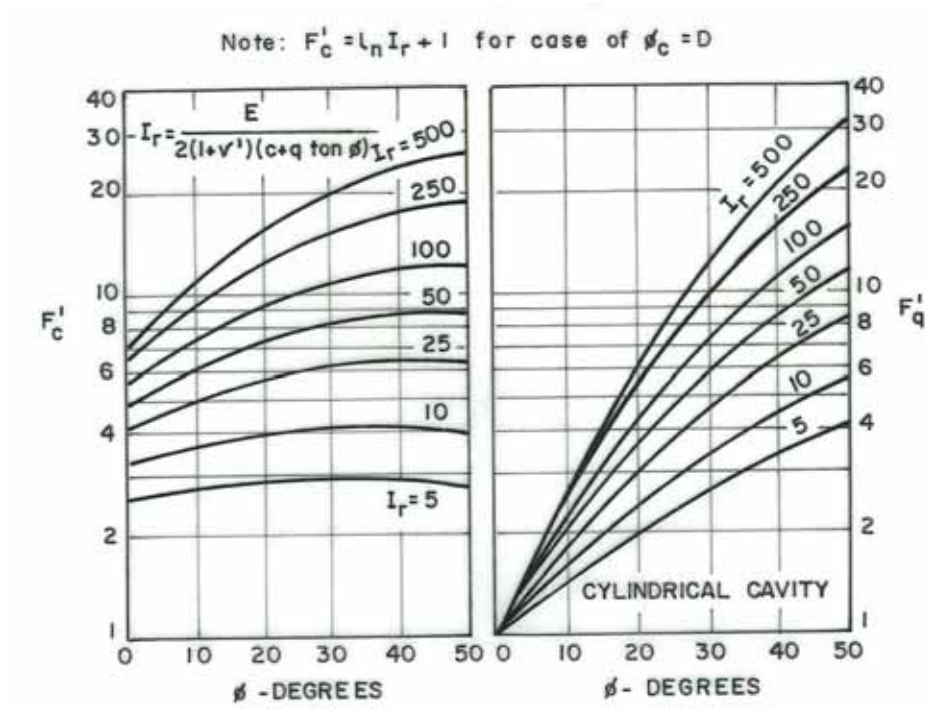

Figure 2.11 Vesic cylindrical cavity expansion factors (Vesic, 1972)

2.3.4.1.3 Short Stone Columns

A short stone column may fail either by a general or local bearing capacity failure of the stone and surrounding soil (Fig. 2.2b), or else by punching into a soft underlying soil (Fig. 2.2c). The ultimate capacity for a punching failure

can be determined by calculating the end bearing capacity of the stone column using conventional bearing capacity theories and adding the skin friction load developed along the side of the column.

A general bearing capacity failure could occur at the surface where the overburden surcharge effect is the smallest. Madhav and Vitkar (1978) have presented a plain strain solution for a general bearing capacity failure of a trench filled with granular material constructed in a frictionless soil. As shown in Figure 2.12, the loading may be applied to both the granular stone and the adjacent soft clay. From their solution bearing capacity is given for a plain strain loading as:

$$q_{ult} = \frac{1}{2}\gamma_c B N_\gamma + c N_c + D_f \gamma_c N_q \qquad (2.17)$$

where N_g, N_c and N_q are bearing capacity factors given in Figure 2.12, and the other terms used in the equation are also defined in the figure.

2.3.4.1.4 Summary

For single isolated granular piles, the most probable failure mechanism is bulging failure. This mechanism develops whether the tip of the pile is floating in the soft soil or fully penetrating and bearing on a firm layer. The lateral confining stress that supports the granular pile is usually taken as the ultimate passive resistance that the surrounding soil can mobilize as the pile bulges outward. Most of the discussed approaches in predicting the ultimate bearing capacity of a single, isolated granular pile have been developed based on this assumption. Some researchers have presented the relationship between the bearing capacities of a single, isolated stone column and other parameters.

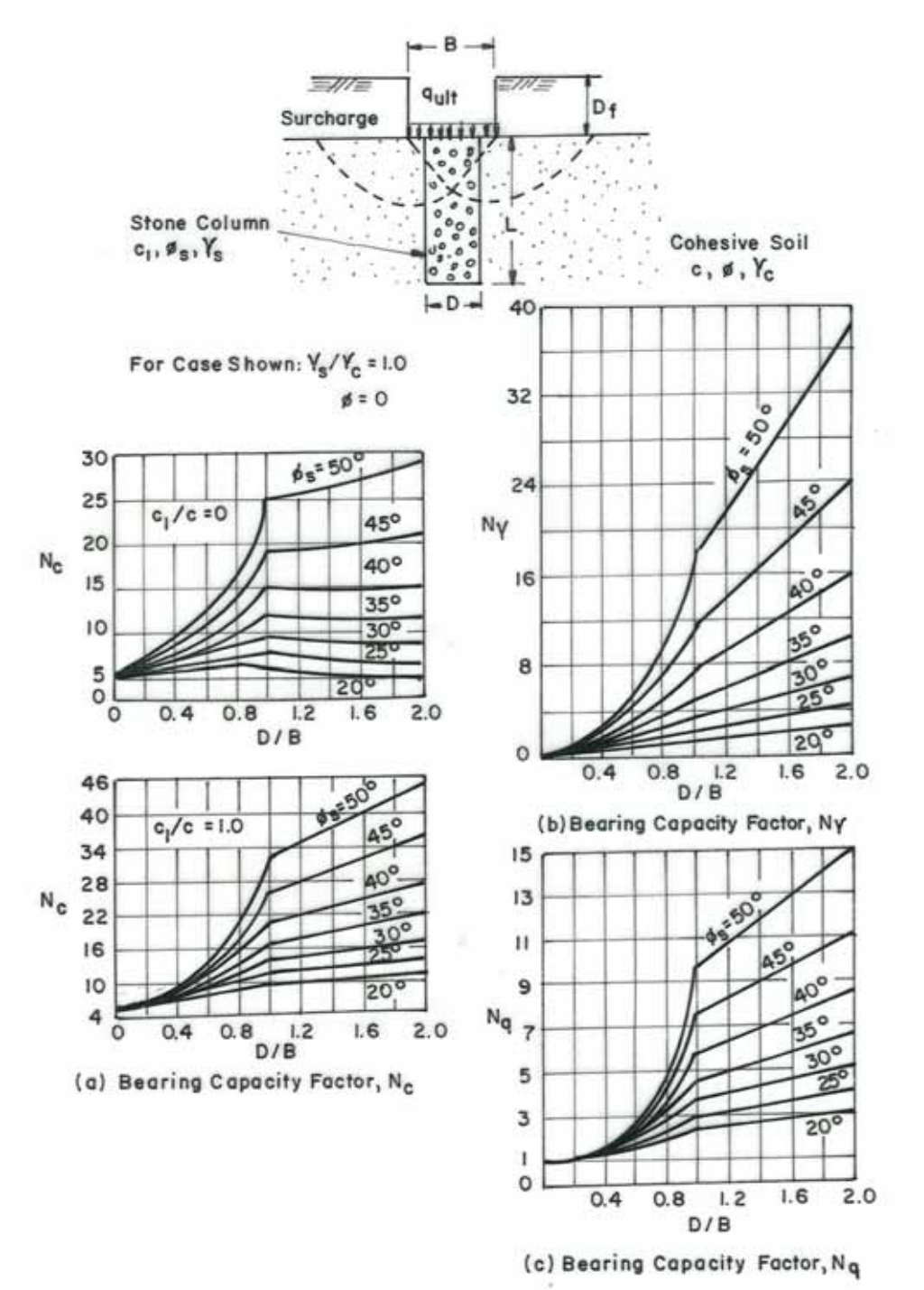

Figure 2.12 General bearing capacity failures for strip load and stone column–plain strain (Madhav and Vitkar, 1978)

Aboshi and Suematsu (1985) (referenced by Bergado et. al. 1994) presented a relationship between bearing capacity and area replacement ratio as illustrated in Figure 2.13.

The relationship between internal friction angle of granular material, strength of the surrounding clay, and the ultimate bearing capacity of single granular piles is shown in Figure 2.14 (Bergado and Lam, 1987)

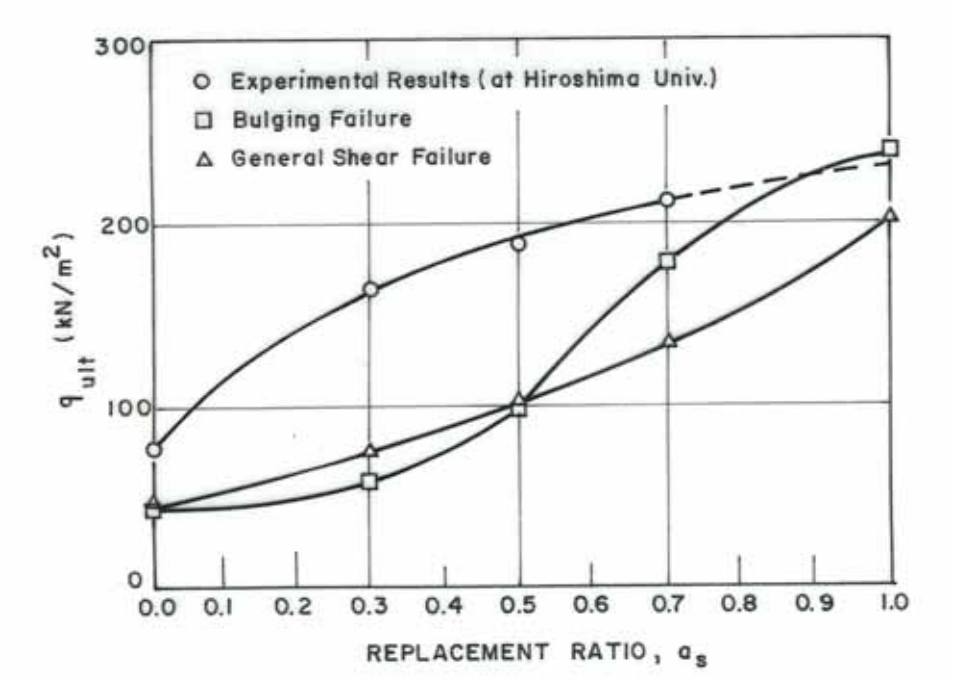

Figure 2.13 Relationship between ultimate bearing capacity and area replacement ratio (after Aboshi and Suematsu 1985) (Bergado et. al. 1994)

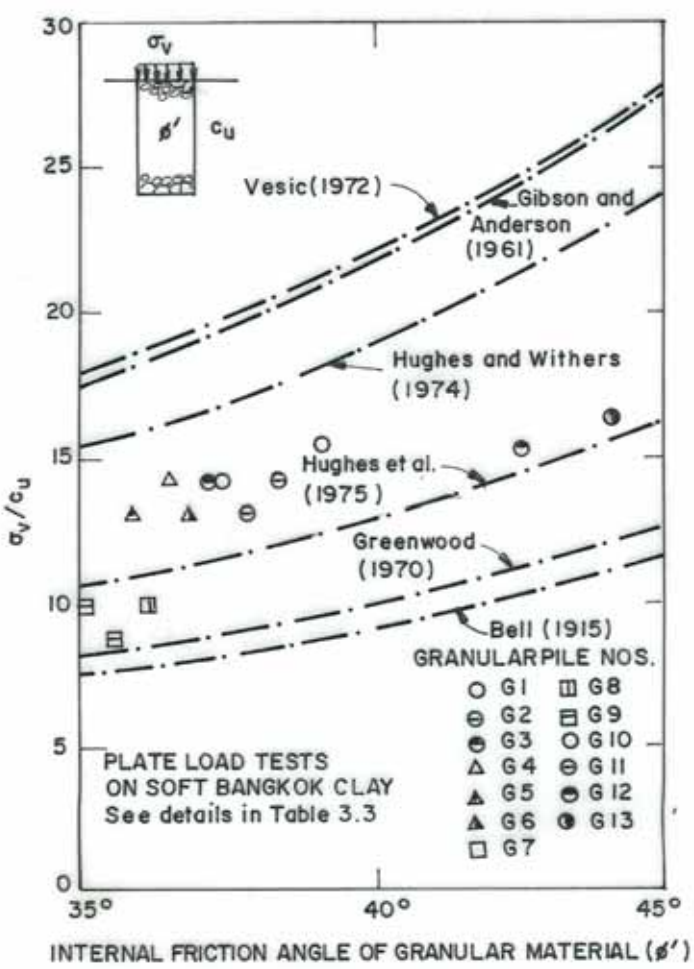

Figure 2.14 Relationship between internal friction angle of granular material, strength of surrounding clay and ultimate bearing capacity of single granular piles (Bergado and Lam, 1987)

2.3.4.2 Ultimate Bearing Capacity of Stone Column Groups

The common method for estimating the ultimate bearing capacity of stone column groups assumed that the angle of internal friction in the surrounding cohesive soil and the cohesion in the granular pile are negligible. Furthermore, the full strength of both the granular pile and cohesive soil has been mobilized. The pile group is also assumed to be loaded by rigid foundation. The ultimate bearing capacity of granular pile groups as suggested by Barksdale and Bachus

(1983) is determined by approximating the failure surface with two straight rupture lines as shown in Figure 2.15. Assuming the ultimate vertical stress, q_{ult}, and the ultimate lateral stress, σ_3, to be the principle stresses, then the equilibrium of the wedge requires:

$$q_{ult} = \sigma_3 \tan^2 \beta + 2c_{avg} \tan \beta \quad (2.18)$$

where

$$\sigma_3 = \frac{\gamma_c B \tan \beta}{2} + 2c \quad (2.19)$$

$$\beta = 45 + \frac{\phi_{avg}}{2} \quad (2.20)$$

$$\phi_{avg} = \tan^{-1}(\mu_s a_s \tan \phi_s) \quad (2.21)$$

$$c_{avg} = (1 - a_s)c \quad (2.22)$$

γ_c = saturated or wet unit weight of the cohesive soil

B = foundation width

β = failure surface inclination

c = undrained shear strength within the unreinforced cohesive soil

ϕ_s = angle of internal friction of the granular soil

ϕ_{avg} = composite angle of internal friction

c_{avg} ;= composite cohesion on the shear surface

The development of the above approach did not consider the possibility of a local bulging failure of the individual pile. Hence the approach is only applicable for firm and strongly cohesive soils having undrained strength greater than 30-40 kN/m^2 (Bergado et.al., 1994). However it is useful for approximately determining the relative effects on ultimate bearing capacity design variables such as pile diameter, spacing, gain in strength due to consolidation and angle of internal friction.

For the case of the soft and very soft cohesive soils the pile group capacity is predicted using the capacity of a single, isolated pile located within a group and to be multiplied by the number of piles (Barksdale and Bachus, 1983). The ultimate bearing capacity of an isolated stone column or a stone column located within a group can be expressed in terms of an ultimate stress applied over the stone column:

$$q_{ult} = cN_c' \qquad (2.23)$$

where N_c' = composite bearing capacity factor for the stone column which ranges from 18 to 22.

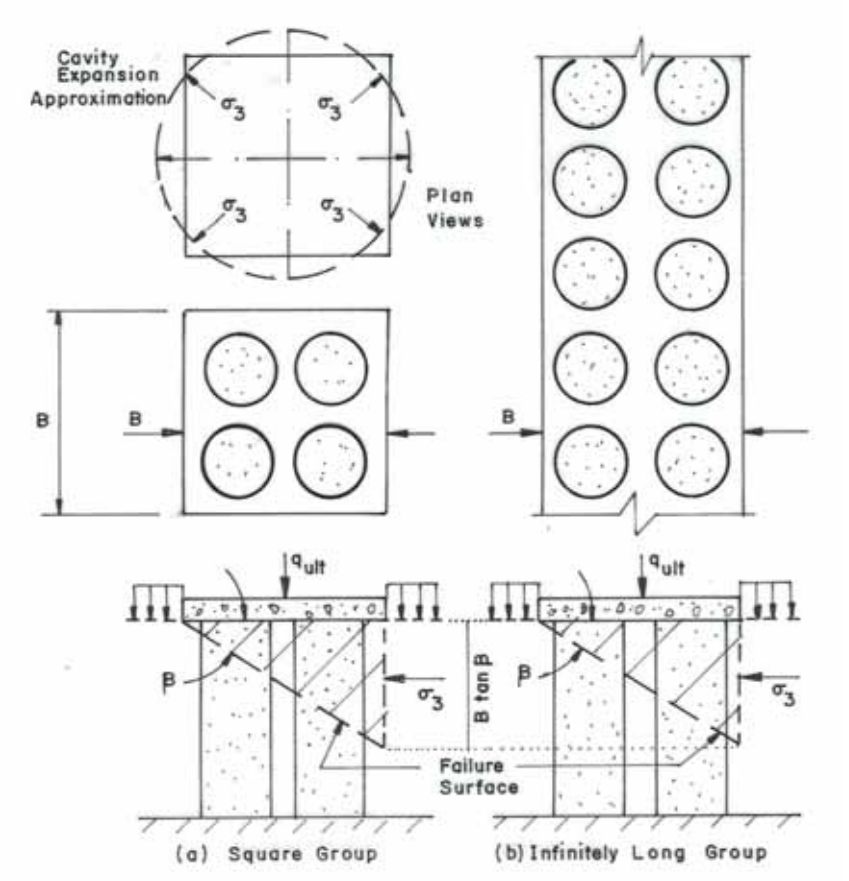

Figure 2.15 Stone column group analysis (Barksdale and Bachus, 1983)

Cavity expansion theory shows that the ultimate capacity and hence N'_c is dependent upon the compressibility of the soil surrounding the stone column. For soils (inorganic soft to stiff clays and silts) having a reasonably high initial stiffness an N'_c of 22 is recommended; for soils (peats, organic cohesive soils and very soft clays with plasticity indices greater than 30) with low stiffness, an N'_c of 18 is recommended by Barksdale and Bachus (1983). For the soft Bagkok clay, N'_c ranges from 15 to 18 (Bergado and Lam, 1987).

Mitchell (1981) recommends using an N'_c of 25 for vibro-replacement stone columns. Datye et. al. (1982) recommend using 25 to 30 for vibro-replacement columns, 45 to 50 for cased, rammed stone columns and 40 for uncased, rammed stone columns.

Vesic cavity expansion theory, Equations (2.14)-(2.16), is recommended primarily used with the group bearing capacity theory to calculate the confining pressure for a square group. For use in Vesic cavity expansion theory, a modulus E of 11c is recommended for soft to stiff, non-organic soils. For organic or very soft soils with a plasticity index greater than 30, an E of 5c is recommended. An angle of internal friction of 42 to 45^0 should be used in the analysis for a good quality crushed stone and 38 to 42^0 for gravel.

2.3.5 Settlement Analysis

Presently available methods for calculating settlement can be classified as either (1) simple, approximate methods which make important simplifying assumptions or (2) sophisticated methods based on fundamental elasticity and/or plasticity theory (such as finite elements) which model material and boundary conditions. Several of the more commonly used approximate methods are presented first. Following this, a review is given of selected theoretically sophisticated elastic and elastic-plastic methods and design charts are presented. All of these approaches for estimating settlement assume an

infinitely wide, loaded area reinforced with stone columns having a constant diameter and spacing. For this condition of loading and geometry the unit cell concept is theoretically valid and has been used by the Aboshi et.al,(1979) Barksdale and Takefumi (1990), Priebe (1990 and 1993), Goughnour and Bayuk (1979) and in the infinite element method to develop theoretical solutions for predicting settlement. As discussed in the next major section, the reduction in settlement can be approximately considered due to the spreading of stress in groups of limited size.

2.3.5.1 Equilibrium Method

The equilibrium method described for example by Aboshi et.al.(1979) and Barksdale and Goughnour (1984), Barksdale and Takefumi (1990) is the method is in Japanese practice for estimating the settlement of sand compaction piles. In applying this simple approach the stress concentration factor, n, must be estimated using past experience and the results of previous field measurements of stress.

The following assumptions are necessary in developing the equilibrium method: (1) the extended unit cell idealization is valid, (2) the total vertical load applied to the unit cell equals the sum of the force carried by the stone and the soil, (3) the vertical displacement of stone column and soil is equal, and (4) a uniform vertical stress due to external loading exists throughout the length of stone column, or else the compressible layer is divided in to increments and the settlement of each increment is calculated using the average stress increase in the increment. Following this approach, as well as the other methods, settlement occurring below the stone column reinforced ground must be considered separately; usually these settlements are small and can often be neglected (Barksdale and Bachus, 1983).

The change in vertical stress in the clay, σ_c, due to the applied external stress is equal to:

$$\sigma_c = \mu_c \sigma \tag{2.24}$$

where σ is the average externally applied stress (Figure 2.8c), and μ_c is given by Equation (2.7a). From conventional one-dimensional consolidation theory

$$S_t = \left(\frac{C_c}{1+e_0} \right) \log_{10} \left(\frac{\sigma_0^{'} + \sigma_c}{\sigma_0^{'}} \right) H \tag{2.25}$$

where S_t = primary consolidation settlement occurring over a distance H of stone column treated ground

H = vertical height of stone column treated ground over which settlements are being calculated.

$\sigma_0^{'}$ = average initial effective stress in the clay layer

σ_c = change in stress in the clay layer due to the externally applied loading, Equation (2.7a)

C_c = compression index from one-dimensional consolidation test

e_o = initial void ratio

From Equation (2.25) it follows that for normally consolidated clays, the ratio of settlements of the stone column improved ground to the unimproved ground, S_t/S, can be expressed as

$$S_t / S = \frac{\log_{10} \left(\frac{\sigma_0^{'} + \mu_c \sigma}{\sigma_0^{'}} \right)}{\log_{10} \left(\frac{\sigma_0^{'} + \sigma}{\sigma_0^{'}} \right)} \tag{2.26}$$

This equation shows that the level of improvement is dependent upon (1) the stress concentration factor n, (2) the initial effective stress in the clay, and (3) the magnitude of applied stress σ. Equation (2.26) indicates if other factors constant, a greater reduction in settlement is achieved for longer columns and smaller applied stress increments.

For very large σ_0' (long length of stone column) and very small applied stress σ, the settlement ratio relatively rapidly approaches

$$S_t / S = 1/[1 + (n-1)a_s] = \mu_c \qquad (2.27)$$

where all terms have been previously defined. Equation (2.27) is shown graphically in Figure 2.16; it gives a slightly unconservative estimate of expected ground improvement and is useful for preliminary studies.

The stress concentration factor n required calculating σ_c is usually estimated from the results of stress measurements made for full-scale embankments, but could be estimated from theory. From elastic theory assuming a constant vertical stress, the vertical settlement of the stone column can be approximately calculated as follows:

$$S_s = \frac{\sigma_s L}{D_s} \qquad (2.28)$$

where S_s = vertical displacement of the stone column

σ_s = average stress in the stone column

L = length of the stone column

D_s = constrained modulus of the stone column (the elastic modulus, E_s, could be used for an upper bound)

Using Equation (2.28) and its analogous from for the soil, equate the settlement of the stone and soil to obtain

$$\frac{\sigma_s}{\sigma_c} = \frac{D_s}{D_c} \tag{2.29}$$

where σ_s and σ_c are the stresses in the stone column and soil, respectively and D_s and D_c are the appropriate module of the two materials.

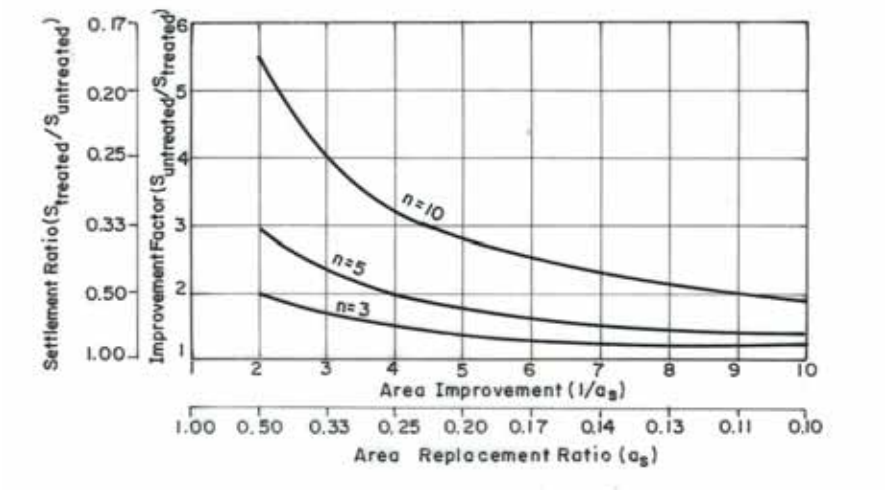

Figure 2.16 Maximum reductions in settlement that can be obtained using stone columns- equilibrium method of analysis (Barksdale and Bachus, 1983)

Use of Equation (2.29) gives values of the stress concentration factor n from 25 to over 500, which is considerably higher than measured in the field. Field measurements for stone columns have shown n to generally be in the range of 2 to 5 (Goughnour and Bayuk, 1979). Therefore, use of the approximate compatibility method, Equation (2.29), for estimating the stress concentration factor is not recommended for soft clays (Barksdale and Bachus, 1983). For settlement calculations using the equilibrium method, a stress concentration factor n of 4.0 to 5.0 is recommended based on comparison of calculated settlement with observed settlements (Aboshi et.al. 1979).

2.3.5.2 Priebe Method

The method proposed by Priebe (Bauman and Bauer, 1974; Priebe, 1988, 1993 and 1995; Mosoley and Priebe, 1993) for estimating reduction in settlement due to ground improvement with stone columns also uses the unit cell model. Furthermore the following idealized conditions are assumed:

- The column is based on a rigid layer
- The column material is incompressible
- The bulk density of column and soil is neglected

Hence, the column cannot fail in end bearing and any settlement of the load area results in a bulging of the column, which remains constant all over its length.

The improvement achieved at these conditions by the existence of stone columns is evaluated on the assumption that the column material shears from beginning whilst the surrounding soil reacts elastically. Furthermore, the soil is assumed to be displaced already during the column installation to such an extend that its initial resistance corresponds to the liquid state, i.e. the coefficient of earth pressure amounts to K=1. The results of evaluation, taking Poisson's ratio, μ=1/3, which is adequate for the state of final settlement in most cases, is expressed as basic *improvement factor* n_o:

$$n_0 = 1 + \frac{A_c}{A}\left[\frac{5 - A_c / A}{4K_{ac}(1 - A_c / A} - 1\right] \qquad (2.30)$$

where A_c = cross section area of single stone column

A = unit cell area

The relation between the improvement factor n_o, the reciprocal area ratio A/A_c and the friction angle of the backfill material ϕ_c is illustrated in Figure 2.17 by

Barksdale and Bachus (1983) comparing the equilibrium method solution (equation 2.27) for stress concentration factors of n 3.5 and 10.

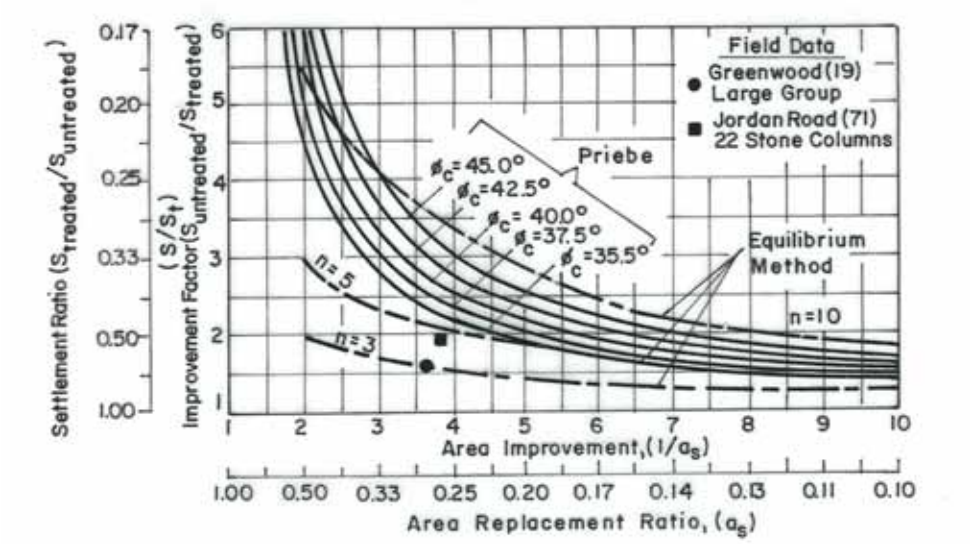

Figure 2.17 Settlement reduction due to stone column- Priebe and Equilibrium Methods (Barksdale and Bachus, 1983).

The Priebe curves generally fall between the upper bound equilibrium curves for n between 5 and 10. The Priebe improvement factors are substantially greater than for the observed variation of the stress concentration factor from 3 to 5. Measured improvement factors from two sites, also given in Figure 2.17, show good agreement with the upper bound equilibrium method curves, for n in the range of 3 to slightly less than 5. Barksdale and Bachus (1983) underlined that the curves of Priebe appear, based on comparison with the equilibrium method and limited field data, to over predict the beneficial effects of stone columns in reducing settlement.

Later Priebe (1995) considered the compressibility of the backfill material and recommended the additional amount on the area ratio $\Delta(A/A_c)$ depending on the ratio of the constrained moduli D_c/D_s which can be readily taken from Figure 2.18.

Priebe (1995) also stated that weight of the columns and of the soil has to be added to the external loads. Under consideration of these additional loads (overburden), he defined the depth factor, f_d and illustrated in Figure 2.19. The improvement ratio n_0 (corrected for consideration of the column compressibility, Fig. 2.18) should be multiplied by f_d.

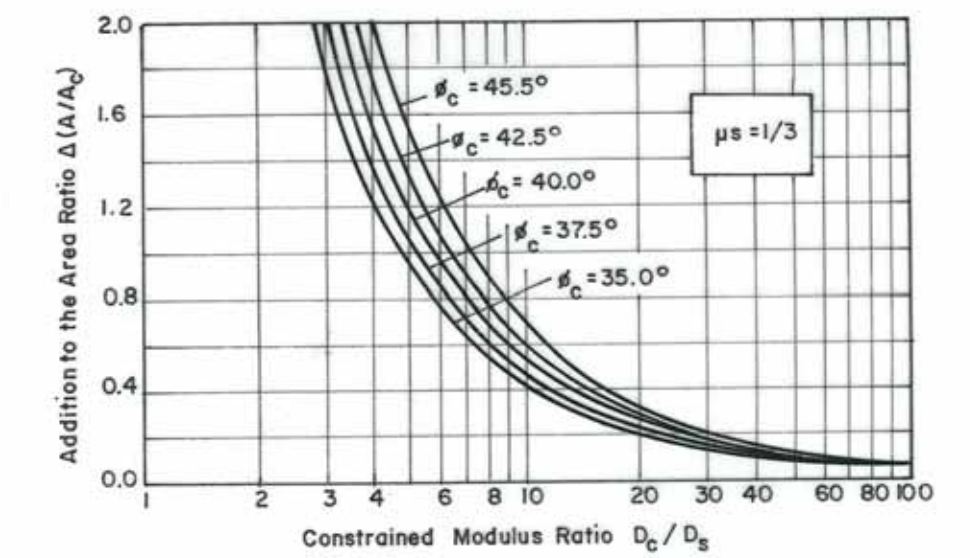

Figure 2.18 Consideration of column compressibility (Priebe, 1995)

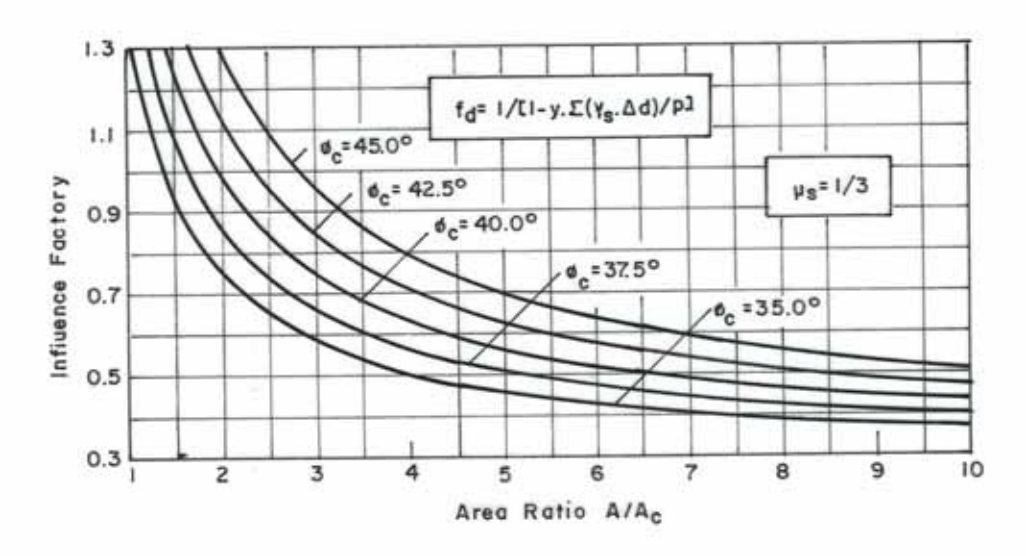

Figure 2.19 Determination of the depth factor (Priebe, 1995)

Due to the compressibility of the backfill material, the depth factor reaches a maximum value, which can be taken from the diagram given by Priebe (1995) in Figure 2.20.

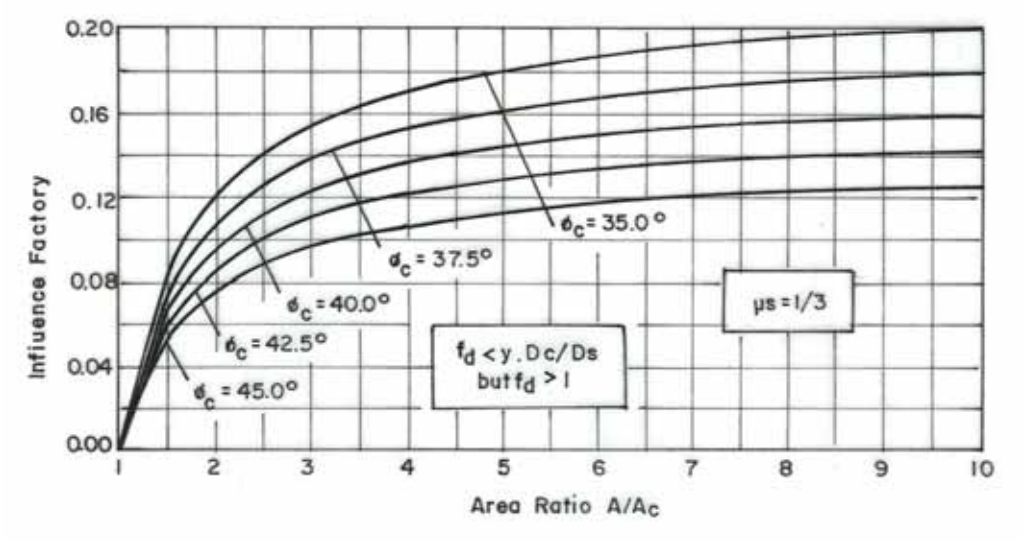

Figure 2.20 Limit value of the depth factor (Priebe, 1995)

The basic system of Priebe's Method discussed so far assumes improvement by a large grid of stone columns. Accordingly, it provides the reduction in the settlement of large slab foundation. For small foundations, Priebe (1995) offers diagrams, given in Figure 2.21a and 2.21b, which allow a simple way to determine the settlement performance of isolated single footings and strip foundations from the performance of a large grid. The diagrams are valid for homogeneous conditions only and refer to settlement ***s*** up to a depth ***d*** which is the second parameter counting from foundation level.

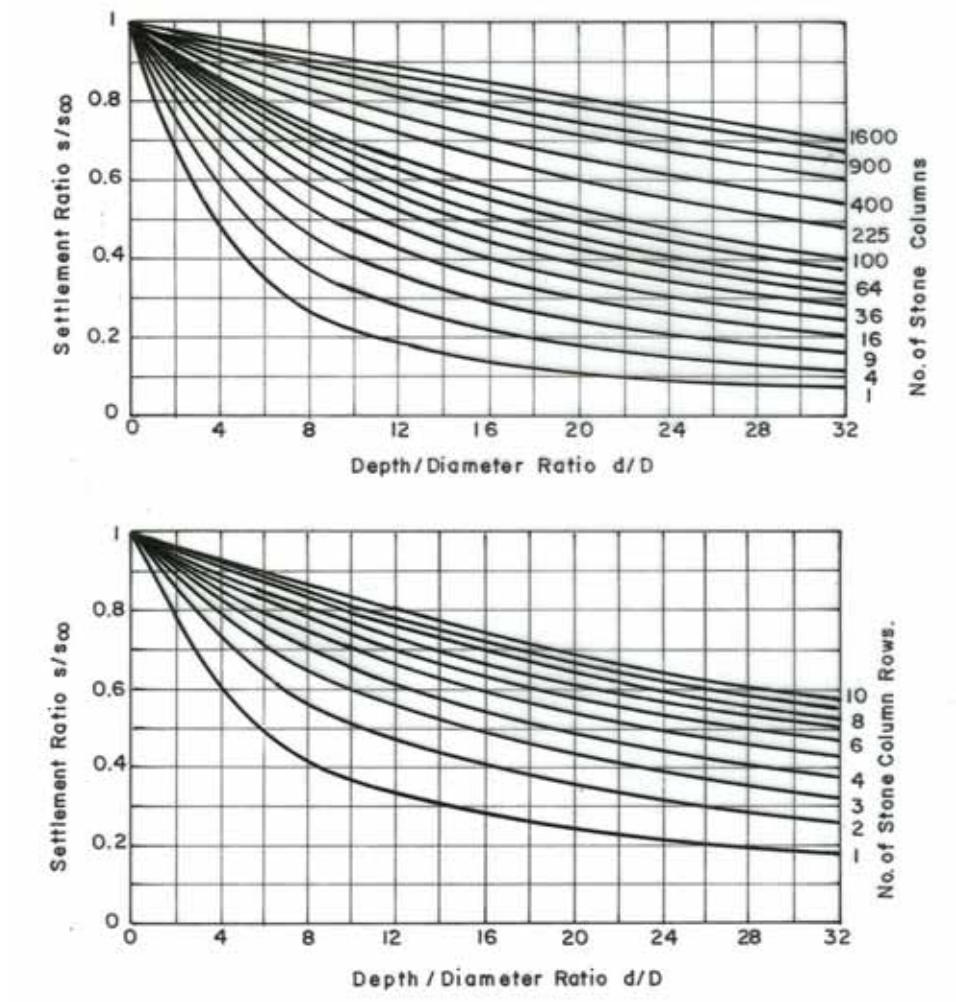

Figure 2.21 Settlement of small foundations a) for single footings b) for strip footings (Priebe, 1995)

2.3.5.3 Greenwood Method

Greenwood (1970) has presented empirical curves, which are based on field experience, giving the settlement reduction due to ground improvement with stone columns as a function of undrained soil strength and stone column spacing. These curves have been replotted by Barksdale and Bachus (1989) and presented in Figure 2.22 using area ratio and improvement factor rather than column spacing and settlement reduction as done in the original curves.

The curves neglect immediate settlement and shear displacement and columns assumed resting on firm clay, sand or harder ground. In replotting the curves a stone column diameter of 0.9m was assumed for the c_u = 40 kN/m^2 upper bound curve and a diameter of 1.07m for the c_u = 20 kN/m^2 lower bounds curve. Also superimposed on the figure is the equilibrium method upper bounds solution, Equation 2.27 for stress concentration factors of 3, 5, 10 and 20. The Greenwood curve for vibro-replacement and shear strength of 20 kN/m^2 generally corresponds to stress concentration factors of about 3 to 5 for the equilibrium method and hence appears to indicate probable levels of improvement for soft soils for area ratio less than about 0.15. For firm soils and usual levels of ground improvement ($0.15 \leq a_s \leq 0.35$), Greenwood's suggested improvement factors on Figure 2.22 appear to be high. Stress concentration n decreases as the stiffness of the ground being improved increases relative to the stiffness of the column. Therefore, the stress concentration factors greater than 15 required developing the large level of improvement is unlikely in the firm soil.

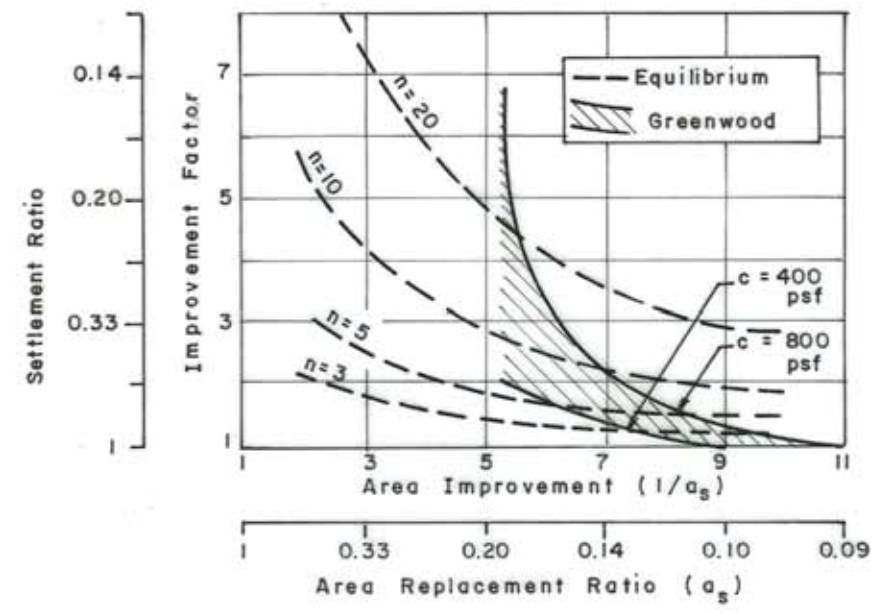

Figure 2.22 Comparison of Greenwood and Equilibrium Methods for predicting settlement of stone column reinforced soil
(Barksdale and Bachus, 1989)

2.3.5.4 Incremental Method

The method for predicting settlement developed by Goughnour and Bayuk (1979b) is an important extension of methods presented earlier by Hughes et. al. (1975), Bauman and Bauer (1974). The unit cell model is used together with an incremental, iterative, elastic-plastic solution. The loading is assumed to be applied over a wide area. The stone is assumed to be incompressible so that all volume change occurs in the clay. Both vertical and radial consolidations are considered in the analysis. The unit cell is divided into small, horizontal increments. The vertical strain and vertical and radial stresses are calculated for each increment assuming all variables are constant over the increment.

Both elastic and plastic responses of the stone column are considered. If stress levels are sufficiently low the stone column remains in the elastic range. For most design stress levels, the stone column bulges laterally yielding plastically over at least a portion of its length.

The assumption is also made that the vertical and, radial and tangential stresses at the interface between the stone and soil are principle stresses. Therefore no shear stresses are assumed to act on the vertical boundary between the stone column and the soil. Both Goughnour and Bayuk (1979b) and Barksdale and Bachus (1983) noted that because of the occurrence of relatively small shear stresses at the interface (generally less than about 10 to 20 kN/m^2), this assumption appears acceptable.

In the elastic range the vertical strain is taken as the increment of vertical stress divided by the modulus of elasticity. Upon failure of the stone within an increment; the usual assumption (Hughes and Withers, 1974, Bauman and Bauer, 1974, Aboshi et.al. 1979) is made that the vertical stress in the stone equals the radial stress in the clay at the interface times the coefficient of passive pressure of the stone. Radial stress in the cohesive soil is calculated following the plastic theory considering equilibrium within the clay. This gives

the change in radial stress in the clay as a function of the change in vertical stress in the clay, the coefficient of lateral stress in the clay, the geometry and the initial stress state in the clay. Radial consolidation of the clay is considered using one-dimensional consolidation theory. Following this approach the vertical stress in the clay is increased to reflect greater volume change due to radial consolidation.

For a realistic range of stress levels and other conditions the incremental method was found to give realistic results.

2.3.5.5 Finite Element Method

The finite element method offers the most theoretically sound approach for modeling stone column improved ground. Nonlinear material properties, interface slip and suitable boundary conditions can all be realistically modeled using the finite element technique. Although 3-D modeling can be used, from a practical standpoint either n axisymmetric or plane strain model is generally employed. Most studies have utilized the axisymmetric unit cell model to analyze the conditions of either uniform load on a large group of stone columns (Balaam et.al. 1977, Balaam and Booker, 1981) or a single stone column (Balaam and Poulos, 1983); Aboshi et.al.(1979) have studied a plane strain loading condition.

Balaam et.al.(1977) analyzed by finite elements large groups of stone columns using the unit cell concept. Undrained settlements were found to be small and neglected. The ratio of modulus of the stone to that of the clay was assumed to vary from 10 to 40, and the Poisson's ratio of each material was assumed to be .3. A coefficient of at rest earth pressure K_0 = 1 was used. Only about 6% difference in settlement was found between elastic and elastic-plastic response. The amount of stone column penetration into the soft layer and the diameter of

the column were found to have a significant effect on settlement (Figure 2.23); the modular ratio of stone column to soil was less importance.

Balaam and Poulos (1983) found for a single pile that slip at the interface increases settlement and decreases the ultimate load of a single pile. Also assuming adhesion at the interface equal to the cohesion of the soil gave good results when compared to field measurement.

Balaam and Booker (1981) found, for the unit cell model using linear elastic theory for a rigid loading (equal vertical strain assumption), that vertical stresses were almost uniform on horizontal planes in the stone column and also uniform in the cohesive soil. Also stress state in the unit cell was essentially triaxial. Whether the underlying firm layer was rough or smooth made little difference. Based upon these findings, a simplified, linear elasticity theory was developed and design curves were given for predicting performance. Their analysis indicates that as drainage occurs, the vertical stress in the clay decreases and the stress in the stone increases as the clay goes from the undrained state. This change is caused by a decrease with drainage both the modulus and Poisson's ratio of the soil.

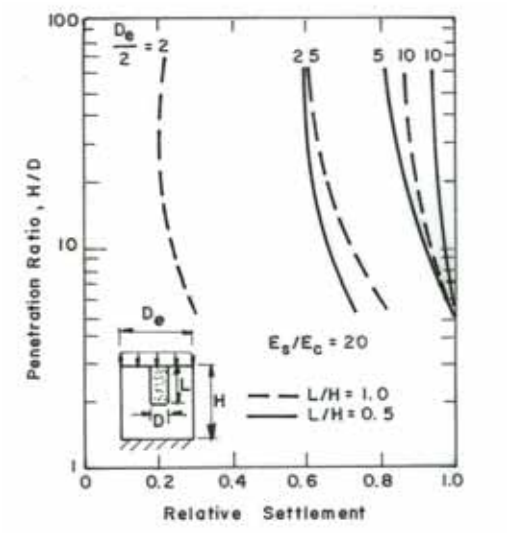

Figure 2.23 Effect of stone column penetration length on elastic settlement (Balaam et.al., 1977)

2.3.5.6 Design Curves

Barksdale and Bachus (1983) presented some design curves for predicting primary consolidation settlement. The finite element program was used in their study. For a nonlinear analysis load was applied in small increments and total stresses were performed by solving a system of linear, incremental equilibrium equations for the system.

Curves for predicting settlement of *low compressibility soils* such as stone column reinforced sands, silty sands and some silts were developed using linear elastic theory. Low compressibility soils are defined as those soils having modular ratios $E_s/E_c \leq 10$ where E_s and E_c are the average modulus of elasticity of the stone column and soil, respectively. The settlement curves for area ratios of 0.1, 0.15 and 0.25 are given in Figure 2.24.

The elastic finite element study utilizing the unit cell model shows a very nearly linear increase in stress concentration in the stone column with increasing modular ratio (Figure 2.25, Barksdale and Bachus, 1983). The approximate linear relation exists for area replacement ratios a_s between 0.1 and 0.25, and length to diameter ratios varying from 4 to 20. For a modular ratio E_s/E_c of 10, a stress concentration factor n of 3 exists. For modular ratios greater than about 10, Barksdale and Bachus (1983) noted that elastic theory underestimates drained settlements due to excessively high stress concentration that theory predicts to occur in the stone and lateral spreading in soft soils.

To calculate the consolidation settlement in *compressible cohesive soils* ($E_s/E_c \geq 10$), design curves were developed assuming the clay to be elastic-plastic and the properties of the stone to be stress dependent (non-linear stress-strain properties). To approximately simulate lateral bulging effects, a soft boundary was placed around the unit cell to allow lateral deformation. Based on the field measurements, a boundary 25mm thick having an elastic modulus of 83 kN/m^2 was used in the model, which causes maximum lateral deformations due to

lateral spreading, which should occur across the unit cell. To obtain the possible variation in the effect of boundary stiffness (lateral spreading), a relatively rigid boundary was also used, characterized by a modulus of 6900 kN/m^2.

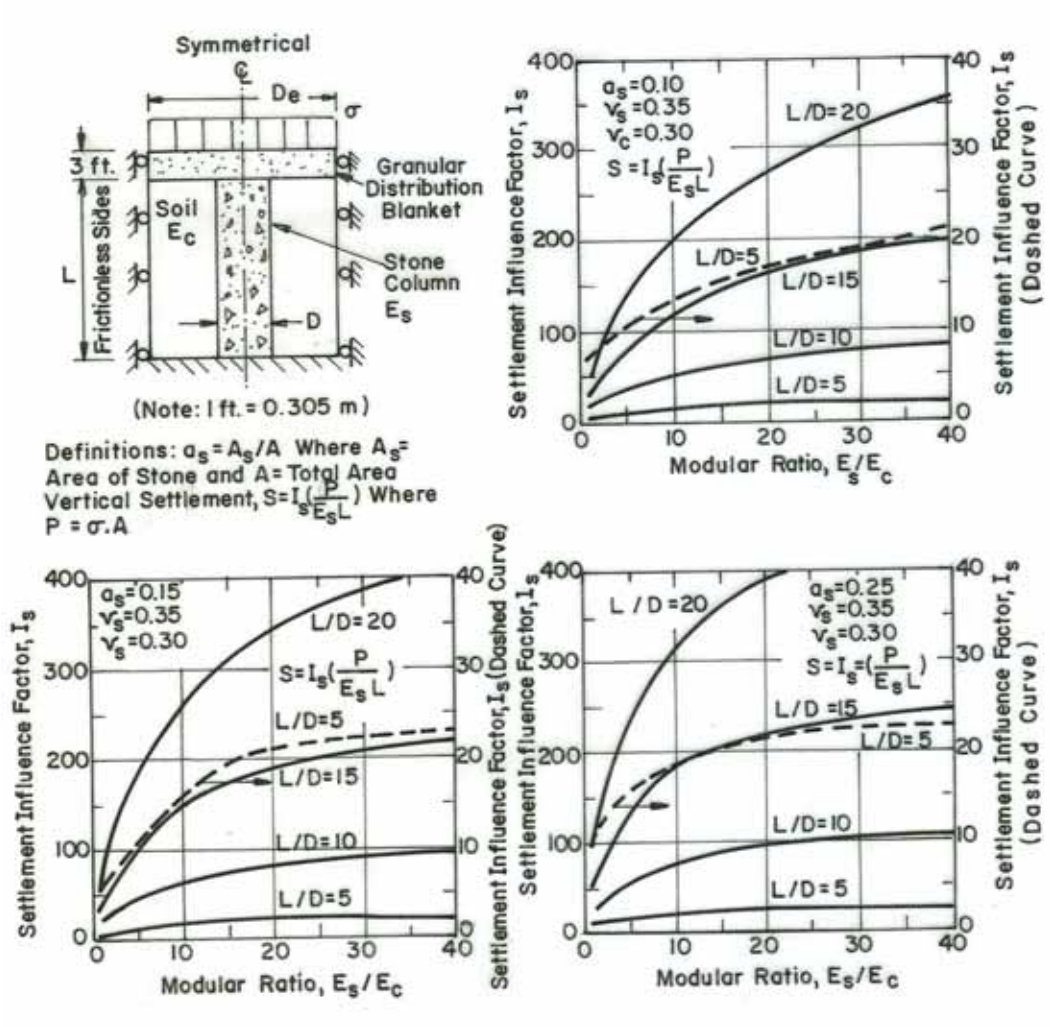

Figure 2.24 Notations used in unit cell linear elastic solutions and linear elastic settlement influence factors for area ratios, a_s = 0.10, 0.15, 0.25 (Barksdale and Bachus, 1983).

The unit cell model and notation used in the analysis is summarized in Figure 2.26. The design charts developed using this approach is presented in Figure 2.27. Settlement is given as a function of the uniform, average applied pressure σ over the unit cell, modulus of elasticity of the soil E_c, area replacement ratio a_s, length to diameter ratio, L/D, and boundary rigidity. The charts were developed for a representative angle of internal friction of the stone $\phi_s = 42^0$, and a coefficient of at rest earth pressure K_0 of 0.75 for both the stone and soil. For soils having a modulus E_c equal to or less than 1100 kN/m^2, the soil was assumed to have a shear strength of 19 kN/m^2. Soils having greater stiffness did not undergo an interface or soil failure; therefore, soil shear strength did not affect the settlement.

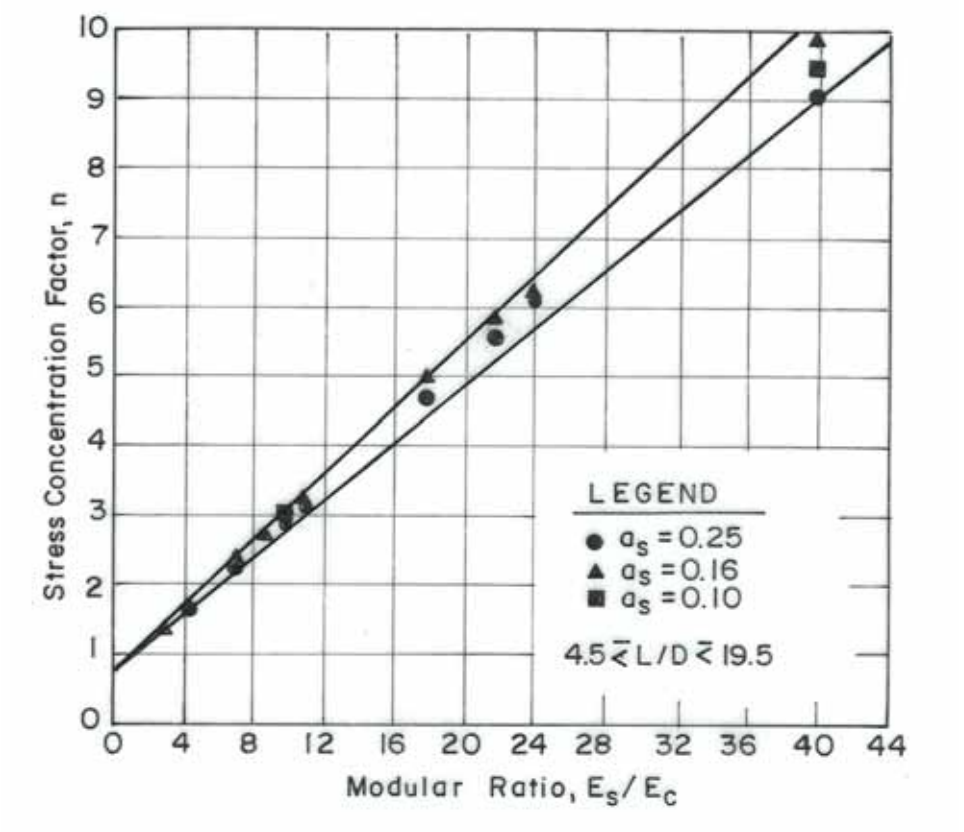

Figure 2.25 Variation of stress concentration factor with modular ratio- Linear elastic analysis (Barksdale and Bachus, 1983)

Figure 2.28 is given by Barksdale and Bachus (1983), which shows the theoretical variation of the stress concentration factor n with the modulus of elasticity of the soil and length to diameter ratio, L/D. Stress concentration factors in the range of about 5 to 10 are shown for short to moderate length columns reinforcing very compressible clays (E_c <1380 to 2070 kN/m^2). These results conclude that the nonlinear theory may predict settlements smaller than those observed (Barksdale and Bachus, 1983).

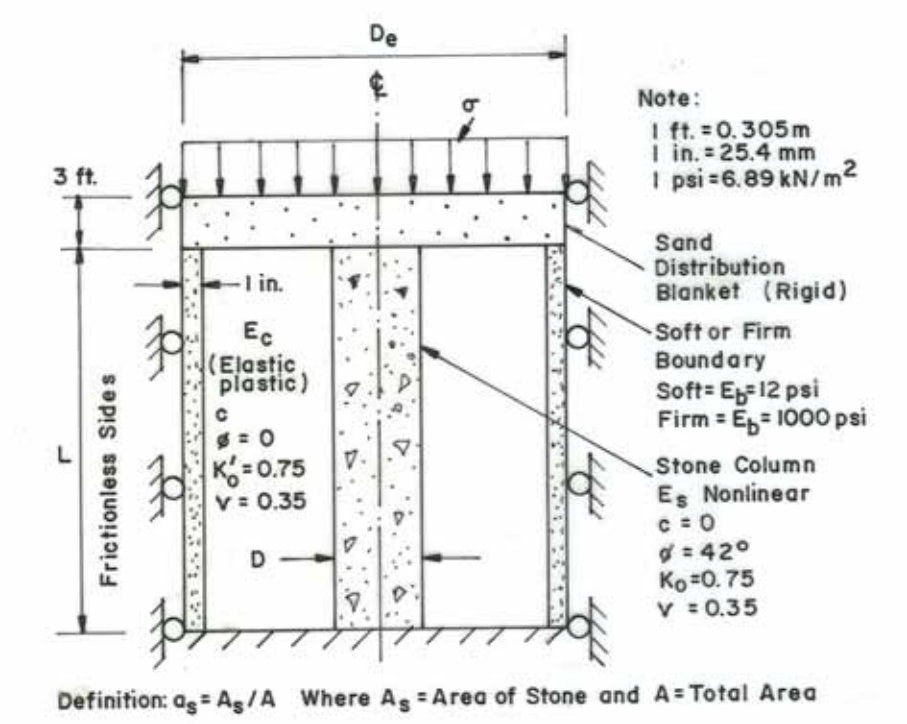

Figure 2.26 Notation used in unit cell nonlinear solutions given in Figure 2.27

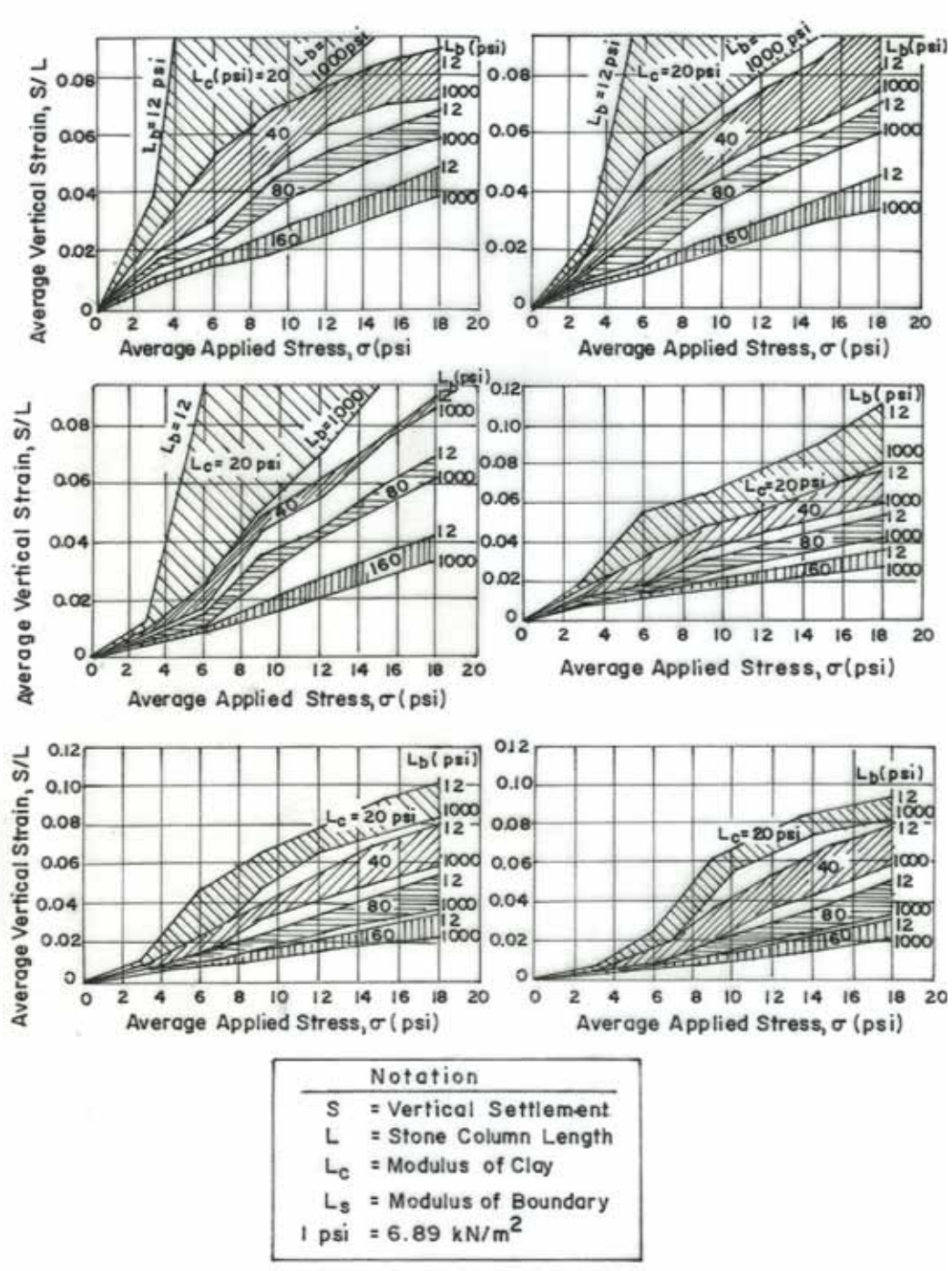

Figure 2.27 Nonlinear Finite Element unit cell settlement curves (Barksdale and Bachus, 1983).

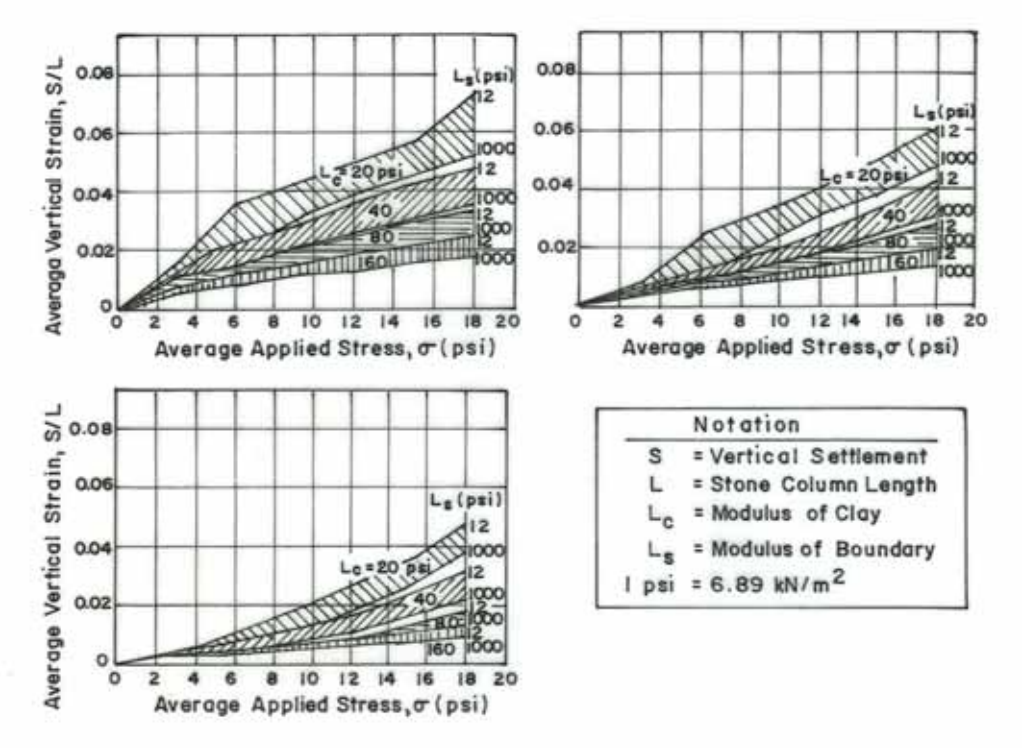

Figure 2.27 (Cont.)

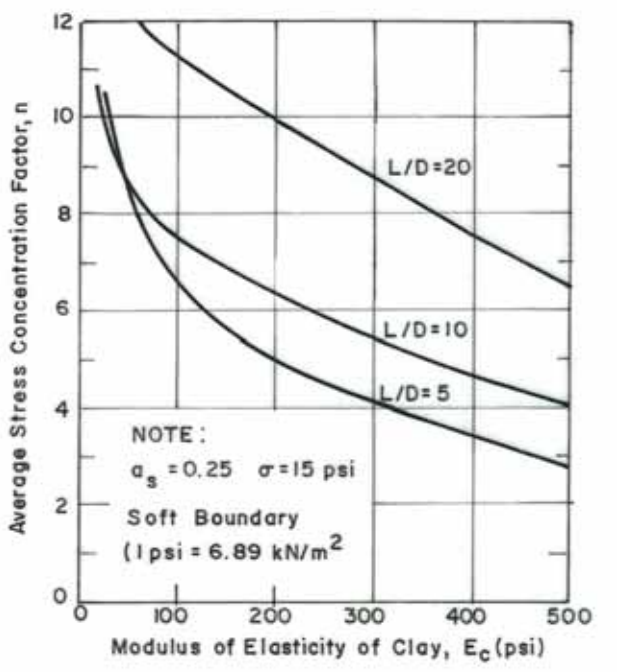

Figure 2.28 Variation of stress concentration with modular ratio-nonlinear analysis (Barksdale and Bachus, 1983)

2.3.5.7 Granular Wall Method

A simple way of estimating the improvement of the settlement behavior of a soft cohesive layer due to the presence of stone columns has presented by Van Impe and De Beer (1983) by considering the stone columns to deform, at their limit of equilibrium, at constant volume. The only parameters to be known are the geometry of the pattern of the stone columns, their diameter, the angle of shearing strength of the stone material, the oedometer modulus of the soft soil and its Poisson's ratio. They also presented a diagram for estimating effective vertical stress in the stone material.

In order to express the improvement on the settlement behavior of the soft layer reinforced with the stone columns, the following parameters are defined:

$$m = \frac{F_1}{F_{tot}} = \alpha \frac{\sigma'_{v,1}}{P_0} \qquad (2.31)$$

$$\beta = \frac{s_v}{s_{v,0}} \qquad (2.32)$$

where F_1 = the vertical load transferred to the stone column

F_{tot} = the total vertical load on the area a, b (Fig. 2.29).

S_v = the vertical settlement of the composite layer of soft cohesive soil and stone columns

$S_{v,0}$ = the vertical settlement of the natural soft layer without stone columns

In Figure 2.30, the relationship between m and α is given for different values of ϕ_1 and for chosen values of the parameters P_0/E and μ.

In the Figure 2.31, the β (settlement improvement factor) values as a function of α are given for some combination of P_0/E and μ and for different ϕ_1 values.

The vertical settlement of the composite layer of soft cohesive soil and stone columns, s_v is expressed as:

$$s_v = \beta H(1-\mu^2)\left[1-\frac{\mu^2}{1-\mu^2}\right]\frac{P_0}{E} \qquad (2.33)$$

where $\beta = f(a, b, \phi_s, \mu, P_0/E)$, obtained from Fig. 2.29

μ = Poisson's ratio of the soft soil

ϕ_1 = angle of shearing strength of the stone material

E = oedometer modulus of the soft soil

P_o = vertical stress

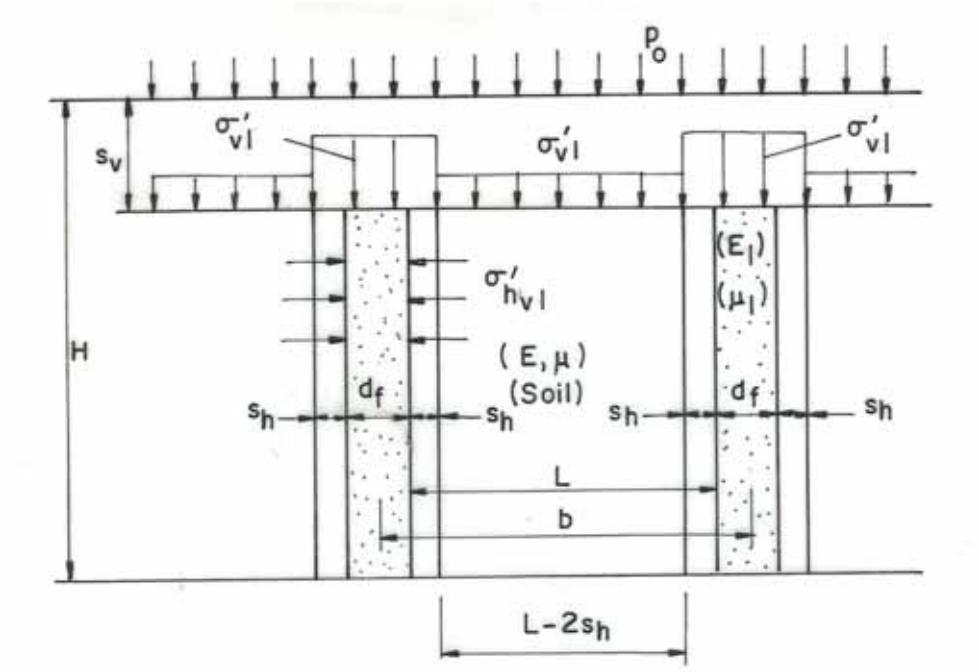

Figure 2.29 Definitions for Granular Wall Method
(Van Impe and De Beer, 1983)

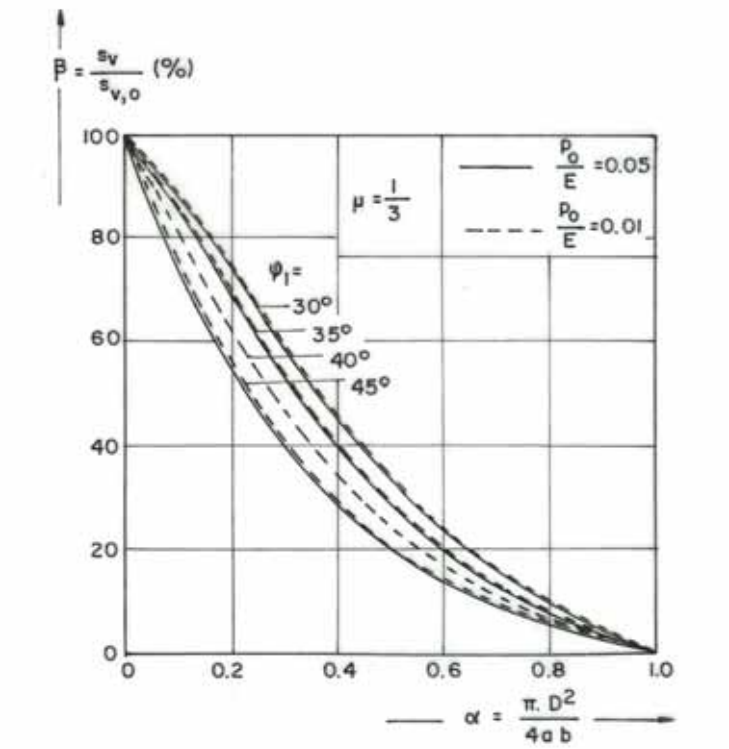

Figure 2.30 Stress distribution of stone columns (Van Impe and De Beer, 1983)

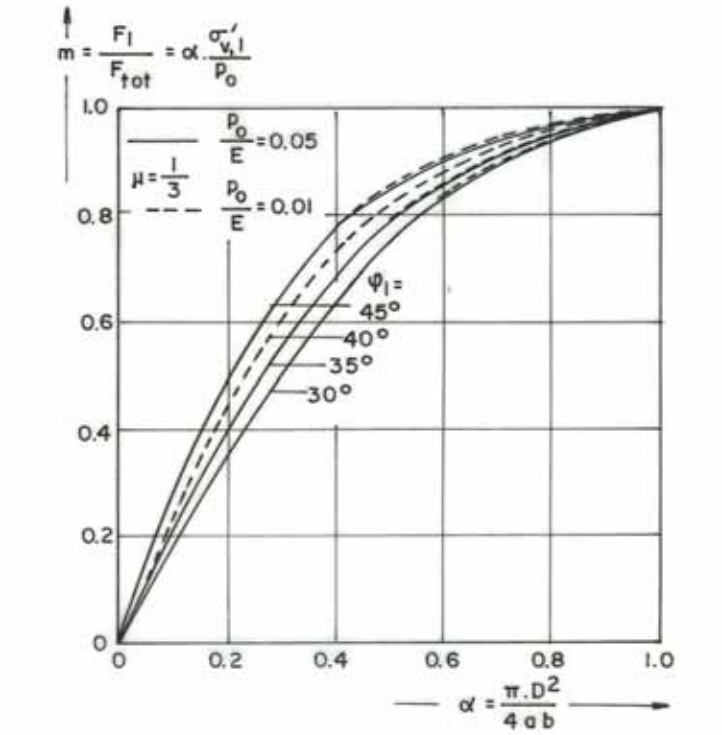

Figure 2.31 Improvement on the settlement behavior of the soft layer reinforced with the stone columns (Van Impe and De Beer, 1983)

2.3.5.8 Stress Distribution in Stone Column Groups

Knowledge of the stress distribution within the stone column improved soil is necessary to estimate the consolidation settlement.

The stress applied to a stone column group of limited size spreads out laterally with depth into the surrounding cohesive soil.

Aboshi et.al. (1979) have presented results of a finite element study comparing the vertical distribution of stress in ground reinforced with sand compaction piles to a homogeneous soil. In the reinforced ground the stiff columns extended to near the sides of the load, with the width of loading being equal to the depth of the reinforced layer as shown in Figure 2.32. The vertical stress in the cohesive soil just outside the edge of the reinforced soil is quite similar to the vertical stress outside the loading in the homogeneous soil.

The best approach at the present time for estimating the vertical stress distribution beneath loadings of limited size supported by stone column reinforced ground is to perform a finite element analysis.

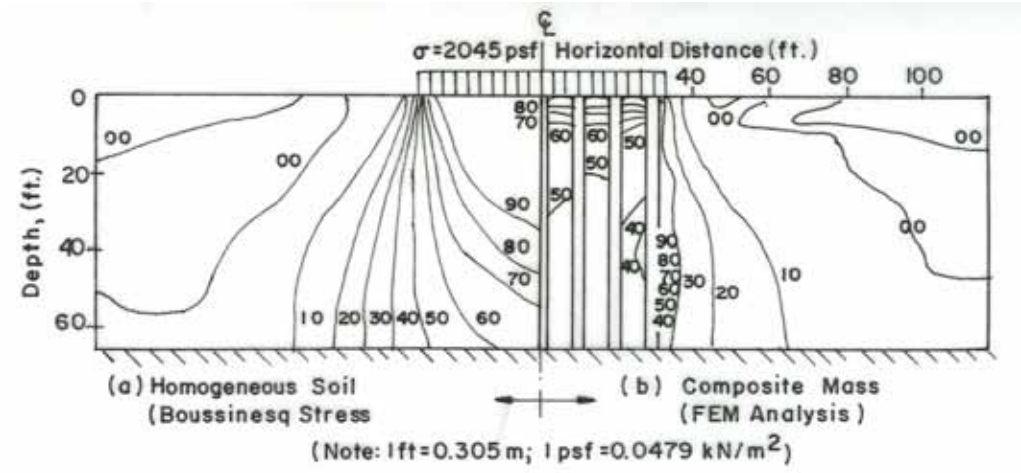

Figure 2.32 Comparison of Boussinesq stress distribution with finite element analysis of the composite mass-plain strain loading (Aboshi et.al. 1979)

2.3.5.9 Discussion for Settlement Predictions

One approach for predicting primary consolidation settlement of a ***wide group*** of stone columns resting on a firm stratum is to use elastic finite element theory for low compressibility soils (Fig. 2.24) or nonlinear finite element theory for high compressibility soils (Fig. 2.26 and Fig. 2.27). To predict long-term primary consolidation settlements the drained modulus of elasticity of the cohesive soil must be used. If drained triaxial tests have not been performed, the drained modulus of elasticity of the cohesive soil can be calculated from the results of one-dimensional consolidation test using:

$$E = \frac{(1+\mu)(1-2\mu)(1+e_0)\sigma_{va}}{0.435(1-\mu)C_c} \qquad (2.34)$$

where E = drained modulus of elasticity

e_0 = initial void ratio

C_c = compression index

μ = Poisson's ratio (drained)

σ_{VA} = average of initial and final stress state applied in the field (vertical stress)

The primary limitation in estimating E from Equation (2.34) is the ability to choose the correct value of Poisson's ratio, since E is very sensitive to the value of the μ used.

The modulus of elasticity of the stone column varies with the state of stress developed within the column both during and after construction. Because of confinement, long stone columns should therefore have a greater average modulus of elasticity than short columns. The modulus of elasticity E_s of the stone column can be calculated using

$$E_s = (\sigma_1 - \sigma_3)/\varepsilon_a \qquad (2.35)$$

where σ_1-σ_3 = deviator stress under the applied loading

σ_1 = vertical stress in stone column

σ_3 = lateral stress in stone column

ε_a = axial strain

In the absence of field load test or triaxial test results, the modulus of the stone can be estimated using the expression developed by Duncan and Chang (1970)

$$E_s = K\sigma_\theta^n \left[1 - \frac{(\sigma_1 - \sigma_3)R_f}{\left(\frac{2(c\cos\phi_s + \sigma_3 \sin\phi_s}{1 - \sin\phi_s} \right)} \right] \qquad (2.36)$$

where E_s = stress dependent secant modulus of the stone

K,n = constants defining the initial modulus of the stone (under low deviator stress)

c = cohesion of the stone (normally taken as zero)

ϕ_S = angle of internal friction of the stone

R_f = failure ratio

$\sigma_\theta = \sigma_1+\sigma_2+\sigma_3$

In the absence of specific test data, the following constants can be used for soft clays (Barksdale and Bachus, 1983): K=88.6, n=1.14, R_f = 0.86, c=0, and typically $\phi_s = 42^0$ to 45^0 where σ_θ and E_s are in psi.

Both the incremental and elastic methods require the modulus of elasticity E_s of the stone column. By back-calculation using measured field settlements, many researchers determined E_s between 30 MPa to 58 MPa. for vibro-replacement stone columns. For rammed stone columns Datye (1982) found by back calculation from measured settlements that E_s = 48 MPa.

For stone column groups less than about 20 to 40 columns (***limited groups***) the methods for estimating settlement using the unit cell idealization are overly conservative (Barksdale and Bachus, 1983). In groups of limited size, the vertical stress spreads outward from the stone column and decreases with depth. This reduction in stress can be readily considered in the equilibrium, incremental and finite element methods.

The approximate elastic solution for pile groups given by Poulos and Mattes (1974) has also been used for predicting settlements of small groups (Datye, 1982). Figure 2.33 shows a comparison between observed group settlements and the bounds for typical geometries and material properties used in the Poulos (1974) theory. The linear elastic theory developed in this study, which uses the unit cell idealization to model an infinite group of stone columns, assumes low compressibility soil having modular ratio of 10, is also shown on the figure.

The theories reasonably bound the limited number of measured group settlements. Of practical importance is the finding that a three-column group settles twice as much as a single pile and a seven-column group three times as much. Barksdale and Bachus (1983) states that using his interaction curves, Balaam predicted a settlement ratio of about 1.8 compared to the measured value of 3 for the seven-column group described by Datye and Nagaraju (1975); the stone columns were constructed by the ramming technique. Balaam also underpredicted group settlements by about 25% for a three-column model group using his interaction factors.

The settlements of a ten-column group may be as much as 3 to 4 times or more than of a single pile. Therefore, similarly to a load test performed on a conventional pile, group settlements are appreciably greater than indicated from the results of a single stone column load test. If load tests are performed on single columns or small groups, the results should be extrapolated to consider settlement of the group using Figure 2.33 for a preliminary estimate.

Finally different methods discussed so far for estimating the settlement of the composite ground are summarized in Table 2.6.

Figure 2.34 shows the relationships between the settlement reduction ratio and the aforementioned parameters based on different methods together with the results from the work of Bergado and Lam (1987) on soft Bangkok clay.

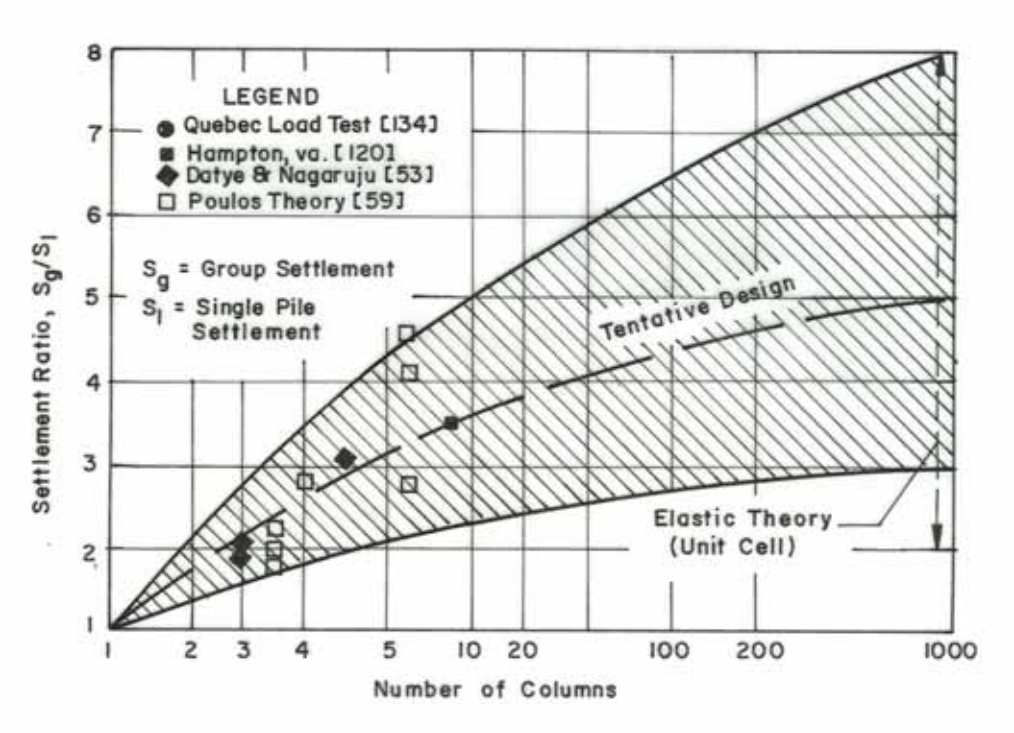

Figure 2.33 Group settlement as a function of number of stone columns: s = 2D (Barksdale and Bachus, 1983)

Table 2.6 Estimation of settlement of composite ground (Bergado et. al, 1994)

Method	Contents	References
Equilibrium method	$S_t = m_v(\mu_c\sigma)H$ $\mu_c = \frac{1}{1+(n-1)a_s}$	Aboshi et. al. (1979)
Priebe method	$\frac{1}{\mu_c} = 1 + a_s\left[\frac{1/2 + f(\mu, a_s)}{(K_A)_s f(\mu, a_s)} - 1\right]$ $f(\mu, a_s) = \left[\frac{1-\mu^2}{1-\mu-2\mu^2}\right]\left[\frac{(1-2\mu)(1-a_s)}{1-2\mu+a_s}\right] (K_A)_s = \tan^2\left(45^0 - \frac{\phi_s}{2}\right)$	Priebe (1976)
Granular wall method	$S = \beta H(1-\mu^2)\left(1 - \frac{\mu^2}{1-\mu^2}\right)\frac{P_0}{E}$ $\beta = f(a, b, \phi_1, \mu, P_0/E)$	Van Impe and De Beer (1983)
Incremental method	$\varepsilon_v = (1-a_s)\frac{C_c}{1+e_0}\log_{10}\left[\frac{(P_0)_{vc} + \Delta P}{(P_0)_{vc}}\right]$ $\Delta P = \frac{(\Delta P)^*_{vc}}{1+2K_0}[1 + K + K_o(K \text{ if } K > 1), (1 \text{ if } K \le 1)]$ $K = K_0 + \frac{1}{\varepsilon_v}\left[\sqrt{\frac{1}{1-\varepsilon_v}} - 1\right]\frac{\sqrt{a_s}}{1-\sqrt{a_s}}$	Goughnour and Bayuk (1979b) Goughnour (1983)
	$(\Delta P)^*_{vc} = \frac{(\Delta P)^*_v + (P_0)_{vc}a_s - K_0(P_0)_{vc}a_s\tan^2(45+\phi_s/2)}{KFa_s\tan^2(45+\phi_s/2)}$	Baumann and Bauer (1974)

Table 2.6 Cont.

Incremental method	$R_p = \dfrac{\varepsilon_v}{\dfrac{C_c}{1+e_0}\log_{10}\left[\dfrac{(P_0)_{vc}+(\Delta P)_v^*}{(P_0)_{vc}}\right]}$	Hughes et.al. (1975)
Finite element method	$\{K_E\}\{\Delta\sigma^{(m-1)}\} = \left(\{\Delta F_E\}+\left[K_c^{(m)}\right]\{\Delta\sigma^{(m)}\}+\{\Delta F_{DN}^{(m)}\}\right)$	Balaam and Poulus (1983)

Note :

$(K_A)_s$ = active earth pressure coefficient of sand pile
ε_v = vertical strain (same for stone and clay)
$(P_0)_{vc}$ =initial vertical stress in clay
$(\Delta P)_{vc}^*$ = effective vertical stress increase in the clay averaged over the horizontal projected area of unit cell
$(\Delta P)_v^*$ = effective vertical stress increase averaged over horizontal projected area of unit cell.
K = earth pressure coefficient applying to the load increments.
R_p =settlement reduction factor
$[K_E]$= elastic stiffness matrix
ΔF_E = vector of incremental nodal forces due to applied tractions
ΔF_{DN} = vector of incremental nodal forces at the dual nodes along the pile clay interface

refer to text for other notations

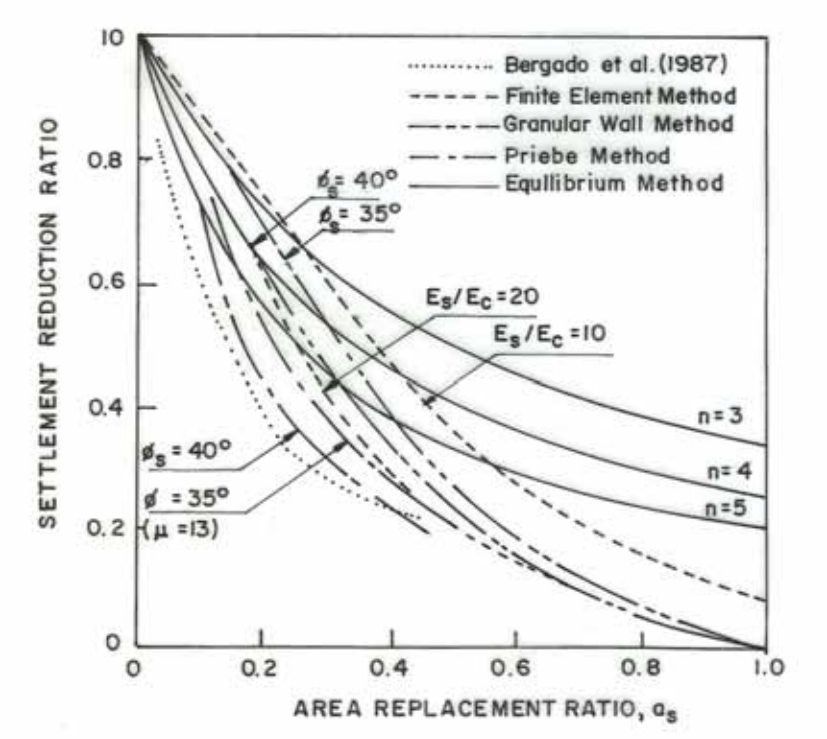

Figure 2.34 Comparison of estimating settlement reduction of improved ground (Bergado et. al., 1994)

2.3.5.10 Rate of Primary Consolidation Settlement

Stone columns act as similarly to sand drains in decreasing the distance which water has to flow in the radial direction for primary consolidation to occur. As a result installation of stone columns can decrease the time required for primary consolidation. Under these conditions, the presence of stone columns will greatly accelerate the gain in shear strength of the cohesive soil as primary consolidation occurs. Time rate of primary consolidation settlement should be estimated using the sand drain consolidation theory.

The horizontal permeability of many strata in which stone columns are constructed is likely to be 3 to 5 times or more the vertical permeability.

In constructing stone columns a zone of soil adjacent to the column becomes smeared. Further, the soil immediately adjacent to the stone column is disturbed, and soil may intrude into the pores of the stone near the periphery. These factors reduce the permeability of a zone around the outside of the stone column, and hence reduce its effectiveness in draining water radially. The combined effects of smear, disturbance, and intrusion are generally simply referred to as "*smear*". In predicting time rate of settlement, the effects of smear can be correctly handled using a reduced drain diameter.

Goughnour and Bayuk (1979a) have performed a comprehensive analysis of the results of the Hampton, Virginia load tests on stone columns. Assuming the horizontal permeability to be 3 times the vertical permeability, a smear factor of 2.5 was found to give a good approximation of the measured time rate of settlement. A smear factor of 2.5 is equivalent to dividing the actual stone column radius by about 18.

An analysis of the Jourdan Road load test results (Barksdale and Bachus, 1983) suggested that the smear factor was probably less than 0.6, which corresponds to using ½ the radius of the stone columns.

In the absence of other data on the effect of smear, a reduction in diameter of from 1/2 to 1/15 of the actual diameter is tentatively recommended by Barksdale and Bachus (1983).

2.3.5.11 Secondary Compression Settlement

Secondary settlement, equal to or even greater than primary consolidation settlement, can occur in highly organic soils and some soft clays; important secondary settlement can also occur in highly micaceous soils. Highly organic soils and soft clays are likely candidates for reinforcement with stone columns

to support embankment loads. Secondary compression settlement will therefore be an important consideration in many stone column projects.
Neither stone columns nor sand drains accelerate the time for secondary settlement. For sites where secondary settlement is important, consideration should be given to surcharge loading.

2.3.6 Slope Stability Analysis of the Composite Ground

General stability of the earth mass is often a serious problem when embankments are constructed over soft underlying soils. Use of stone columns to improve the underlying soft soil is one alternative for increasing the factor of safety to an acceptable level with respect to a general rotational or linear type stability failure. Stone columns are also used to increase the stability of existing slopes under-going landslide problems.

The method of stability analysis on a composite ground is performed exactly in the same manner as for a normal slope stability problem except that stress concentration is considered. When circular rotational failure is expected, the Simplified Bishop Method of Slices is recommended. Stability analyses are usually carried out with the implementation of computer programs.

Three general techniques that can be used to analyze the stability of stone column reinforced ground are described in this section.

2.3.6.1 Profile Method

In the profile method, each row of the stone columns is converted in to an equivalent, continuous strip with width, w. The continuous strips have the same volume of stone as the tributary stone columns as shown in Figure 2.35. Each

strip of stone and soil is then analyzed using its actual geometry and material properties.

For an economical design, the stress concentration developed in the piles must be taken into consideration (Bergado et.al. 1994). The stress concentration in the stone column results in an increase in resisting shear force. In computer analysis, the effects of stress concentration can be handled by placing thin, fictitious strips of soil above the foundation soil and stone columns at the embankment interface (Fig. 2.35). The weight of the fictitious of soil placed above the stone column is relatively large to cause the desired stress concentration when added to stress caused by the embankment. The weight of the fictitious soil placed above the in situ soil must be negative to give proper reduction in stress when added to that caused by ht embankment. The fictitious strips placed above the in situ soil and stone piles would have no shear strength and their weights are respectively expressed as:

$$\gamma_f^c = \frac{(\mu_c - 1)\gamma_1 H'}{\bar{T}} \qquad (2.37)$$

$$\gamma_f^s = \frac{(\mu_s - 1)\gamma_1 H'}{\bar{T}} \qquad (2.38)$$

where μ_c and μ_s are the stress concentration factors of the in situ soil and stone column, respectively, and the other terms are defined as indicated in Figure 2.35.

It must be noted that limits should be imposed on the radius and/or grid size of circle centers so that critical circle should not be controlled by the weak, fictitious interface layer (Barksdale and Bachus, 1983).

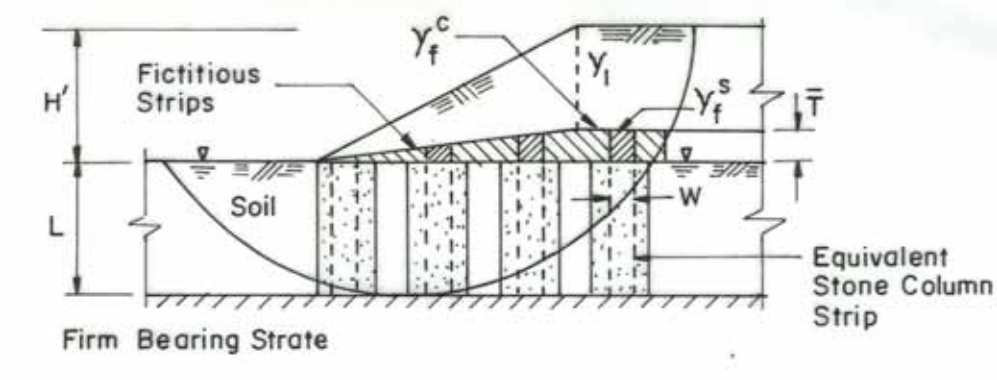

Figure 2.35 Stone column strip idealization and fictitious soil layer for slope stability analysis (Barksdale and Bachus, 1983).

2.3.6.2 Average Shear Strength Method

The average shear strength method is widely used in stability analysis for sand compaction piles (Aboshi et. al. 1979, Barksdale and Takefumi, 1990). The method considers the weighted average material properties of the materials within the unit cell (Fig. 2.36). The soil having the fictitious weighted material properties is than used in stability analysis. Since average properties can be readily calculated, this approach is appealing for both hand and computer calculations. However, average properties cannot be generally used in standard computer programs when stress concentration in stone columns is considered in the analysis (Bergado et.al. 1994).

When stress concentration is considered, hand calculation is preferred. The effective stresses in the stone column and the total stress surrounding soil are respectively expressed as:

$$\bar{\sigma}_z^s = \bar{\gamma}_s z + \bar{\sigma}\mu_c \qquad (2.39)$$

$$\sigma_z^c = \gamma_c z + \bar{\sigma}\mu_c \qquad (2.40)$$

where $\bar{\gamma}_s$ = buoyant weight of the stone

γ_c = saturated unit weight of the surrounding soil,

z = depth below the ground surface.

σ = stress due to embankment loading

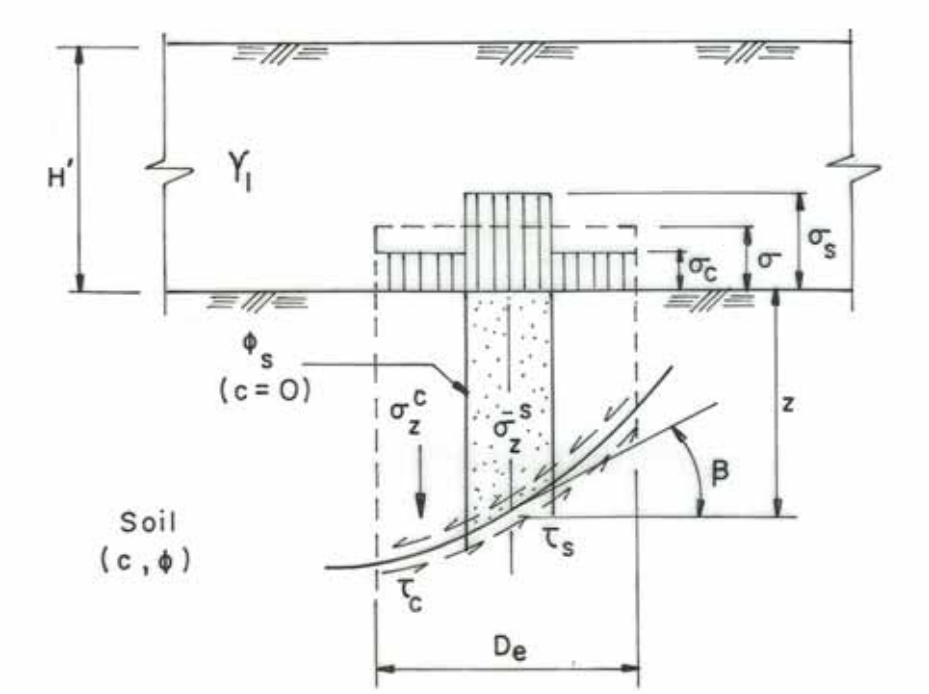

Figure 2.36 Average stress method of stability analysis
(Barksdale and Bachus, 1983)

The shear strength of the stone column and the surrounding cohesive soil are:

$$\tau_s = (\bar{\sigma}_z^s \cos^2 \beta) \tan \phi_s \qquad (2.41)$$

$$\tau_c = c + (\sigma_z^c \cos^2 \beta) \tan \phi_c \qquad (2.42)$$

where β = inclination of the shear surface with respect to the horizontal

The average weighted shear strength within the area tributary to the stone column is:

$$\tau = (1 - a_s)\tau_c + a_s\tau_s \tag{2.43}$$

The weighted average unit weight within the composite ground used in calculating the driving moment is:

$$\gamma_{avg} = \gamma_s a_s + \gamma_c a_c \tag{2.44}$$

where γ_s and γ_c are the saturated unit weight of the stone and the in situ soil respectively. In this approach, the weighted shear strength and unit weight are calculated for each row of stone columns and then used in conventional hand calculation.

When stress concentration is not considered, as in the case of some landslide problems, a standard computer analysis employing average strengths and unit weights can be performed using a conventional computer program. Neglecting the cohesion in the granular materials and the stress concentration, the shear strength parameters for use in the average shear strength method are:

$$c_{avg} = c(a_s) \tag{2.45}$$

$$(\tan\phi)_{avg} = \frac{\bar{\gamma}_s a_s \tan\phi_s + \gamma_c a_c \tan\phi_c}{\bar{\gamma}_{avg}} \tag{2.46}$$

where $\bar{\gamma}_{avg}$ is given by Equation 2.44 using buoyant weight for $\bar{\gamma}_s$ and saturated weight for γ_c.

Di Maggio (1978) (referring Bergado et.al. 1994) reported that the use of $(\tan\phi)_{avg}$ based just on the area ratio is not correct as can be demonstrated by considering the case when ϕ_c =0. If averages based on the area were used, then:

$$(\tan\phi)_{avg} = a_s \tan\phi_s \qquad (2.47)$$

The above expression would be appropriate to use if $\bar{\gamma}_{avg} = \bar{\gamma}_s$, but incorrect if $\bar{\gamma}_{avg}$ is used to calculate the driving moment.

2.3.6.3 Lumped Moment Method

The lumped moment method can be used to determine the safety factor of selected trial circles by either hand calculation or with the aid of computer. Following this approach the driving moment M_d and resisting moment M_r are calculated for the condition of no-ground improvement with stone columns. The correct excess resisting moment ΔM_r and driving moment ΔM_d due to the stone columns are then added to the previously calculated moments M_r and M_d, respectively. The safety factor of the improved ground is then calculated by

$$SF = \frac{(M_r + \Delta M_r)}{(M_d + \Delta M_d)} \qquad (2.48)$$

In general this approach is most suited for hand calculation. The approach can also be used with computer programs, which permit adding in ΔM_r and ΔM_d that could be calculated by hand.

2.3.7 Increase In Shear Strength Due to Consolidation

The shear strength of a soft cohesive soil increase during and following construction of an embankment, tank, or foundation on soft cohesive soils. The additional stress due to construction results in an increase in pore pressure causing consolidation accompanied by an increase in shear strength.

For a cohesive soil having a linear increase in shear strength with effective stress, the increase in undrained shear strength Δc_t with time due to consolidation can be expressed for stone column improved ground as

$$\Delta c_t = K_1(\sigma\mu_c)[U(t)] \qquad (2.49)$$

where Δc_t = increase in shear strength at time t of the clay due to consolidation

σ = average increase in vertical stress in the unit cell on the shear surface due to the applied loading

μ_c = stress concentration factor in the clay

U (t) = degree of consolidation of the clay at time t

2.4 Field Load Tests on Stone Columns

Field load tests are an important part of the overall design verification for stone columns just as conventional pile load tests are commonly used in practice. Load tests are performed to evaluate the (1) ultimate bearing capacity, (2) settlement characteristics, (3) shear strength of the stone column or the composite stone column-soil strength, and (4) to verify the adequacy of the overall construction process.

For shear strength characteristics of the stone column, i.e. angle of internal friction of stone column and/or composite shear behavior, double ring direct shear test should be performed in the field.

To evaluate ultimate bearing capacity of stone column reinforced ground, short-term, rapid load tests are recommended (Barksdale and Bachus, 1983). The load test program should be planned to permit testing to failure rather than going to 1.5 or 2.0 times the design load. In general more information would be obtained from testing a single stone column to failure than testing a group of two columns to 1.5 times the design load.

Model test studies indicate that the method of applying the loading influences the mode of failure and hence the ultimate capacity of a stone column. In general, the loading should not be applied to just the area of the stone column; the effect of lateral confinement and soil strength should also be included in test by using a larger plate.

Many potential stone column applications such as bridge bents and abutments limit the design settlement to relatively low levels. For such applications settlement considerations will generally restrict the design load per column to values well below ultimate. In cohesionless soils, the immediate settlement, which can be defined by a short-term load test, will be most important. In cohesive soils, however, primary and secondary settlements will be much larger than the immediate settlement. Therefore, long-term load test are required to define settlement characteristics; rapid load tests would only indicate ultimate bearing capacity. In general, dead loading is most practical for long term test. The design load should be left on long enough to achieve at least 80 to 90 percent of primary consolidation. The load test should performed using as many stone columns as possible; more stone columns will lead to a more reliable settlement estimate. Twenty-three stone columns, for example, were used beneath the load at Hampton, Virginia and 100 percent of the primary settlement was achieved in about 4 months (Goughnour and Bayuk, 1979).

2.5 Selected Stone Column Case Histories

2.5.1 Expansion of Regional Hospital, Atlanta, Georgia (Lawton et.al., 1994)

In an expansion to a regional hospital in Atlanta, Georgia, two major structural towers were added to provide additional office space and hospital rooms. The idealized geological profiles for south tower is 3.50m fine sandy micaceous silt at the top with an average N=10 and E_d = 7.66 MPa, and 1.5m fine sandy micaceous silt with an average N=22 and E_d = 16.9 MPa, underlain by weathered rock. The rectangularly linear aggregate piers with widths of 0.61m were installed by excavating a trench about 1.83m below the bearing elevation and compressing the soils at the bottom of the trench to a depth about 0.15m, resulting in a total height of the short aggregate piers of about 1.98m. To estimate the settlement of a shallow foundation bearing on an aggregate pier-reinforced soil, the subgrade is divided into an upper zone (UZ) and a lower zone (LZ). The upper zone is assumed to consist of the composite soil comprised of the aggregate piers and matrix soil, plus the zone of appreciable densification and prestressing immediately underlying the pier, which is estimated to be equal to the width of one pier. For this case, piers were 1.98m high and 0.61m wide, with the height of the upper zone equal to 2.59m. The lower zone consists of all strata beneath the upper zone. Settlements are calculated individually for the UZ and LZ, with the two values combined to yield an estimate of the total settlement. Assuming that the footing is perfectly rigid and a subgrade modulus approach, the following equations apply:

σ_p = bearing stress applied to aggregate piers = $\sigma R_s / (a_s * R_s - a_s + 1)$
σ_m = bearing stress applied to matrix soil
S_{uz} = settlement of the UZ = $\sigma_p / k_p = \sigma_m / k_m$

where σ = average design bearing pressure = Q/A; R_s = subgrade modulus ratio = k_p/k_m; a_s = area ratio = A_p/A; Q = vertical design load at the bearing level; A

= total area of the footing; A_p = total area of aggregate piers supporting footing; k_m = subgrade modulus for matrix soil, k_p = subgrade modulus of aggregate piers.

The authors suggested that values of moduli for the aggregate piers can be determined either by static load tests on individual piers or by estimation from previously performed static load tests within similar soil conditions, although this is considered conservative since static load tests does not consider the beneficial effect of confining pressures of matrix soil. Subgrade moduli for the matrix soils are either determined from static load tests or estimated from boring data. In this project, authors were estimated k_p, as 76 MN/m3 and k_m as 5.8 MN/m3 from the results of previously performed static load tests. Using R_s = 13.3 and these values for k_p and k_m, as well as the values for $_s$ and a_s, calculated values for σ_p, σ_m, and S_{uz} for both footings are summarized in Table 2.7

The procedure used by the authors to estimate vertical stress increase at the UZ-LZ interface is a modification of the 2:1 method, and involves the use of engineering judgment. For estimates of the lower zones settlements (S_{LZ}) for this project, a stress dissipation slope through the UZ of 1.67:1 is used. Bowles' (1988) modified elastic theory method is used to estimate settlements of lower zone and to estimate settlements for comparable footings without aggregate piers (S_{UN}). The results of these calculations are summarized in Table 2.7. The minimum value of predicted settlement with aggregate piers is slightly larger than or equal to the maximum value of actual settlement, suggesting that the settlement method used by the authors gives reasonable estimates.

Table 2.7 Predicted and Actual Settlements of South Tower of Regional Hospital, Atlanta, Georgia

Loacation and Found. Type	Dimensions of Foundation	σ kPa	a_s	σ_p kPa	σ_m kPa	S_{UZ} mm	Predicted Settlement (mm)				Predicted Sett. (mm) $S_{UZ}+S_{LZ}$	Actual Settlement (mm)
							S_{LZ} (mm)		S_{UN} (mm)			
							Schmert.	Bowles	Schmert.	Bowles		
ST, square ftg	2.74 m	225	0.35	563	42	7.4	0.8	4.6	43.2	40.4	8-12	<6
ST, rect. ftg.	3.66x5.03m	239	0.33	630	47	8.3	1.5	7.9	51.8	58.2	10-16	<10

2.5.2 Mississippi Air National Guard Hangar, Meridian, Mississippi

A hangar was built at an Air National Guard field in Meridian, Mississippi. Design uplift forces from wind loads were as great as 1,156 kN per column (Lawton et.al, 1994).

The authors have successfully used aggregate piers as hold-down anchors during compressive static load tests on aggregate piers, with two significant characteristics observed during tests conducted in silt sands and sandy silts: (1) The uplift capacity of an aggregate pier was significant; and (2) in 31 of 32 piers where uplift deflections were measured, the rebound upon removal of the load was 100%. These results suggest that the uplift loads were transferred primarily as shear stress along the aggregate pier-matrix soil interface, and that stresses were within the elastic range for the interfacial materials. The maximum uplift forces per aggregate pier in these tests were typically between 200 to 214 kN, with measured uplift deflections mostly less than 25 mm and always less than 51 mm, and in no cases did failure occur. The results from uplift tests in sandy clays have shown less than 100% rebound, indicating some plastic soil behavior.

The key hangar is located within the Coastal Plain geological region. The subsoil profile at the location of the uplift load test consisted of 1.4m of medium dense, well-graded sand fill overlying a zone of loose, very clayey sand. The ground water was 0.3m above the bottom of the pier excavation, at a depth of about 1.8m.

Rectangularly prismatic aggregate piers were used. The test pier was 1.8m high, 0.61m wide and 1.5m long, with top of the pier at a depth of 0.3m. The uplift loads were transferred to the bottom of the pier by steel tension rods located along the perimeter of the pier, which were attached to a continuous steel plate at the bottom of the pier.

The load test was performed in accordance with ASTM D1194. The deflection at the maximum load of 267 kN, was 23mm, and the load-deflection curve is

fairly linear. In addition, 100% rebound was measured upon released of the load, indicating that the soil behaved elastically within the range of stresses applied in the test. From the results of this load test, a design capacity of 178 kN per aggregate pier was approved.

2.5.3 A three-story Wood Frame Assisted Care Facility Structure in Sumner, Washington

In 1997, a three-story wood framed assisted care facility structure was planned for construction in the city of Sumner, Washington on a site containing peat soils. CPTs taken to depths of 18.3m located no reliable data capable of supporting deep foundations to those depths (Fox and Edil, 2000). Subsurface conditions encountered consisted of a 0.4m zone of top soil, underlain by soft layers of organic silts interbedded with layers of peat extending to depths ranging between 2.3m to 5.3m below grade. The organic silts and peat zones were underlain by loose to firm sand and soft to firm sandy silt with some thin lenses of peat. Perched groundwater was found at a depth of about 1.5m.

This structure, with lightly bearing walls and columns, needed to be supported on a foundation system capable of limiting settlements to approximately 25mm. Driven piles would have to extend to depths greater than 18.3m. Alternative support methods of over excavation and replacement of the soft organic silts and peat, and of traditional vibro-replacement stone columns, were rejected because of groundwater problems and anticipated poor reinforcement, respectively.

As a result, shallow foundations designed with a maximum allowable bearing pressure of 215 kN/m^2 and supported by a system of Geopier elements, were designed and constructed. The aggregate piers were made by drilling 762mm diameter holes to depths of 5 m from ground surface and 4 m below footing bottoms. A small volume of crushed stone without fines, maximum diameter 50mm, was placed at the bottom of each cavity. This aggregate was than

densified with a high energy impact rammer (not vibration energy), to form a bottom bulb. An undulated-sided pier shaft was formed in 300mm thick lifts using well-graded highway base course stone, that was again, highly densified by the ramming action of the beveled tamper head.

The piers are designed to improve the composite stiffness of the upper layer in which the footing-induced stresses are the highest, in order to control the long term settlements to meet design criteria of 25 mm. Settlement calculations were made using a two-zone method (described in the previous sections) , estimating settlement contributions from the Upper Zone (the aggregate pier-matrix soil zone) and from the underlying Lower Zone, and adding the two contributions together to provide an estimate of total settlements.

The Upper Zone analysis method uses a spring analogy and considers the stiff pier acting as a stiff spring, while the less stiff matrix soil acts as a soft spring (Lawton and Fox, 1994 and Lawton et.al. 1994). Estimates of settlement components from the Lower Zone soils were computed using conventional geotechnical settlement analysis methods that rely on estimating the degree of load spreading below the footing and estimating the compressibility of the soils. The analysis includes the assumption that vertical stress intensity within the Lower Zone is the same as that of a bare footing without the stiffened Upper Zone, using solutions for a footing supported by an elastic half space. This assumption is conservative because the presence of the stiff piers results in a stress concentration on the pier, and a more efficient stress transfer with depth below the footing bottoms than what would occur for conventional bare footings. This has been shown during full-scale pier-supported footing tests that were instrumented with pressure cells (Lawton, 1999).

Finally the authors concluded that aggregate piers, 4 to 7m long, replaced deep piles estimated to be on the order of 24 m or greater for the described project and settlements of supported footings for the structure were observed to be less than 25 mm.

CHAPTER III

SITE WORKS

3.1 Introduction

An appropriate site should have been found to study the behavior of the floating aggregate piers by full-scale field tests. Moreover, the existence of poor site conditions should have been suspected before beginning the subsurface investigation from local experience.

A site around Lake Eymir with poor soil conditions was found and the entrance of Lake Eymir was accepted as an appropriate test area to perform the study.

This chapter describes the proposed test project, the area covered by the project, the subsurface investigations performed at the site and the construction methods of aggregate piers. In short, all site works necessary to perform prior to tests is explained in this chapter.

3.2 Preparation of Test Site

The test area which is approximately 10mx30m is located at the left side of the main entrance of Lake Eymir.

In November 2000, a preliminary boring of 10.0m depth, SKT-1, was opened to make an initial prediction about soil profile. The results of SPT performed in this boring and laboratory testing on soil samples had indicated the soft soil profile.

Site works were initiated in June 2001, after a heavy winter period by cleaning the rushes covering the whole area. After all rushes had cleaned as shown in Figure 3.1 a working platform composed of stone blocks with finer fill material was compacted to provide safe working condition for heavy construction machines. These works can be seen on Figures 3.2 and 3.3.

Figure 3.1 Preparation of test area by cleaning rushes

Figure 3.2 Spreading of blocks at the base of working platform

Figure 3.3 Site view after completion of working platform

3.3 Subsurface Investigations

Site investigations included five boreholes and sampling, four CPT soundings, and SPT and laboratory testing.

Drilling works were initiated in November 2000 at the test site, with preliminary boring of 10m depth, named SKT-1. In June 2001, four additional investigation borings were opened, which are named as SK-1, SK2, SK-3 and SK-4. SK-1 of 8m depth was located at the left corner of the test site. 10m deep borehole, SK-2 was at the center of the test site. 11m deep borehole SK-3 was between SK-1 and SK-2 and SK-4 which is 13.5m deep was opened alongside o the preliminary boring, SKT-1. Location of the boreholes is given in Figure 3.4.

The borings were opened by a truck-mounted Mobile Drill. Temporary casings of NW (having outer diameter of 89mm and inner diameter of 76mm) types were used in the borings of whole depth during penetration (Figure 3.5). At each borehole, Standard Penetration Test was performed at every 1m intervals. Disturbed samples by SPT tests and undisturbed samples were taken. Since the soil profile is sandy clay at some depths, UD samples taken at those depths by Shelby tubes which have either insufficient length or were empty.

The ground water is located near at the surface.

Laboratory testing on the disturbed and undisturbed soil samples were performed at METU Soil Mechanics Laboratory. The results of these tests will be discussed in Chapter IV.

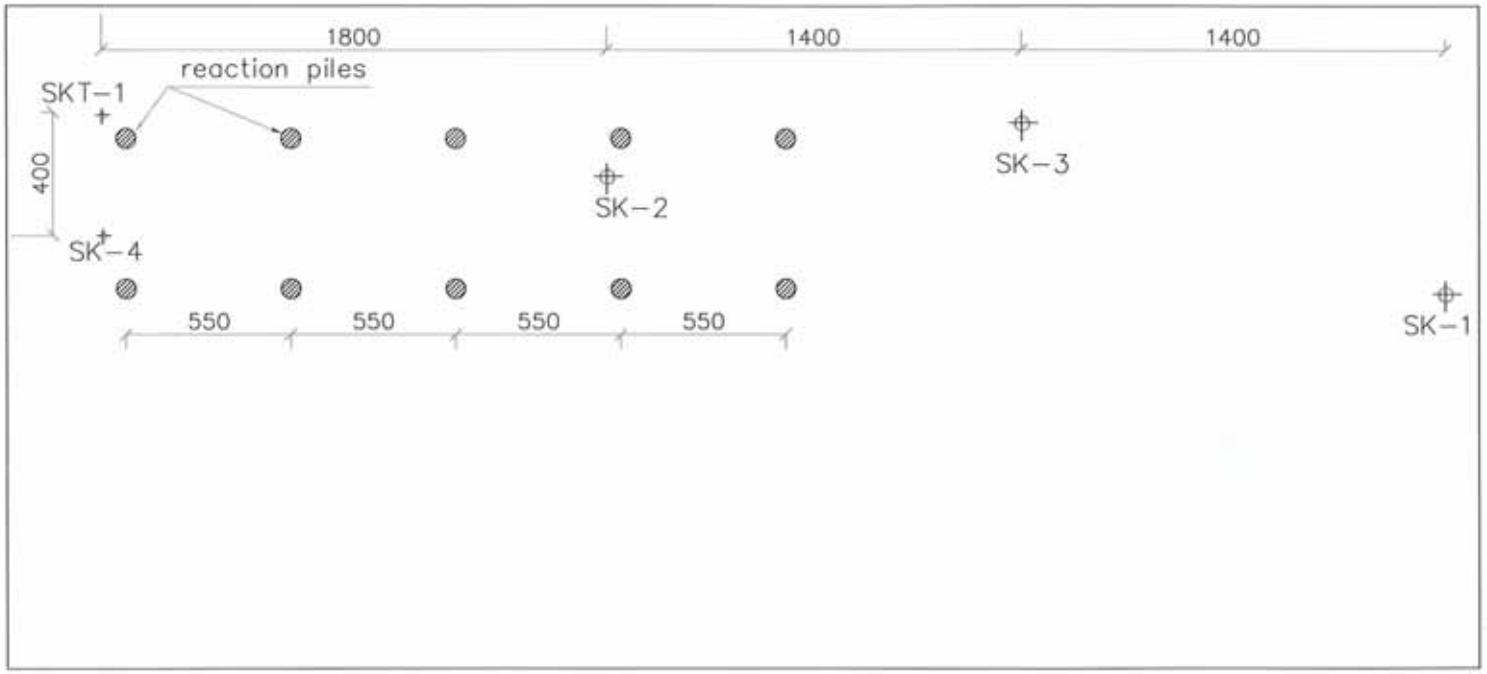

Figure 3.4 Location of boreholes and reaction piles

Figure 3.5 A view from boring works

3.4 Construction of Reaction Piles

Ten reinforced bored piles each of 12m in length and 65cm in diameter were constructed to be used as a reaction piles. They were bored using Casagrande B150 model hydraulic piling rig with using temporary casing to maintain stability. Longitudinal and transverse spacing of constructed bored piles were 5.50m and 5.0m respectively. A view from construction of reaction piles can be seen in Figure 3.6.

Figure 3.6 Construction of reaction piles with casing

As longitudinal and transverse reinforcement, 10Φ22 and ϕ10/20 were placed, respectively. Concreting is performed with tremie pipe and BS 20 type of concrete was used.

3.5 Construction of Aggregate Piers

3.5.1 Properties of Crushed Stone Used For Pier Backfill

Uniform, well-graded backfill material is obtained as a mixture of three types of crushed stone (30-60mm, 15-30mm, 7-15mm) with the ratio of 50%, 30% and 20%, respectively.

The crushed stones were stored at the site and mixed according to the aforementioned ratios with the help of loader as can be seen in Figure 3.7.

Samples were taken from the mixture to perform some laboratory tests to determine the gradation curve and compacted density of the backfill material. In Figure 3.8, the gradation range of the crushed stone used as column backfill is depicted. Compacted and loose densities of the backfill mixture were determined as 1.74 gr/cm^3 and 1.40 gr/cm^3, respectively.

Figure 3.7 Mixing operations of crushed stones at the site

3.5.2 Aggregate Pier Construction

In this study aggregate piers were constructed by using bored piling equipment. Thus the constructed piers are those known as rammed aggregate piers.

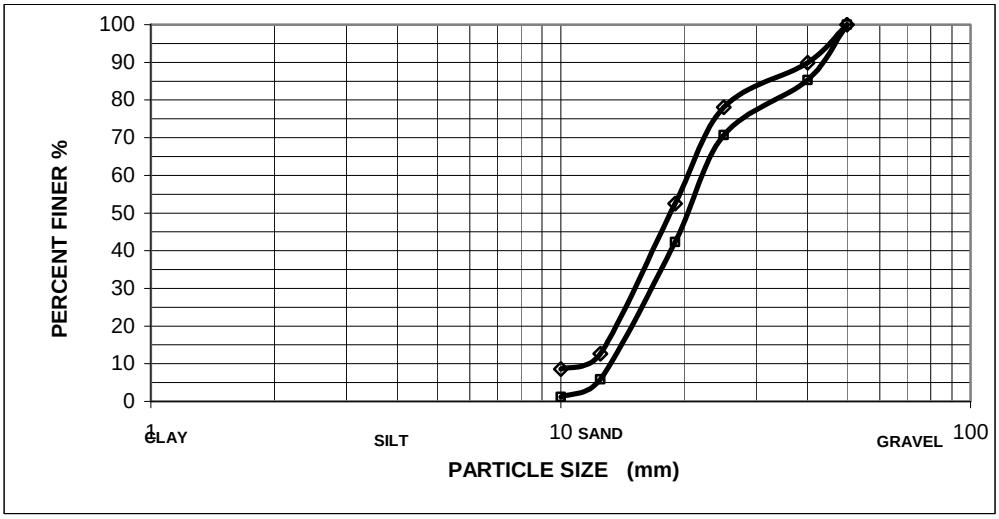

Figure 3.8 Gradation curves of the crushed stone used as a column backfill

Firstly, an open-ended casing with a diameter of 65cm was driven to a certain depth and then augering was performed. Subsequently, the casing was driven to further depths and then cleaned out by auger. This operation can be seen in Figure 3.9. This procedure was repeated until a specified depth was reached. Following this stage, the granular material was poured into the cased borehole in consecutive stages. First, 1.0 to1.5m thick layer was filled with granular material and compacted by dropping a weight of 1.5 tons from a height of 1.0m for 10 times. A view from filling the granular material into borehole and ramming operation can be seen in Figures 3.10 and 3.11, respectively. During first compaction, the casing was kept in place. Following the first compaction phase, the granular material was continued to pour for the next 1.0 to 1.5m thick layer. After filling operation casing was withdrawn partially and backfill was rammed to the specified set (10 blows from 1.0m height). It was ensured that bottom of the casing was at least 0.3m below the top of the rammed fill. These procedures were repeated until the full granular pile of specified length was reached (Figure 3.12). Figure 3.13 illustrates the method of execution of aggregate piers by piling rig.

Figure 3.9 Cleaning operation of borehole with auger

A total of 28 piles with a diameter of 65cm were installed by Casagrande B150E hydraulic piling rig with a spacing of 1.25m in a triangular pattern. The piles were grouped into 3 categories. In Group A, 7 piles, each of 3.0m in length were constructed as floating aggregate piers. Similarly Group B consisted of 7 floating aggregate piers, each of 5.0m in length. Whereas, Group C was a patch of 7 end bearing aggregate piers each of 8.0m in length. In addition to these three groups, there were 7 individual aggregate piers, 4 of which were 3.0m in length, 2 of which were 5.0m in length and remaining one was 8.0m long. Location of aggregate pier groups together with reaction piles and investigation bore holes is given in Figure 3.14. The plan view of completed aggregate pier groups can be seen in Figure 3.15.

Figure 3.10 Filling the granular material into the borehole

Figure 3.11 A view from ramming operation

Figure 3.12 A view from completion of aggregate pier

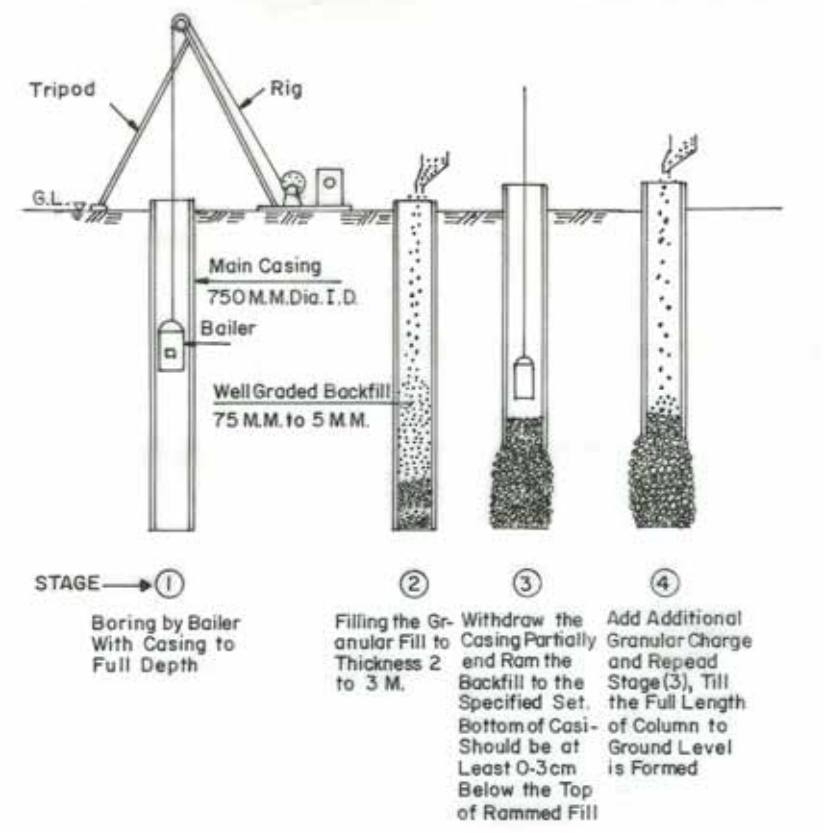

Figure 3.13 Method of execution of aggregate pier by piling rig

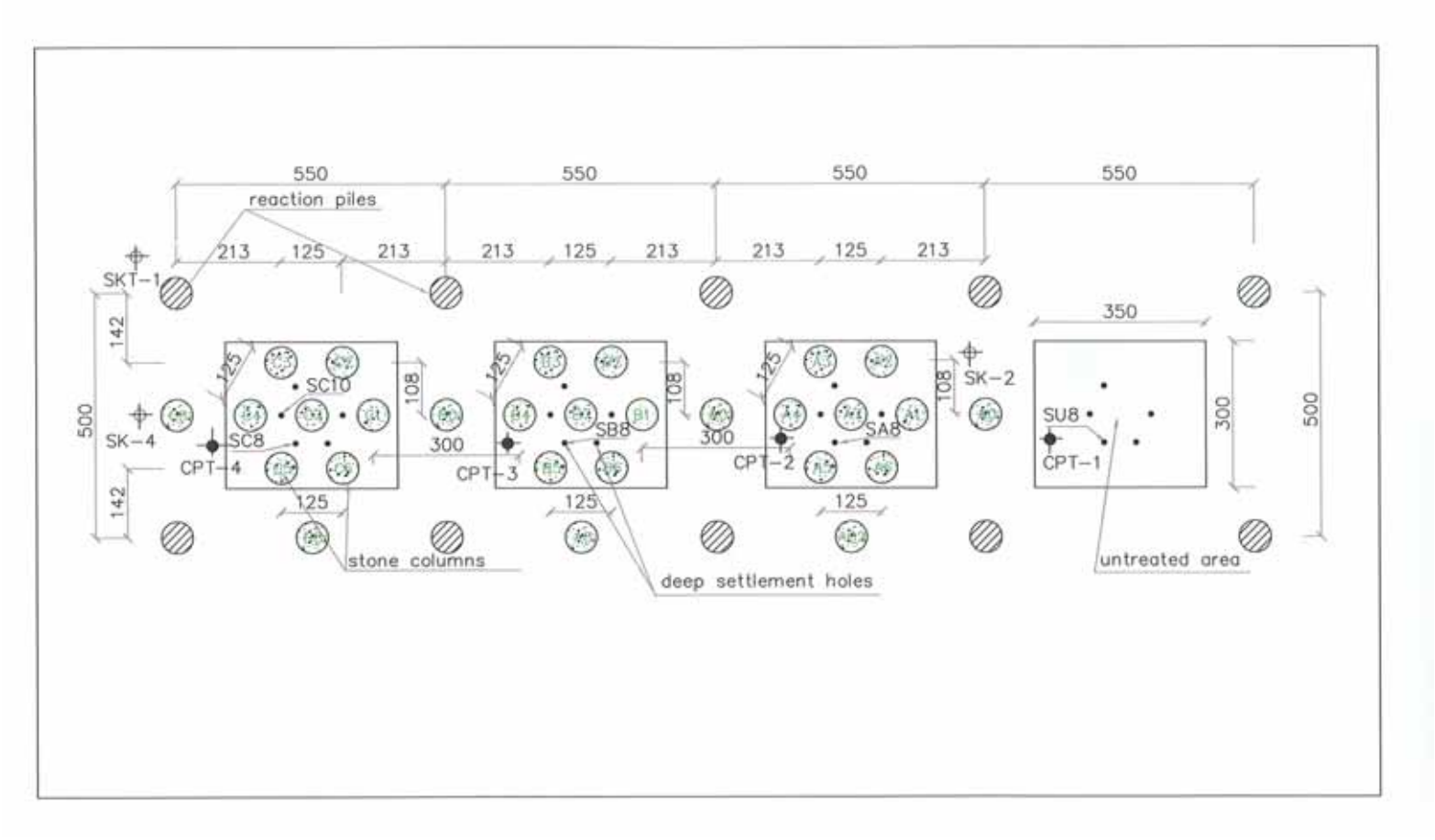

Figure 3.14 Location of aggregate piers together with reaction piles and investigation boreholes

Figure 3.15 The plan view of completed aggregate pier groups

3.6 Placing of Deep Settlement Plates

For each group of aggregate piers, five bore holes of 1.5m, 3m, 5m, 8m and 10m deep were opened with temporary casing in between aggregate piers. Then PVC tubes of 5cm in diameter were placed at each bore hole. A steel bar with a plate welded at the end, was used as a deep settlement plate. Three nails were also welded at the back side of the plate to stick it into soil. The deep settlement plates can be seen in Figure 3.16. After placing the deep settlement plates into the hole, the space between the PVC tube and the hole were filled with fine sand (Figure 3.17).

Figure 3.16 Deep settlement plates

Figure 3.17 Filling the space between PVC tube and bore hole with fine sand

3.7 Large Plate Load Test Apparatus

3.7.1 General

There were four number of reaction piles in each load test to provide adequate reactive capacity. Three test beams of sufficient size and strength were used to avoid excessive deflection under load with sufficient clearance between bottom flanges of the test beams and the top of the test pile group to provide the necessary bearing plates, hydraulic jack and load cell. It can be seen from the Figure 3.18 that all the reference beams and wires were independently supported with supports firmly embedded in the ground. They were sufficiently stiff to support the instrumentation and cross connected to provide additional rigidity.

Figure 3.18 Test arrangements for applying load

3.7.2 Loading Plate

Loading plate was a steel plate with dimensions of 300x350x5cm. It was stiffened with 5cm thick triangular steel plates to transfer the load through the edge of the plate and also to supply additional rigidity. These four additional steel plates were welded to the main loading plate and circular ring that is also welded to the main plate centrally. Schematic drawing of loading plate is given in Figure 3.19.

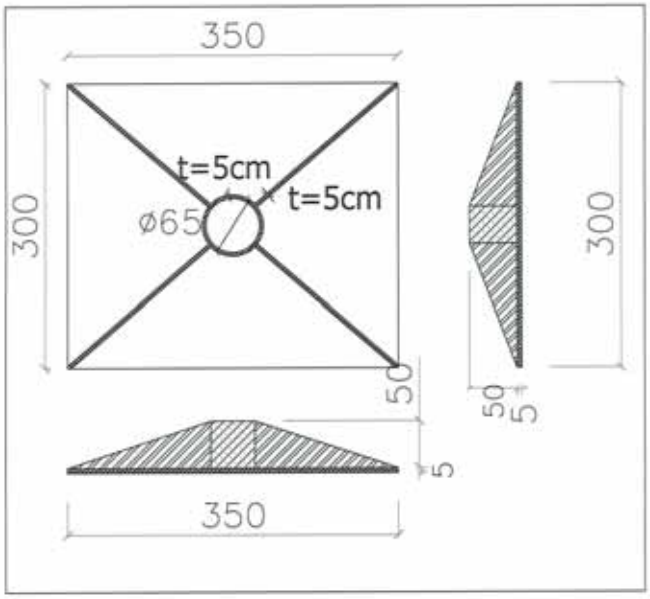

Figure 3.19 Schematic drawing of loading plate

3.7.3 Dial Gages

Two 25mm and five 10mm travel dial gages which have a precision of 0.25mm were used. Dial gages having 25mm travel were placed at the center and corner points of the loading plate. Others were used to measure deep settlements.

3.7.4 Hydraulic Jacking System

The complete jacking system including the hydraulic jack, hydraulic pump and pressure gage was calibrated as a unit in Istanbul Technical University before test program. The calibration certificate is given in Appendix C. The use of a single high-capacity (400 tons) jack manufactured by Hidromekanik A.Ş. was used.

3.7.5 Total Pressure Cell and Readout Unit

The total pressure cell used in the loading tests was a vibrating wire total pressure cell, model TPC manufactured by ROCTEST, Canada with range of 3000 kPa. The TPC consists of two steel discs welded around their periphery and then recessed on both sides to provide a central flexible oil filled pressure pad. The TPC, equipped with vibrating wire pressure transducers, are fitted with watertight cable to allow remote reading of pressure changes. Its thickness and diameter are 0.63cm and 23cm, respectively.

The read out unit used in the loading tests was a vibrating wire datalogger, model MB-6TL manufactured by ROCTEST, Canada. It is a self-powered, portable unit. Mainly, its operation principal is as follows: It generates a frequency sweep to cause the wire to vibrate. This step is the excitation of the wire. Once the wire excited, the MB-6TL amplifies the signal created by the wire vibrating in proximity to the coil, and measures the vibration period. The calibration certificate of total pressure cell is given in Appendix C.

3.8 Large Plate Load Tests

3.8.1 Preparation of Aggregate Pier Groups Loading Area

Totally four load tests were performed in this study; one was untreated zone loading, others were aggregate pier group loadings.

Before loading set-up preparations, fill material that was laid at the very beginning as a working platform was excavated and the natural ground surface was revealed. Then approximately 10cm thick sand layer was laid and compacted to level the surface. In Figure 3.20, laying and compaction process can be seen. After placing total pressure cell on top of the center aggregate pier, as shown in Figure 3.21, a second layer of sand was laid and compacted to embed the pressure cell. Next step was to place the loading plate with the help of crane and to pass the deep settlement plate's PVC tubes into the holes on the loading plate, as shown in Figure 3.22.

Figure 3.20 Laying and compaction process of sand layer on the loading surface

After placing of loading plate, test beams were positioned and welding works were completed. Then, test set-up was ready for loading.

Figure 3.21 Placing of total pressure cell on top of the center aggregate pier

Figure 3.22 Placing of loading plate

3.8.2 Loading Procedure

Totally four load tests were performed in this study; one was untreated zone loading, others were aggregate pier group loadings.

The loading sequence for untreated zone load test was as follow: 25, 50, 25, 75, 25, 100, 50, 150, 75, 0, 200, 100, 0, 250, 175, 100, 0 kPa. With this cyclic loading procedure, both loading and unloading characteristics of natural soil were investigated. At each increment, load was kept constant until the settlement rate almost zero.

The loading sequence was 50, 100, 150, 200, 250, 150, 0 kPa. for aggregate pier group loading tests. Similar to untreated zone loading test, each incremental load was kept constant until the displacement rate became almost zero.

Two surface movements, one at the corner and one at the center of the loading plate, and five deep movement (at 1.5, 3.0, 5.0, 8.0 and 10.0m depth) measurements were taken with respect to time. In addition, pressure cell readings were taken from central column with respect to time, in aggregate pier group loading tests.

3.9 Single Aggregate Pier Load Tests

Three short- term, rapid load tests were performed on the single aggregate piers. Test piers are 3, 5 and 8m long and 65cm in diameter. The load is applied to just on the area of the pier with rigid steel plate with a thickness of 5cm.

Single aggregate pier, test arrangements and apparatus for individual pier loading test can be seen in Figures 3.23, 3.24 and 3.25 respectively. There were

two reaction piles in each load test to provide adequate reactive capacity. A test beam of sufficient size and strength was used to avoid excessive deflection under load with sufficient clearance between bottom flanges of the test beam and the top of the test pile to provide for the necessary bearing plate and hydraulic jack. It can be seen from the Fig. 3.25 that all the reference wires which the dial gages were attached were independently supported with supports firmly embedded in the ground.

The load tests were performed essentially in accordance with ASTM D1143. A total of eight loading increments were applied, with 2 tons per each increment. The time between loading increments was at least 15 minutes; each load increment was maintained until the rate of settlement is not greater than 0.3 mm/hour. The maximum load of 15 tons was held for two hours. The maximum load was removed in three decrements.

Movements were measured with two 25mm travel dial gages which have a precision of 0.25mm. Dial gages were placed at the top of the loading plate.

Figure 3.23 A view from single test pier

Figure 3.24 Single aggregate pier load test arrangement

Figure 3.25 Apparatus for loading and measuring settlements

3.10 Cone Penetration Tests

Four cone penetration soundings were performed by Zemar Ltd. at the site as a final work (Figure 3.26). Each borehole was 10.0m depth. CPT logs are given in the Appendix B. In addition to tip and skin friction resistance, pore pressure was also measured at the tests. Location of CPT bore holes can be seen in Figure 3.14. Evaluation of test results will be carried out in the next chapter.

Figure 3.26 A view from Cone Penetration Test

CHAPTER IV

GEOLOGICAL AND SITE CONDITIONS

4.1 Introduction

Site investigations included five boreholes and sampling, four CPT soundings, and SPT and laboratory testing.

Drilling works were initiated in November 2000 at the test site, with preliminary boring of 10m depth, named SKT-1. In June 2001, four additional investigation borings were opened, which are named as SK-1, SK2, SK-3 and SK-4. SK-1 of 8m depth was located at the left corner of the test site. 10m deep borehole, SK-2 was at the center of the test site. 11m deep borehole SK-3 was between SK-1 and SK-2 and SK-4 which is 13.5m deep was opened alongside o the preliminary boring, SKT-1. Location of the boreholes is given in Figure 4.1.

In each of these borings Standard Penetration Tests, SPT were performed and both disturbed and undisturbed samples were taken.

In addition, SPT and sampling were performed at five different holes, which were drilled to position the deep settlement plates. They are named as SU8 (located in the unreinforced loading area), SA8 (located in the loading area having aggregate piers of 3.0m length), SB8 (located in the loading area having aggregate piers of 5.0m length), SC8 and (located in the loading area having

aggregate piers of 8.0m length). SU8, SA8,SB8 and SC8 were 8m deep, whereas SC10 was 10m.

Four CPT soundings, which are 9.5m each, were performed at the site in October, 2003.

Borehole logs and CPT results are given in Appendix B.

4.2 Evaluation of SPT Results

Variation of SPT-N values with depth is given in Figure 4.2. It can be seen that, N values are in the range of 6 to 12 with an average of 10 in the first 8m. After 8m depths, SPT-N values are greater than 20.

The variation of SPT-N_{60} values, obtained from CPT correlations, with depth is given in Figure 4.3. Same trend is observed as regard to the variation of SPT-N values with respect to depth.

4.3 Laboratory Works

Particle size analysis and Atterberg Limit tests were performed on all disturbed and undisturbed samples to determine the basic and index properties of the compressible layer. Specific gravity, clay content percentage and natural water content were determined for some samples. Additionally undrained-unconsolidated triaxial tests (UU) were performed on limited number of samples because UD samples taken by Shelby tubes had insufficient lengths or the tubes were just empty since the soil profile was sandy clay.

Variation of fine content (-No.200) and coarse content (+No.4) of the compressible layer with depth are given in Figure 4.4 and 4.5 respectively. As seen from these figures, fine and coarse contents of the compressible layer change in the range of 25% to 40 % and 10% to 25%, respectively.

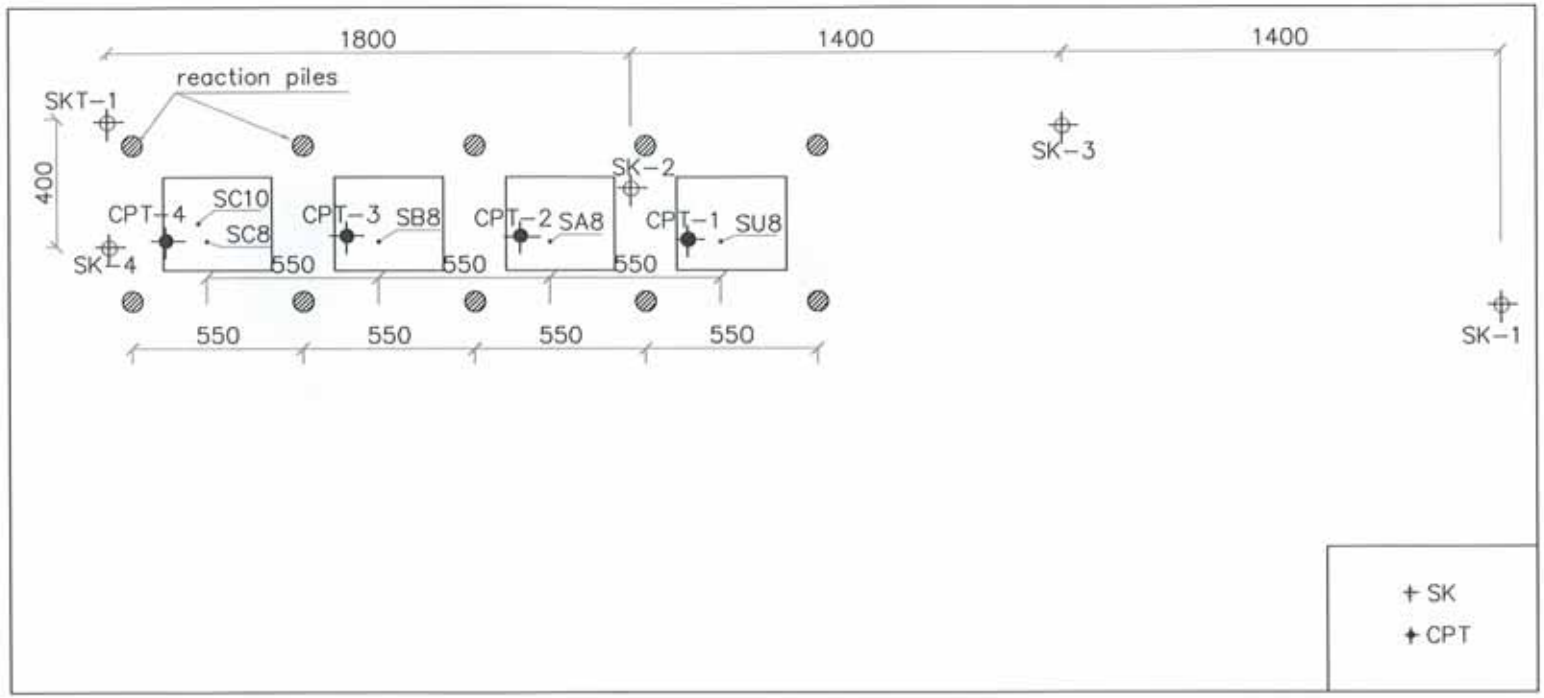

Figure 4.1 Location of investigation boreholes and CPT soundings

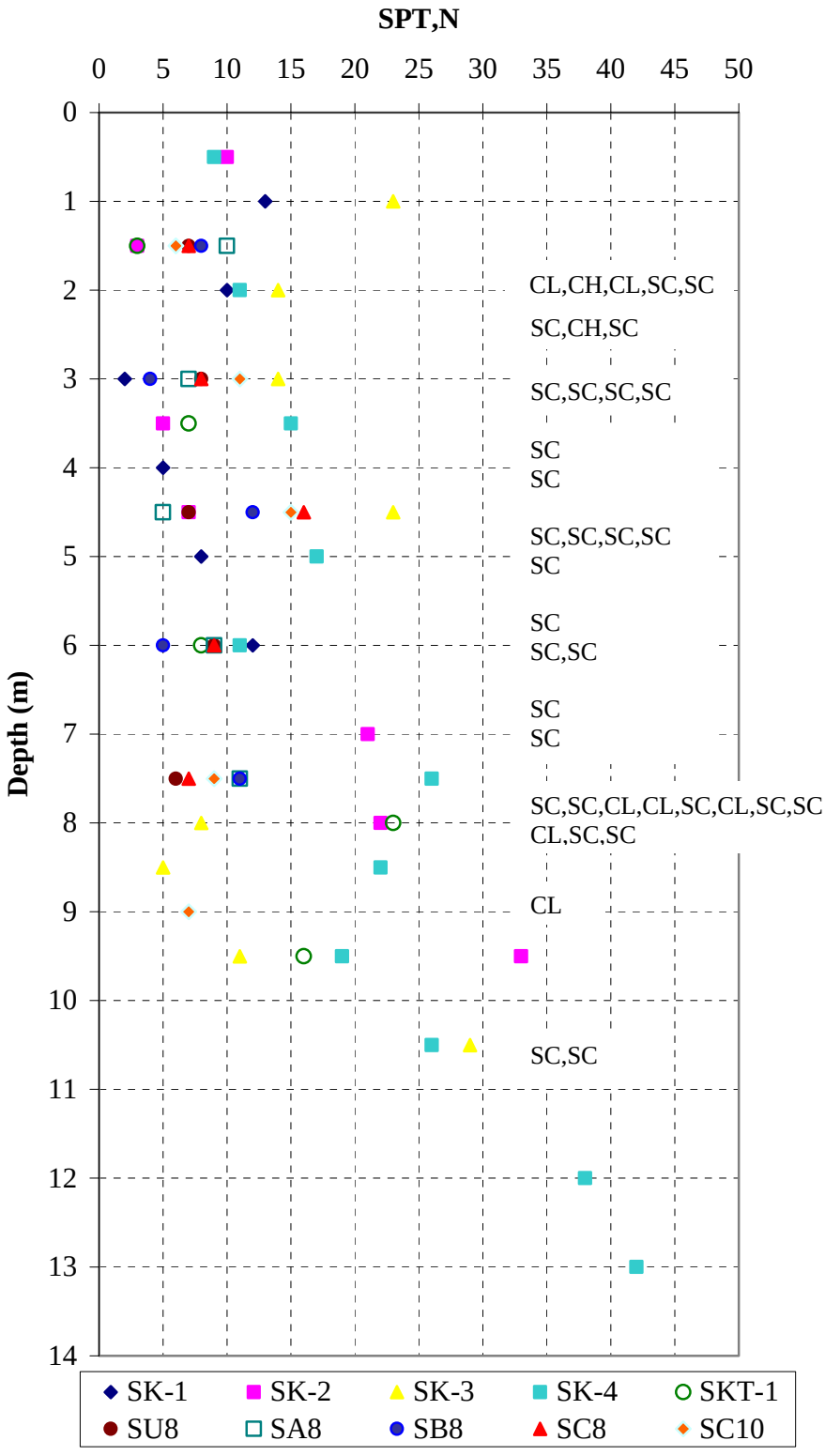

Figure 4.2 Variation of SPT N values with depth

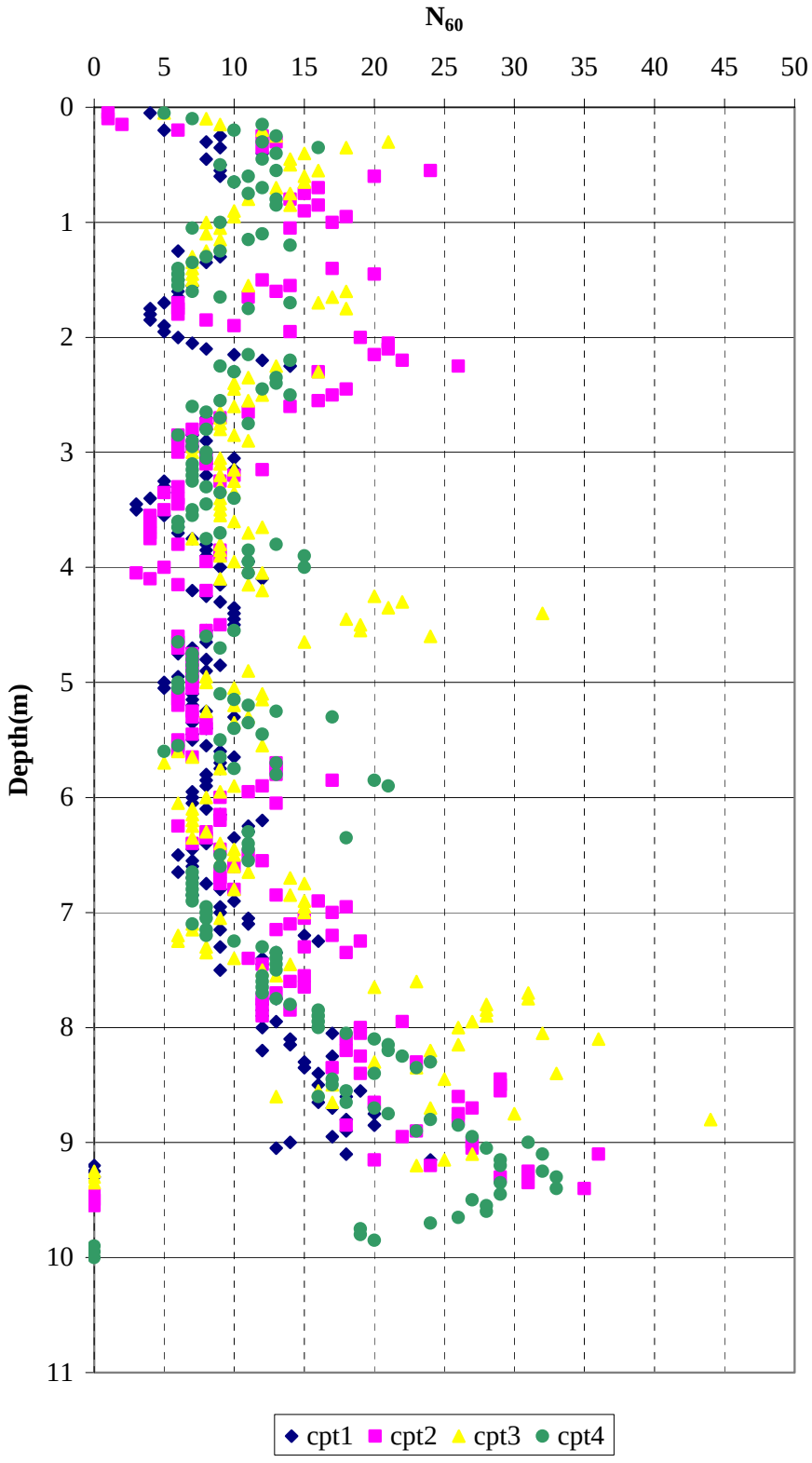

Figure 4.3 Variation of N_{60} values obtained from CPT correlations with depth

Figure 4.6 and 4.7 show the variation of liquid limit and plastic limit throughout the depth of compressible layer, respectively. As Liquid limit of the compressible layer changes predominantly in the range of 27 to 43% with an average of 30%, the plastic limit changes in the range of 14 to 20% with an average of 15%.

Based on the laboratory test results, which are provided in Appendix B, the compressible layer is classified as CL and SC according to Unified Soil Classification System (USCS).

4.4 Evaluation of CPT Results

The variations of tip and friction resistance of the compressible soil layer, obtained from CPT soundings, with depth are given in Figure 4.8 and 4.9, respectively.

These figures indicate that, the averages of the tip and friction resistance of the compressible soil strata can be taken as 1.1 MN/m^2 and 53 kN/m^2, respectively.

Figure 4.10 gives the variation of soil classification based on CPT correlations with depth. It can be said that, although the soil profile consists of thin silty sand to sandy silt layers, it is generally cohesive type of soil that is silty clay to clay, generally.

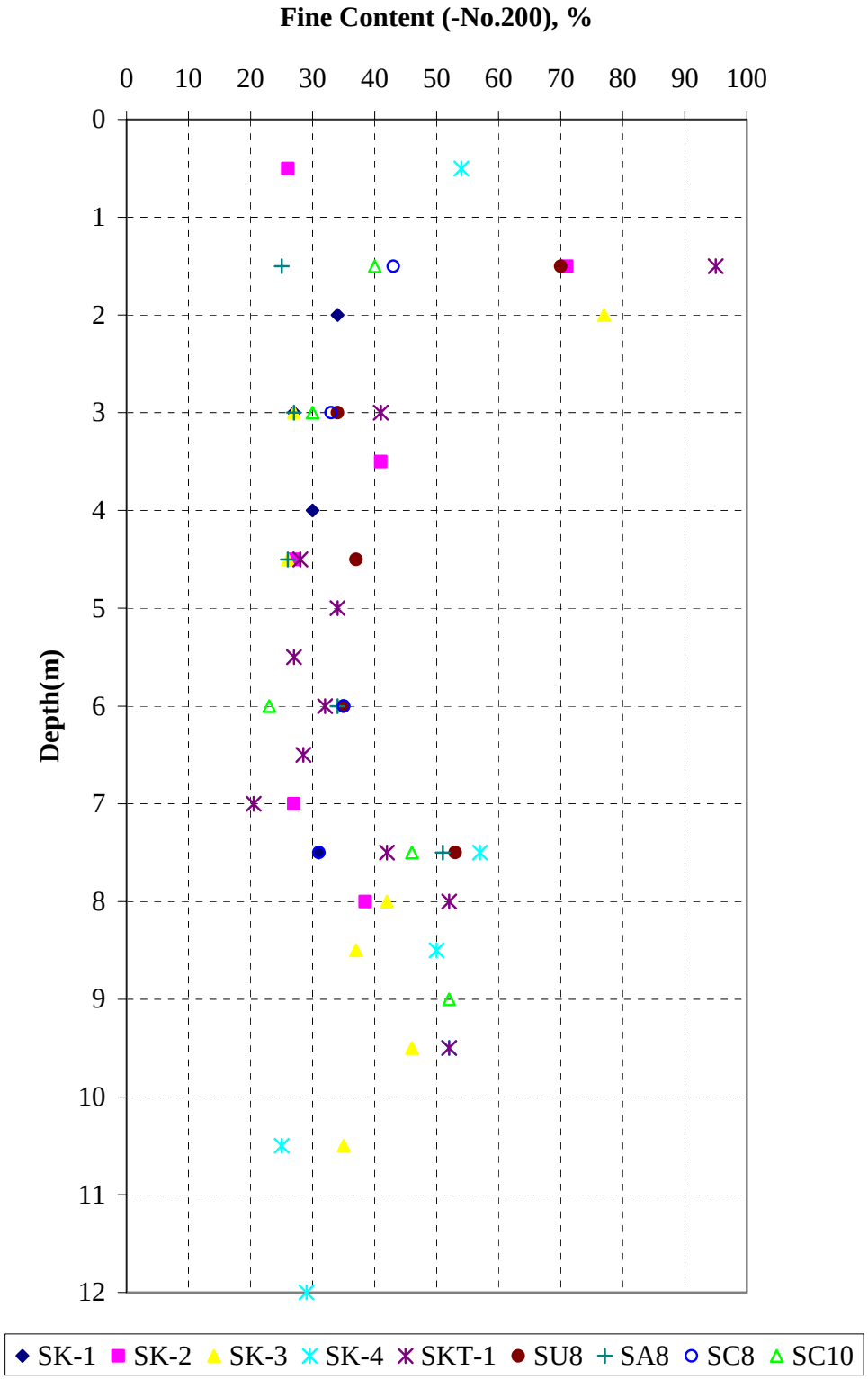

Figure 4.4 Variation of fine content (-No.200) with depth

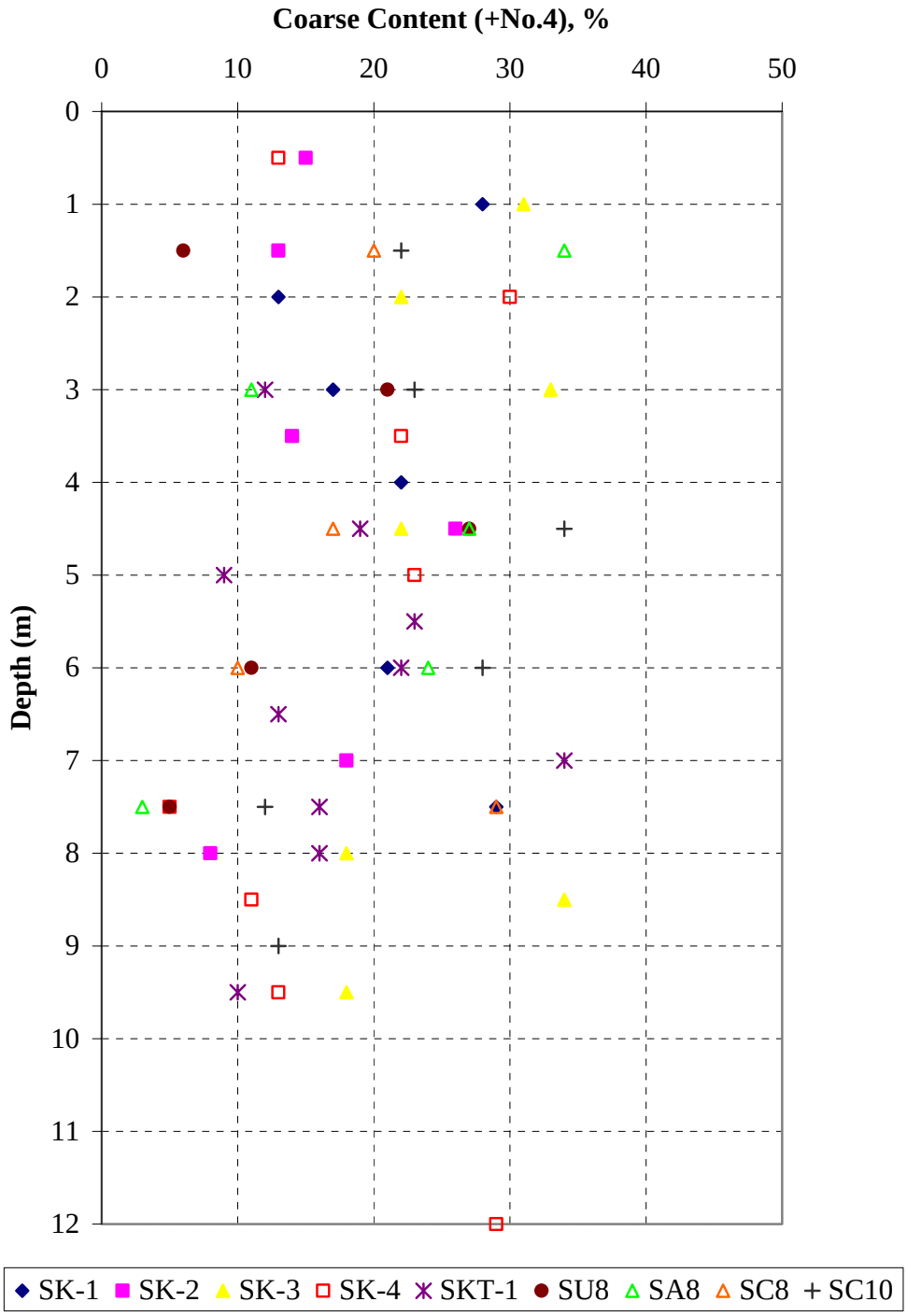

Figure 4.5 Variation of coarse content (+No.4) with depth

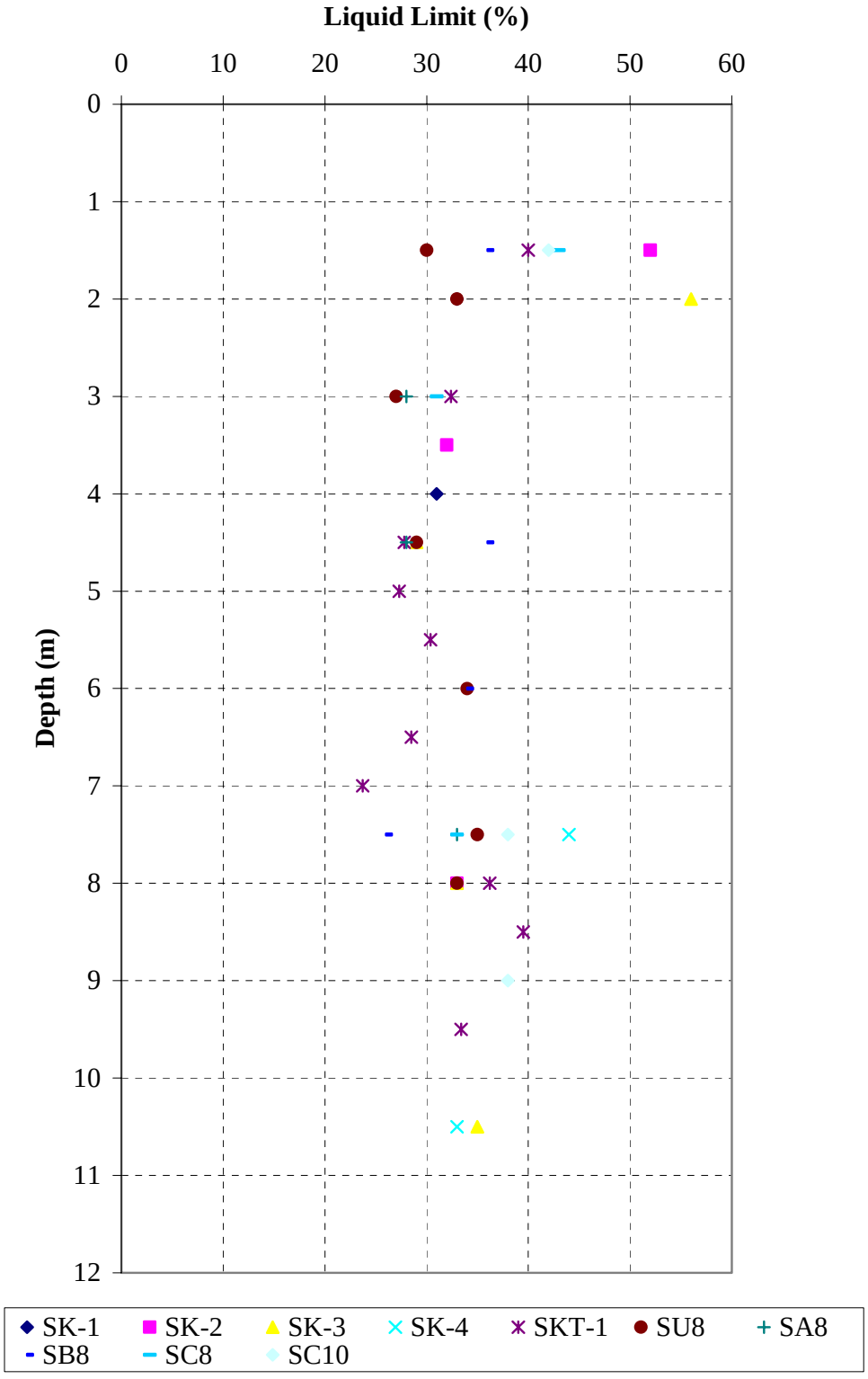

Figure 4.6 Variation of Liquid Limit with depth

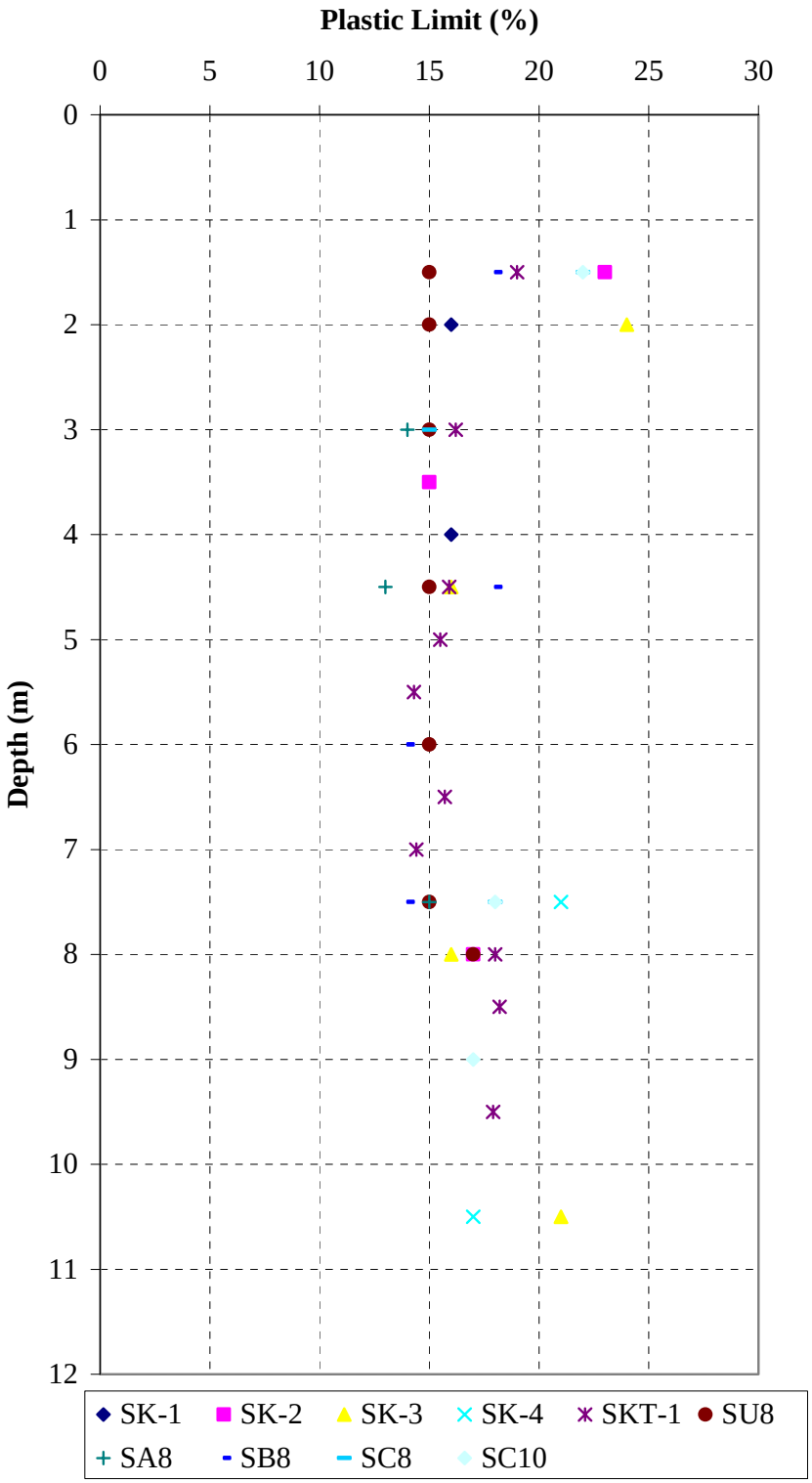

Figure 4.7 Variation of Plastic Limit with depth

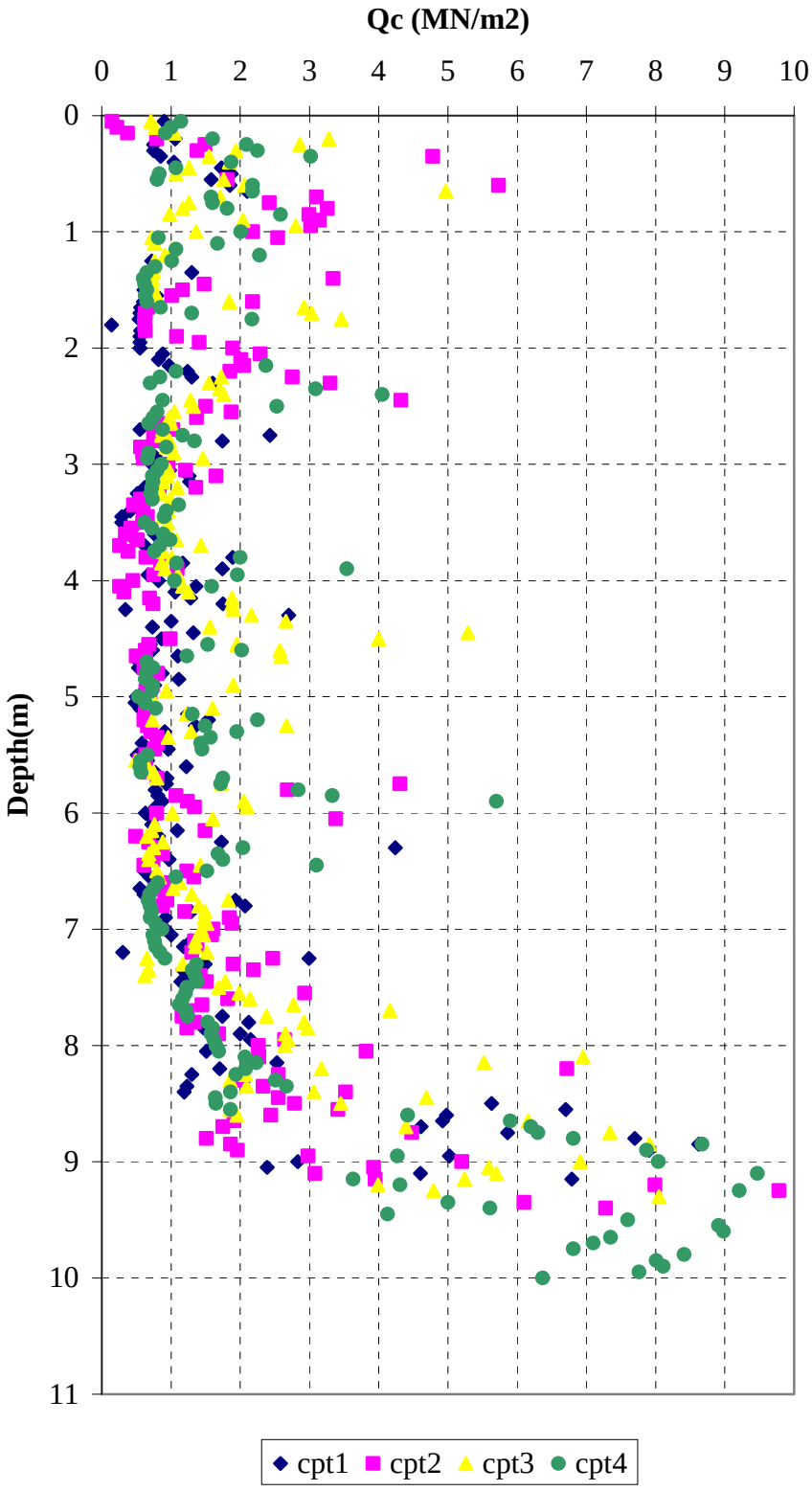

Figure 4.8 Variation of tip resistance with depth

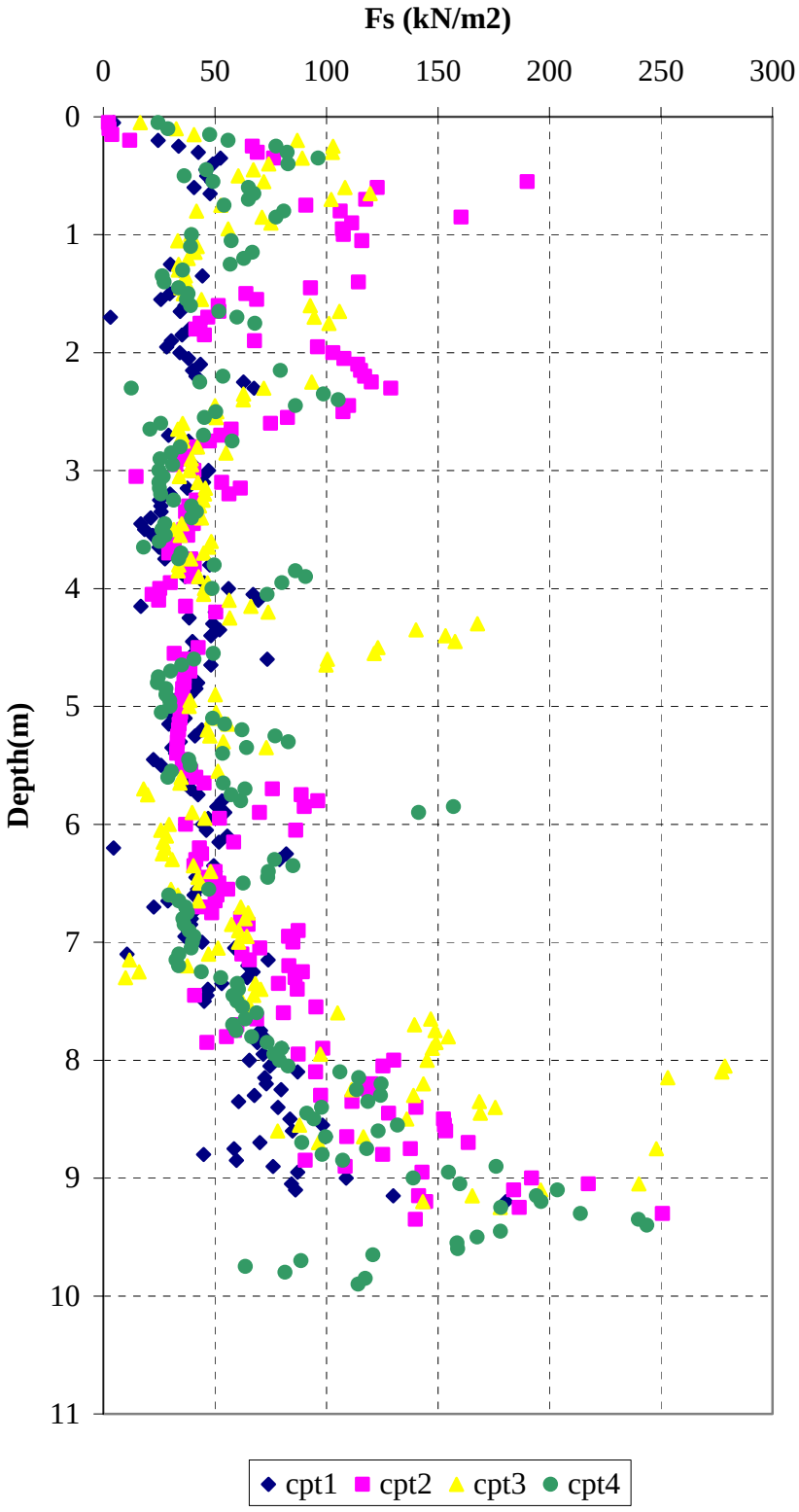

Figure 4.9 Variation of friction resistance with depth

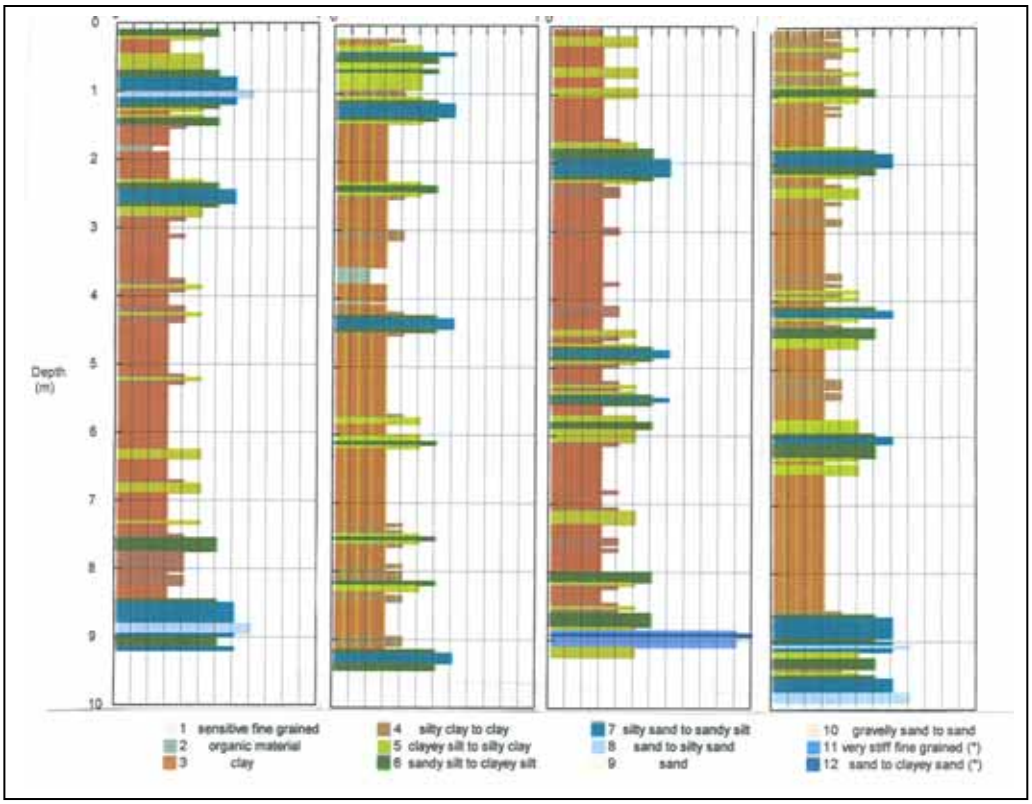

Figure 4.10 Variation of soil classification based on CPT correlations

CHAPTER V

PRESENTATION OF TEST RESULTS

5.1 Introduction

In this study, four large plate load tests were conducted. First load test was on untreated soil. Second load test was Group A loading on improved ground with floating aggregate piers of 3.0m length, third load test was Group B loading on improved ground with floating aggregate piers of 5.0m length and finally fourth load test was Group C loading on improved ground with end-bearing aggregate piers of 8.0m length.

During these tests, the settlement of the large loading plate and the settlements in the different levels of soil profile were measured. In addition, in Group A, B and C loadings, stress on the center pier were measured.

In this chapter, results of these tests will be presented.

5.2 Settlement Behavior Results of Load Tests

5.2.1 Load Test on Untreated Soil

In the beginning of the field study, a load test on untreated clayey soil (not supported by aggregate piers) was performed to be a reference for comparisons and interpretations with other tests in the later stages of the study.

In the load test, loads were applied in stages and settlement readings were taken continuously with time. Surface settlement readings were taken from the center and the corner points of the loading plate. At higher pressure values the center and the corner settlement values departed from each other, most probably due to the slight rotation of loading plate. As a result, average value of these is used as a surface settlement of untreated soil profile. Deep settlement readings were taken from the deep settlement gages installed at 1.5, 3.0, 5.0 and 8.0 depths. The loading sequence for untreated soil load test was as follow: 25, 50, 25, 75, 25, 100, 50, 150, 75, 0, 200, 100, 0, 250, 175, 100, 0 kPa.

The surface settlement-time and deep settlement-time relationships of the untreated soil are given in Figure 5.1 and 5.2 respectively.

Final surface and deep settlement magnitudes of the untreated soil at the end of each loading stage are summarized in Table 5.1.

Variations of settlements through depth in untreated soil are plotted in Figure 5.3 for all stress ranges.

Table 5.1 Final surface and deep settlement magnitudes of the untreated soil at the end of each loading stage

Applied Surface Pressure σ (kPa)	**Untreated Soil Settlements (mm)**				
	Surface	**d=1.5m**	**d=3.0m**	**d=5.0m**	**d=8.0m**
25	11.7	5.0	2.7	1.8	0.0
50	20.0	8.7	5.1	3.6	0.0
25	19.0	8.3	4.4	2.8	0.2
75	30.3	15.8	8.0	5.5	2.4
25	26.5	15.5	6.4	4.5	1.2
100	43.8	25.7	14.4	6.5	2.4
50	31.6	20.9	8.7	5.3	1.2
150	84.8	54.0	36.9	19.8	5.7
75	81.8	54.0	34.8	18.4	5.1
0	61.9	46.1	25.0	16.5	4.1
200	149.2	99.7	78.8	39.7	9.1
100	145.7	99.9	76.4	38.1	9.8
0	116.5	81.0	61.6	30.5	8.3
250	350.9	249.4	194.2	68.6	24
175	345.9	245.6	193.9	72.3	24.7
100	336.8	238.7	192.8	73.1	25.2
0	298.6	213.8	178.2	72.2	26.6

* d= depth of the settlement gage

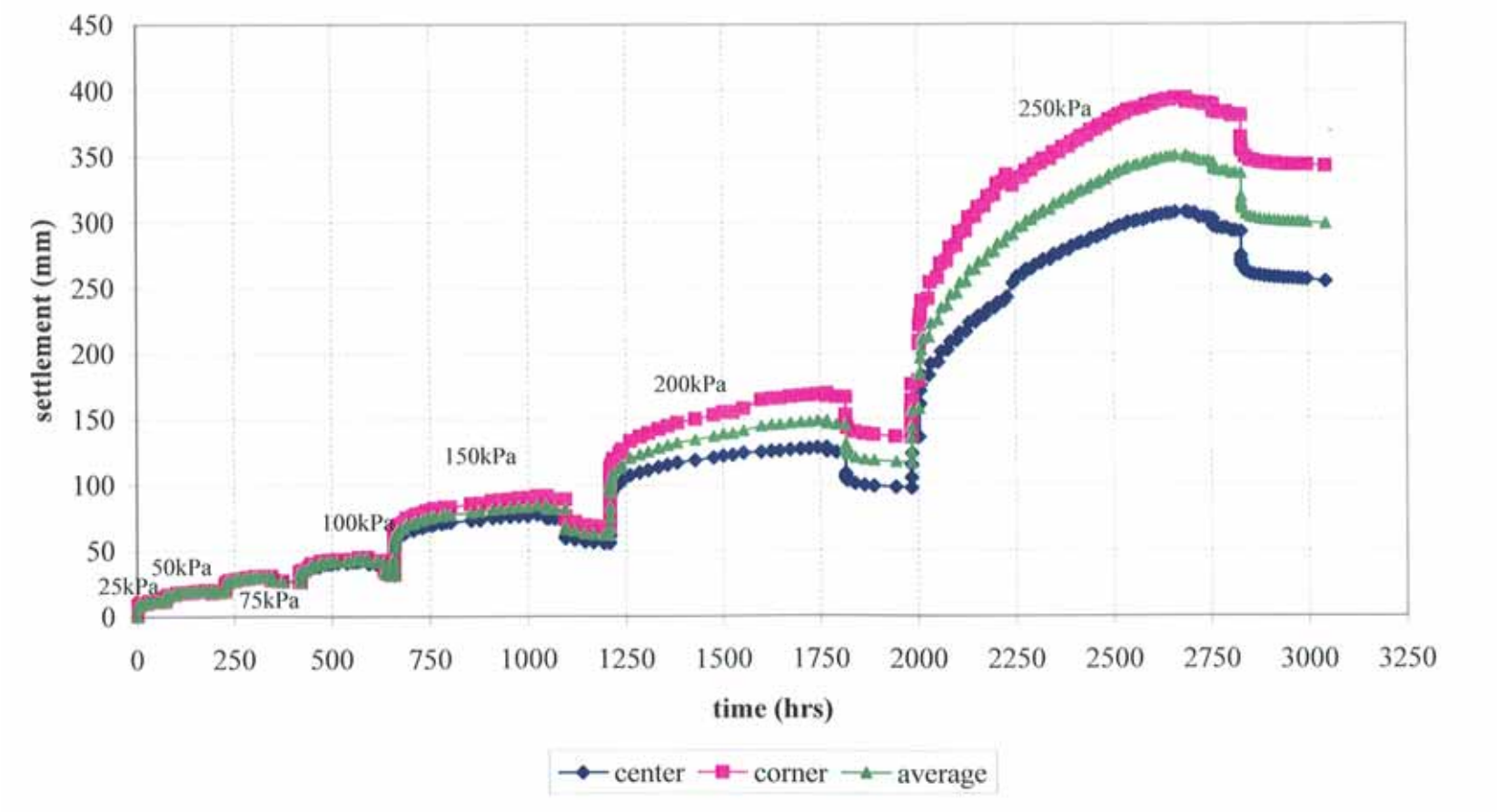

Figure 5.1 Surface settlement-time relationships of untreated soil

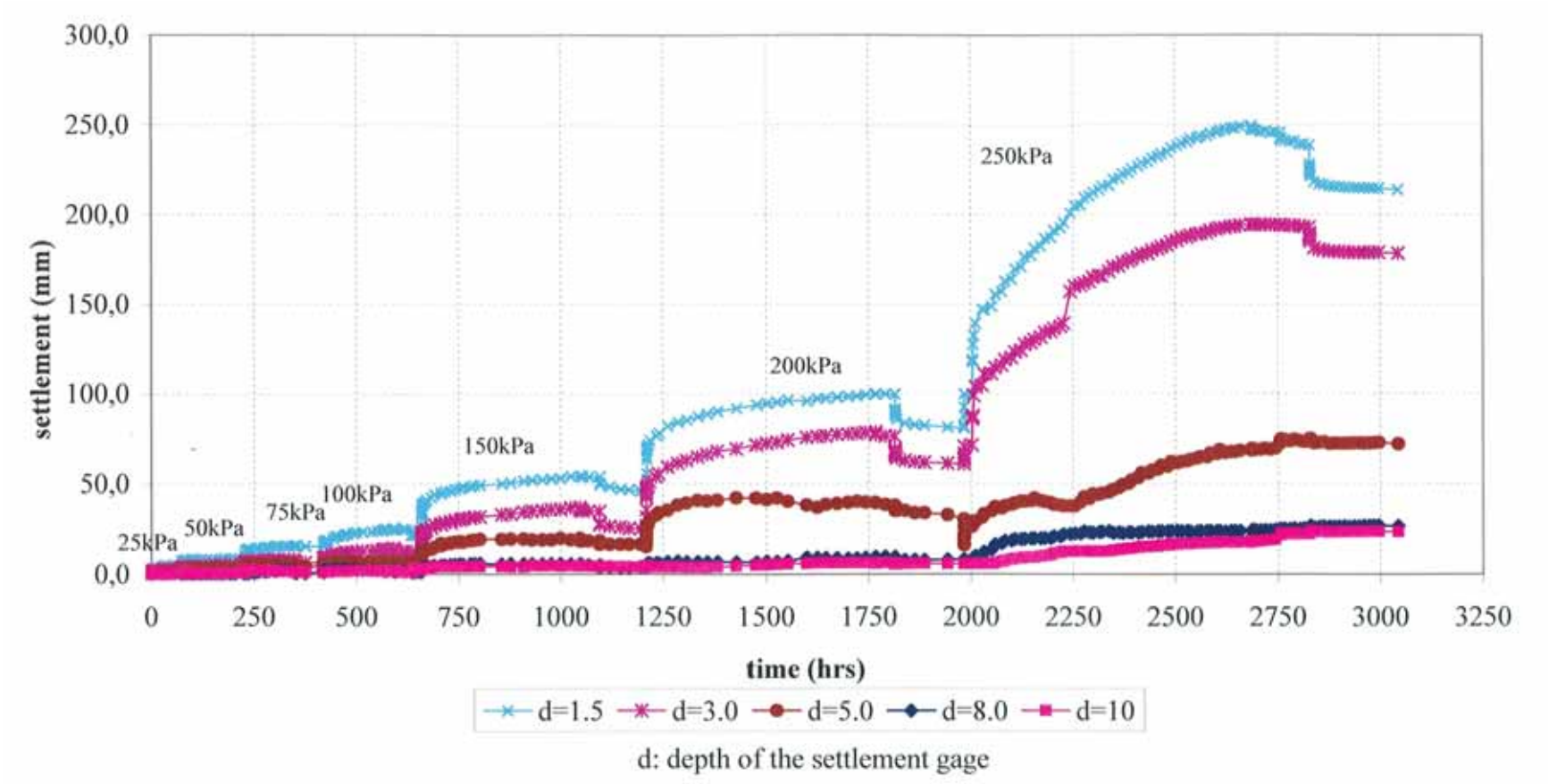

Figure 5.2 Deep settlement-time relationships of untreated soil

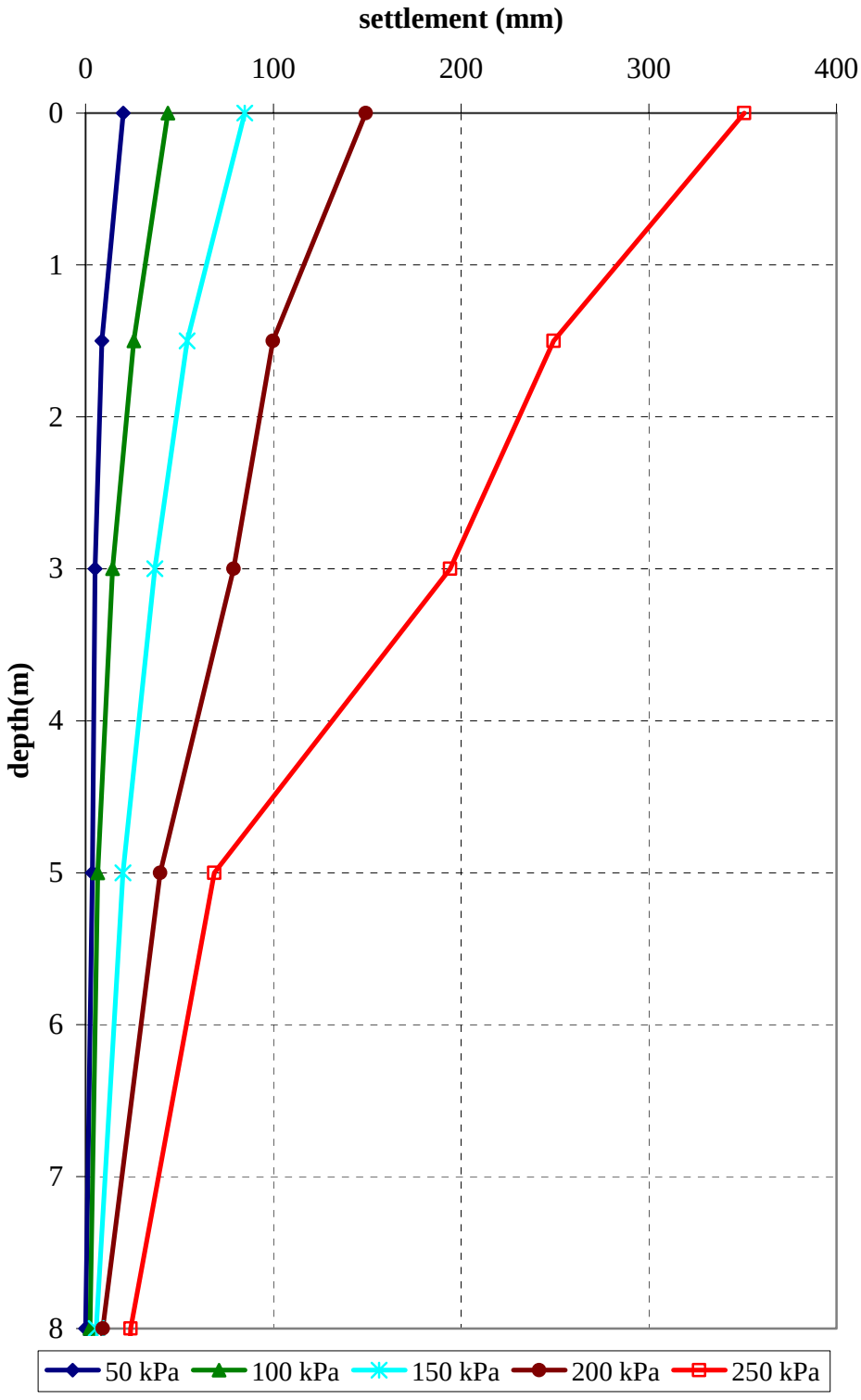

Figure 5.3 Variation of settlements with depth in the untreated soil

5.2.2 Load Test on Group A (Load Test on the Improved Soil with 3.0m lengths of Aggregate Piers)

A load test was performed on the improved soil with 3.0m lengths of aggregate piers.

In the load test, loads were applied in stages and settlement readings were taken continuously with time. Surface settlement readings were taken from center and corner points of loading plate. Average value of these is used as a surface settlement. Deep settlement readings were taken from the deep settlement gages installed at 1.5, 3.0, 5.0 and 8.0 depths. The deep settlement gage at 8.0m depth did not work satisfactorily and settlements below the gage elevation could not be measured. The loading sequence for this group load test was as follow: 50, 100, 150, 200, 250, 150, 0 kPa.

The surface settlement-time and deep settlement-time relationships of Group A where the soil profile is reinforced by 3m long piers are given in Figure 5.4 and 5.5 respectively.

Final surface and deep settlement magnitudes of group A at the end of each loading stage are summarized in Table 5.2.

Variations of settlements through depth in improved soil are plotted in Figure 5.6 for all stress ranges.

Table 5.2 Final surface and deep settlement magnitudes of the Group A at the end of each loading stage

Applied Surface Pressure σ (kPa)	**Group A Settlements (L=3.0m)**				
	Surface	**d=1.5m**	**d=3.0m**	**d=5.0m**	**d=8.0m**
50	10.7	2.8	2.2	0.7	
100	22.9	10.3	4.4	1.6	
150	36.2	20.2	9.7	5.2	
200	58.4	37.6	20.2	15.0	
250	86.7	62.7	38.5	26.6	
150	85.2	61.7	37.8	26.3	
0	69.3	52.7	33.6	26.1	

5.2.3 Load Test on Group B (Load Test on the Improved Soil with 5.0m lengths of Aggregate Piers)

A load test was performed on the improved soil with 5.0m lengths of aggregate piers.

In the load test, loads were applied in stages and settlement readings were taken continuously with time. Surface settlement readings were taken from center and corner points of loading plate. Average value of these is used as a surface settlement. Deep settlement readings were taken from the deep settlement gages installed at 1.5, 3.0, 5.0, 8.0 and 10.0m depths. The loading sequence for this group load test was as follow: 50, 100, 150, 200, 250, 100, 0 kPa.

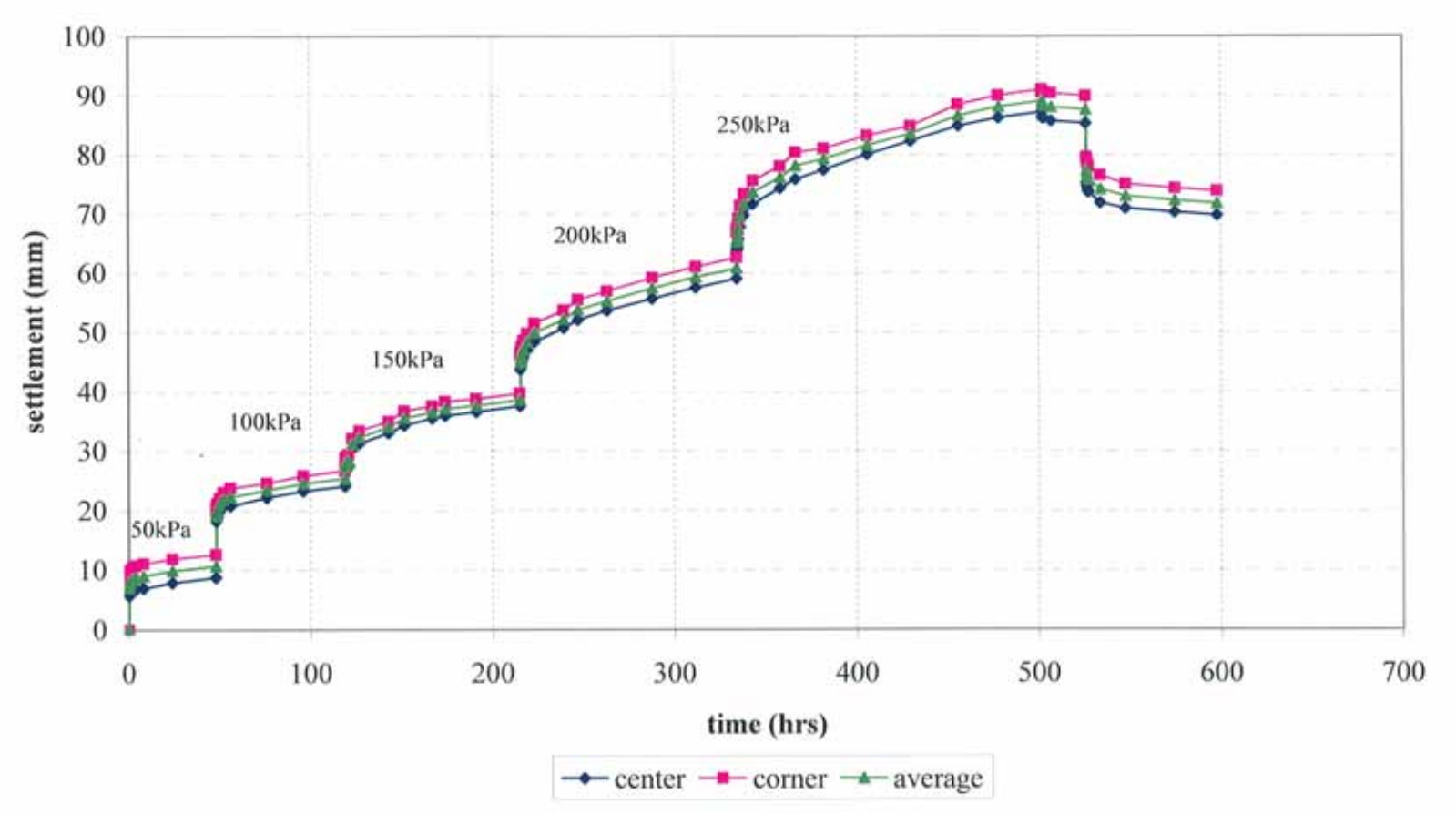

Figure 5.4 Surface settlement-time relationship for L=3.0m aggregate pier group loading (Group A)

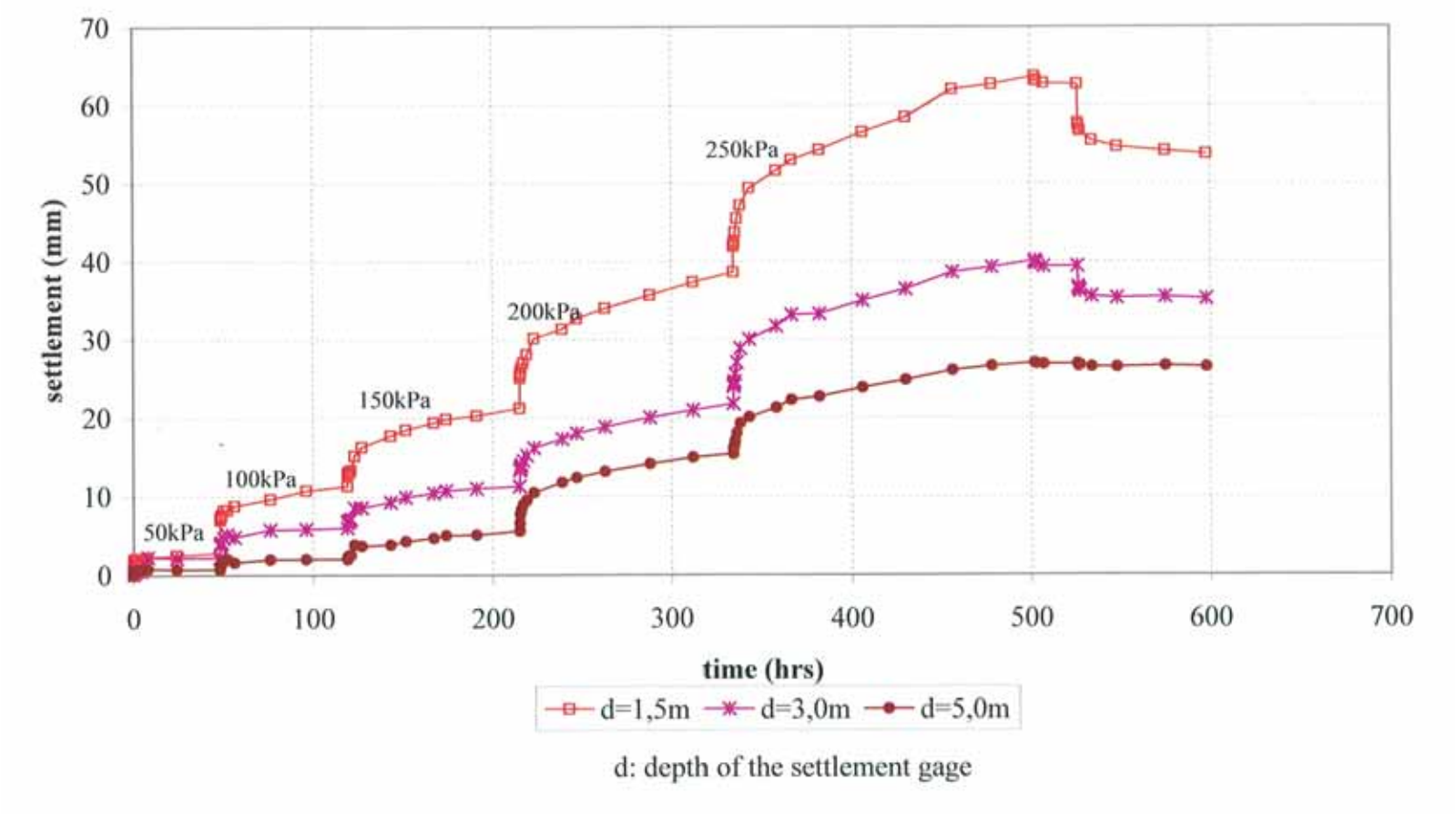

Figure 5.5 Deep settlement-time relationship for L=3.0m aggregate pier group loading (Group A)

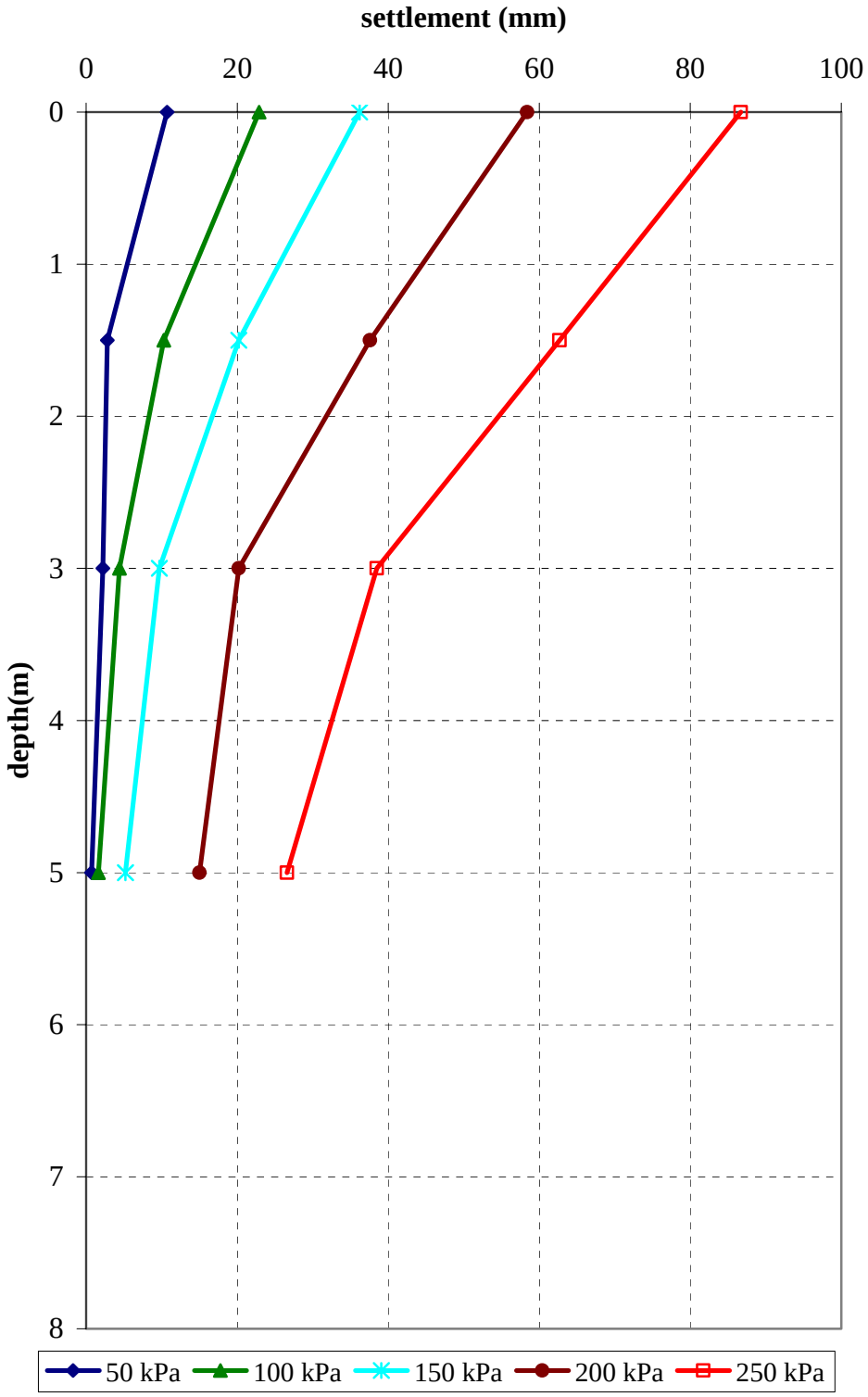

Figure 5.6 Variation of settlements with depth in the soil improved with 3.0m lengths of aggregate piers (Group A)

The surface settlement-time and deep settlement-time relationships of Group B where the soil profile is reinforced by 5 m long piers are given in Figure 5.7 and 5.8, respectively.

Final surface and deep settlement magnitudes of Group B at the end of each loading stage are summarized in Table 5.3.

Variations of settlements through depth in improved soil are plotted in Figure 5.9 for all stress ranges.

Table 5.3 Final surface and deep settlement magnitudes of the Group B at the end of each loading stage

Applied Surface Pressure σ (kPa)	**Group B Settlements (L=5.0m)**				
	Surface	**d=1.5m**	**d=3.0m**	**d=5.0m**	**d=8.0m**
50	11.7	3.0	2.0	0.6	0.3
100	22.0	7.3	7.3	1.5	2.1
150	33.9	13.2	14.4	3.0	2.9
200	55.7	27.3	27.8	4.9	4.6
250	73.3	39.6	37.8	7.2	6.3
100	71.9	38.9	37.4	7.1	6.3
0	57.9	32.9	34.5	6.9	6.5

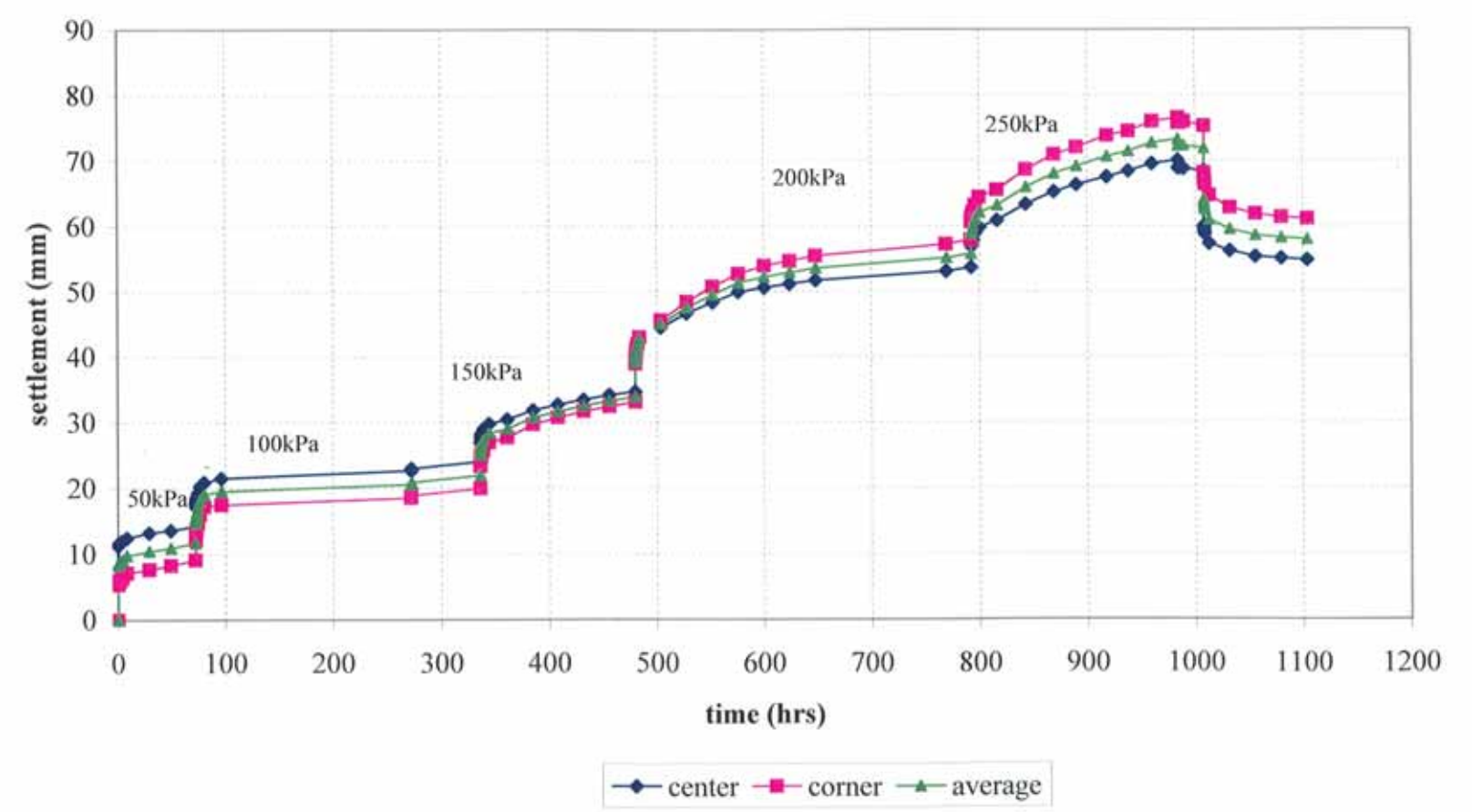

Figure 5.7 Surface settlement –time relationship for L=5.0m aggregate pier group loading (Group B)

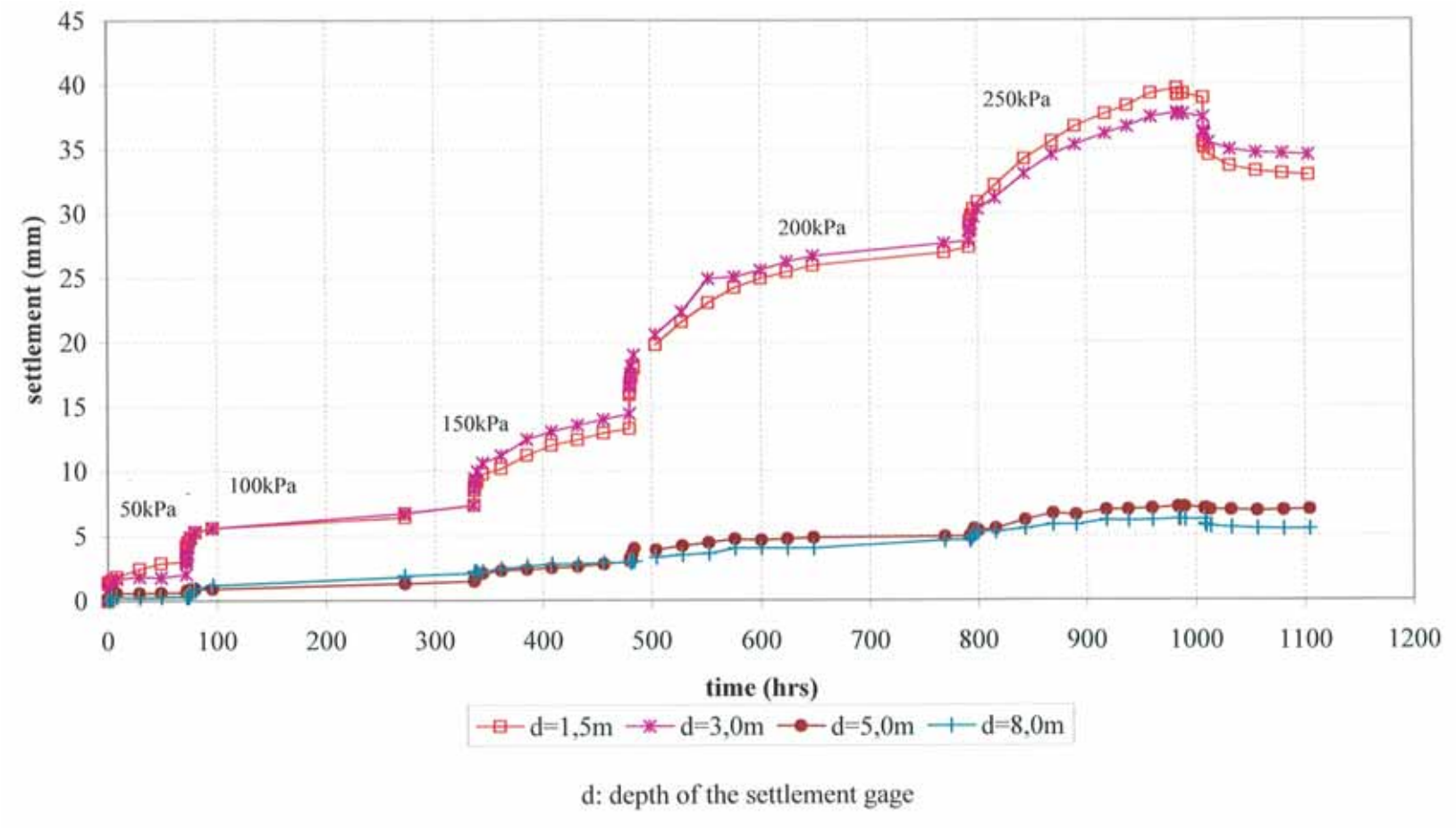

Figure 5.8 Deep settlement-time relationship for L=5.0m aggregate pier group loading (Group B)

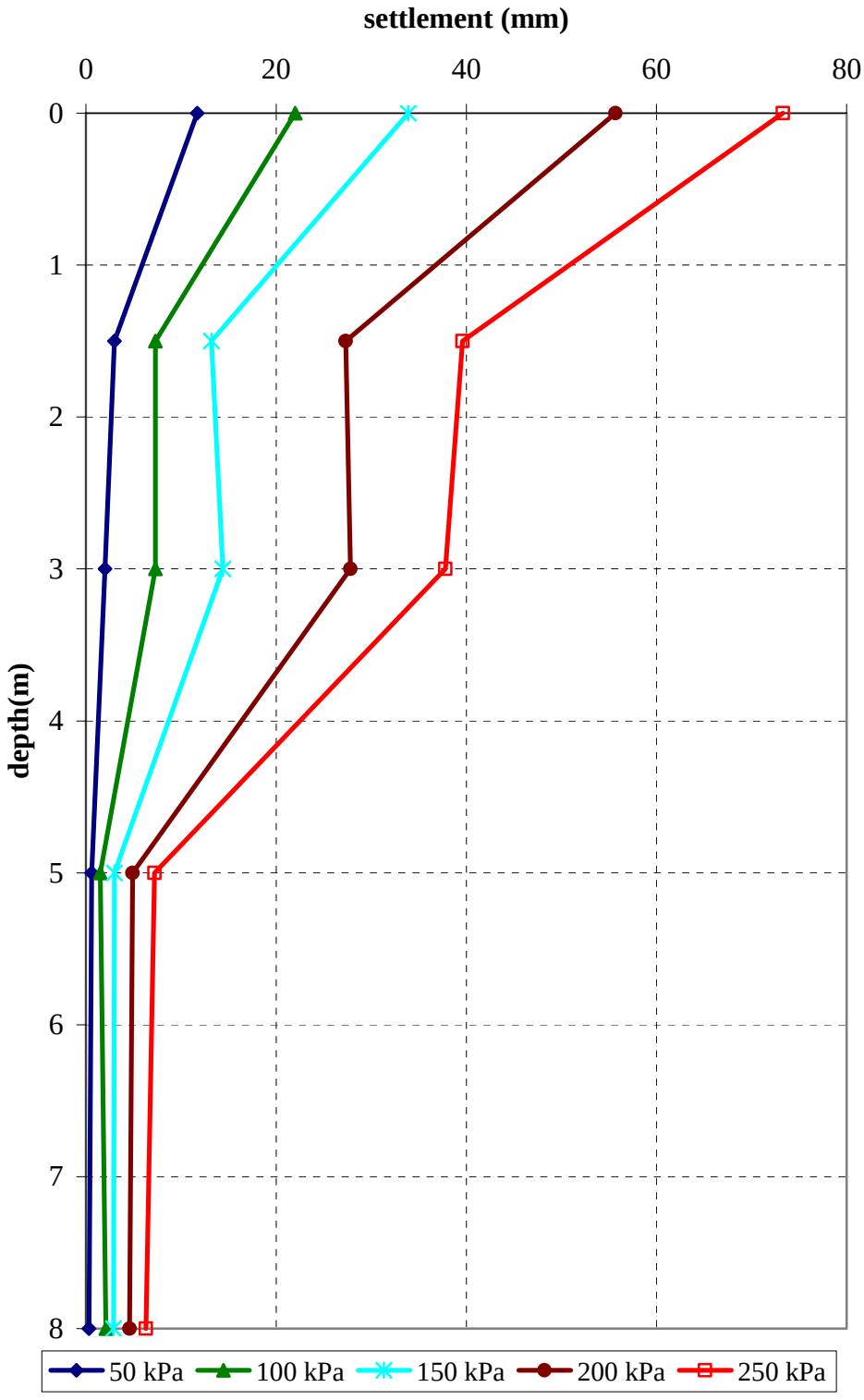

Figure 5.9 Variation of settlements with depth in the soil improved with 5.0m lengths of aggregate piers (Group B)

5.2.4 Load Test on Group C (Load Test on the Improved Soil with 8.0m lengths of Aggregate Piers)

A load test was performed on the improved soil with 8.0m lengths of end-bearing aggregate piers.

In the load test, loads were applied in stages and settlement readings were taken continuously with time. Surface settlement readings were taken from the center and the corner points of the loading plate. Average value of these is used as a surface settlement. Deep settlement readings were taken from the deep settlement gages installed at 1.5, 3.0, 5.0 and 8.0 depths. The loading sequence for this group load test was as follow: 50, 100, 150, 200, 250, 150, 0 kPa.

The surface settlement-time and deep settlement-time relationships of Group C where the soil profile is reinforced by 8 m long end-bearing piers are given in Figure 5.10 and 5.11, respectively.

Final surface and deep settlement magnitudes of Group C at the end of each loading stage are summarized in Table 5.4.

Variations of settlements through depth in improved soil are plotted in Figure 5.12 for all stress ranges.

Table 5.4 Final surface and deep settlement magnitudes of the Group C at the end of each loading stage

Applied Surface Pressure σ (kPa)	**Group C Settlements (L=8.0m)**				
	Surface	**d=1.5m**	**d=3.0m**	**d=5.0m**	**d=8.0m**
50	8.3	1.8	0.6	0.3	1.0
100	21.6	8.5	3.4	1.4	1.0
150	34.0	17.0	5.6	2.4	1.7
200	41.7	23.2	10.1	3.4	2.4
250	62.1	39.3	15.1	5.6	3.5
150	61.0	38.6	14.0	5.3	3.3
0	45.5	29.9	12.9	4.9	2.7

5.3 Stress Measurement Results in Aggregate Pier Groups

In this study, the stress on center column was measured by means of a pressure cell. In the computation of the stresses on the clay, σ_c it is assumed that the same vertical stress is mobilized in the other six piers and the stress on the clay is uniform under the rigid steel plate. Thus the difference between the total vertical load and the sum of the loads on the piers is divided by the clay area to obtain the σ_c values.

In Table 5.5, the measured stress on aggregate pier, σ_s and the back-calculated stress on clay, σ_c are summarized.

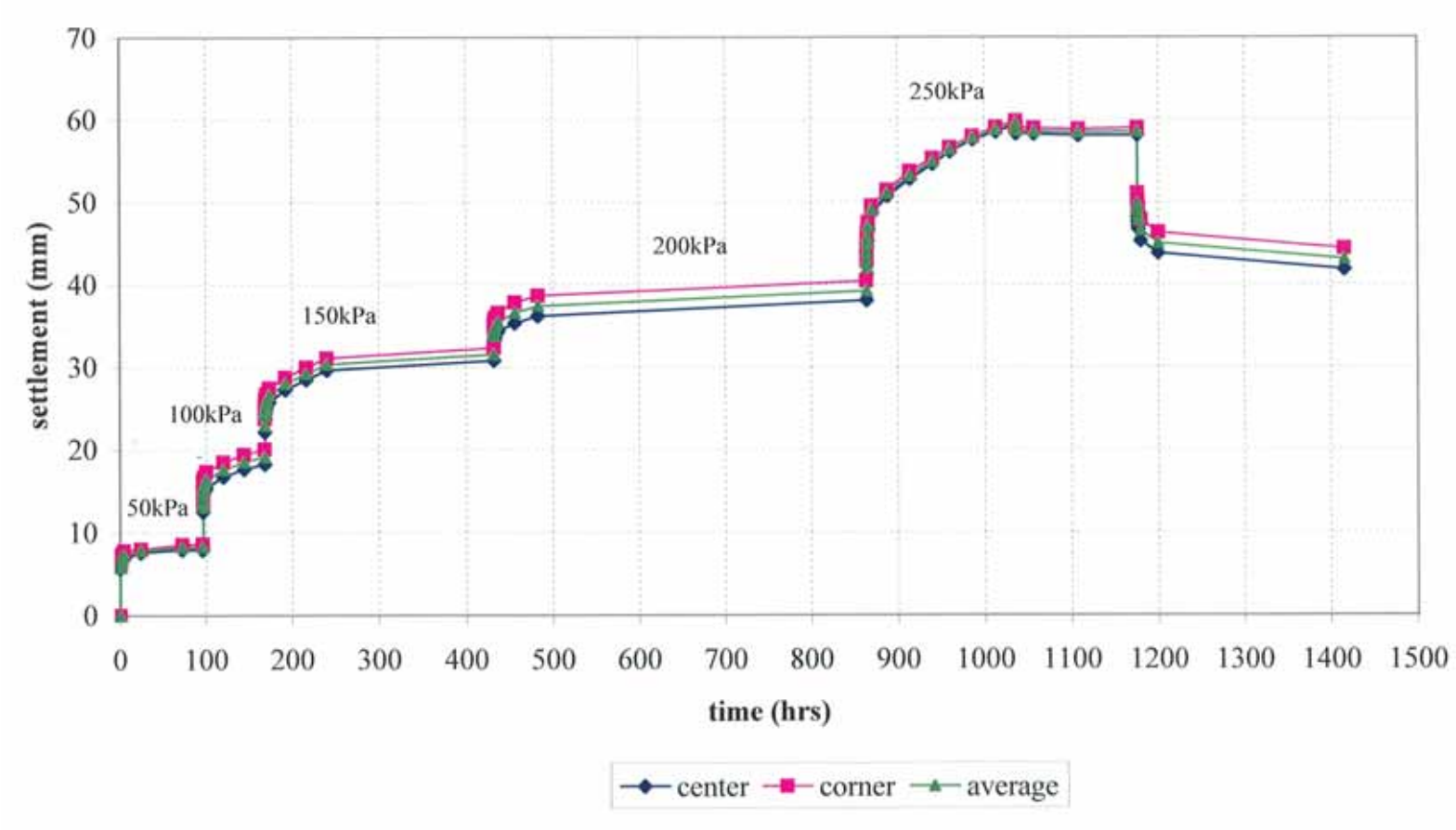

Figure 5.10 Surface settlement-time relationship for L=8.0m aggregate pier group loading (Group C)

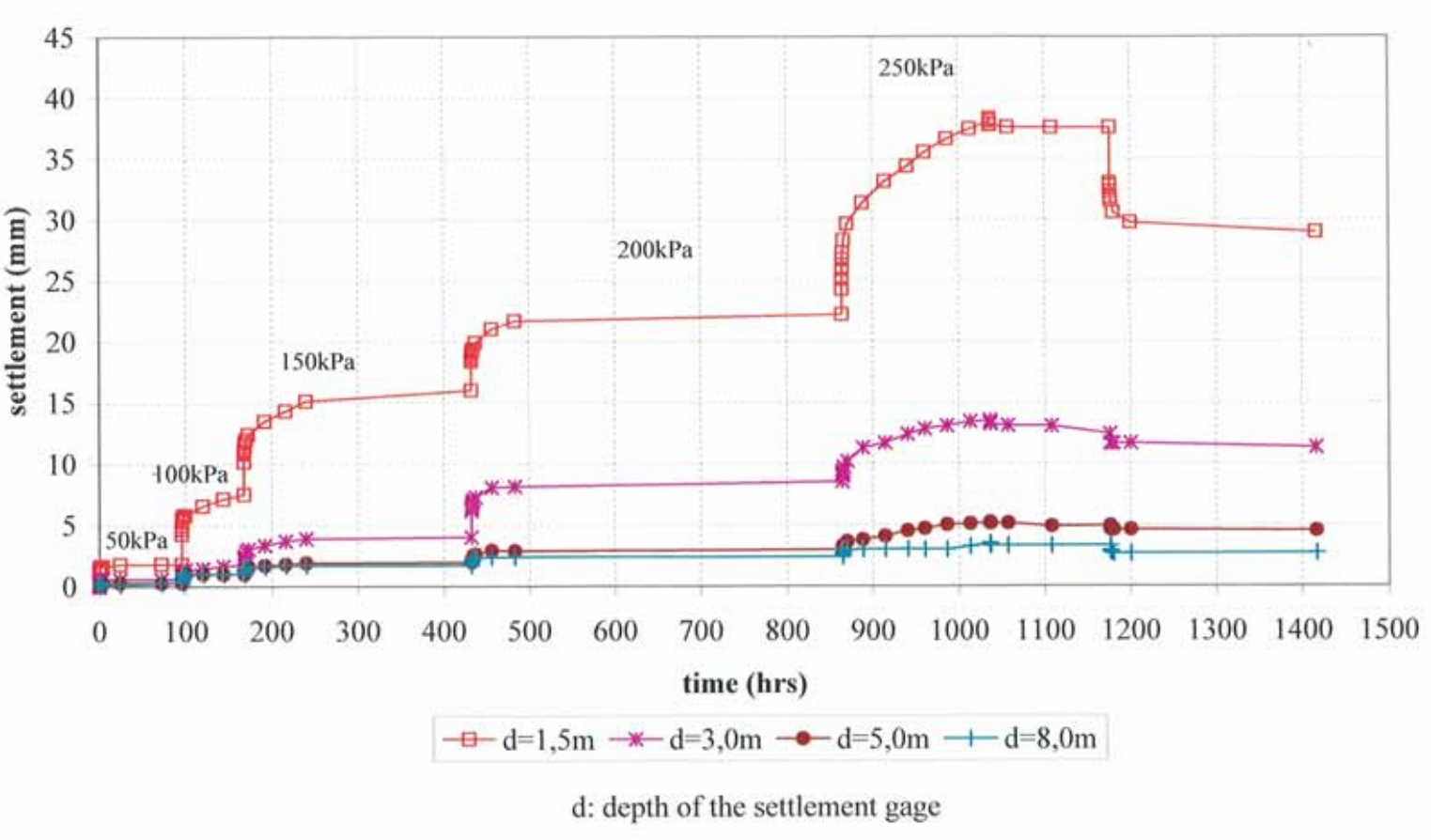

Figure 5.11 Deep settlement-time relationship for L=8.0m aggregate pier group loading (Group C)

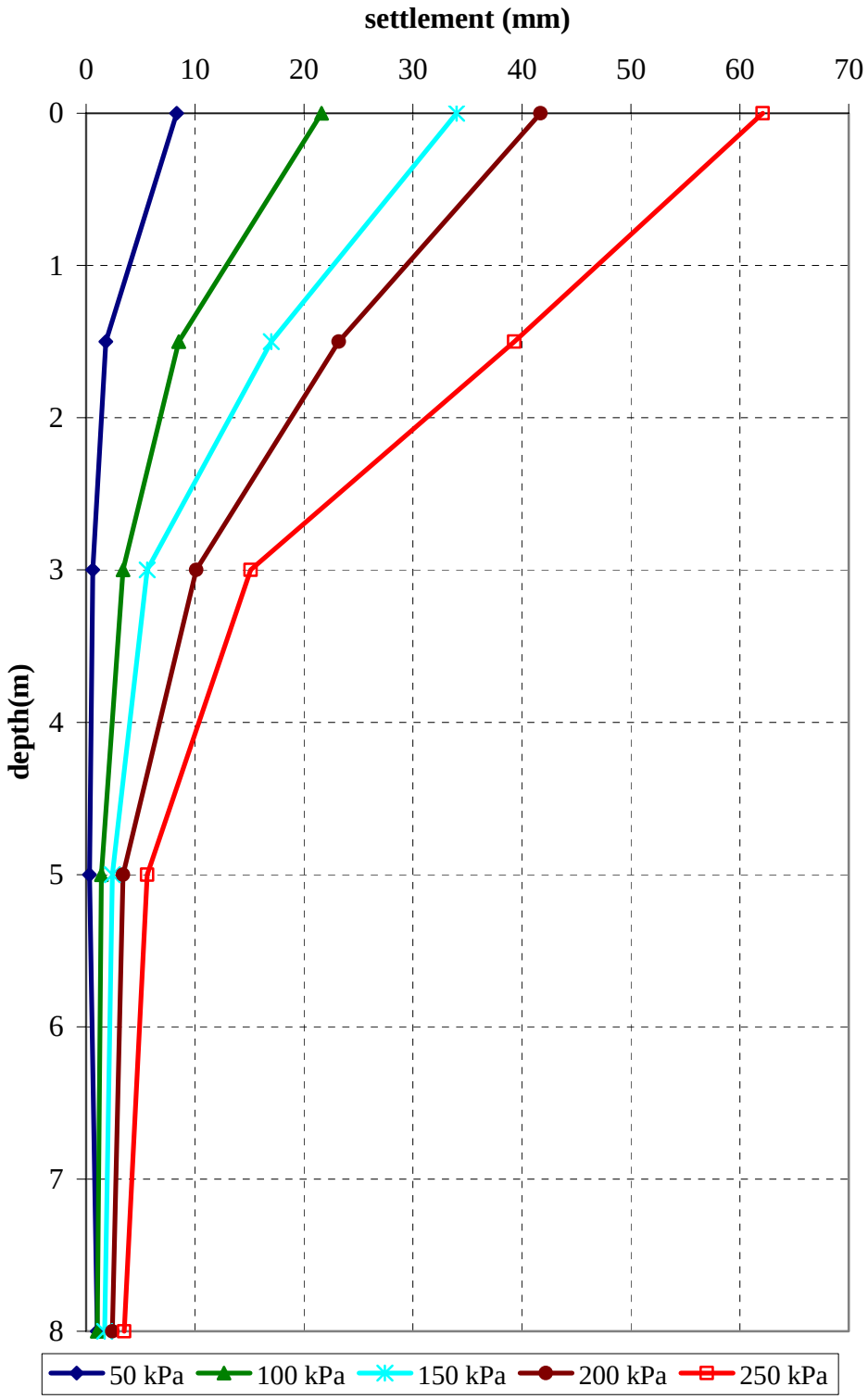

Figure 5.12 Variation of settlements with depth in the soil improved with 8.0m lengths of aggregate piers (Group C)

In Figure 5.13 the measured stress on aggregate pier, σ_s, and the back-calculated stress on clay, σ_c, are shown as a function of applied surface pressure. It is observed that stress on aggregate pier, σ_s, and stress on clay, σ_c, linearly increase with increasing applied stress.

Table 5.5 The measured stress on aggregate pier, σ_s, the back-calculated stress on clay, σ_c and the stress concentration factor, n for each aggregate pier groups

Applied Surface Pressure σ (kPa)	**Group A (L=3.0m)**		**Group B (L=5.0m)**		**Group C (L=8.0m)**	
	σ_s (kPa)	**σ_c** (kPa)	**σ_s** (kPa)	**σ_c** (kPa)	**σ_s** (kPa)	**σ_c** (kPa)
50	161	13	216	-	176	8
100	260	47	220	60	234	56
150	338	87	314	96	318	94
200	405	132	375	142	393	136
250	462	179	410	197	441	186

The variation of σ_s with time can be seen in Figure 5.14 for 3.0m length of aggregate pier group loading. The stress on aggregate pier is approximately constant with time.

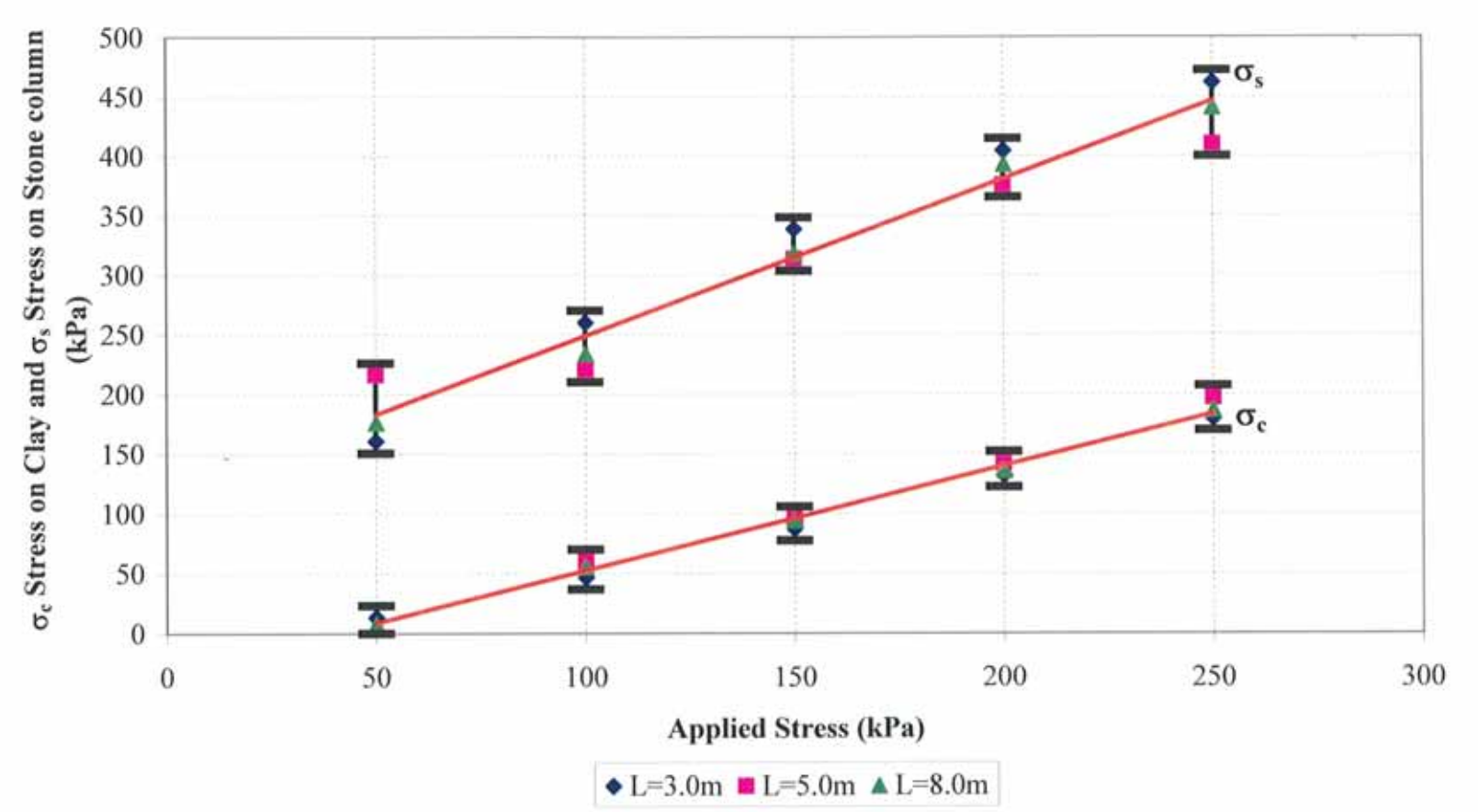

Figure 5.13 Variation of σ_s and σ_c with applied surface pressure

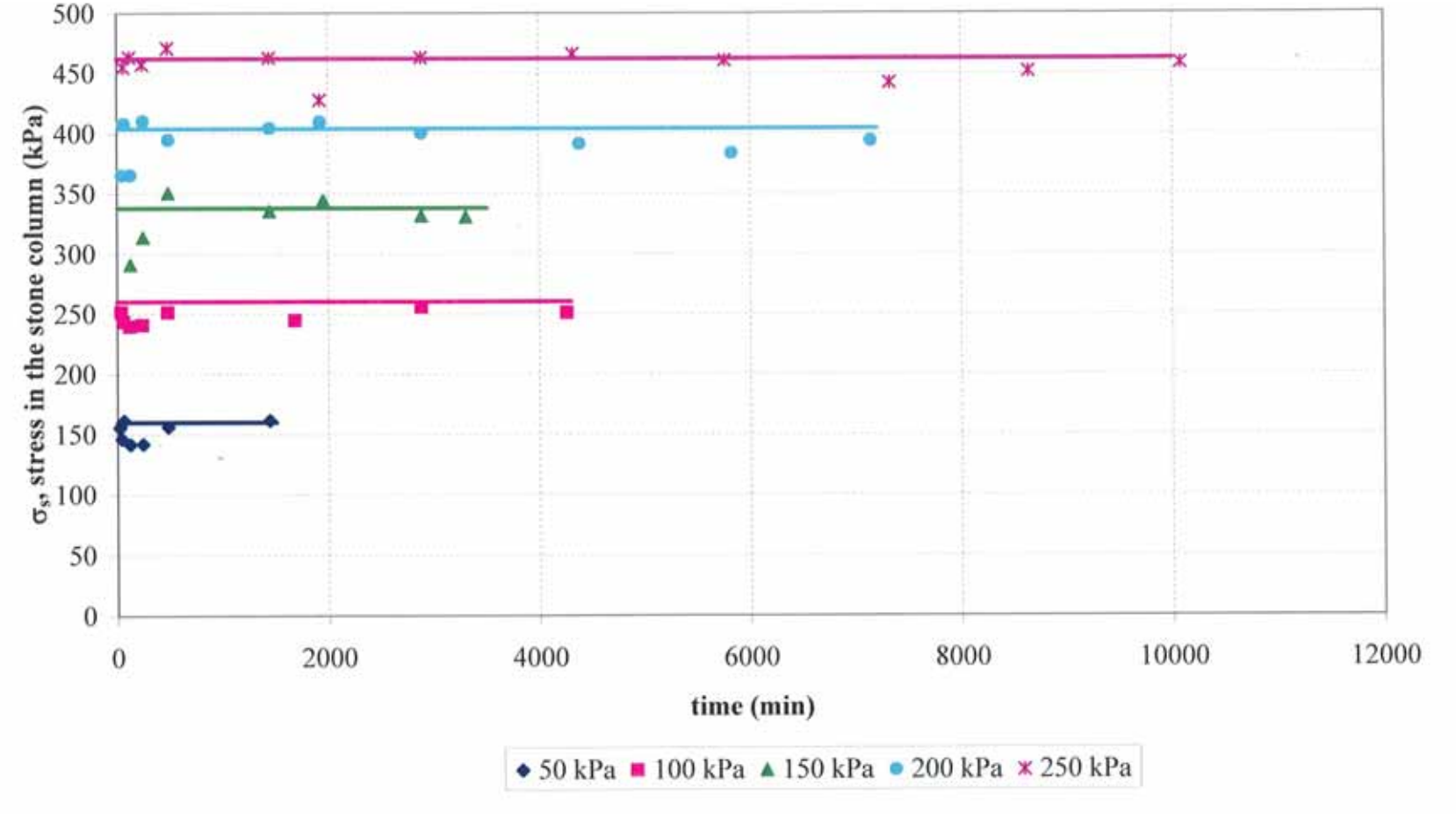

Figure 5.14 Variation of σ_s with time for 3.0m length of aggregate pier group loading

5.4 Single Pier Load Test Results

The single pier load tests were performed on three individual aggregate piers of 3, 5 and 8m in length. The procedure of the tests was given in Chapter III, Section 3.9.

The measured settlements of 3, 5 and 8m length of single aggregate piers at each applied load increments are tabulated in Table 5.6.

Either end bearing or free floating stone columns greater than about 2-3 diameters in length fail in bulging (Barksdale and Bachus, 1983). Similarly, Hughes and Withers (1974) states that the considerable vertical and lateral distortion which occurs at the top of the column rapidly diminishes with depth and at failure, about 4 diameters length of the column is being significantly strained. Therefore, it may be expected that the load –settlement behaviors of 3, 5 and 8m length of aggregate piers are very close to each other. In this study, the load-settlement behavior of 3 and 5 m length of individual aggregate pier are close to each other, on the other hand 8m length of individual did not reflect the expected behavior. As a result, the average settlements of 3 and 5 m length of piers are taken as a general trend of the individual pier load-settlement behavior.

The load-settlement behaviors observed in these tests are shown in Figure 5.15.

Table 5.6 The measured settlements of single pier tests

Pressure (kPa)	**Settlement of L=3.0m pier (mm)**	**Settlement of L=5.0m pier (mm)**	**Settlement of L=8.0m pier (mm)**	**Average settlement of L=3m and L=5m piers**
30	1.4	1.1	2.9	1.3
90	3.7	3.0	6.1	3.4
151	6.0	5.0	10.3	5.5
211	8.4	7.0	13.8	7.7
271	10.6	9.1	18.7	9.9
331	13.3	11.5	24.2	12.4
392	16.3	14.3	30.7	15.3
452	19.2	17.5	37.7	18.4
301	19.1	17.0	37.6	18.1
151	18.4	16.2	37.2	17.3
0	14.9	14.1	34.0	14.5

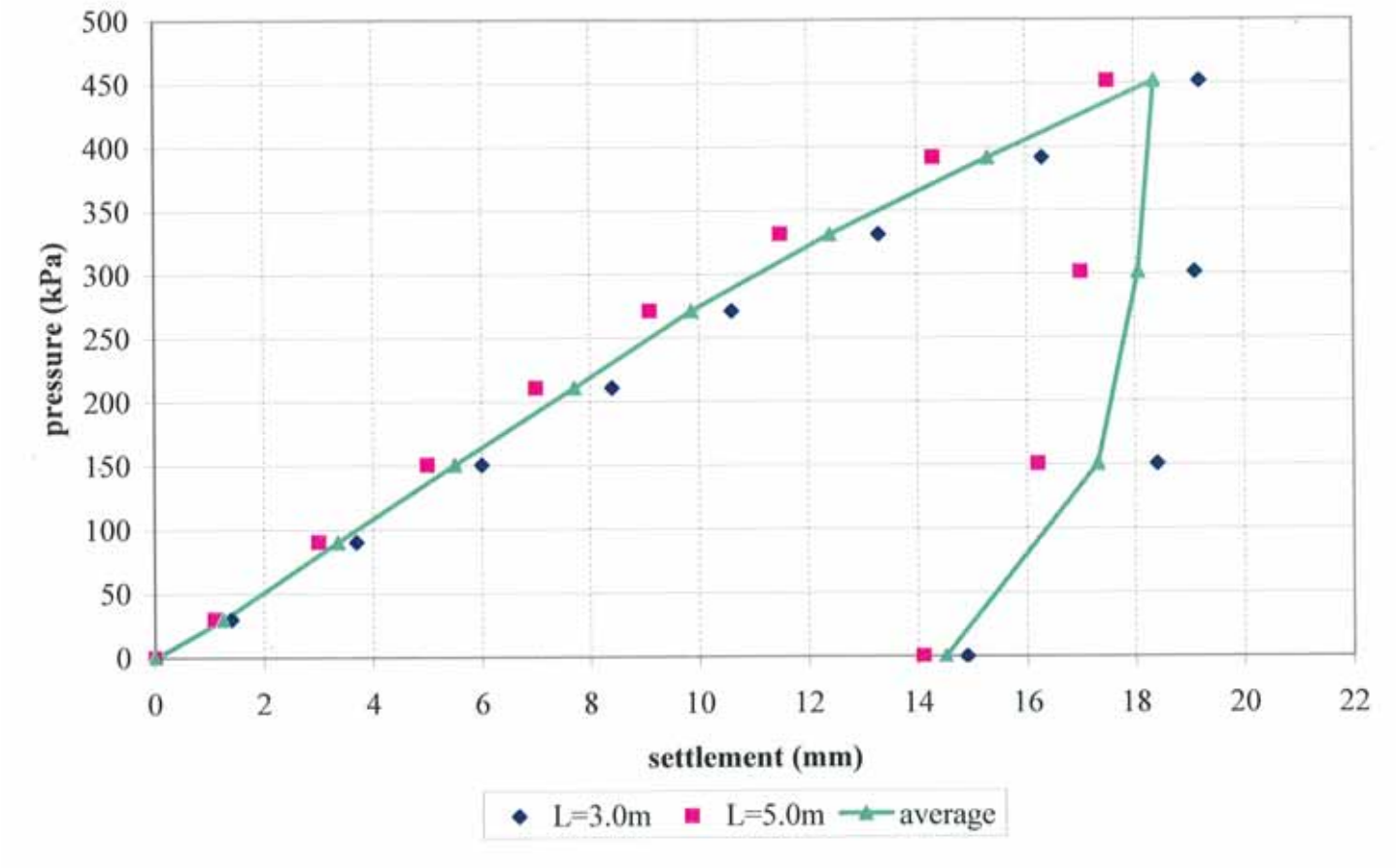

Figure 5.15 The load-settlement behavior of 3 and 5 m lengths of individual aggregate piers

CHAPTER VI

DISCUSSION OF TEST RESULTS

6.1 Introduction

The results obtained from field measurements were given in Chapter V. This chapter includes the discussion on the settlement behavior and the stress distribution of the floating and end-bearing type of aggregate pier groups.

In the proceeding sections the improvement in settlement, comparison of the settlement reduction ratio with conventional methods will be discussed.

Elastic modulus and modulus of subgrade reaction of the untreated soil and aggregate pier will be analyzed.

6.2 Settlement Improvement

The surface settlement-pressure relationships of the untreated soil and aggregate pier group loadings are given in Figure 6.1 and Figure 6.2 respectively. It is observed that at small magnitude of vertical stress the measured settlements are close to each other at different pier length. The effect of pier length in reducing the settlements becomes effective at relatively higher vertical stress range.

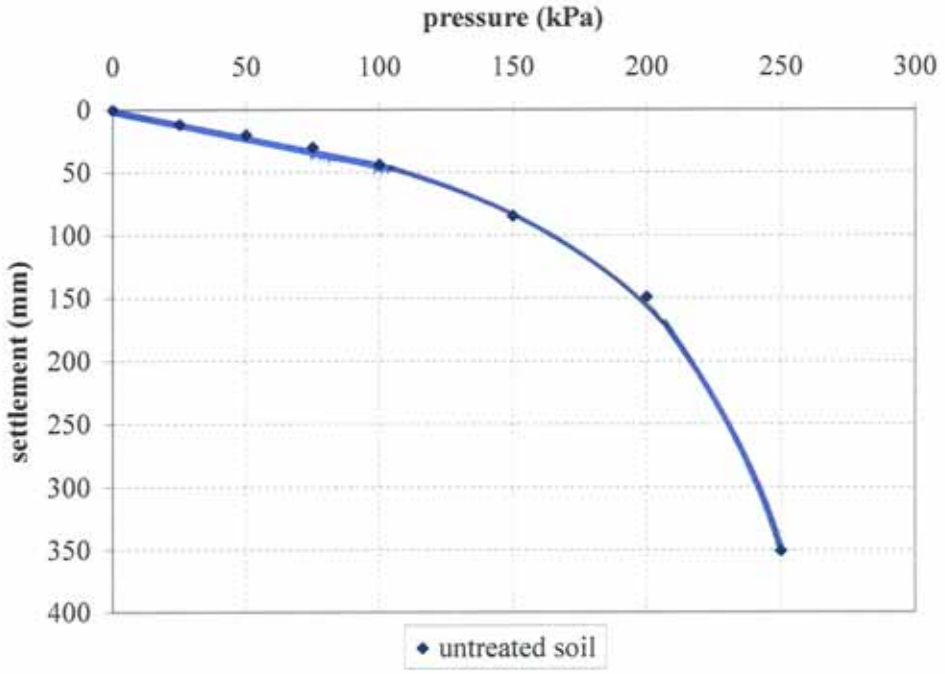

Figure 6.1 Surface settlement-pressure relationships for untreated soil

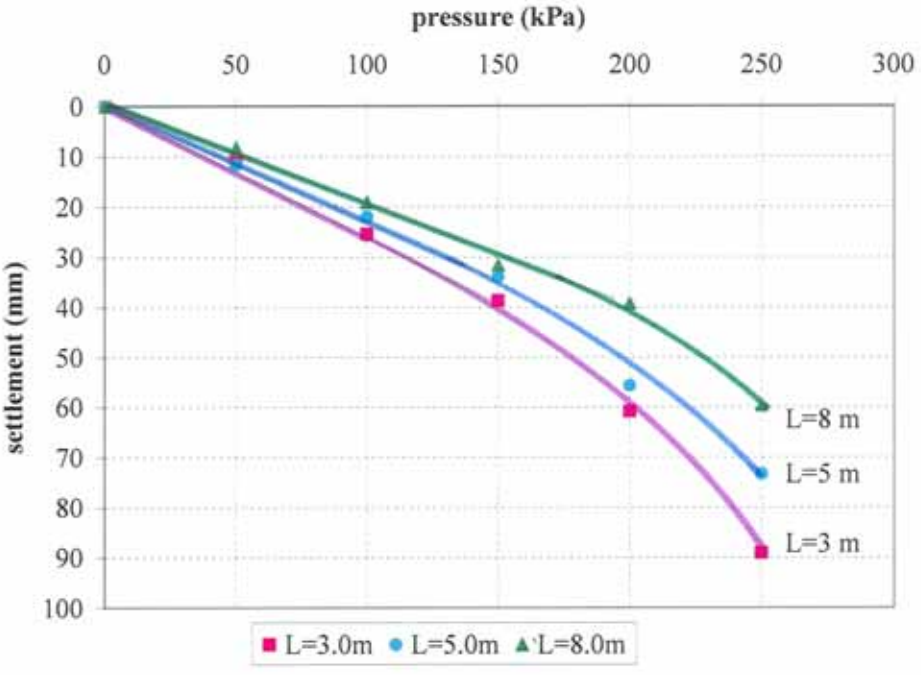

Figure 6.2 Surface settlement-pressure relationships for aggregate pier groups

It is also observed that the rate of settlements with respect to applied vertical stress increases significantly for the stresses exceeding 200 kPa. This behavior indicates that the ultimate bearing capacity of the untreated soil is reached at about 200 kPa normal stress. This behavior can also be seen in Figure 5.1.

In Figures 6.3 to 6.7 settlement variations of aggregate pier reinforced soil with depth under each applied pressure can be seen. It is observed that in Group B tests (lengths of piers are 5.0m) the deep settlement gage at 3.0m depth did not function properly to reflect the expected behavior. Therefore in the interpretations, these gage readings were disregarded.

6.2.1 Settlement Reduction Ratio, S_t/S

The magnitude of S_t/S ratios (the ratio of settlements of the aggregate pier improved ground to the unimproved ground) are tabulated in Table 6.1.

Variation of S_t/S ratio with applied pressure is given in Figure 6.8.

Table 6.1 S_t/S ratios (the ratio of settlements of the aggregate pier improved ground to the unimproved ground)

Applied Surface Pressure σ (kPa)	**S_t/S** (the ratio of settlements of the aggregate pier improved ground to the unimproved ground)			
	Group A (L=3.0m)	**Group B (L=5.0m)**	**Group C (L=8.0m)**	**Average**
50	0.535	0.585	0.415	0.560
100	0.523	0.502	0.493	0.508
150	0.427	0.400	0.400	0.414
200	0.391	0.373	0.279	0.335
250*	0.247	0.209	0.177	0.212

* Bearing Capacity Failure (BFC) is reached.

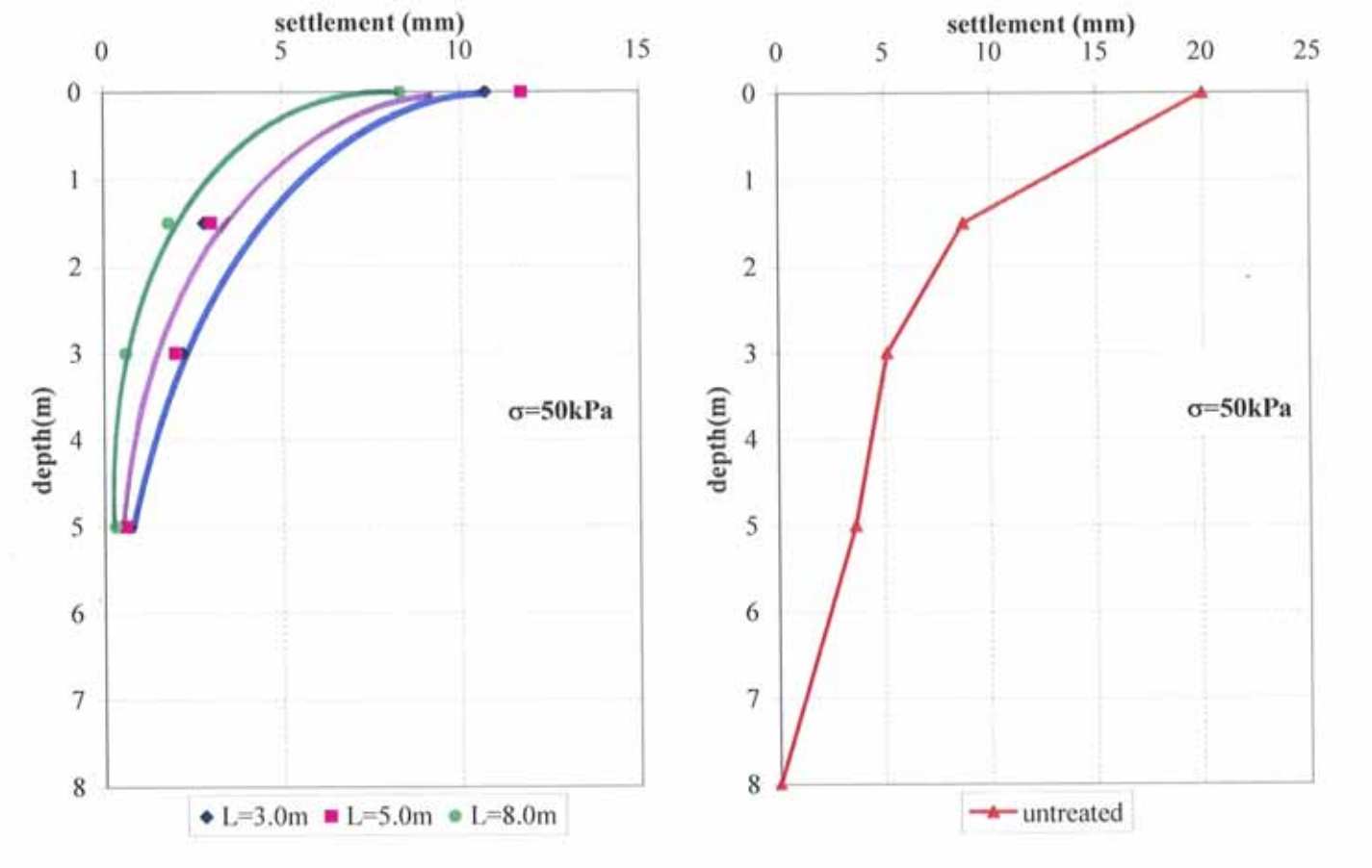

Figure 6.3 Settlement-depth relationship for aggregate pier groups at σ=50 kPa

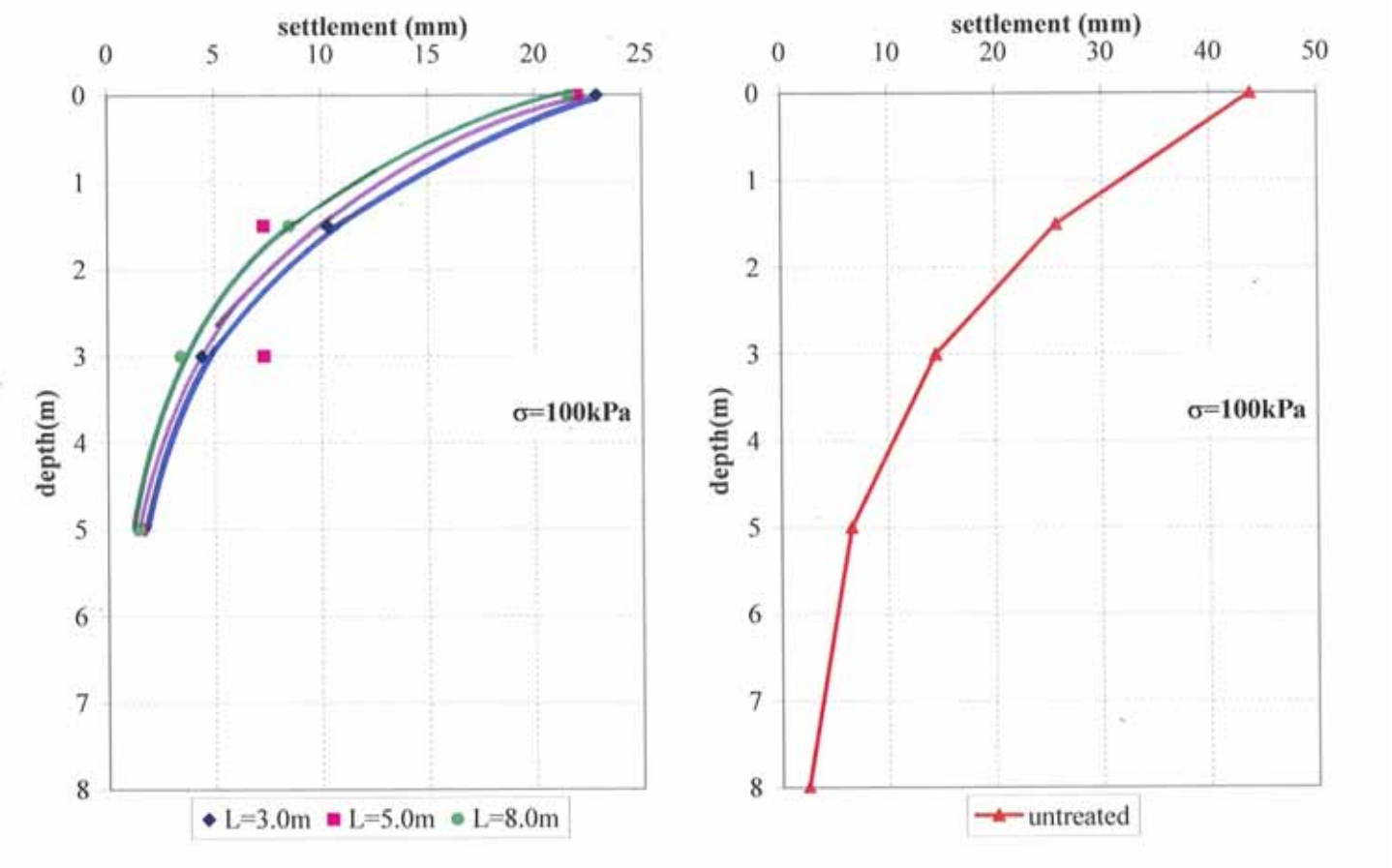

Figure 6.4 Settlement-depth relationship for aggregate pier groups at σ=100 kPa

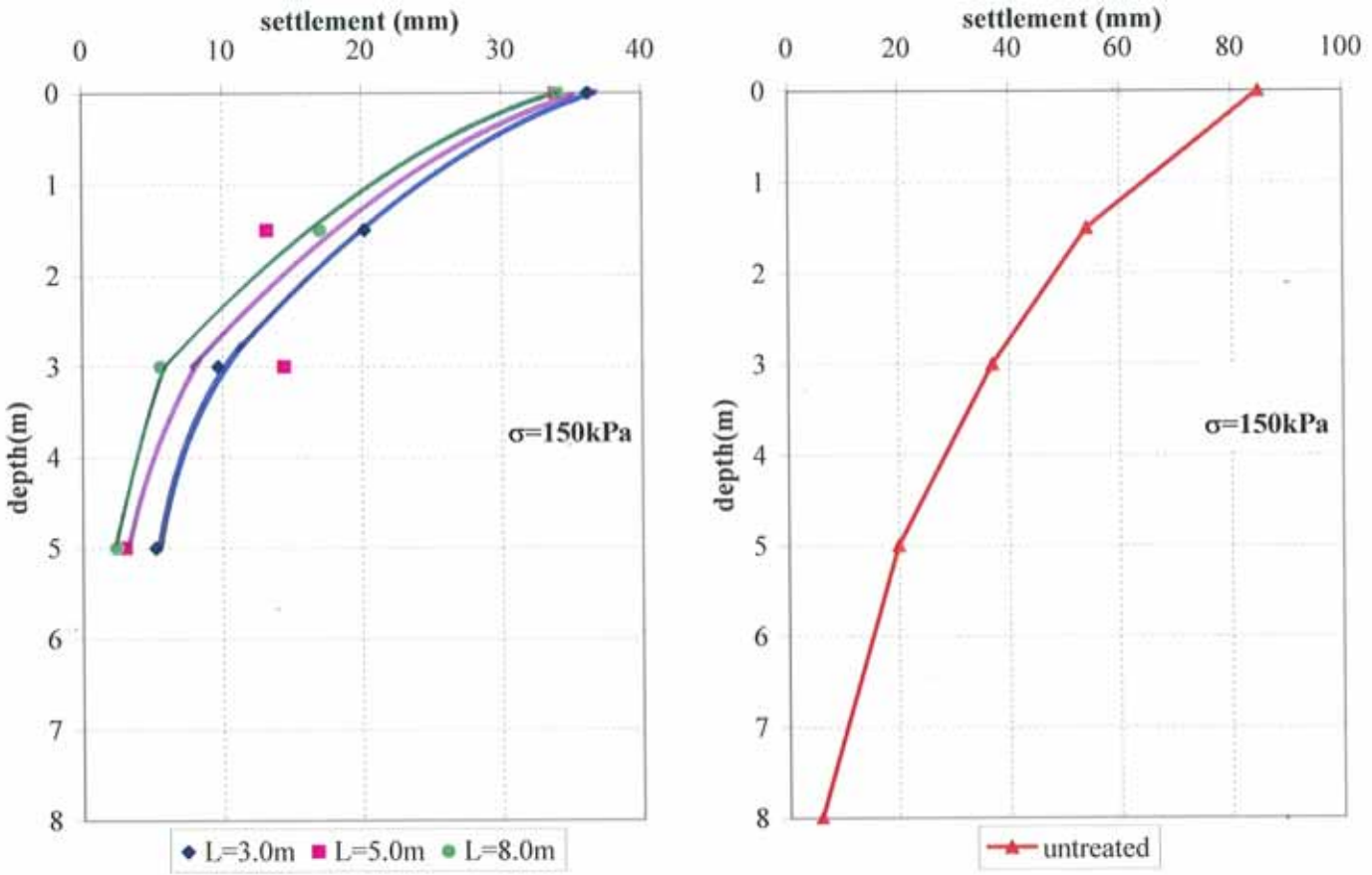

Figure 6.5 Settlement-depth relationship for aggregate pier groups at σ=150 kPa

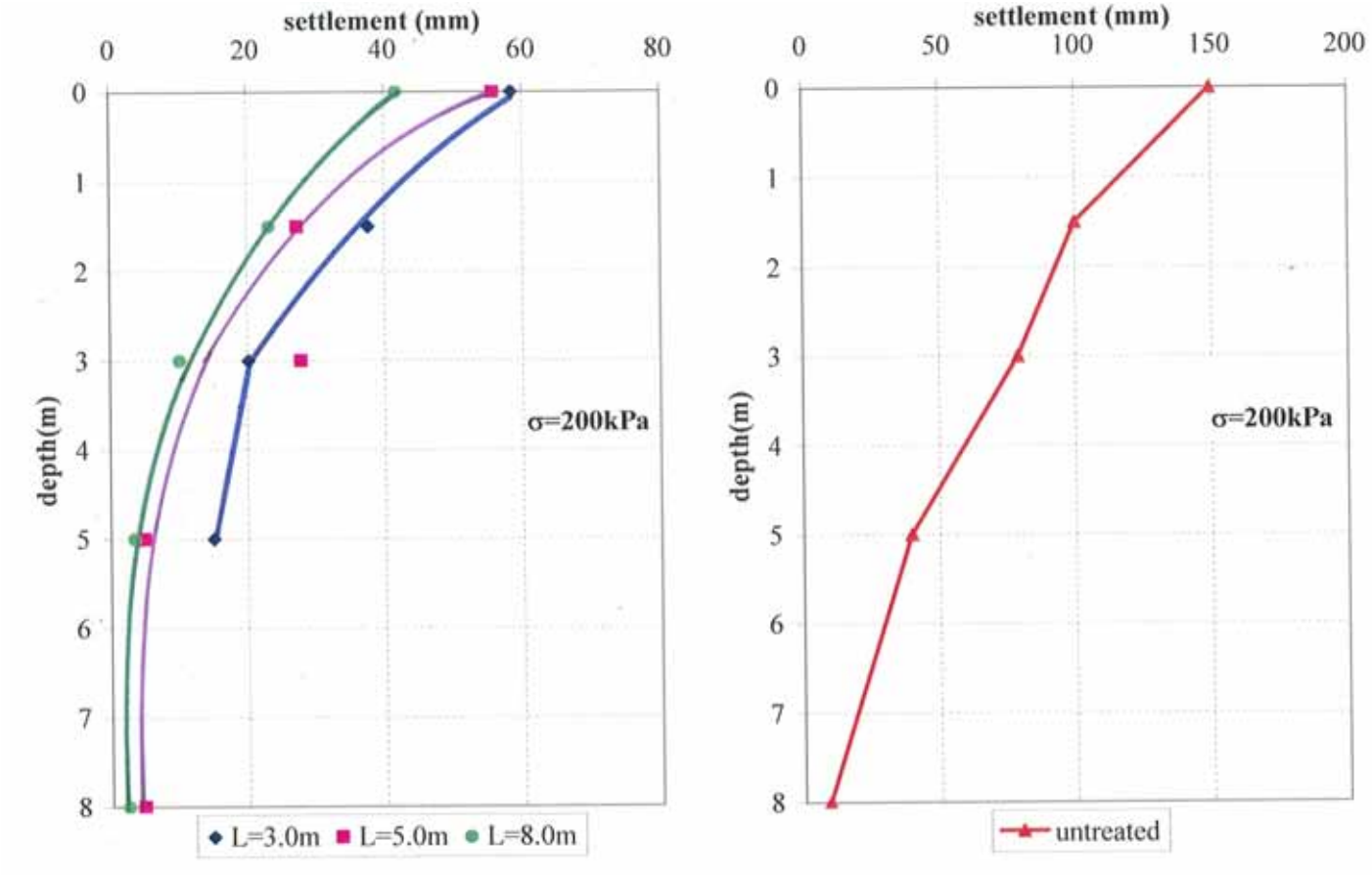

Figure 6.6 Settlement-depth relationship for aggregate pier groups at σ=200 kPa

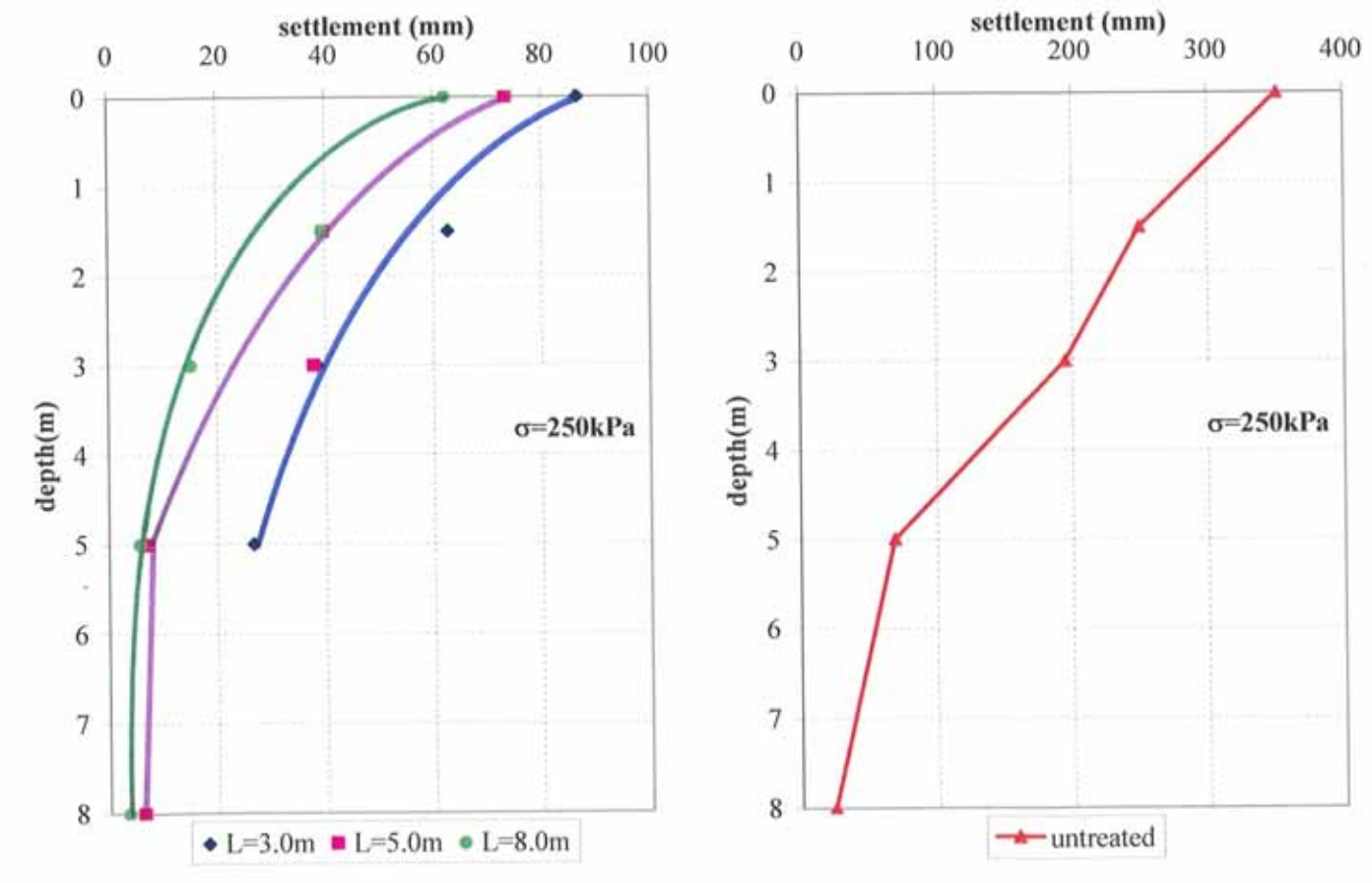

Figure 6.7 Settlement-depth relationship for aggregate pier groups at σ=250 kPa

The settlement improvement ratio calculated from the surface settlements shows a decreasing trend with increasing vertical stress in the staged loading conditions. The magnitude of the improvement ratio is at the order of 0.6 at 50 kPa and is reduced to an average value of 0.34 at 200 kPa of vertical stress. This means that the efficiency of the piers in reducing the settlements becomes more effective at relatively higher vertical stress range.

S_t/S values are plotted with respect to pier length at every applied load stage in Figure 6.9. The settlement reduction factor in the group with 3m long piers was in the range from 0.39 to 0.54. Whereas the magnitude of the settlement reduction factor in the 8m length end bearing columns are in the range from 0.28 to 0.42, revealing that increasing the column length from 3m to 8m, could only marginally improve the settlements, and major improvement in the settlements take place at relatively short column lengths. In settlement improvement ratio versus pier length plot, the data trends show an inconsistent behavior at first stage loading of 50 kPa probably due to a seating problem at the beginning of the test.

It is found that the relationship between settlement reduction ratio and the applied stress is approximately linear within the pressure range of 0-200 kpa. The slope line is steeper after 200 kPa reflecting the effect of bearing capacity failure.

6.2.2 Settlement Reduction Ratio beneath the Treated Zone, $(S_t/S)_b$

It has been observed that, the settlements measured in the clay situated below aggregate pier are consistently smaller as compared to untreated soil settlements. This improvement in the settlements below the piers is illustrated in Figure 6.10. In this figure, s_1 corresponds to settlement of the untreated loading and s_2 is the settlement of the treated loading below the treated zone. The difference in settlements is denoted as Δs. Then a settlement reduction ratio beneath the treated zone is defined as $(S_t/S)_b = s_2/s_1$.

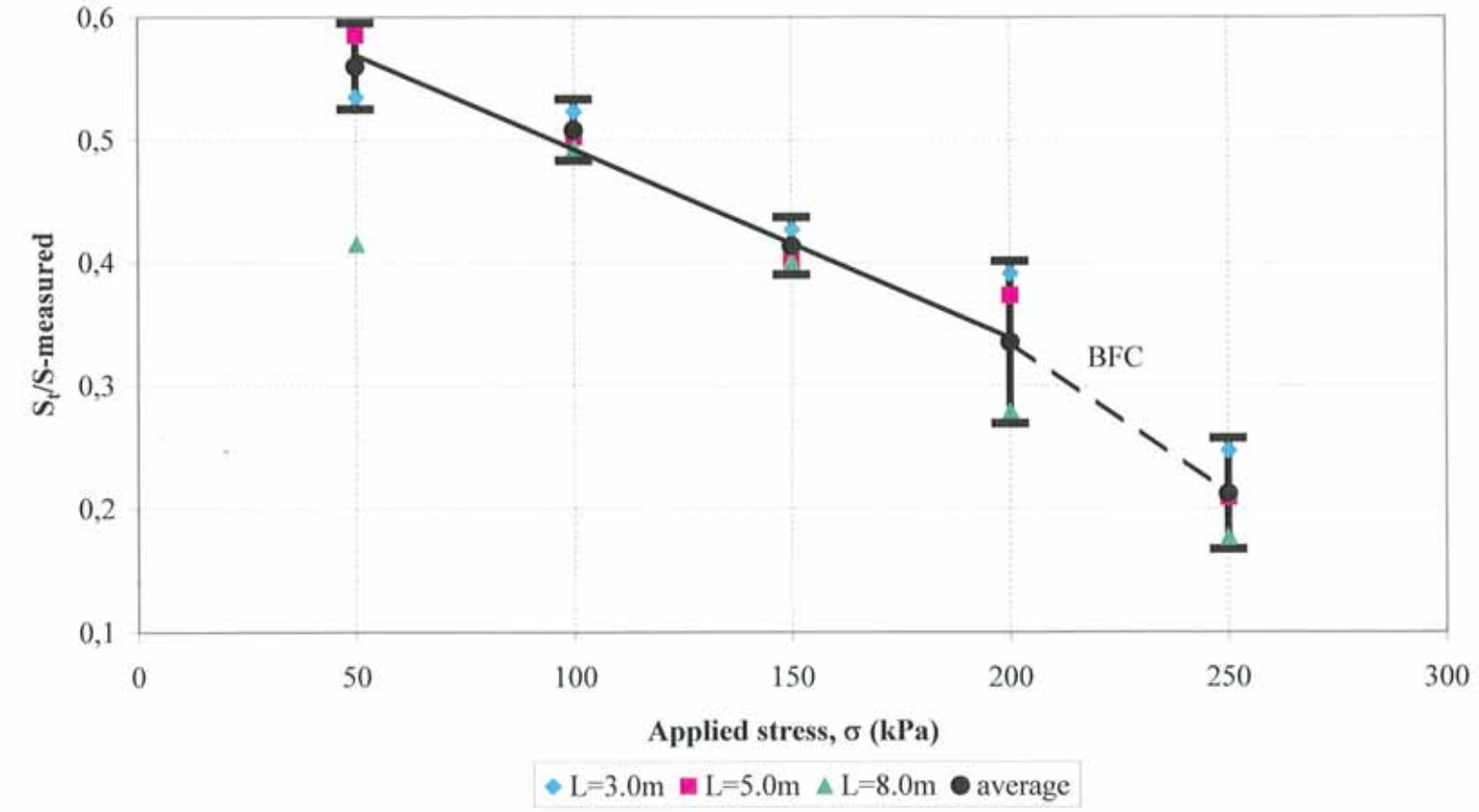

Figure 6.8 Variation of St/S ratio with applied pressure

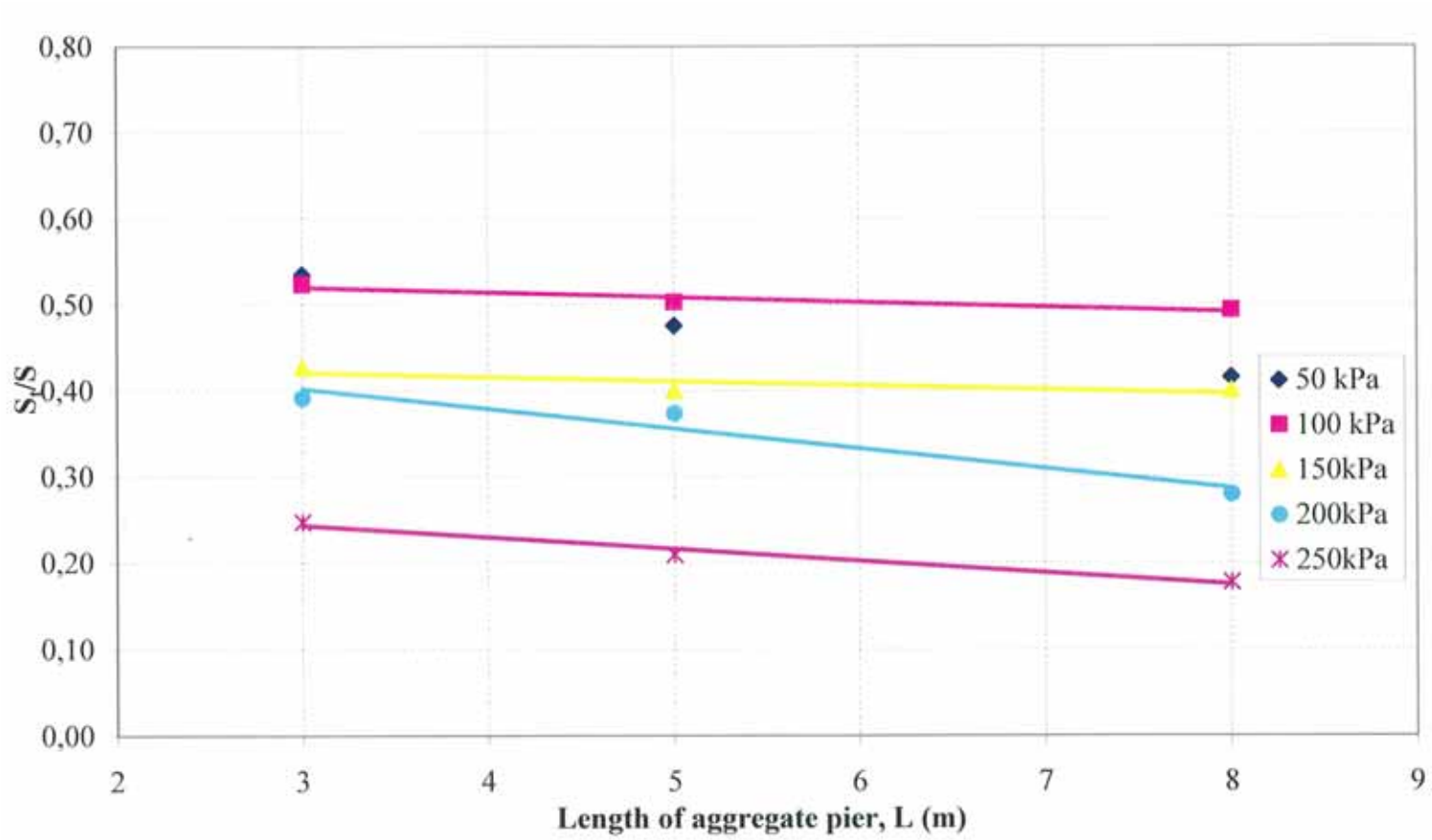

Figure 6.9 Variation of S_t/S ratio with pier length

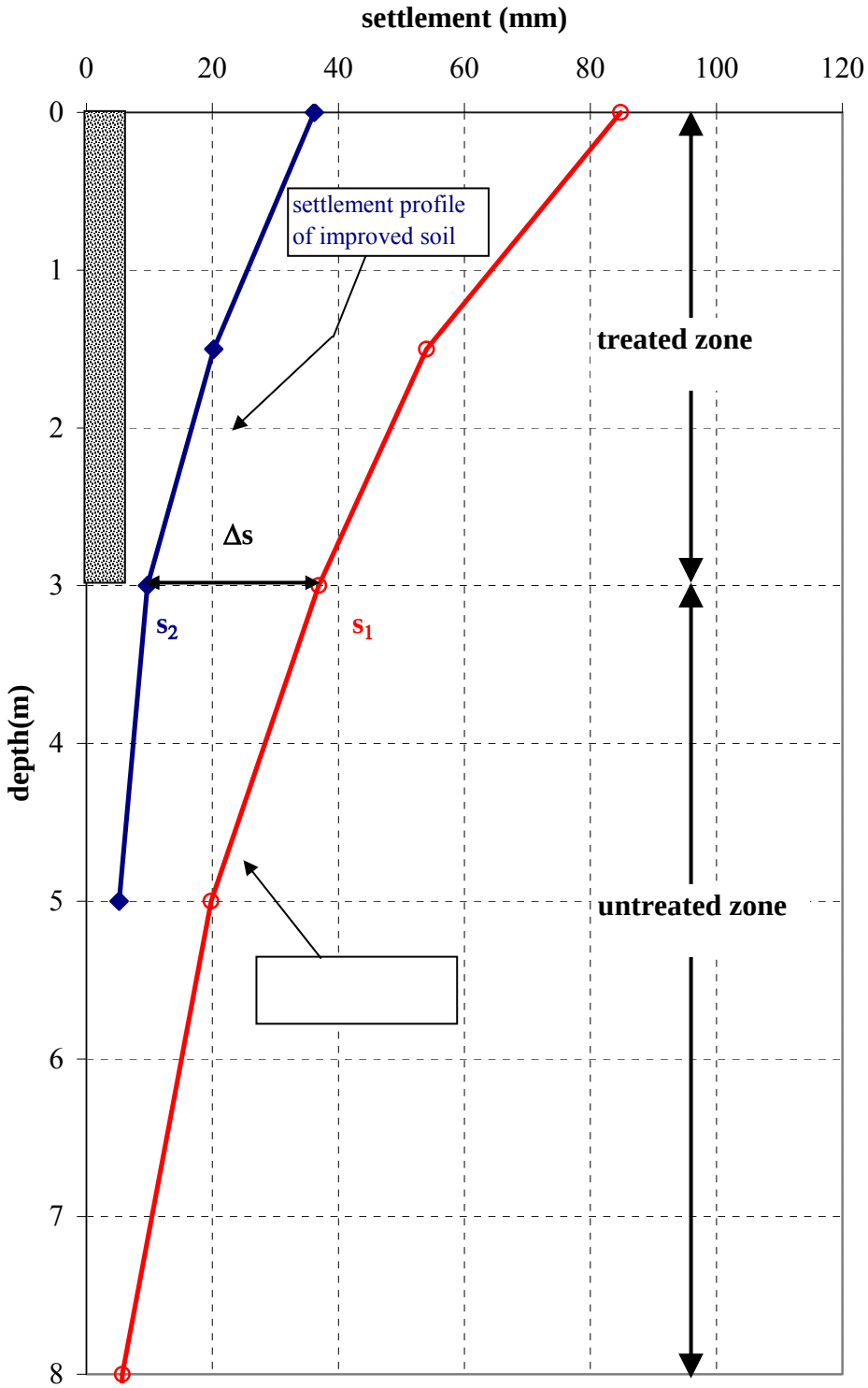

Figure 6.10 Descriptive sketch showing the improvement in settlements beneath the treated zone (data taken from Group A loading under σ=150 kPa)

The calculated $(S_t/S)_b$ values are given in Table 6.2 for Group A (improved soil with 3.0m lengths of aggregate piers) and Group B (improved soil with 5.0m lengths of aggregate piers) loadings. The cumulative settlement reduction ratios, S_t/S are also given in this table.

Table 6.2 S_t/S and $(S_t/S)_b$ values at each applied loading

Applied Surface Pressure σ (kPa)	**Group A (L=3.0m)**		**Group B (L=5.0m)**	
	S_t/S	**$(S_t/S)_b$**	**S_t/S**	**$(S_t/S)_b$**
50	0.535	0.431	0.585	0.167
100	0.523	0.306	0.502	0.231
150	0.427	0.263	0.400	0.152
200	0.391	0.256	0.373	0.123
250*	0.247	0.198	0.209	0.105

* BCF (bearing capacity failure)

As shown in Table 6.2 the $(S_t/S)_b$ ratios for Group B loading have remarkable small values possibly not reflecting the expected trend. This is due to the fact that the stress transmitted to a depth of 5.0m under plate of 3.0x3.5 sq.m for Group B loading is almost negligible and therefore the settlement below 5.0m depth is insignificant. Thus consideration of improvement in settlements below 5.0m depth is not quite relevant for discussion of $(S_t/S)_b$ ratios in the case studied.

The comparison of (S_t/S) and $(S_t/S)_b$ values in Group A loading shown in Figure 6.11 indicates that the improvement in the untreated zone of reinforced soil is more than the cumulative surface settlement improvements.(i.e. $(S_t/S)_b<(S_t/S)$).

Akdoğan (2001) also reports an improvement in the settlements below the untreated zone of reinforced soil from the model footing tests results. Magnitude of $(S_t/S)_b$ ratios were on the order of 0.6-0.7 and are higher than the (S_t/S) ratios reported in this study.

The results clearly indicate that, there is a net reduction in settlements in the untreated zone of the reinforced soil as compared to untreated soil profile. Since the compressibility of the clay remains the same in both reinforced and unreinforced soil (i.e. below the piers), this improvement should be due to the difference in the transmitted magnitude of vertical stress in the two cases.

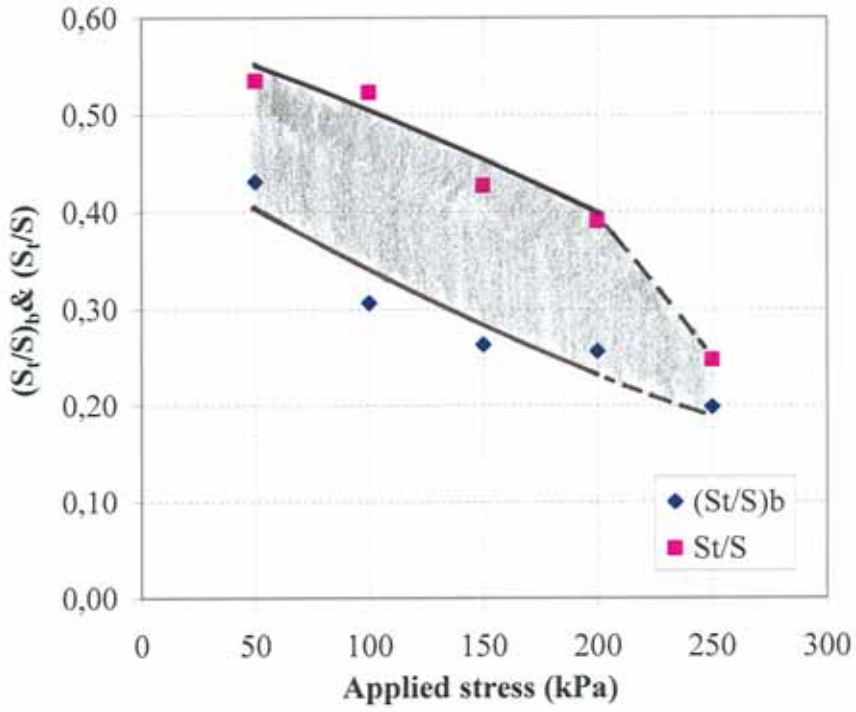

Figure 6.11 $(S_t/S)_b$ variation with applied pressure in Group A loading

An estimate of the applied stress transmitted to the interface between the lower zone (untreated clay strata) and the upper zone (composite strata) is needed so that predicted settlements in the zones can be calculated. Burmister's (1958, referring to Lawton et.al. 1994) and Fox (1948) methods on two layered elastic strata of infinite horizontal extend clearly showed that the presence of a stiffer upper layer substantially reduces the applied stress transmitted to the lower, more compressible layer compared to the case of a homogeneous soil. For example, for a uniform circular load, E_1/E_2=10, and a thickness of the upper layer equal to the radius of the loaded area, the vertical normal stress beneath the centerline of the loaded area at the interface between the two materials is about 30% of the applied stress, compared to about 65% for a homogeneous soil (Boussinesq-type analysis) at the same depth. Similarly, for a uniform circular load, E_1/E_2 = 10, and a thickness of the upper layer equal to the twice the radius of the loaded are, i.e. represents Group A in this study, the vertical normal stress at the interface is about 10% of the applied stress, compared to about 30% for a homogeneous soil at the same depth as shown in Figure 6.12.

Lawton et al. (1994) suggest an approximate stress dissipation slope as V:H= 1.67:1 instead of conventional V:H=2:1 approach, to reflect the effect of stiffer upper layer on the vertical stress distribution in practical applications.

6.3 Stress Distribution in Aggregate Pier Groups

The stress concentration factor n required calculating σ_c, magnitude of the stress in the clay, is usually preferred to estimate from the results of stress measurements made in full-scale load tests instead of driving from the elastic theory. It has been stated that stress concentration factor n is dependent on a number of variables including relative stiffness between natural soil and the pier material, length of the aggregate pier, area ratio, characteristics of the granular blanket placed over the aggregate pier (Barksdale and Bachus, 1983).

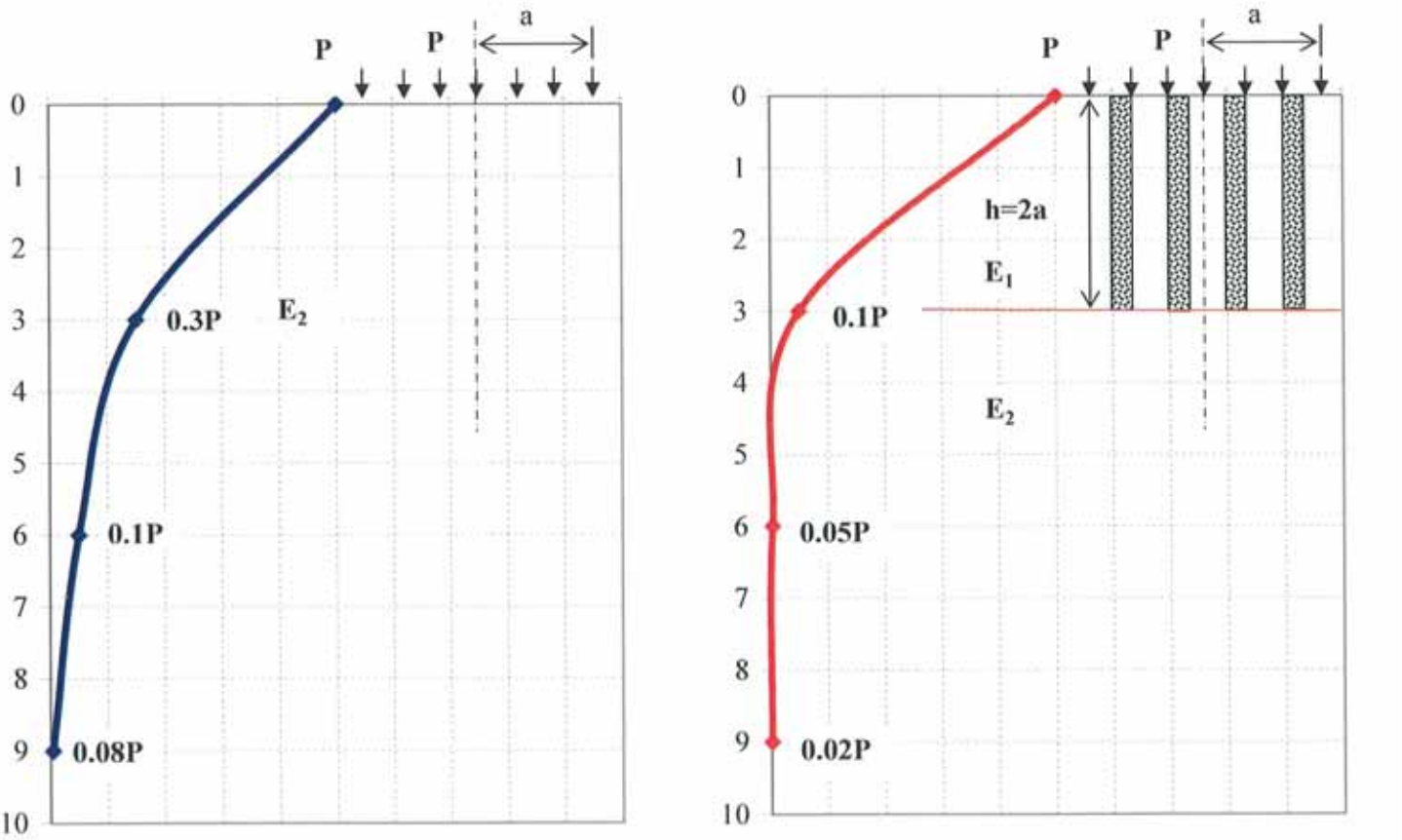

Figure 6.12 Axial stress as percentage of applied loading of uniform vertical loading on a circular area in two layer system, E_1/E_2 =10 and in homogeneous soil (Poulos and Davis, 1974)

Values of stress concentration factor measured in field and laboratory studies have generally varied between 2.5 and 5.0. The stress concentration factor measured in the studies was either approximately constant or increased with time as consolidation occurred (See Table 2.4).

The variation of stress on the piers, σ_s with time can be seen in Figure 5.14 for 3.0m length of aggregate pier group loading. In this study, the stress on aggregate pier is observed to be constant with time, consequently the stress concentration factor, n does not vary with time.

In Table 6.3 the measured stress on aggregate pier, σ_s, the back-calculated stress on clay, σ_c and the stress concentration factor, n are summarized for each aggregate pier group.

The variation of stress concentration factor, n with applied surface pressure is given in Figure 6.13. The n values are presented for the stress range from 100 kPa to 250 kPa excluding the first stage loading of 50 kPa. At the first stage loading the data deviates from the general trend possibly due to the seating problem of the plate over the loose blanket layer, and therefore not included in Figure 6.13.

As a general trend the n factor has a tendency to decrease with increasing vertical stress and the trend is practically linear. In this study, values of stress concentration factor, n have been between 2.1 and 5.6 with an average of 3.5, which is comparable with the previously reported values of n.

The variation of n values with pier length as well as stress level is given in Figure 6.14. The data trends shown in Figure 6.14 indicates that L=5.0m and L=8.0m pier length mobilize similar n values, and slightly higher n values are measured for the L=3.0m pier length. The difference in the behavior of 3.0m pier length as compared to the longer ones is probably due to the stress distribution in the two cases compared. The longer columns (i.e. 5 and 8m

lengths) behave as end bearing column since the stress transmitted to depth 5m or more is in significant.

Table 6.3 The measured stress on aggregate pier, σ_s, the back-calculated stress on clay, σ_c and the stress concentration factor, n for each aggregate pier

Applied Surface Pressure σ (kPa)	**Group A (L=3.0m)**			**Group B (L=5.0m)**			**Group C (L=8.0m)**		
	σ_s (kPa)	**σ_c** (kPa)	**n**	**σ_s** (kPa)	**σ_c** (kPa)	**n**	**σ_s** (kPa)	**σ_c** (kPa)	**n**
50	161	13	12.4	216	-		176	8	22
100	260	47	5.5	220	60	3.7	234	56	4.2
150	338	87	3.9	314	96	3.3	318	94	3.4
200	405	132	3.1	375	142	2.7	393	136	2.9
250	462	179	2.6	410	197	2.1	441	186	2.4

In the aggregate pier terminology generally the ratio of the stress on clay to the total stress (σ_c/σ) is denoted as μ_c and the ratio of stress on pier to total stress (σ_s/σ) as μ_s. The variation of μ_c and μ_s with applied surface pressure can be seen in Figures 6.15 and 6.16 respectively.

Granular Wall Method presented by Van Impe and De Beer (1983) is explained in Section 2.3.5.7. Stress distribution of stone columns given in Figure 2.30 gives m=0.5 and 0.57 for area ratio and as = 0.25 and internal friction angle of stone column, $\phi'_s = 40^0$ and $\phi'_s = 45^0$ respectively. In this method the parameter m is defined as $m= \alpha\ \sigma_s/\sigma = \alpha\ \mu_s = a_s\mu_s$. This means that the ratio of stress on aggregate pier, μ_s is in the range of 2 to 2.3 for a range of an internal friction angle of stone column , $\phi'_s = 40^0$ to 45^0. This range for μ_s is very compatible with measured μ_s values in this study which is in the range of 1.7 to 3.8.

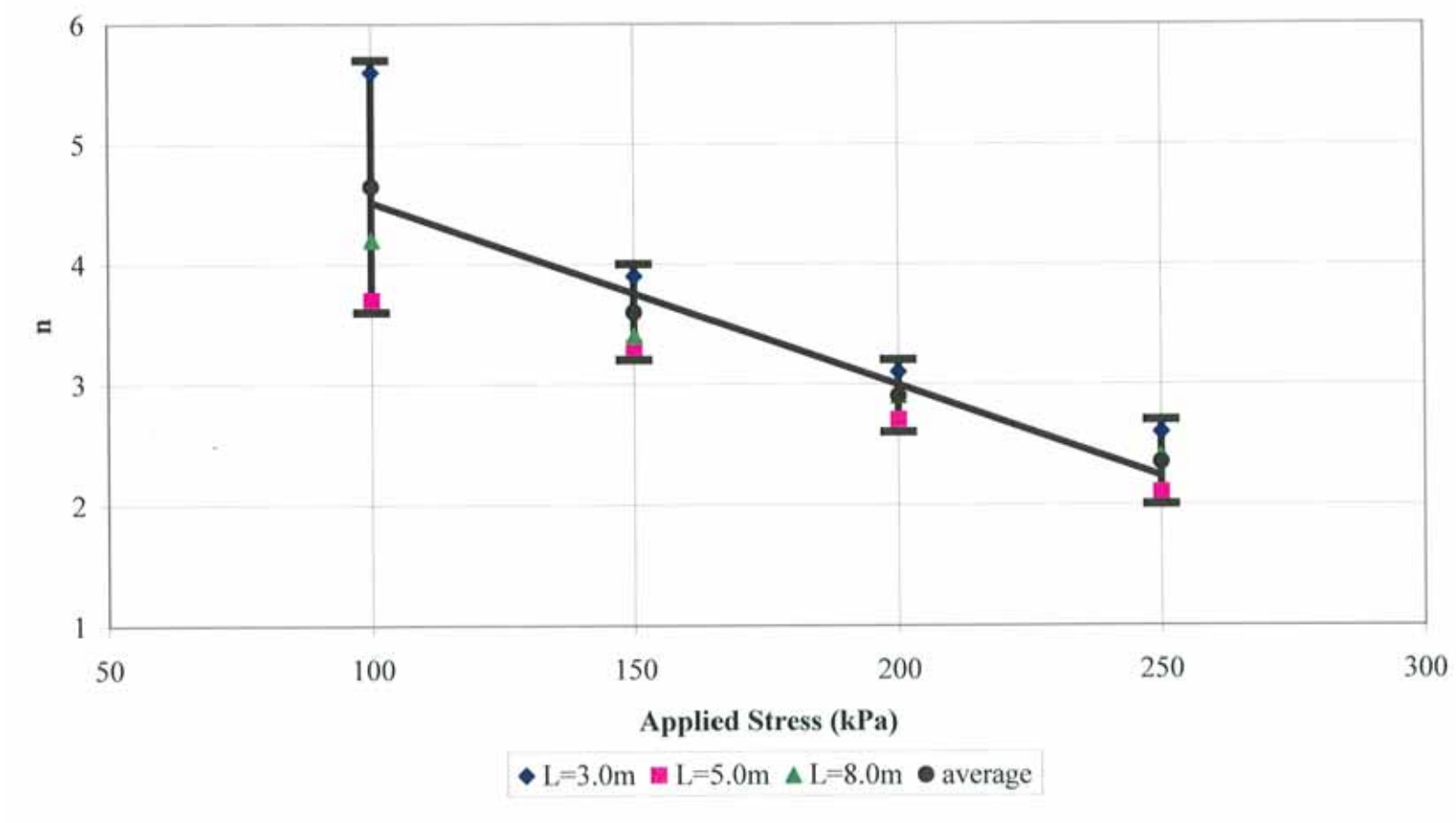

Figure 6.13 Variation of n value with applied surface pressure

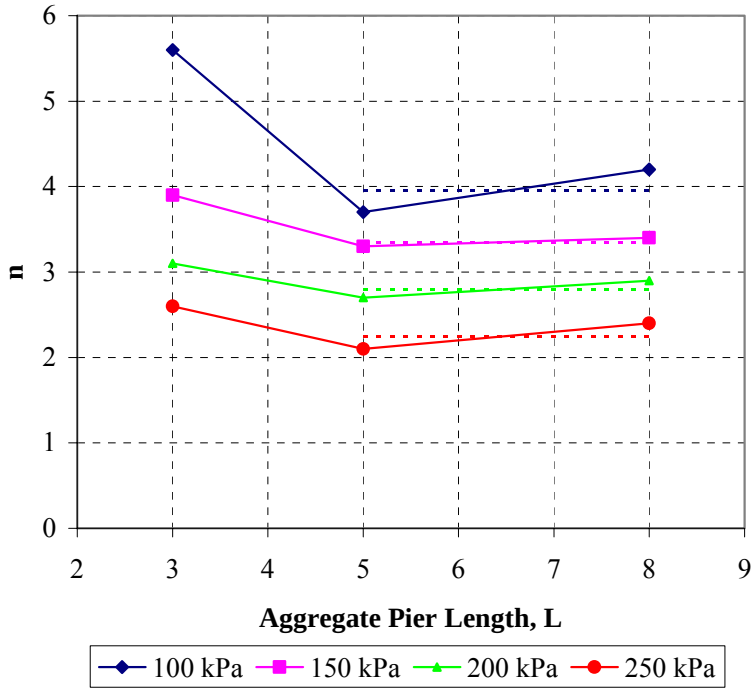

Figure 6.14 Variation of n with pier length

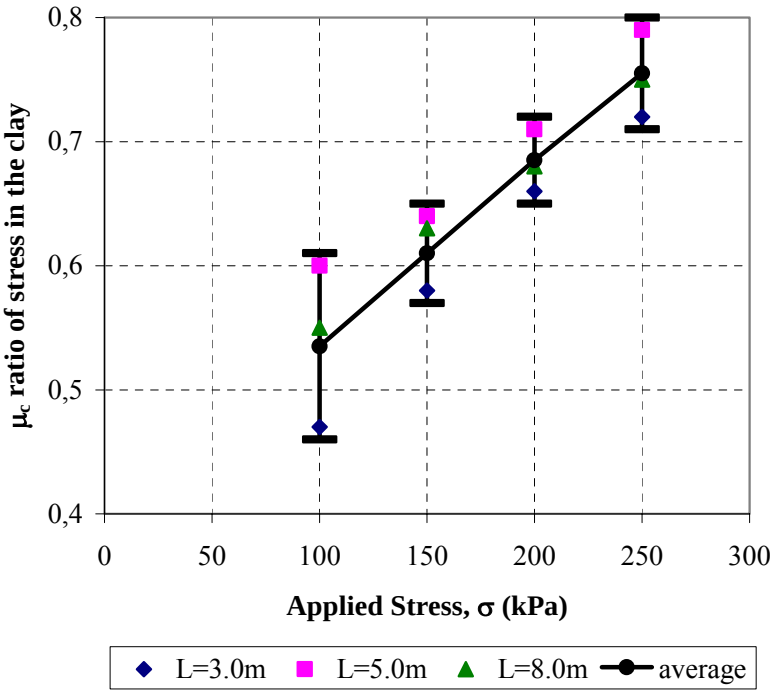

Figure 6.15 Variation of μ_c with applied surface pressure

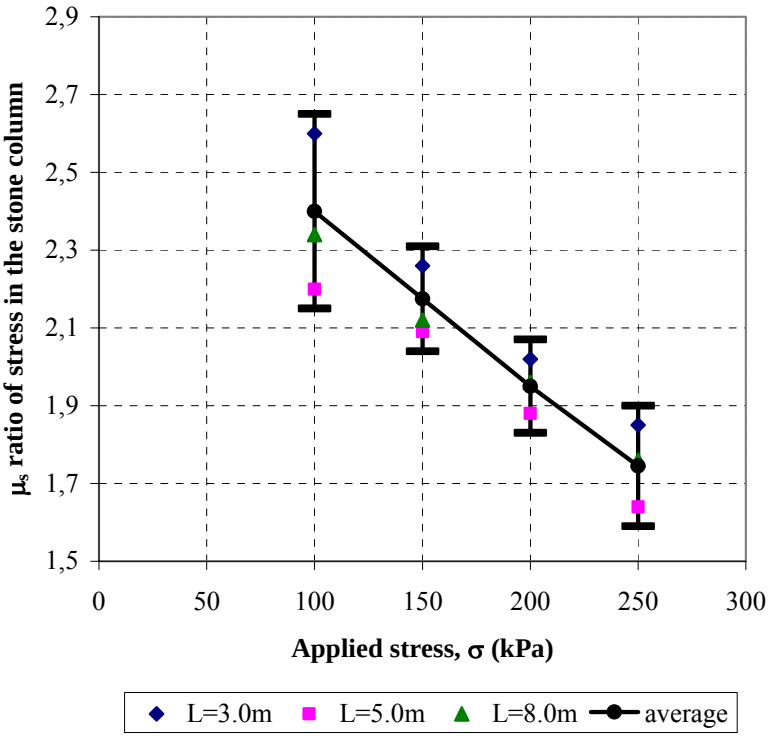

Figure 6.16 Variation of μ_s with applied surface pressure

6.4 Determination of Elastic Moduli

6.4.1 Modulus of Elasticity of Clay

To determine the elastic modulus of the clay, approximate solution for the vertical displacement of a rigid rectangle on semi-infinite mass given by Whitman and Richard, (1967) is used:

$$\rho_z = \frac{p\left(1-\upsilon^2\right)}{\beta_z \sqrt{BL}\, E} \qquad (6.1)$$

where p = total vertical load

B,L = rectangle dimensions

β_z = factor dependent on L/B given in Table 6.4.

Table 6.4 β factor (Pells, 1983)

L/B	1	2	4	10
β	1.07	1.1	1.2	1.4

Elastic modulus of the native soil was back-calculated from the measured settlement under the known magnitude of applied vertical stress using above elastic solution. Poisson's ratio of native soil was taken as 0.35. In Table 6.5 calculated elastic moduli values are given for each applied vertical stress.

Table 6.5 Back-calculated drained elastic moduli of native soil

σ (kPa)	**P (kN)**	**ρ_z (mm)**	**E (kPa)**
25	262.5	11.7	5684
50	525	20	6650
75	787.5	30.3	6584
100	1050	43.8	6073
150	1575	84.8	4705
200	2100	149.2	3566
250	2625	350.9	1895

At the first stage of loading (at 25 kPa), the measured settlement includes the seating of the loose sand blanket under the loading plate. Because of this seating problem, calculated elastic module deviates from the general trend at the first stage of loading. Also, the behavior of the native soil is not elastic for the load exceeding 100kPa. as could be seen on the load-settlement behavior shown in Figure 6.1. Therefore, the elastic modulus of the native soil is taken

as the average of calculated values between loadings of 50 kPa to 100 kPa because the elastic behavior of the native soil is represented in this vertical pressure range. Thus

E_c (elastic modulus of native soil) = 6450 kPa

is considered in further interpretations in the proceeding sections.

6.4.2 Modulus of Elasticity of Aggregate Pier

Elastic modulus of aggregate pier E_s was back-calculated from the measured settlement of single aggregate pier under the known magnitude of applied vertical stress by carrying out a finite element analysis using PLAXIS. An axisymmetry model of single aggregate pier load test was created and material properties and boundary conditions were specified. Loading plate was modeled as a circular rigid footing with an external uniform pressure on it. Linearly elastic model was used in the analysis. The deformed mesh of the single pier with 3m length is given in Figure 6.17.

Elastic modulus and poisson's ratio of clay were set to 6.4 MPa (as computed previously in Section 6.4.1) and 0.35 respectively. Poisson's ratio of aggregate pier was set to 0.3. By changing the elastic modulus of the aggregate pier in the range of 20 MPa to 40 MPa, E_s (elastic modulus of pier) versus settlement relationships were obtained for each applied stress increment as shown in Figure 6.18. Analyses were performed for 3 and 5 length of single aggregate pier, but since the difference was negligible, average settlement-E_s relationship was used in back-calculation.

In Table 6.6, back-calculated elastic moduli of aggregate pier values under each applied vertical load increment are given.

Due to the seating problem of the plate over the loose sand blanket, back-calculated value at the first stage of loading was excluded. At the last three loading stage aggregate pier shows non-elastic behavior, therefore these three calculated values were also excluded. As a result, by taking the averages of back-calculated values at 90 to 271 kPa of applied pressure, elastic modulus of aggregate pier was determined as:

E_s (elastic modulus of aggregate pier) = 39 MPa.

Table 6.6 Back-calculated drained elastic modules of aggregate pier

P (ton)	**σ (kPa)**	**ρ_z average sett. of 3 and 5m length of single piers (mm)**	**E (kPa)**
1	30	1.3	32643
3	90	3.4	38630
5	151	5.5	39732
7	211	7.7	39424
9	271	9.9	39603
11	331	12.4	37587
13	392	15.3	34745
15	452	18.4	31934

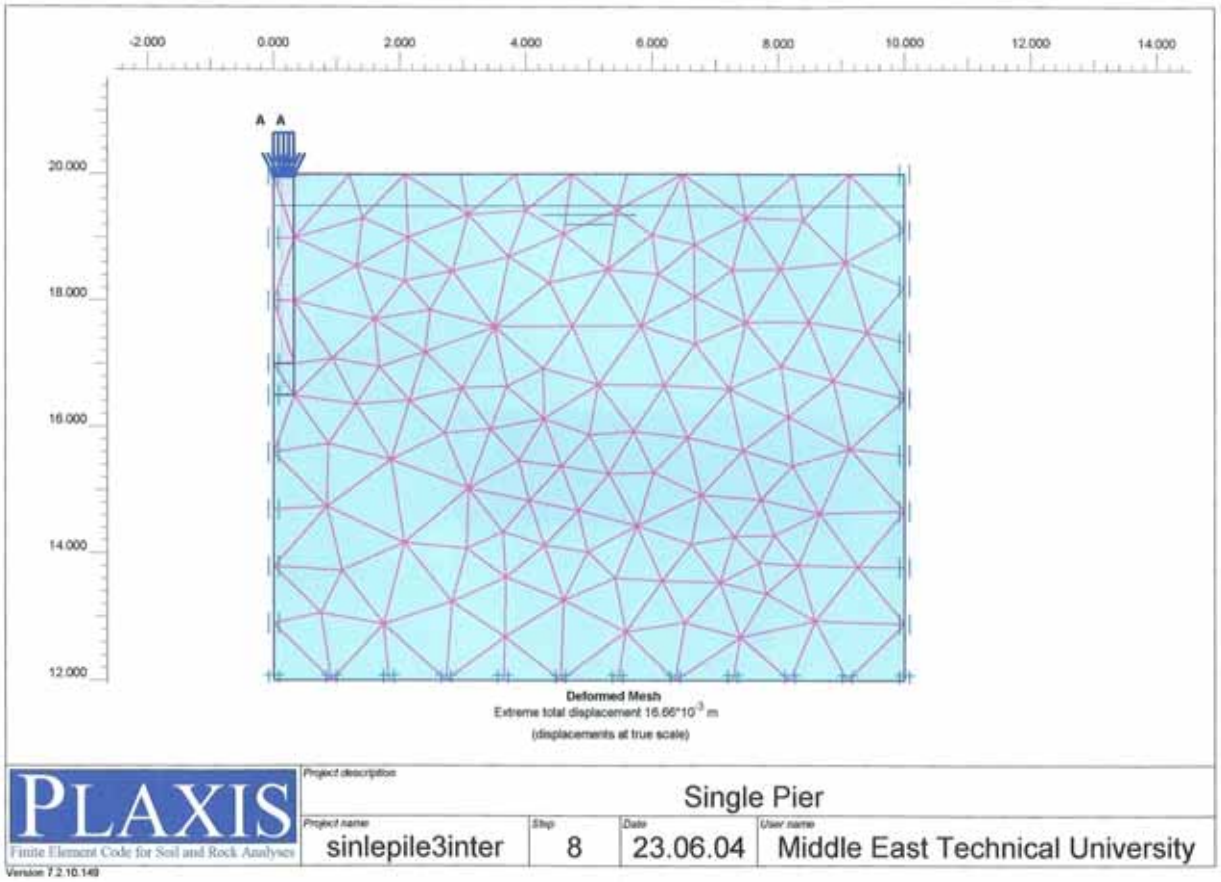

Figure 6.17 Deformed mesh of L=3m single pier

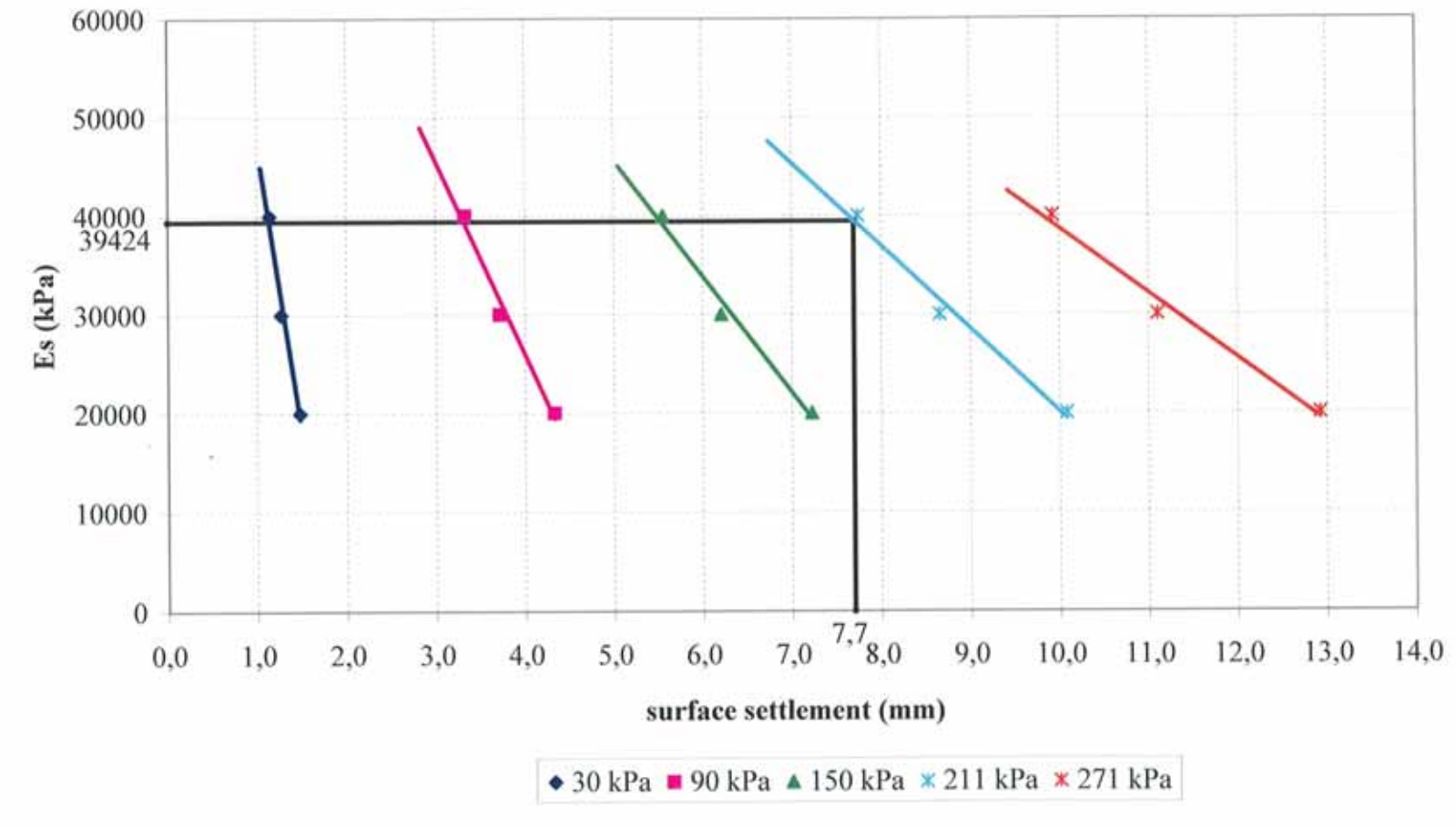

Figure 6.18 Elastic modulus of pier-settlement relationships under applied vertical stress obtained from FEM

By back calculation using measured field settlements, Vautrain (1977) determined E_s actually developed was about 30 MPa for the vibroreplacement aggregate piers at Rouen. Balaam (1978) estimated E_s to be 50 MPa from the linear portion of the undrained load settlement curve obtained at Canvey Island. Englehart and Kirsh recommend using a value of 58 MPa. For rammed aggregate piers Datye et.al (1982) found by back-calculating from measured settlements that E_s was 48 MPa. It is found that the pier stiffness obtained in this study is in agreement with the values reported in the literature.

By assuming constant vertical settlement of the aggregate pier and tributary soil (by equating the settlement of the stone and soil, the following equation can be obtained:

$$n = \frac{\sigma_s}{\sigma_c} = \frac{E_s}{E_c} \qquad (6.2)$$

Using equation (6.2) gives values of the stress concentration factor, n of 6.0 which is higher than measured in the field. In this study, field measurements give following relationship between stress concentration factor, n and ratio of the elastic moduli of the two materials used:

$$n = (0.93 - 0.35)\frac{E_s}{E_c} \qquad (6.3)$$

Therefore, use of Equation (6.2) for estimating the stress concentration factor is not recommended.

6.5 Determination of Subgrade Moduli

The settlement of an aggregate pier-supported footing or mat is a complex soil-structure interaction problem consisting of interaction between footing and

piers, footing and matrix soil, and matrix soil and piers, and the modulus of subgrade reaction, “k” which is defined as the ratio of stress to deformation, is a conceptual relationship between soil pressure and deflection that is widely used in the structural analysis of foundation members. It is used for footings, mats, and various types of pilings.

The modulus of subgrade reaction can be obtained from initial tangent or secant line of the pressure-deformation result of the plate-load test. In this study, the moduli of subgrade reactions are obtained from initial tangent line of the pressure-settlement relationships of the large plate load tests.

6.5.1 Subgrade Modulus of the Clay

From the surface settlement-pressure relationship of untreated soil given in Figure 6.1, the modulus of subgrade reaction of untreated, native soil, k_c is determined for a vertical pressure range of 0-100 kPa as:

$$k_c = \frac{\Delta\sigma}{\Delta\delta} = \frac{100}{0.0438} \cong 2280\,kN/m^3$$

6.5.2 Subgrade Modulus of Composite Soil

From the surface settlement-pressure relationships of composite soil reinforced by 3, 5 and 8m length of aggregate piers (given in Figure 6.2), the modulus of subgrade reaction of composite soil is determined as:

$k_{p,L}$ = the modulus of subgrade reaction of composite soil reinforced with L m lengths of aggregate piers

$$k_{p,3} = \frac{\Delta\sigma}{\Delta\delta} = \frac{100}{0.0254} \cong 3940\,kN/m^3$$

$$k_{p,5} = \frac{\Delta\sigma}{\Delta\delta} = \frac{100}{0.022} \cong 4550\,kN/m^3$$

$$k_{p,8} = \frac{\Delta\sigma}{\Delta\delta} = \frac{100}{0.0191} \cong 5240\,kN/m^3$$

Variation of subgrade reaction of composite soils with pier length is given in Figure 6.19. As length of aggregate pier increases, the reaction of subgrade modulus of composite soil increases.

6.5.3 Subgrade Modulus of Aggregate Pier

From the average settlement-load result of single aggregate pier load test (given in Figure 5.15), the modulus of subgrade reaction of aggregate pier, k_p is determined as:

$$k_p = \frac{\Delta\sigma}{\Delta\delta} = \frac{211}{0.0077} = 27400\,kN/m^3$$

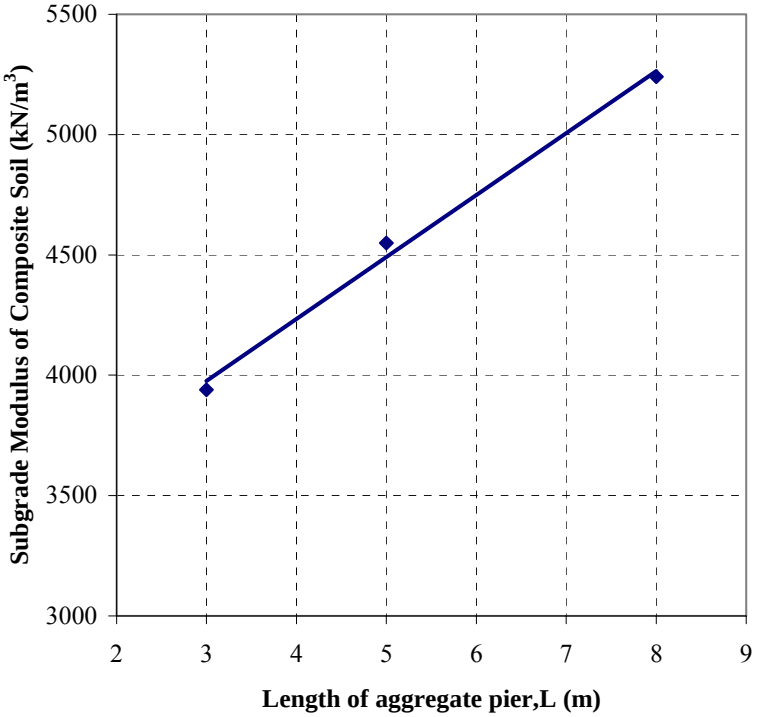

Figure 6.19 Variation of subgrade modulus of composite soil with pier length

6.6 Discussion of Settlement Reduction Ratio -Comparison of Settlement Reduction Ratio with Conventional Methods

The equilibrium method described by Aboshi et.al. (1979) is the method in Japanese practice for estimating the settlement of sand compaction piles. In applying this simple approach, the stress concentration factor, n must be estimated. The details of this method were discussed in Section 2.3.5.1. The general equation of this method (Equation 2.26) shows that the level of improvement is dependent upon the stress concentration factor, n, the initial effective stress in the clay, and the magnitude of applied stress σ. It indicates that if other factors are constant, a greater reduction in settlement is achieved for longer columns since the average initial effective stresses along the column are higher and for a smaller applied stress increments. For very large σ_0' (long length of aggregate pier) and very small applied surface stress σ, the settlement ratio approaches the ratio of stress on the clay, μ_c.

In this study the S_t/S ratio is evaluated for L=8.0m pier lengths (Group C test) to compare the observed improvement in the settlements with the prediction by Aboshi's Method. All pier lengths are considered although the method is given primarily for end bearing columns. In computation of the S_t/S ratio, the n values measured at different magnitudes of vertical stress given in Table 6.3 are used. In Table 6.7 calculated S_t/S ratio for 3,5 and 8m pier lengths by Aboshi Method and observed S_t/S ratios in the field for Group A, B and C are all summarized.

The variation of both the evaluated S_t/S ratio by Aboshi's Method and the average observed S_t/S ratios for Group A, B, C with applied pressure are illustrated in Figure 6.20.

As S_t/S ratio calculated by Aboshi (equilibrium) Method slightly increases with applied pressure, the observed S_t/S ratios decrease, showing a contradicting trend.

As the range of S_t/S ratio evaluated by Aboshi Method varies between 0.73 to 0.84, with an average of 0.78; the range of observed St/S ratios vary between 0.56 to 0.34 with an average of 0.44. Thus, it is concluded that the method proposed by Aboshi for prediction of settlement improvement in soils does not reflect the field behavior of the piers as obtained from the large scale load tests performed in this study.

Our findings in general are in agreement with the findings of Akdoğan (2001) who studied the sand column behavior using laboratory small scale model tests, as shown in Figure 6.20.

An attempt has been made to compare the observed improvement ratios with the ones predicted by Priebe's Method. For this purpose first the end bearing pier with L=8.0m length data is considered since the method is specially proposed for end bearing columns. However in the experimental program,

L=5.0m pier length may also be considered as an end bearing column since the vertical stress increment below 5m (≈1.5B)is not significant. Therefore Group B test results are also used.

Table 6.7 Comparison of the observed S_t/S ratios with Aboshi Method

Applied vertical stress σ (kPa)	**S_t/S**							
	Aboshi Method				**This Study**			
	L=3.0m	**L=5.0m**	**L=8.0m**	**Average**	**GroupA L=3.0m**	**GroupB L=5.0m**	**GroupC L=8.0m**	**Average**
50					0.535	0.585	0.415	0.560
100	0.76	0.72	0.71	0.73	0.523	0.502	0.493	0.508
150	0.82	0.79	0.78	0.80	0.427	0.401	0.400	0.414
200	0.86	0.83	0.82	0.84	0.391	0.373	0.279	0.335
250*	0.9	0.87	0.87	0.88	0.247	0.209	0.177	0.212

*Bearing Capacity Failure (BFC)is reached

In this study the area ratio, a_s was 0.25 and the angle of shearing resistance of the pier material, ϕ'_s could not be determined due to the fact that a large scale direct shear apparatus is not available. However a probable range of ϕ'_s values for the gradation of the material used could be in the range of 42^0-45^0 (Barksdale and Bachus, 1983). The ratio of constrained modulus of pier material to clay D_s/D_c is evaluated from the E_c and E_s values reported in the Sections 6.4.1 and 6.4.2 respectively, using the following relationship:

$$D = \frac{E(1-\upsilon)}{(1+\upsilon)(1-2\upsilon)} \qquad (6.2)$$

As a result ratio of constrained modulus of pier to clay was calculated as D_s/D_c = 5.1.

Using parameters described above, Priebe method, explained in Section 2.3.5.2 gives S_t/S ratio (corrected for column compressibility) as 0.43 for $\phi'_s = 42^0$ and 0.42 for $\phi_s = 45^0$. As can be seen in Figure 6.21, the predictions using Priebe's method are in agreement with average of measured S_t/S ratios of Group B and Group C tests, in this study.

On the contrary, this method is proposed for the prediction of large grid of aggregate piers. For small single foundations, Priebe (1995) offers the diagrams given in Figure 2.21. For the 7 number of stone columns under the footing, S_t/S ratio can be predicted as 0.33 and 0.42 for the ratio of depth to diameter, d/D=7.7 and 12.3 (for Group B and Group C) and, respectively. These values are also in agreement with the measured values.

Greenwood Method, described in Section 2.3.5.3 gives the level of improvements for the area ratio of a_s<0.15, so it is not applicable for this study.

Granular Wall Method presented by Van Impe and De Beer (1983) explained in Section 2.3.5.7 gives an improvement ratio depending on area ratio, a_s and internal friction angle of stone column, ϕ'_s (Figure 2.31). Improvement ratio, S_t/S can be predicted as in the range of 0.55 and 0.50 for an area ratio of 0.25 and for a range of an internal friction angle of stone column, $\phi'_s = 40^0$ to 45^0, respectively. Comparing with field data of this study, this method slightly underestimates the expected improvements in the settlements, as shown in Figure 6.21.

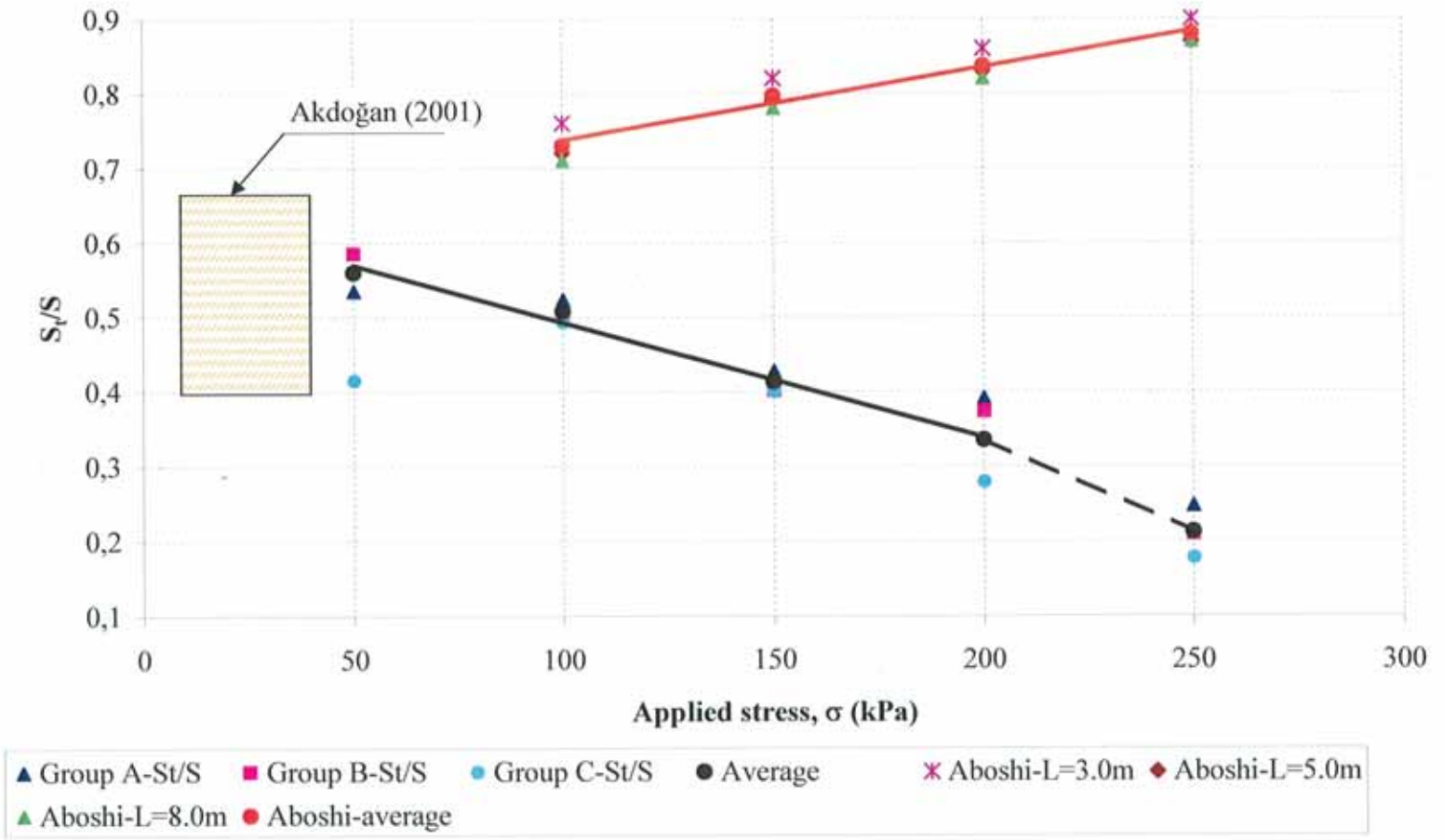

Figure 6.20 Comparison of Measured S_t/S Ratios with Equilibrium Method

An attempt has been made to compare the observed improvement ratios with the ones predicted from curves for estimating settlement of low compressibility soils (defined as those soils having modular ratios $E_s/E_c \leq 10$) such as aggregate pier reinforced sands, silty sands and some silts developed by Barksdale and Bachus (1983) using linear elastic theory (Figure 2.24).

These curves give settlement influence factor, I_s depending on modular ratio, E_s/E_c , area ratio, a_s and L/D ratio. For modular ratio, E_s/E_c = 6.0 (from the values reported in the Sections 6.4.1 and 6.4.2) and for L/D ratio of 12.3 and 7.7 (for Group B and Group C), settlement influence factor I_s can be estimated as 85 and 40, respectively. Thus, settlements under 50, 100, 150, 200 and 250 kPa can be evaluated using following equation:

$$s = I_s\left(\frac{P}{E_s L}\right) \tag{6.3}$$

where $P=\sigma A$

The calculated settlement magnitudes from design curves obtained by Barksdale and Bachus (1983) and measured ones are tabulated in Table 6.8 and illustrated in Figure 6.22.

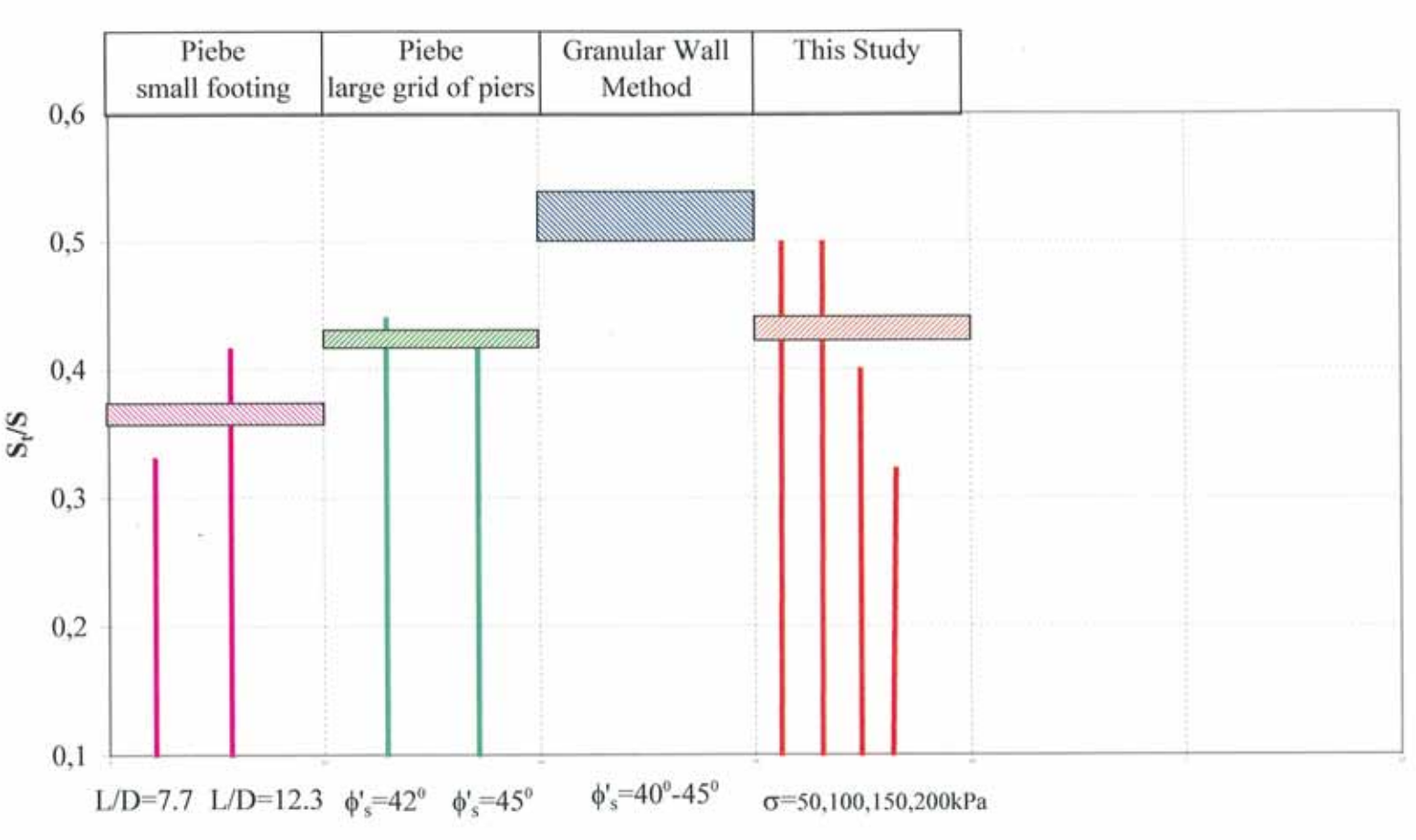

Figure 6.21 Comparisons of Measured S_t/S Ratios with Priebe and Granular Wall Method

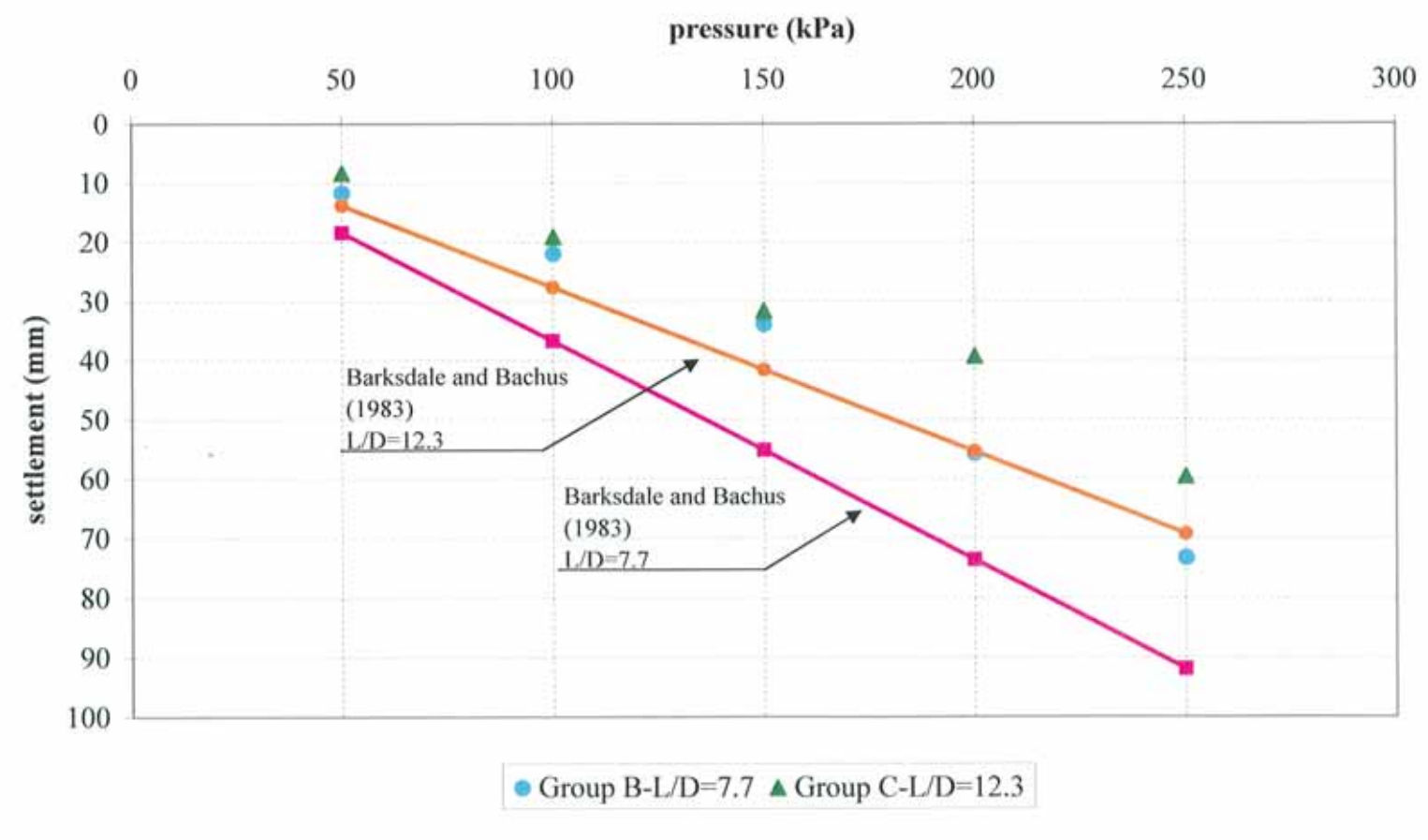

Figure 6.22 Comparisons of measured settlements of improved ground with ones predicted from design curves by Barksdale and Bachus (1983)

Table 6.8 Comparison of settlements of stone column improved ground predicted from design curves by Barksdale and Bachus (1983) with measured field data

Applied vertical stress σ (kPa)	**Settlements of stone column improved ground (mm)**			
	Barksdale and Bachus (1983)		**Measured at the Field**	
	L/D=12.3	**L/D=7.7**	**L/D=12.3 (Group C)**	**L/D=7.7 (Group B)**
50	18.4	13.8	8.3	11.7
100	36.8	27.7	21.6	22.0
150	55.2	41.6	34.0	33.9
200	73.6	55.4	41.7	55.7
250	92	69.3	62.1	73.3

6.7 Proposed Method to Estimate the Settlement of a Shallow Foundation Bearing on an Aggregate Pier Reinforced Soil

Lawton et.al. (1994) described a method for estimating settlements of the aggregate pier-reinforced soil. In this method, subgrade is divided into an upper zone (UZ) and a lower zone (LZ). The upper zone is assumed to consist of the composite soil comprised of the aggregate piers and native soil, plus the zone appreciable densification and prestressing immediately underlying the pier, which is estimated to be equal to the width (or diameter) of one pier. The lower zone consists of all strata beneath the upper zone. Settlements are calculated individually for the UZ and LZ, with the two values combined to yield an estimate of the total settlement. The authors have conducted settlement analyses for the UZ using the finite grid method (Bowles, 1988), which have shown that little error is introduced in the settlement calculations by assuming

that the footing is perfectly rigid. Using this assumption and a subgrade modulus approach, the following equations apply:

σ_s = bearing stress applied to aggregate piers = $n\sigma / [1+ (n-1) a_s]$ (6.4)

σ_c = bearing stress applied to native soil = σ_s/n (6.5)

$$n = \frac{k_s}{k_c} \quad (6.6)$$

S_{UZ} = settlement of the $UZ = \frac{\sigma_s}{k_s} = \frac{\sigma_c}{k_c}$ (6.7)

where k_s = subgrade modulus of aggregate piers

k_c = subgrade modulus of native soil

The authors suggest that the values of subgrade moduli of the aggregate piers are determined either by static load tests on individual piers or by estimation from previously performed static load tests within similar soil conditions and similar aggregate pier materials. Similarly subgrade moduli of the native soil are either determined from static load tests or estimated from boring data.

An estimate of the applied stress transmitted to the interface between the UZ and the LZ is needed so that predicted settlements in the LZ can be calculated. The procedure used by authors to estimate vertical stress increase at the UZ-LZ interface is a modification of the 2:1 method, which is a stress dissipation slope through the UZ of 1.67:1.

In Table 6.9, the predicted settlements of an improved ground reinforced with 3.0m lengths of aggregate piers (Group A) by Lawton's Method is given for each applied loading stage. The values of subgrade moduli of the aggregate piers, k_s and native soil, k_c was taken as 27400 kN/m^3 and 2280 kN/m^3 respectively (values reported in Sections 6.5.1 and 6.5.3). The thickness of the

compressible zone was taken as 2B = 6.0m from the ground surface. The thickness of the UZ and LZ was taken as 3.5m (≈ pier length+ one diameter of the pier) and 2.5m respectively. A stress dissipation slope of 1.67:1 was used to estimate the stress transmitted to the interface between the UZ and LZ. Consolidation settlement formula was used to calculate the settlement of LZ by taking coefficient of volume compressibility, $m_v = 1/D_c = 1x10^{-4}$ m^2/kN; where D_c is constrained modulus of the native soil and reported in Section 6.7.

Table 6.9 Comparison of settlements of aggregate piers improved ground predicted from method proposed by Lawton et.al (1994) with measured field data

Applied vertical stress σ (kPa)	**Predicted Settlements Lawton's Method**			**Measured Settlements (Group A) (mm)**
	S_{UZ} (mm)	**S_{LZ} (mm)**	**S_{total} (mm)**	
50	5.8	1.6	7.4	10.7
100	11.6	3.2	14.8	25.4
150	17.3	4.8	22.1	38.7
200	23.1	6.4	29.5	60.9
250	28.9	8.0	36.9	89.1

The calculated settlements of aggregate piers improved ground predicted from method proposed by Lawton et.al are lower than the measured settlements of this study.

It is proposed that instead of using subgrade modulus of piers, k_s, using subgrade modulus of composite soil, k_{comp} gives reasonable estimates of the settlements of the aggregate pier- reinforced soil, using following equations:

$$k_{comp} = a_s k_s + (1 - a_s) k_c \tag{6.8}$$

$$n = \frac{k_{comp}}{k_c} \tag{6.9}$$

$$S_{UZ} = \frac{\sigma_s}{k_{comp}} \tag{6.10}$$

which result in

$$k_{comp} = 0.25x27400 + (1 - 0.25)x2280 = 8560\,kN/m^3$$

and

$$k_{comp} = n_{av} * k_c = 3.5 * 2280 = 8000\,kN/m^3$$

In Tables 6.10 and 6.11, the predicted settlements of aggregate pier-reinforced ground by this approach using Equations 6.8 to 6.10 and measured ones at the field both for Group A and Group B are summarized, respectively.

The comparisons of predicted and measured settlements for both Group A and Group B are given in Figure 6.23. As it can be seen in Figure 6.23, the proposed approach gives reasonable estimates for settlement of aggregate pier-reinforced ground.

Table 6.10 Settlements of aggregate piers improved ground predicted from proposed approach with measured field data for Group A

Applied vertical stress σ (kPa)	**Predicted Settlements Proposed Approach (Group A)**			**Measured Settlements (Group A) (mm)**
	S_{UZ} (mm)	**S_{LZ} (mm)**	**S_{total} (mm)**	
50	12.9	1.6	14.5	10.7
100	25.7	3.2	28.9	25.4
150	38.6	4.8	43.4	38.7
200	51.4	6.4	57.8	60.9
250	64.3	8.0	72.3	89.1

Table 6.11 Settlements of aggregate piers improved ground predicted from proposed approach with measured field data for Group B

Applied vertical stress σ (kPa)	**Predicted Settlements Proposed Approach (Group B)**			**Measured Settlements (Group B) (mm)**
	S_{UZ} (mm)	**S_{LZ} (mm)**	**S_{total} (mm)**	
50	12.9	0.3	13.2	11.7
100	25.7	0.5	26.2	22.0
150	38.6	0.8	39.4	33.9
200	51.4	1.0	52.4	55.7
250	64.3	1.3	64.6	73.3

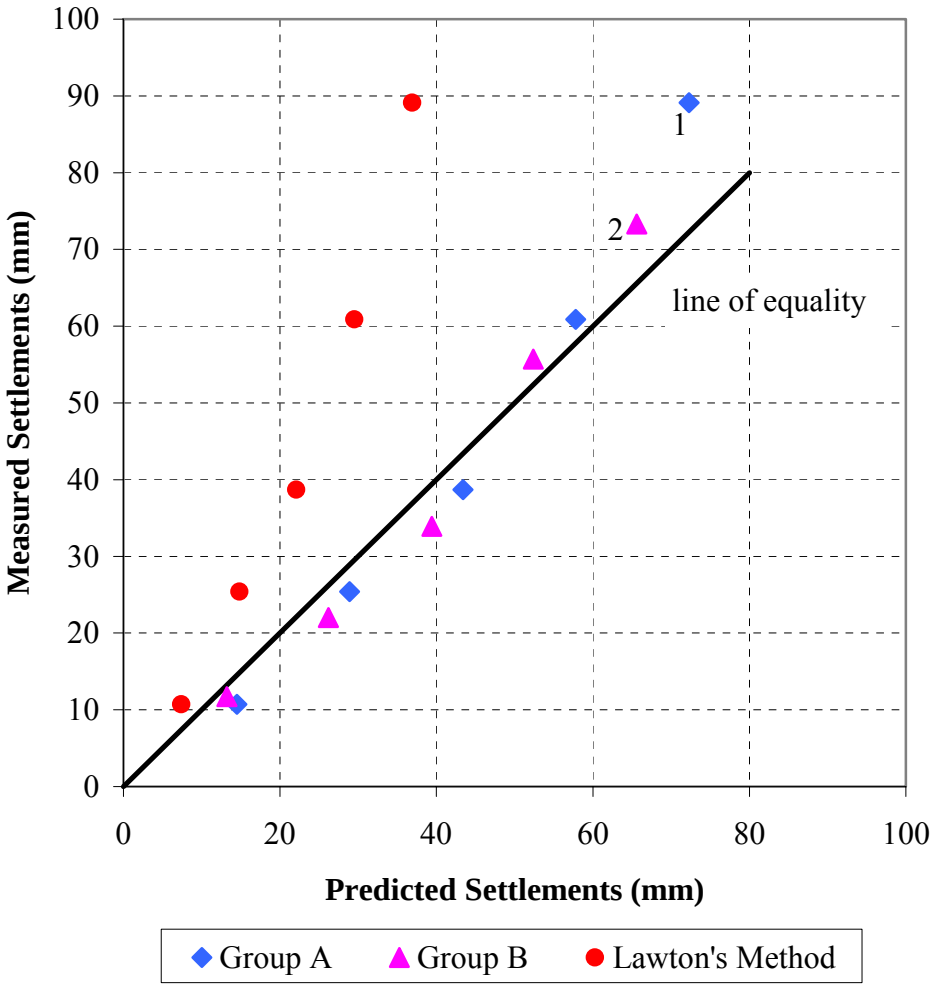

Figure 6.23 Comparison of the predicted settlements by proposed approach with measured settlements at the field

In Figure 6.23, the data points shown with numbers correspond to the settlements which occur under normal stresses in excess of the ultimate bearing capacity (i.e. exceeding 200 kPa). In this pressure range the measured settlements are relatively higher than the predicted ones as compared to the lower pressure range. This behavior is probably due to the yielding of the native soil surrounding the piers. At 250 kPa applied stress, the normal pressure on the native soil reaches to almost 200 kPa which is about the ultimate bearing capacity of the untreated soil, as given in Table 6.3. Thus

plastification of the surrounding soil reveals additional settlements which are not considered in the method proposed by this study. Therefore, the proposed method for prediction of the settlement of the improved ground is not applicable for stress range exceeding the ultimate bearing capacity of the native soil.

CHAPTER VII

CONCLUSIONS

7.1 Summary

A full-scale field study was performed to investigate the floating aggregate pier behavior in a soft clayey soil. Site investigations included five boreholes and sampling, four CPT soundings, and SPT and laboratory testing. The soil profile consisted of 8m thick compressible clay overlying weathered rock.

Four large load test stations were prepared. A rigid steel footing having plan dimensions of 3.0x3.5 m were used for loading. Four 65cm diameter reaction piles and steel cross beams were used to load the soil in each station.

First test comprised of loading the untreated soil up to 250 kPa with increments, and monitoring the surface settlements. Moreover distribution of settlements with depth is recorded by means of deep settlement gages installed prior to loading.

Other three tests were conducted on clay soil improved by rammed aggregate piers. In each station, seven stone columns were installed, having a diameter of 65cm, area ratio of 0.25, placed in a triangular pattern with a center to center spacing of 1.25m. The length of the columns were 3m (Group A), 5m (Group B) in the two station resembling floating columns, and 8m (Group C) in the last station to simulate end bearing columns to observe the level of the

improvement in the floating columns. Field instrumentation included surface and deep settlement gages, and load cell placed on a aggregate pier to determine distribution of the applied vertical stress between the column and the natural soil , thus to find magnitude of the stress concentration factor, n , in end bearing and floating stone columns.

7.2 Settlement Improvement

The settlement improvements due to aggregate piers in cohesive soils were investigated. It is observed that at small magnitude of vertical stress the measured settlements are close to each other at different pier lengths. The effect of pier length in reducing the settlements becomes effective at relatively higher vertical stress range.

7.2.1. Settlement Reduction Ratio, S_t/S

The settlement improvement ratio calculated from the surface settlements shows a decreasing trend with increasing vertical stress in the staged loading conditions. The magnitude of the improvement ratio is at the order of 0.6 at 50 kPa and is reduced to an average value of 0.34 at 200 kPa of vertical stress. This means that the efficiency of the piers in reducing the settlements becomes more effective at relatively higher vertical stress range.

The settlement reduction factor in the group with 3m long piers was in the range from 0.39 to 0.54. Whereas the magnitude of the settlement reduction factor in the 8m length end bearing columns are in the range from 0.28 to 0.42, revealing that increasing the column length from 3m to 8m, could only marginally improve the settlements, and major improvement in the settlements take place at relatively short column lengths.

7.2.2 Settlement Reduction Ratio beneath the Treated Zone, $(S_t/S)_b$

It has been observed that, the settlements measured in the clay situated below aggregate pier are consistently smaller as compared to untreated soil settlements.

The settlement reduction factor beneath the treated zone, $(St/S)_b$ in the group with 3m long piers was in the range from 0.2 to 0.4. The comparison of (S_t/S) and $(S_t/S)_b$ values in Group A loading indicates that the improvement in the untreated zone of reinforced soil is more than the cumulative surface settlement improvements.(i.e. $(S_t/S)_b<(S_t/S)$).

The results clearly indicate that, there is a net reduction in settlements in the untreated zone of the reinforced soil as compared to untreated soil profile. Since the compressibility of the clay remains the same in both reinforced and unreinforced soil (i.e. below the piers), this improvement should be due to the difference in the transmitted magnitude of vertical stress in the two cases.

7.3 Stress Distribution in Aggregate Pier Groups

As a general trend the n factor has a tendency to decrease with increasing vertical stress and the trend is practically linear. In this study, values of stress concentration factor, n have been between 2.1 and 5.6 with an average of 3.5, which is comparable with the previously reported values of n.

The data trends indicates that L=5.0m and L=8.0m pier length mobilize similar n values, and slightly higher n values are measured for the L=3.0m pier length. The difference in the behavior of 3.0m pier length as compared to the longer ones is probably due to the stress distribution in the two cases compared. The longer columns (i.e. 5 and 8m lengths) behave as end bearing column since the stress transmitted to depth 5m or more is insignificant.

7.4 Determination of Elastic Moduli

Elastic Moduli of untreated soil and aggregate pier were back-calculated from the measured settlements. Pier stiffness is obtained as

E_s = 39 MPa

and it is in agreement with the values reported in the literature.

In this study, field measurements give following relationship between stress concentration factor, n and ratio of the elastic moduli of the two materials used:

$$n = (0.93 - 0.35)\frac{E_s}{E_c}$$

7.5 Determination of Subgrade Moduli

In this study, the moduli of subgrade reactions for untreated soil, composite soils and aggregate pier are obtained from initial tangent line of the pressure-settlement relationships of the large plate load tests. It has been shown that, the subgrade reactions of composite soils increase linearly with the increasing pier length.

7.6 Comparison of Settlement Reduction Ratio with Conventional Methods

Settlement reduction ratio values were estimated from the various methods presented in the literature. It has been observed that Priebe Method (1993), Granular Wall Method presented by Van Impe and De Beer (1983) and Barksdale and Bachus Method (1983) are in agreement with the settlement reduction ratios measured in this study.

7.7 Proposed Method to Estimate the Settlement of a Shallow Foundation Bearing on an Aggregate Pier Reinforced Soil

A method which modifies the method given by Lawton et.al (1994) is proposed for estimating the settlement of the aggregate pier-reinforced ground. Using subgrade modulus of composite soil, k_{comp} gives reasonable estimates of the settlements of the aggregate pier- reinforced soil, and subgrade reaction of composite soils, k_{comp} can be estimated from the following equations:

$$k_{comp} = a_s k_s + (1 - a_s) k_c$$

or

$$n = \frac{k_{comp}}{k_c}$$

where k_s , k_c and n are the subgrade reactions of aggregate pier and native soil, and stress concentration factor, respectively.

It is found that this method underestimates the settlements of improved ground for pressure range where the stress transmitted to the clay exceeds the ultimate bearing capacity of the untreated soil.

The values of subgrade moduli of the aggregate piers are determined either by static load tests on individual piers or by estimation from previously performed static load tests within similar soil conditions and similar aggregate pier materials. Similarly subgrade moduli of the native soil are either determined from static load tests or estimated from boring data. Stress concentration factor, n can also be estimated from the results of stress measurements made in full-scale load tests given in the literature.

7.8 Future Research

Field performance information for floating aggregate piers improved ground is needed for future design.

Full-scale embankment or group load tests need to be performed in varying soil conditions with varying L/D ratios of floating aggregate piers to establish the amount of improvement in terms of reduction in settlements.

Considerable additional research is needed to improve existing design methods and develop a complete understanding of the mechanics of *short (floating) aggregate piers.* Field study should be carefully planned to establish the stress distribution along and beneath the piers. Pressure cells should be placed in the aggregate pier and soil at the interface. Pressure cells could also be placed at several levels beneath the surface to develop important information concerning the variation of stress distribution and stress concentration with depth.

REFERENCES

1. ABOSHI, H., ICHIMOTO, E., ENOKI, M., HARADA, K., 1979. "The Compozer- a Method to Improve the Characteristics of Soft Clays by Inclusion of Large Diameter Sand Columns", *Proceedings of International Conference on Soil Reinforcement: Reinforced Earth and Other Techniques,* Paris Vol.1, pp.211-216

2. ABOSHI, H. and SUEMATSU, N., 1985. "Sand Compaction Pile Method: State-of-the-art paper", *Proceedings of 3rd Int. Geotechnical Seminar on Soil Improvement Methods,* Nanyang Technological Institute, Singapore

3. AKDOĞAN, M., 2001. "Settlement Behavior of a Model Footing on Floating Sand Columns", *thesis presented to the Middle East Technical University in partial fulfillment of the requirements for the degree of Doctor of Philosophy.*

4. BACHUS, R.C. and BARKSDALE, R.D., 1984. "Vertical and Lateral Behavior of Model Stone Columns", *Proceedings of Int. Conference on In-Situ Soil and Rock Reinforcement*, Paris, pp.99-104

5. BACHUS, R.C. and BARKSDALE, R.D., 1989. "Design Methodology for Foundations on Stone Columns", *Vertical and Horizontal Deformations of Foundations and Embankments, Proceedings of Settlement'1994,* Texas, ASCE Geotechnical Special Publication No.40, pp.244-257

6. BALAAM, N.P., 1978. "Load-Settlement Behavior of Granular Piles" *thesis presented to the University of Sydney in partial fulfillment of the requirements for the degree of Doctor of Philosophy.*

7. BALAAM, N.P. and BOOKER, J.R., 1981. "Analysis of Rigid Rafts Supported by Granular Piles", *Proceedings of Int. Journal for Numerical an Analytical Methods in Geomechanics*, Vol.5, pp.379-403

8. BALAAM, N.P. and BOOKER, J.R., 1985. "Effect of Stone Column Yield on Settlement of Rigid Foundations in Stabilized Clay", *Proceedings of Int. Journal for Numerical an Analytical Methods in Geomechanics*, Vol.9, pp.331-351

9. BALAAM, N.P. and POULOS, H.G., 1983. "The Behavior of Foundations Supported by Clay Stabilized by Stone Columns", *Proceedings of 8th ECSMFE,* Helsinki, Vol.1, pp.199-204

10. BALAAM, N.P., BROWN, P.T., and POULOS, H.G., 1977. "Settlement Analysis of soft Clays Reinforced with Granular Piles", *Proceedings of 5th Southeast Asian Conference on Soil Engineering*, Bangkok, pp.81-92

11. BARKSDALE, R.D., and BACHUS, R.C., 1983. "Design and Construction of Stone Columns", *Report No. FHWA/RD-83/026*, National Technical Information Service, Virginia, USA.

12. BARKSDALE, R.D., and GOUGHNOUR, R.R., 1984. "Settlement Performance of stone Columns in the US", *Proceedings of Int. Conference on In-Situ Soil and Rock Reinforcement*, Paris, pp.105-110

13. BARKSDALE, R.D., and TAKEFUMI, T., 1990. "Design, Construction and Testing of Sand Compaction Piles", *Symposium on Deep Foundation Improvements: Design, Construction and Testing*, ASTM Publications, STP 1089, Las Vegas

14. BAUMANN, V., and BAUER, G.E.A, 1974. " The Performance of Foundations on Various Soils Stabilized by the Vibro-Compaction Method", *Canadian Geotechnical Journal*, Vol.11, pp.509-530

15. BERGADO, D.T., RANTUCCI, G., WIDODO, S., 1984. "Full Scale Load Tests on Granular Piles and Sand Drains in the Soft Bangkok Clay", *Proceedings of Intl. Conf. on In-Situ Soil and Rock Reinforcement*, Paris, pp.111-118

16. BERGADO, D.T. and LAM, F.L., 1987. "Full Scale Load Test of Granular Piles with Different Proportions of Gravel and Sand in the Soft Bangkok Clay", *Soils and Foundations Journal*, 27, 1: 86-93

17. BERGADO, D.T., ALFARO, M.C., CHAI, J.C., 1991. " The granular pile: Its Present State and Future Prospects for Improvement of Soft Bangkok Clay", *Journal of South Asian Society for Soil Engineering, Geotechnical Engineering*, Vol.22, pp.143-171

18. BERGADO, D.T., ALFARO, M.C., CHAI, J.C., BALASUBRAMAIAM, A.S., 1994. "Ground Improvement Using Granular Piles", *Improvement Techniques of Soft Ground in Subsiding and Lowland Environment,* A.A. Balkema/Rotterdam/Brookfield, pp.57-97

19. BOWLES, E.J., 1988. *Foundation Analysis and Design*, 4th Edition, Mc Graw-Hill Publishing Company

20. BURMISTER, D.M., 1958. "Evaluation of Pavement Systems of the WASHO Road Test by Layered System Methods" *Highway Research Board Bulletin 177*, pp.26-54

21. DATYE, K.R., 1982. "Settlement and Bearing Capacity of Foundation System", *Symposium on Recent Developments in Ground Improvement Techniques*, Bangkok, pp.85-103

22. DATYE, K.R. and NAGARAJU, S.S., 1975. "Installation and Testing of Rammed Stone Columns", *Proceedings of 5th Asian Regional Conf. on Soil Mechanics and Foundation Engineering,* Bangalore, India, pp. 101-104

23. DATYE, K.R. and NAGARAJU, S.S., 1977. "Behavior of Foundations on Ground Improved with Stone Columns", *Proceedings 9th Intl. Conf. on Soil Mechanics and Foundation Engineering*, Tokyo

24. DATYE, K.R. and NAGARAJU, S.S., 1981. "Design Approach and Field Control for Stone Columns", *Proceedings of 10th Intl. Conference on Soil Mechanics and Foundation Engineering,* Stockholm

25. DUNCAN, J.M. and CHANG, C.Y., 1970. " Nonlinear Analysis of Stress Strain in Soils", *Journal of the Soil Mechanics and Foundations Division,* ASCE, Vol.96, No.SM5, pp.1625-1653

26. EDİL, T.B., ŞENOL, A., FOX, N.S., 2000. "Sıkıştırılmış Geokolon-Rammed Aggregate Pier Yöntemi ile Yumuşak Zeminlerin Taşıma Gücünün Arttırılması", *Proceedings of Zemin Mekaniği ve Temel Mühendisliği 8. Ulusal Kongresi,* Istanbul

27. ENGELHARDT, K. and KIRSCH, K., 1977. "Soil Improvement by Deep Vibration Technique", *Proceedings of 5th Southeast Asian Conf. on Soil Engineering*, Bangkok.

28. FOX, E.N., 1948. " The Mean Elastic Settlement of a Uniformly Loaded Area at a Depth Below the Ground Surface", *Proceedings of 2nd Intl. Conf. on Soil Mechanics and Foundation Engineering,* Vol.2, pp.236-246

29. FOX, N.S. and EDİL, T.B., 2000. "Case Histories of Rammed Aggregate Pier, Soil reinforcement Construction over Peat and Highly Organics Soils", *Proceedings of Conf. on the Soft Ground Technology*, Netherlands, ASCE Special Publication No.112, pp.146-157

30. GOUGHNOUR, R.R., 1983. "Settlement of Vertically Loaded Stone Columns in Soft Ground", *Proceedings of 8th ECSMFE*, Helsinki, Vol.1, pp.199-204.

31. GOUGHNOUR, R.R., 1997. " Stone Column Construction by Rotary Method", *Ground Improvement Ground Reinforcement Ground Treatment*, ASCE Geotechnical Special Publication No.69

32. GOUGHNOUR, R.R. and BAYUK, A.A., 1979(a). "A Field Study of Long Term Settlements of Loads Supported by Stone Columns in Soft Ground", *Proceedings of Int. Conf. on In-Situ Soil and Rock Reinforcement,* Paris

33. GOUGHNOUR, R.R. and BAYUK, A.A., 1979(b). "Analysis of Stone Column-Soil Matrix Interaction Under Vertical Load", *Proceedings of Int. Conf. on In-Situ Soil and Rock Reinforcement*, Paris

34. GOUGHNOUR, R.R., SUNG, J.T., RAMSEY, J.S., 1990. " Slide Correction by Stone Columns", *Symposium on Deep Foundation Improvements: Design, Construction and Testing,* ASTM Publications, STP 1089, Las Vegas

35. GREENWOOD, D.A., 1970. "Mechanical Improvement of Soils below Ground Surface", *Proceedings of the Conf. on Ground Engineering*, London, ICE.

36. GREENWOOD, D.A., and KIRSCH, K. 1983. "Specialist Ground Treatment by Vibratory and Dynamic Methods-State-of-the Art", *Proceedings of Conf. on Piling and Ground Treatment*, London, pp.17-45.

37. HUGHES, J.M.O., and WITHERS, N.J., 1974. "Reinforcing of Soft Cohesive Soils with Stone Columns", *Ground Engineering*, Vol.7, No.3, pp.42-49

38. HUGHES, J.M.O., WITHERS, N.J., GREENWOOD, D.A., 1975. "A Field Trial of the Reinforcing Effect of a Stone Column in Soil", *Geotechnique, 25*,1, pp.31-44

39. LAWTON, E.C., and FOX, N.S., 1994. "Settlement of Structures Supported on Marginal or Inadequate Soils Stiffened with Short Aggregate Piers", *Vertical and Horizontal Deformations of Foundations and Embankments, Proceedings of Settlement'1994,* Texas, ASCE Geotechnical Special Publication No.40, pp.244-257

40. LAWTON, E.C., FOX, N.S., HANDY, R.L., 1994, " Control of Settlement and Uplift of Structures Using Short Aggregate Piers" *In-Situ Deep Soil Improvement,* ASCE Geotechnical Special Publication No.45

41. MADHAV, M.R., 1982. "Recent Developments in the Use and Analysis of Granular Piles" *Symposium on Recent Developments in Ground Improvement Techniques*, Bangkok

42. MADHAV, M.R. and MIURA, N, 1994. "Stone Columns" *Proceeding of 13th of ICSMFE,* New Delhi

43. MADHAV, M.R. and VITKAR, P.P., 1978. "Strip Footing on Weak Clay Stabilized with a Granular Trench or Pile", *Canadian Geotechnical Journal*, Vol.5, Nr.2

44. MADHAV, M.R., IYENGAR, N.G.R., VITKAR, R.P. and NANDIA, A., 1979. " Increased Bearing Capacity and Reduced Settlements due to Inclusions in Soil", *Proceedings of Intl. Conf. on Soil Reinforcement: Reinforced Earth and Other Techniques,* Vol.2, Paris, pp. 329-333

45. MITCHELL, J.K., 1982. " Soil Improvement- State-of –the Art Report" *Proceedings of the 10th Int. Conf. on SMFE, Stockholm*, Vol.4, pp.509-565

46. MOSOLEY, M.P., and PRIEBE, H.J., 1993. " Vibro Techniques" *Ground Improvement*, Chapman and Hall

47. MUNFAKH, G.A., ABRAMSON, L.W., BARKSDALE, R.D. and JURAN, I., 1987. " In-Situ Ground Reinforcement" *Proceedings of Conf. on Soil Improvement-A Ten Year Update*

48. MURAYAMA, S., and ICHIMOTO, E., 1982. "Sand Compaction Pile" *Symposium on Recent Developments in Ground Improvement Techniques,* Bangkok

49. NAYAK, N.V., 1982. "Recent Innovations in Ground Improvement by Stone Columns" *Symposium on Recent Developments in Ground Improvement Techniques*, Bangkok

50. POULOS, H.G., 1972. "Difficulties in Prediction of Horizontal Deformations of Foundations", *Journal of the Soil Mechanics and Foundation engineering Division*, ASCE, vol.98, No.SM8, pp. 843-848

51. POULOS, H.G., and MATTES, N.S., 1974. "Settlement of Pile Groups Bearing on Stiffer Strata", *Journal of the Geotechnical Engineering Division,* ASCE, Vol.100, No. GT2, pp. 185-190

52. POULOS, H.G. and DAVIS, E.H., 1974. *Elastic Solutions for Soil and Rock Mechanics*, John Wiley & Sons

53. PRIEBE, H., 1976. "Estimating Settlements in a Gravel Column Consolidated Soil", *Die Bautechnik* 53 pp.160-162

54. PRIEBE, H., 1990. "Vibro Replacement- Design Criteria and Quality Control", *Symposium on Deep Foundation Improvements: Design, Construction and Testing,* ASTM Publications, STP 1089, Las Vegas

55. PRIEBE, H., 1993. "Design Criteria for Ground Improvement by Stone Columns", *Proceedings of 4th National Conference on Ground Improvement*, Lahore

56. PRIEBE, H., 1995. "The design of Vibro Replacement", *Journal of Ground Engineering,* Vol.28, No.10

57. RANJAN, G., and RAO, B.G., 1983. "Skirted Granular Piles for Ground Improvement", *Proceedings of 8th ECSMFE*, Helsinki

58. SLOCOMBE, B.C., and MOSELEY, M.P., 1990. "The Testing and Instrumentation of Stone Columns", *Symposium on Deep Foundation Improvements: Design, Construction and Testing*, ASTM Publications, STP 1089, Las Vegas

59. STARK, T.D., YACYSHYN, M.B., 1990. "Specifications for Constructing and Load Testing Stone Columns in Clays", *Symposium on Deep Foundation Improvements: Design, Construction and Testing,* ASTM Publications, STP 1089, Las Vegas

60. TAVENAS, F., MIEUSSENS, C. and BOURGES, F., 1979. "Lateral Displacements in Clay Foundations under Embankments", *Canadian Geotechnical Journal,* Vol.16, No.3, pp.532-550

61. THORNBOURN, S., 1975. "Building Structures Supported by Stabilized Ground", *Geotechnique,(25),*1, pp. 83-94

62. VAN IMPE, W.F, DE BEER, E., 1983. "Improvement of Settlement Behavior of Soft Layers by Means of Stone Columns", *Proceedings of 8th ECSMFE,* Helsinki

63. VAUTRAIN, J., 1977. "Mur en Terre Armee Sur Colonnes Ballastees", *Proceedings of Int. Symposium on Soft Clay*, Bangkok

64. VESIC, A.S., 1972. "Expansion of Cavities in Infinite Soil Mass", *Journal of Soil Mechanics and Foundations Division*, ASCE, Vol.98, No. SMF3

65. WHITMAN, R.V. and RICHART, F.E., 1967. "Design Procedures for Dynamically Loaded Foundations" *Journal of Soil Mechanics and Foundations Division*, ASCE, Vol.93, No.Sm6, pp.169-193

66. WONG, H.Y., 1975. "Vibrofloatation-Its Effect on Weak Cohesive Soils", *Civil Engineering* 824 pp.44-67

A1. Notation for Tables 2.6 and 2.7

A_s	cross sectional area of sand pile
B	width of loaded area
C_c	compression index of clay
C_o	original undrained shear strength of clay
D_f	depth of foundation
E	modulus of elasticity
F_c^*, F_q^*	cavity expansion factors
H	thickness of layer
K	earth pressure coefficient applying to the load increments
K_{as}	active earth pressure coefficient of sand pile
$[K_c^{(m)}]\{\Delta\sigma^{(m)}\}$	vector of corrections due to yielding of the pile and/or clay; these corrections are treated as an additional external load
$[K_E]$	elastic stiffness matrix
K_o	coefficient of earth pressure at rest
K_{ps}	soil coefficient of passive earth pressure
L	length of sand pile
N_c, N_γ, N_q	dimensionless factors which depend on properties of soil and pile materials and area replacement ratio
$(P_o)_{vc}$	initial vertical stress in clay
R	settlement reduction factor
S_t	settlement of composite foundation
W	width of equivalent granular pile strip
Z	depth from surface of composite foundation
a_s	area replacement ratio
d_s	pile diameter
e_o	initial void ratio
m	iteration number
m_v	modulus of volume compressibility
n	stress concentration factor
q_o	overburden pressure
q_s	bearing capacity of soft soil expressed as $(2/3)\,C_o N_c$
q_{ult}	ultimate bearing capacity
γ_s, γ_c	unit weight of sand and clay, respectively
$\{\Delta F_{DN}\}$	vector of incremental nodal forces at the dual nodes along the pile clay interface
$\{\Delta F_E\}$	vector of incremental nodal forces due to applied tractions (usually applied along the top of the sand pile)
$(\Delta P)^*_{vc}$	effective vertical stress increase in the clay averaged over the horizontal projected area of clay
$(\Delta P)^*_v$	effective vertical stress increase averaged over horizontal projected area of unit cell
$\{\Delta\sigma^{m+1)}\}$	vector incremental deflections
ε_v	vertical strain (same for sand and clay)
θ	vertical angle of sliding surface at each sand pile
μ	Poisson's ratio
μ_c	reduction in stress coefficient of clay
σ	vertical stress
σ_{ro}	initial radial stress along the granular pile
σ_z	overburden pressure at depth z
τ	shear resistance of composite foundation
ϕ_s	angle of internal friction
ψ	angle between the assumed failure surface and foundation

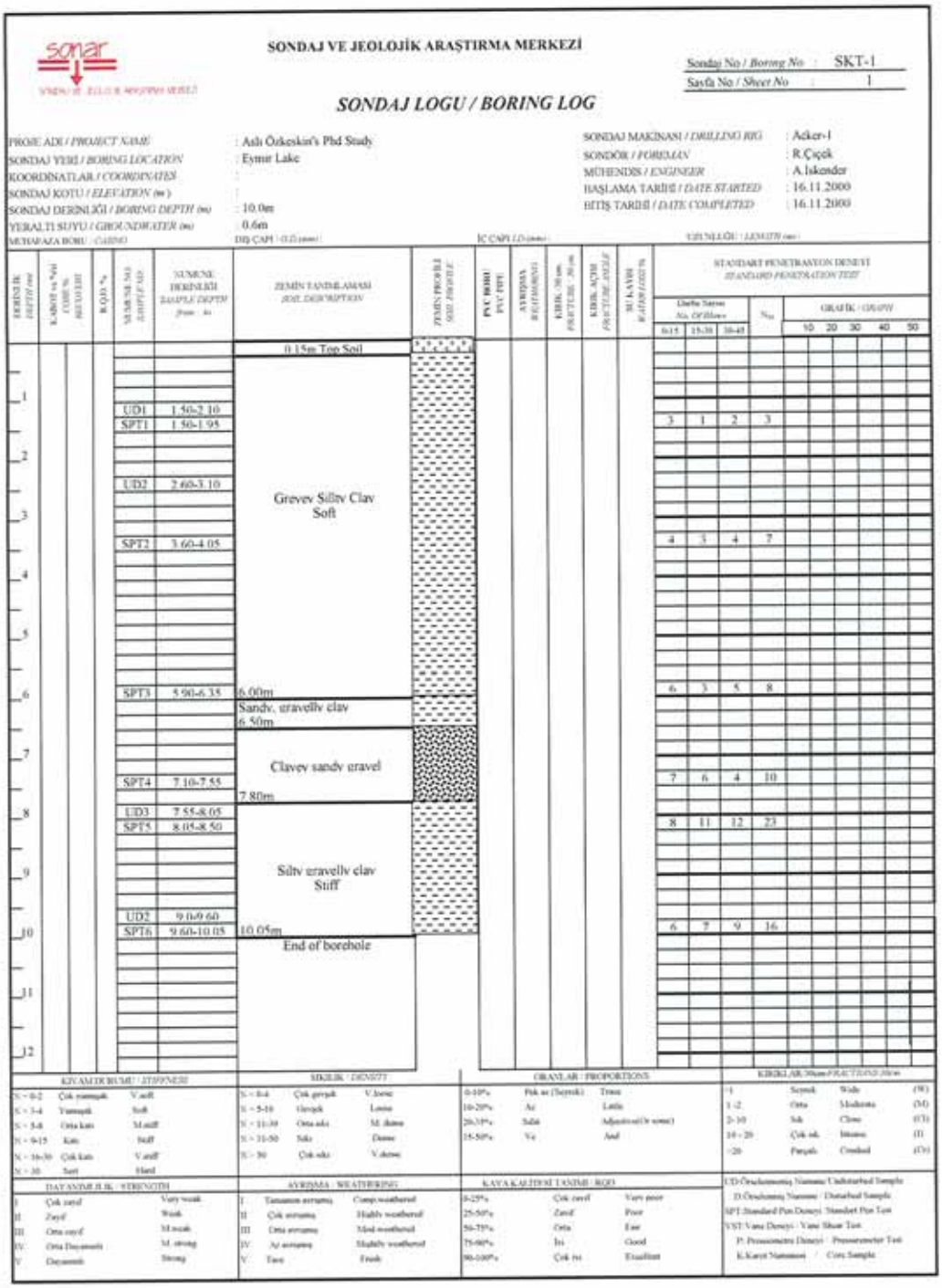

Figure B1. Borehole Log of SKT-1

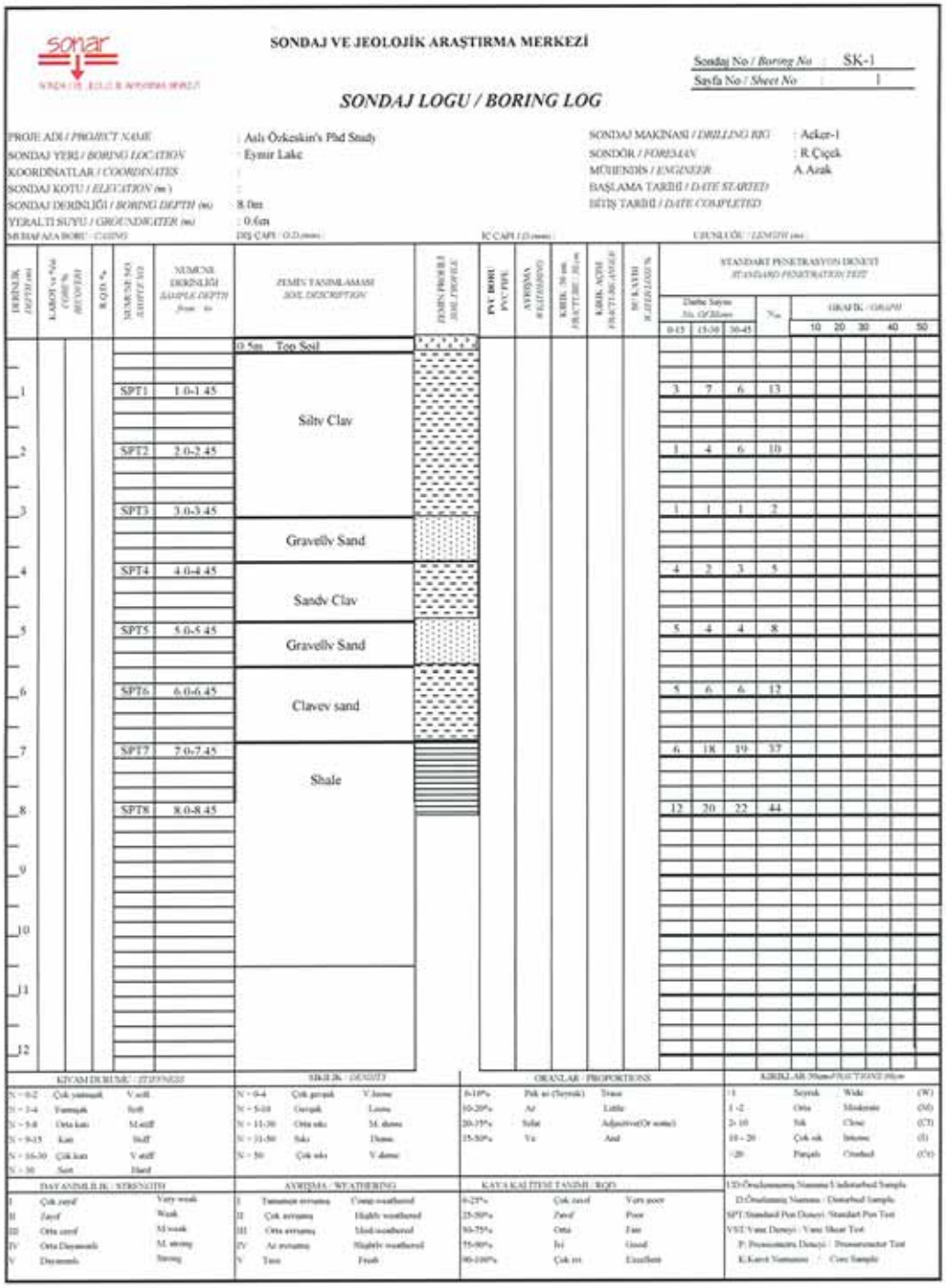

Figure B2. Borehole Log of SK-1

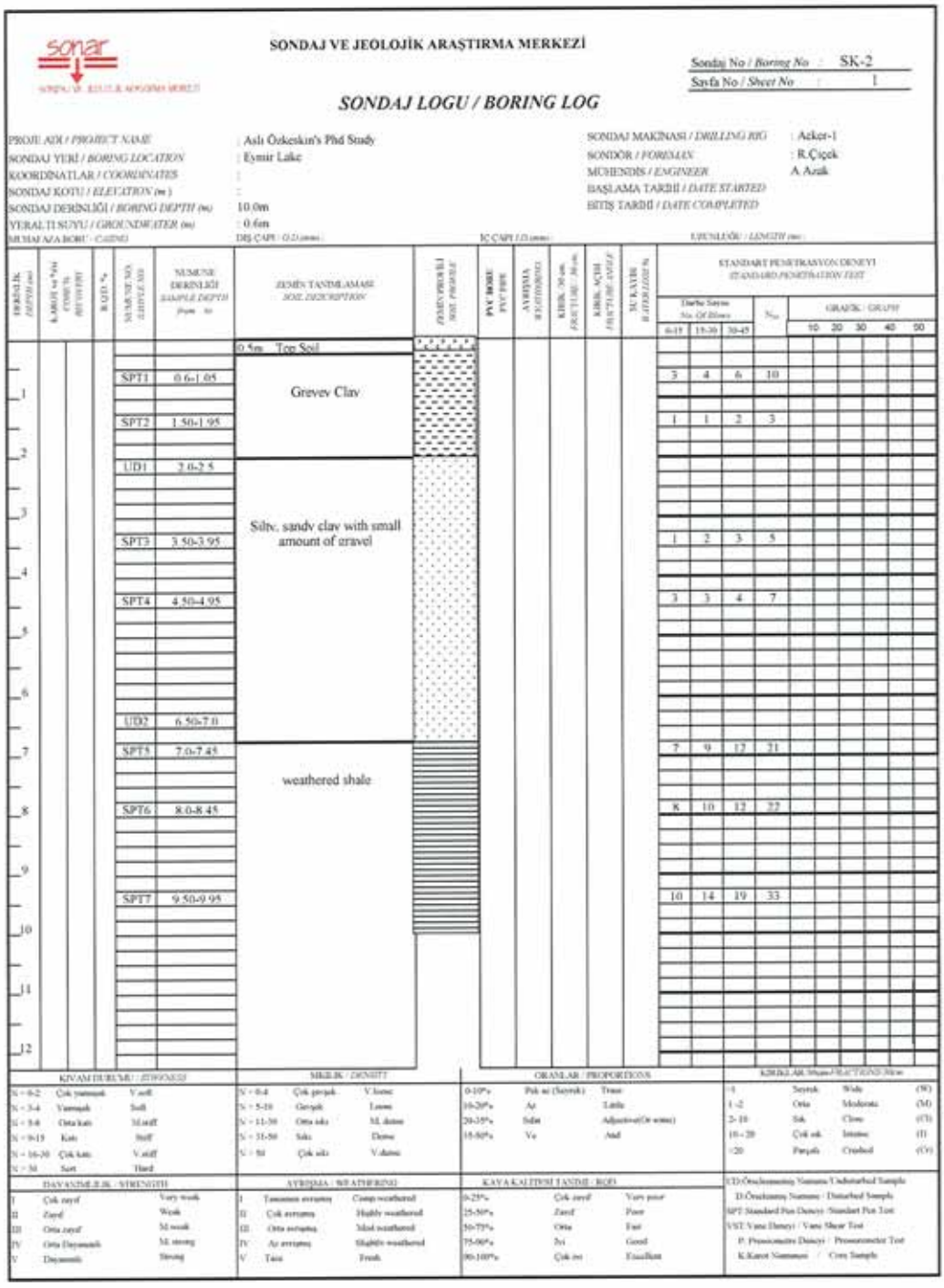

Figure B3. Borehole Log of SK-2

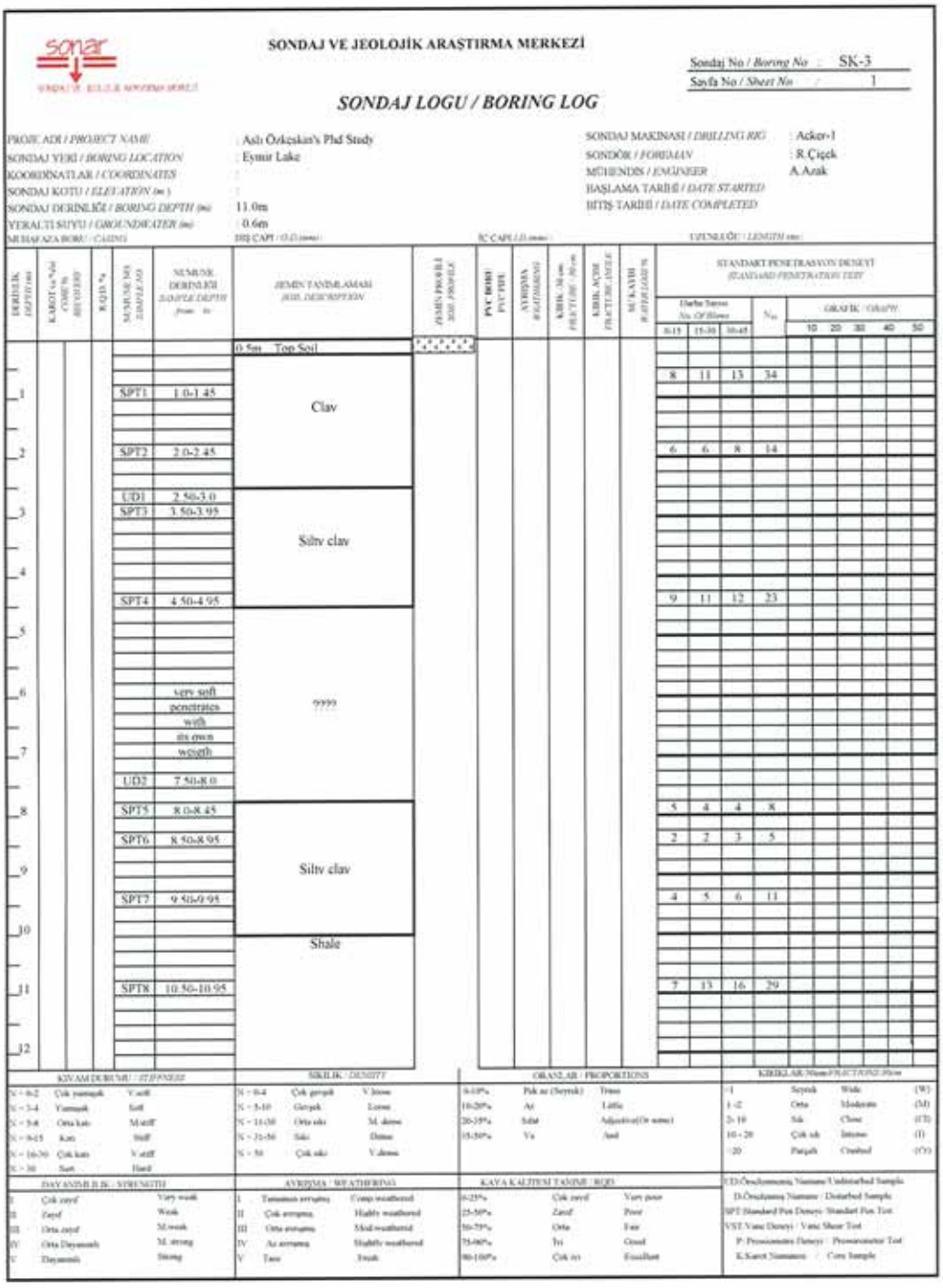

Figure B4. Borehole Log of SK-3

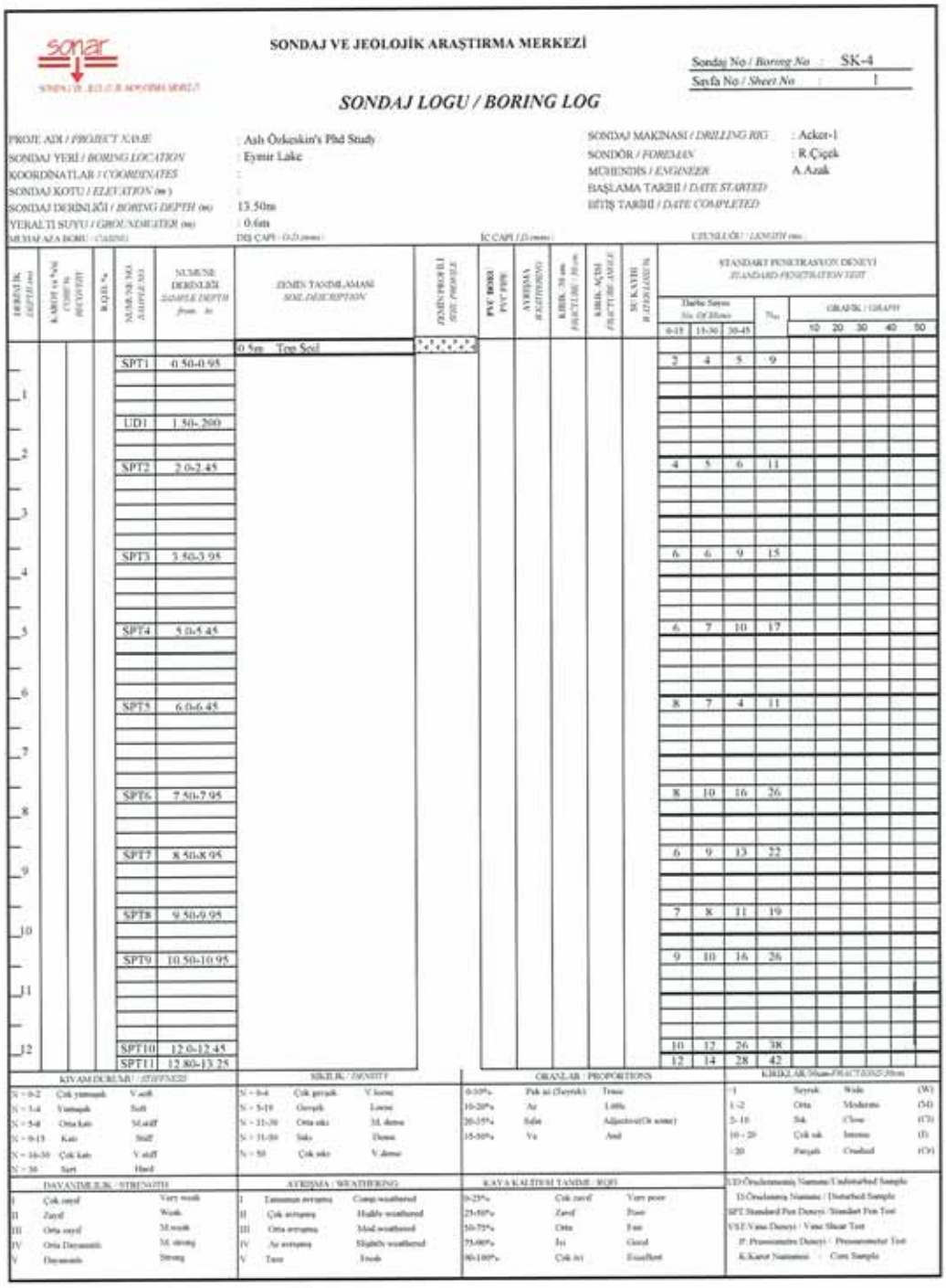

SONDAJ VE JEOLOJİK ARAŞTIRMA MERKEZİ

Sondaj No / *Boreng No* : SK-4
Sayfa No / *Sheet No* : 1

SONDAJ LOGU / BORING LOG

PROJE ADI / *PROJECT NAME* : Ash Özkeskin's Phd Study
SONDAJ YERİ / *BORING LOCATION* : Eymir Lake
KOORDİNATLAR / *COORDINATES* :
SONDAJ KOTU / *ELEVATION* (m) :
SONDAJ DERİNLİĞİ / *BORING DEPTH* (m) : 13.50m
YERALTI SUYU / *GROUNDWATER* (m) : 0.6m
MUHAFAZA BORU / *CASING* : DIŞ ÇAPI / *O.D.* (mm) : İÇ ÇAPI / *I.D.* (mm) : UZUNLUĞU / *LENGTH* (m) :

SONDAJ MAKİNASI / *DRILLING RIG* : Acker-1
SONDÖR / *FOREMAN* : R.Çiçek
MÜHENDİS / *ENGINEER* : A.Azak
BAŞLAMA TARİHİ / *DATE STARTED* :
BİTİŞ TARİHİ / *DATE COMPLETED* :

DERİNLİK *DEPTH* (m)	KAROT % *CORE %*	RQD %	NUMUNE DERİNLİĞİ *SAMPLE DEPTH from to*	ZEMİN TANIMLAMASI *SOIL DESCRIPTION*	ZEMİN PROFİLİ *SOIL PROFILE*	PVC BORU *PVC PIPE*	AYRIŞMA *WEATHERING*	KIRIK ... /30 cm *FRACTURE ... /30 cm*	KIRIK AÇISI *FRACTURE ANGLE*	SU KAYBI *WATER LOSS*	STANDART PENETRASYON DENEYİ *STANDARD PENETRATION TEST* Darbe Sayısı *No. Of Blows*	N_{60}	GRAFİK / *GRAPH*
											0-15 / 15-30 / 30-45		10 20 30 40 50
				0.5m Top Soil									
			SPT1	0.50-0.95							2 4 5	9	
1													
			UD1	1.50-2.00									
2			SPT2	2.0-2.45							4 5 6	11	
3													
			SPT3	3.50-3.95							6 6 9	15	
4													
			SPT4	5.0-5.45							6 7 10	17	
5													
			SPT5	6.0-6.45							8 7 4	11	
6													
			SPT6	7.50-7.95							8 10 16	26	
7													
			SPT7	8.50-8.95							6 9 13	22	
8													
			SPT8	9.50-9.95							7 8 11	19	
9													
			SPT9	10.50-10.95							9 10 16	26	
10													
			SPT10	12.0-12.45							10 12 26	38	
11			SPT11	12.80-13.25							12 14 28	42	

KIVAM DURUMU / *STIFFNESS*

N = 0-2	Çok yumuşak	V.soft
N = 3-4	Yumuşak	Soft
N = 5-8	Orta katı	M.stiff
N = 9-15	Katı	Stiff
N = 16-30	Çok katı	V.stiff
N > 30	Sert	Hard

SIKILIK / *DENSITY*

N = 0-4	Çok gevşek	V.loose
N = 5-10	Gevşek	Loose
N = 11-30	Orta sıkı	M. dense
N = 31-50	Sıkı	Dense
N = 50	Çok sıkı	V. dense

ORANLAR / *PROPORTIONS*

0-10%	Pek az (Sayılmaz)	Trace
10-20%	Az	Little
20-35%	Eşit	Adjective(Or some)
35-50%	Ve	And

KIRIKLAR / *FRACTURES*

> 1	Seyrek	Wide	(W)
1 -2	Orta	Moderate	(M)
2- 10	Sık	Close	(Cl)
10 - 20	Çok sık	Intense	(I)
> 20	Parçalı	Crushed	(Cr)

DAYANIMLILIK / *STRENGTH*

I	Çok zayıf	Very weak
II	Zayıf	Weak
III	Orta zayıf	M.weak
IV	Orta Dayanımlı	M. strong
V	Dayanımlı	Strong

AYRIŞMA / *WEATHERING*

I	Tamamen ayrışmış	Comp.weathered
II	Çok ayrışmış	Highly weathered
III	Orta ayrışmış	Mod.weathered
IV	Az ayrışmış	Slightly weathered
V	Taze	Fresh

KAYA KALİTESİ TANIMI / *RQD*

0-25%	Çok zayıf	Very poor
25-50%	Zayıf	Poor
50-75%	Orta	Fair
75-90%	İyi	Good
90-100%	Çok iyi	Excellent

UD:Örselenmemiş Numune/*Undisturbed Sample*
D:Örselenmiş Numune / *Disturbed Sample*
SPT: Standard Pen Deneyi / *Standart Pen Test*
VST:Vane Deneyi / *Vane Shear Test*
P: Presiometre Deneyi / *Pressuremeter Test*
K:Karot Numunesi / *Core Sample*

Figure B5. Borehole Log of SK-4

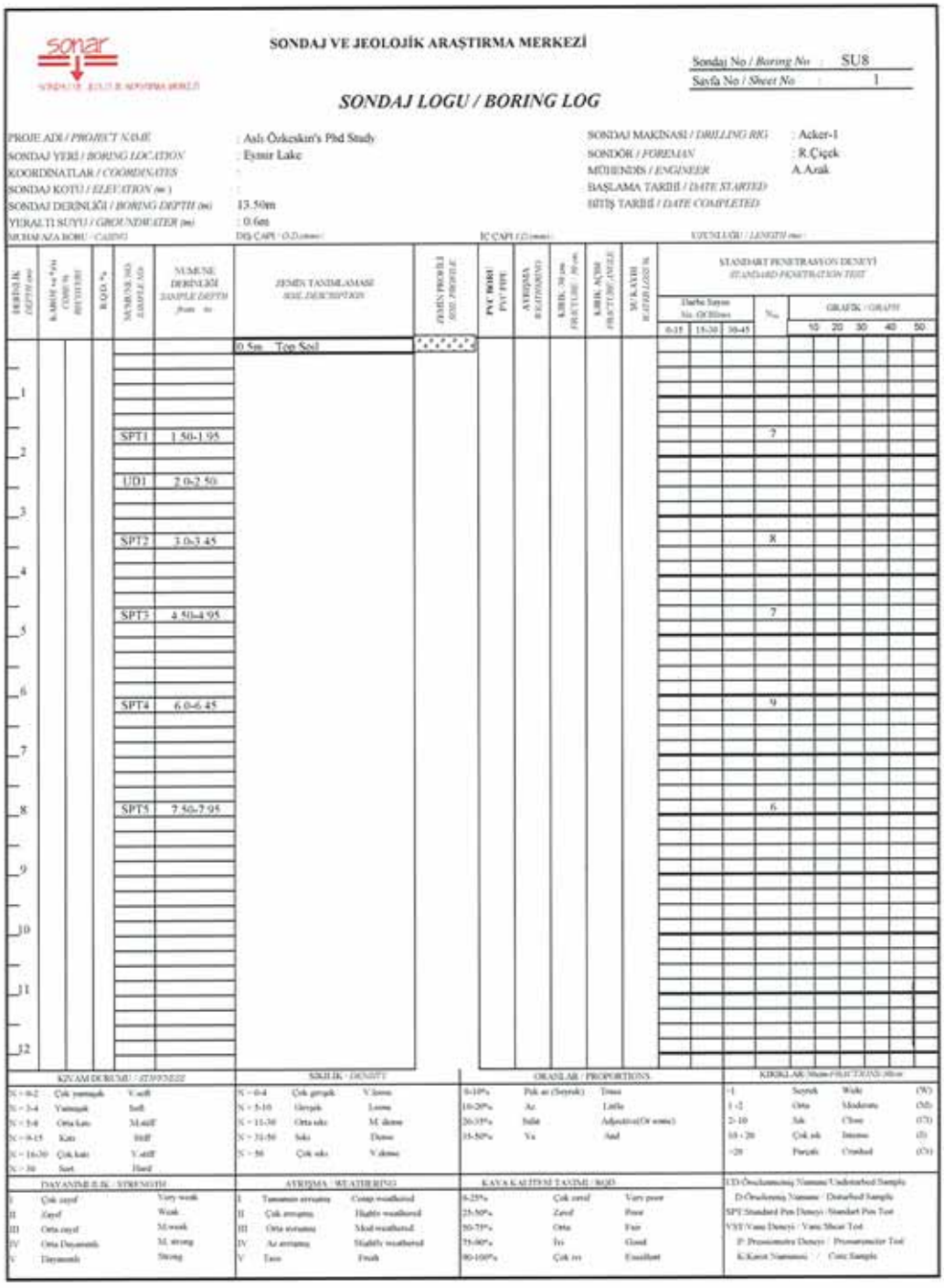

Figure B6. Borehole Log of SU8

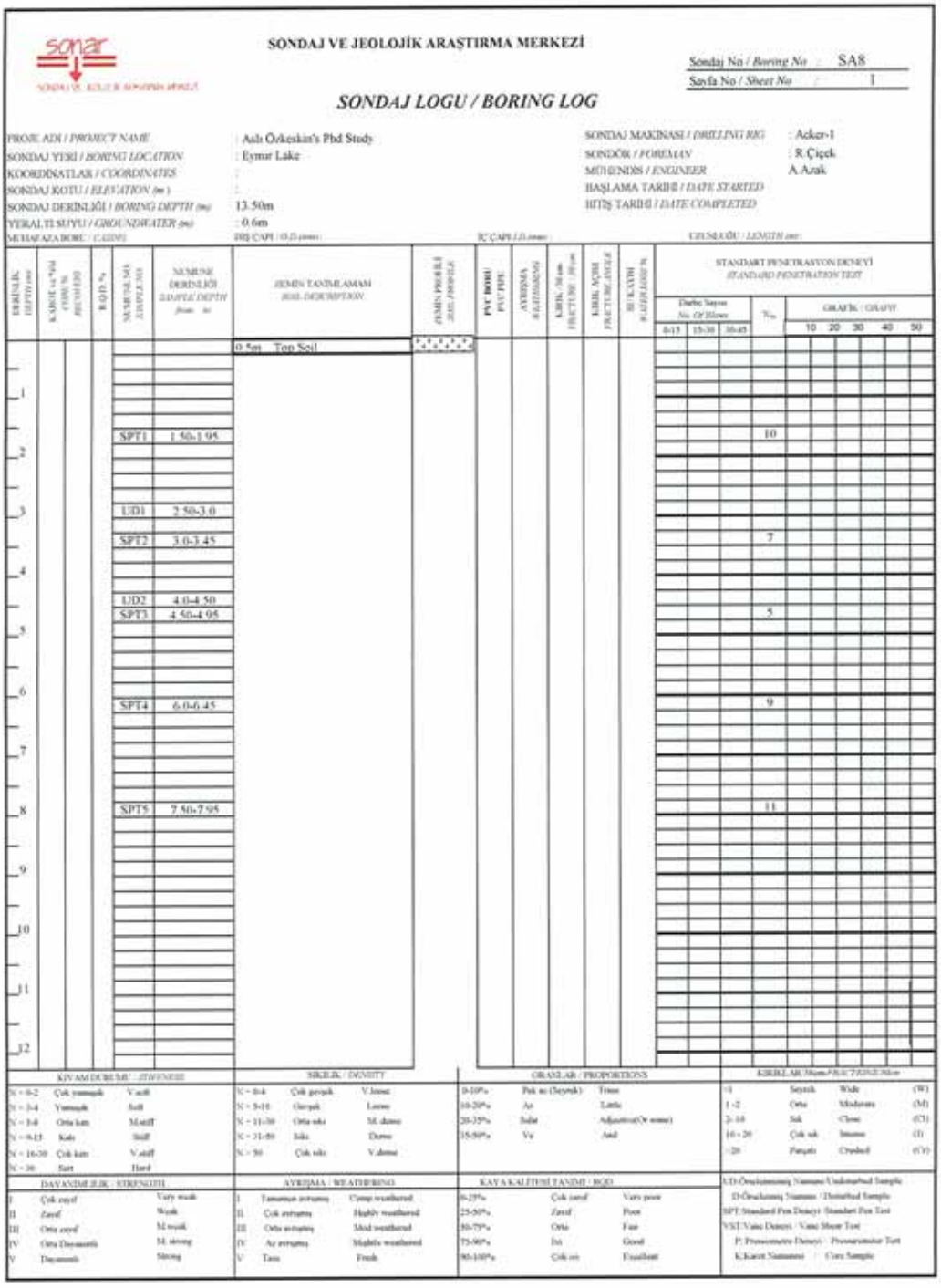

Figure B7. Borehole Log of SA8

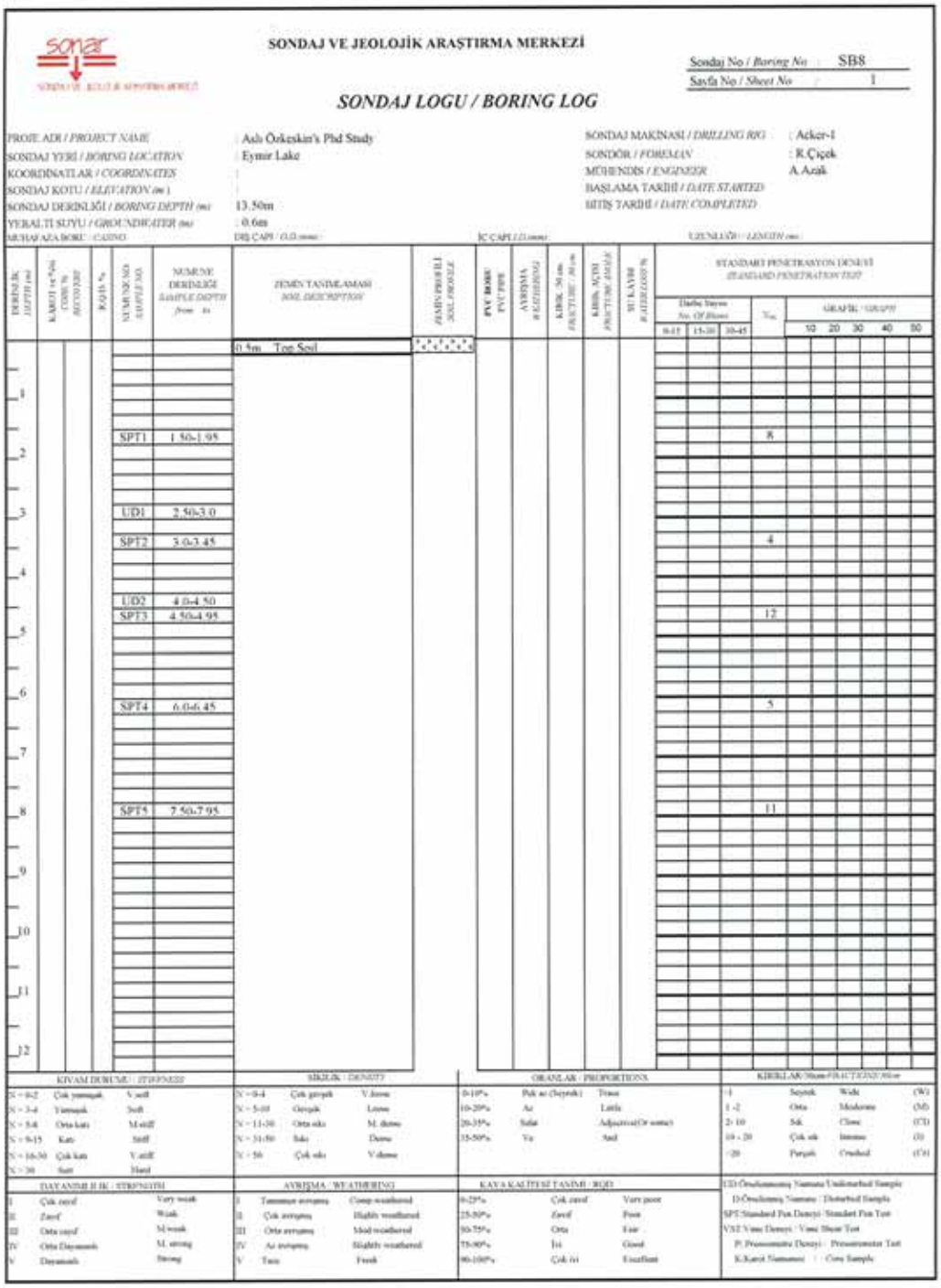

Figure B8. Borehole Log of SB8

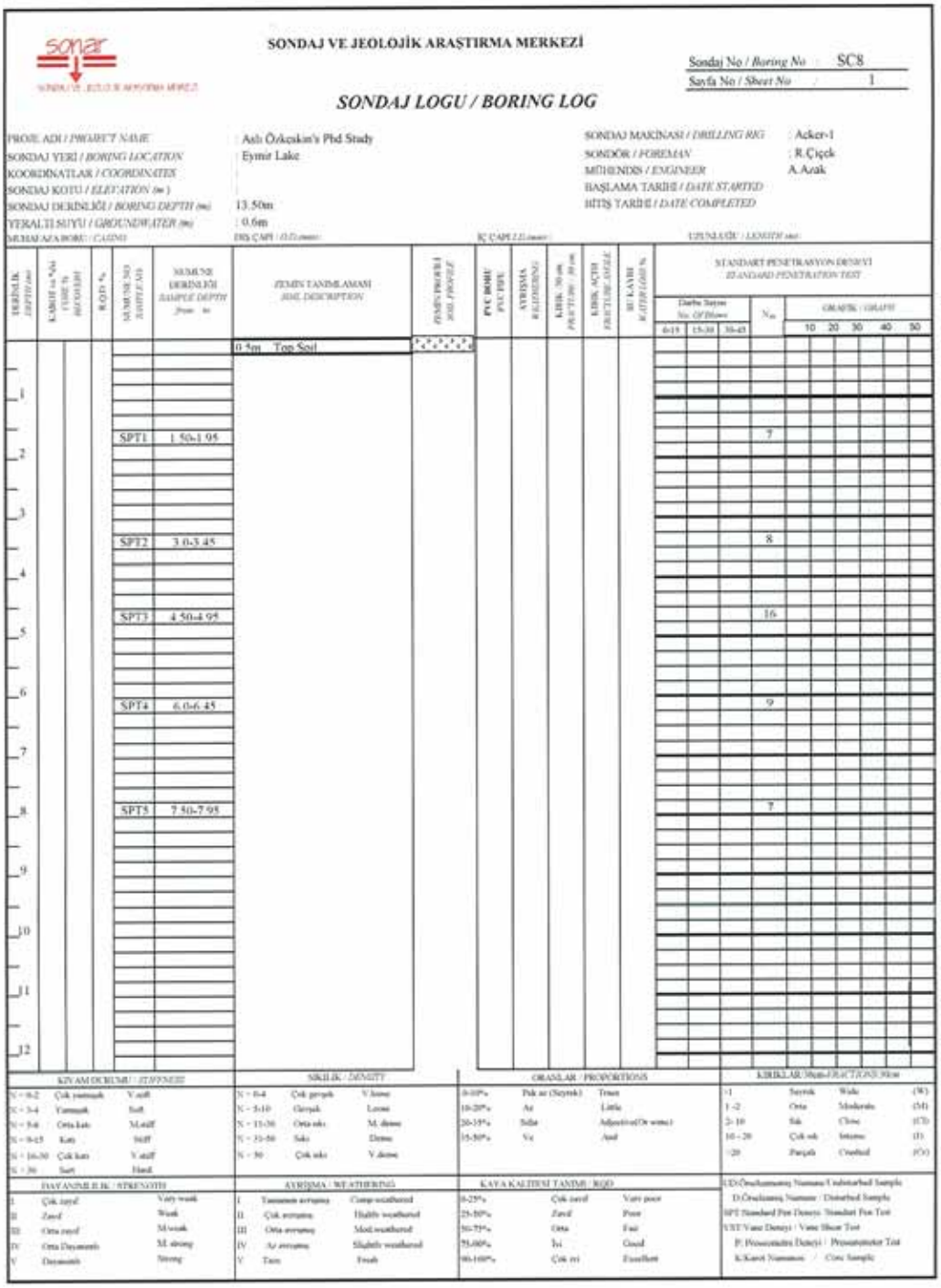

Figure B9. Borehole Log of SC8

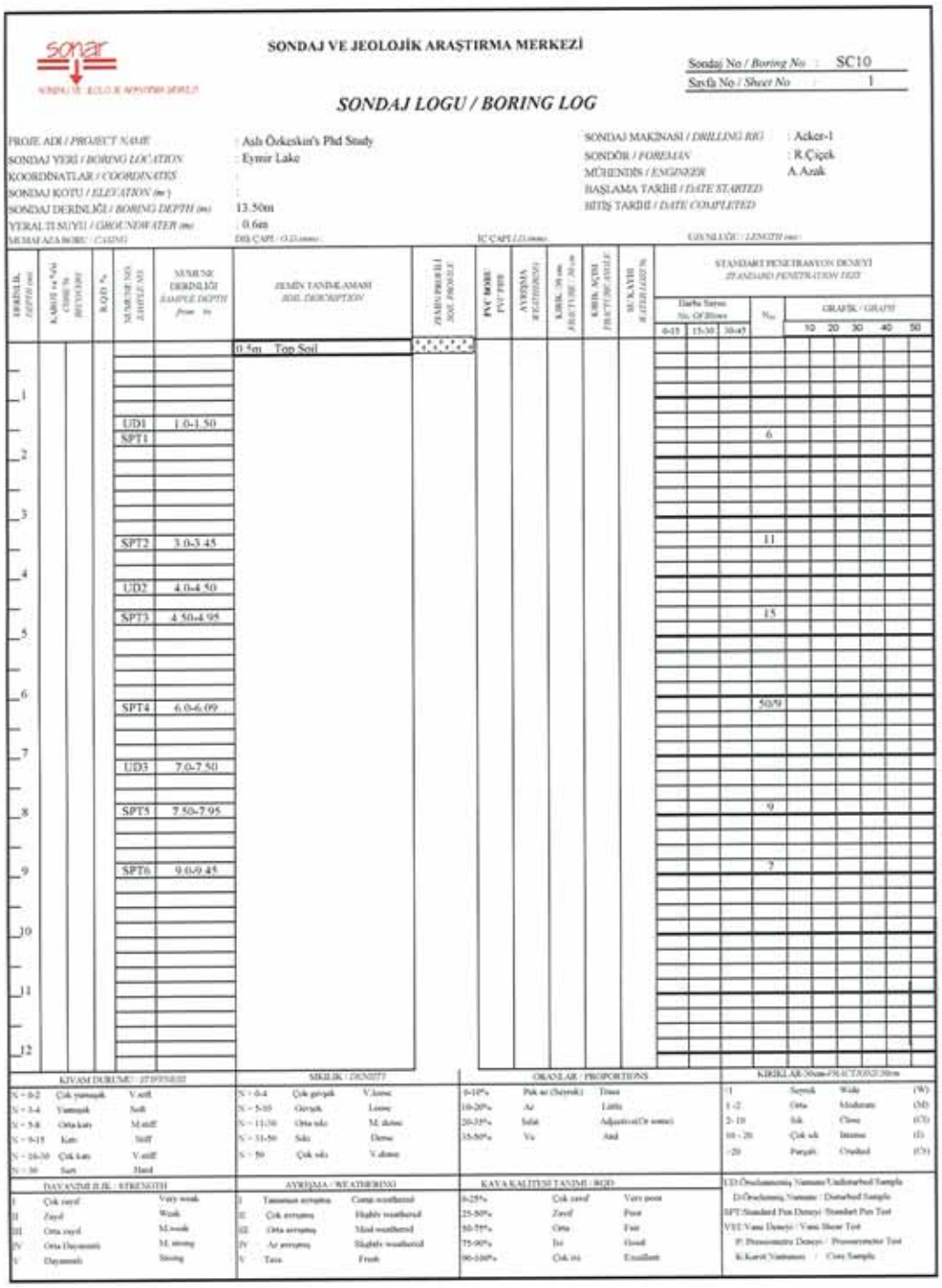

Figure B10. Borehole Log of SC10

M.E.T.U SOIL MECHANICS *LABORATORY*

O.D.T.Ü ZEMİN MEKANİĞİ *LABORATUVARI* **PROJECT/PROJE:** *EYMİR LAKE*

1956

Sondaj Boring No	Numune Sample No	Derinlik Depth (m.)	SPT N	w_n (%)	e_o	γ_n kN/m³	G_s	Elek analizi Sieve analysis -No.4 (%)	-No.200 (%)	Atterberg limitleri Atterberg Limits LL (%)	PL (%)	PI (%)	Uniformluk katsayıları Uniformity numbers C_u	C_c	USCS	Direk Kesme Deneyi Direct Shear Test(CD) c (kPa)	f (°)	Üç Eksenli Bas Den Triaxial Test (UU) c (kPa)	f (°)	Kil Yüzdesi Clay Cont (%)
	SPT-1	1.50-1.95	3				2,672	99,7	95,4	40	19	21,0			CL					25
	UD-1	1.50-2.10		24,6		19,70												55	0	
	UD-2	2.60-3.10																		
	TOR-1	3.00-3.50					2,513	88,3	40,8	32,4	16,2	16,2			SC					11
	SPT-2	3.60-4.05	7					73,3	5,2						SW-SC					–
	TOR-2	4,50					2,648	80,9	27,8	27,8	15,9	11,9			SC					6
	TOR-3	5,00					2,642	90,7	34,5	27,3	15,5	11,8			SC					9
	TOR-4	5.50-6.00					2,671	77,4	27,1	30,4	14,3	16,1			SC					6
SKT-1	SPT-3	5.90-6.35	8					78,4	32,4						SC					
	TOR-5	6.50-7.00					2,574	87,3	28,5	28,5	15,7	12,8			SC					7
	TOR-6	6.80-7.10					2,536	68,5	16,6						SC					5
	SPT-4	7.10-7.55	23				2,673	65,8	20,5	23,7	14,4	9,3			SC					5
	UD-3	7.55-8.05																		
	TOR-7	7.50-8.00					2,685	84,0	42,0	36,2	18,0	18,2			SC					19
	SPT-5	8.00-8.50	16				2,512	83,5	52,2	39,5	18,2	21,3			CL					24
	UD-4	9.00-9.60																		
	SPT-6	9.60-10.05					2,56	89,7	52,0	33,4	17,9	15,5			CL					16

Figure B11. Table of Laboratory Test Results

M.E.T.U SOIL MECHANICS LABORATORY

O.D.T.Ü ZEMİN MEKANİĞİ LABORATUVARI PROJECT/PROJE: EYMİR LAKE

1956

Sondaj Boring No	Numune Sample No	Derinlik Depth (m.)	SPT N	w_n (%)	e_o	γ_n kN/m³	G_s	Elek analizi Sieve analysis -No.4 (%)	-No.200 (%)	Atterberg limitleri Atterberg Limits LL (%)	PL (%)	PI (%)	Uniformluk katsayıları Uniformity numbers C_u	C_c	USCS	Direk Kesme Deneyi Direct Shear Test(CD) c (kPa)	f (°)	Üç Eksenli Bas. Den. Triaxial Test (UU) c (kPa)	f (°)	Kil Yüzdesi Clay Cont. (%)
SK-1	SPT-1	1,00-1,45	13	14,5				71,8	19,1											
	SPT-2	2,00-2,45	10	20,3				86,8	34,4	33	16	17			SC					
	SPT-3	3,00-3,45	2	24,8				83,2	26,7											
	SPT-4	4,00-4,45	5	17,4				78,4	30,0	31	16	15			SC					
	SPT-5	5,00-5,45	8	15,9				59,9	13,5											
	SPT-6	6,00-6,45	12	16,2				78,6	17,1											
	SPT-7	7,00-7,45	37	7,3				50,3	15,1											
	karot	7,50-8,00		9				71,5	30,8											
	SPT-8	8,00-8,45	42	8,4				62,5	20,7											
SK-2	SPT-1	0,60-1,05	10	14,2				84,9	26,4											
	SPT-2	1,50,1.95	3	32,6				86,6	70,6	52	23	29			CH					
	UD-1	2,00-2,50																		
	SPT-3	3,50-3,95	5	18,6				85,8	41,1	32	15	17			SC					
	SPT-4	4,50-4,95	7	13,9				73,8	27,1											
	UD-2	6,50-7,00																		
	SPT-5	7,00-7,45	21	13,9				81,5	26,9											
	SPT-6	8,00-8,45	22	16,1				91,9	38,5	33	17	16			SC					
	SPT-7	9,50-9,95	33	8,5				61,9	20,1											

Figure B11.Cont'n Table of Laboratory Test Results

M.E.T.U SOIL MECHANICS LABORATORY

O.D.T.Ü ZEMİN MEKANİĞİ LABORATUVARI PROJECT/PROJE: EYMİR LAKE

1956

Sondaj Boring No	Numune Sample No	Derinlik Depth (m)	SPT N	w_n (%)	e_0	γ_n kN/m³	G_s	Elek analizi Sieve analysis -No.4 (%)	-No.200 (%)	Atterberg limitleri Atterberg Limits LL (%)	PL (%)	PI (%)	Uniformluk katsayıları Uniformity numbers C_u	C_c	USCS	Direk Kesme Deneyi Direct Shear Test(CD) c (kPa)	f (°)	Üç Eksenli Bas.Den. Triaxial Test (UU) c (kPa)	f (°)	Kil Yüzdesi Clay Cont. (%)
SK-3	SPT-1	1,00-1,45	23	12,3				69,3	15,6											
	SPT-2	2,00-2,45	14	38,7				87,6	77,4	56	24	32			CH					
	UD-1	2,50-3,00																		
	SPT-3	3,00-3,45	14	16,1				66,8	27,2											
	SPT-4	4,50-4,95	23	13,4				78,1	25,6	29	16	13			SC					
	UD-2	7,50-8,00																		
	SPT-5	8,00-8,45	8	18,2				81,8	41,6	33	16	17			SC					
	SPT-6	8,50-8,95	5	16,2				66,5	37,1											
	SPT-7	9,50-9,95	11	15,9				82,5	46,3											
	SPT-8	10,50-10,95	29	16,5				65,5	35,3	35	21	14			SC					
SK-4	SPT-1	0,50-0,95	9	31,3				87,4	54,0											
	UD-1	1,50-2,00																		
	SPT-2	2,00-2,45	11	14,5				70,5	19,7											
	SPT-3	3,50-3,95	15	12,7				78,0	20,5											
	SPT-4	5,00-5,45	17	11,7				76,9	18,8											
	SPT-5	6,00-6,45	11	12,4				63,6	21,5											
	SPT-6	7,50-7,95	26	20,5				94,6	56,6	44	21	23			CL					
	SPT-7	8,50-8,95	22	17,8				88,7	49,5											
	SPT-8	9,50-9,95	19	17,7				87,0	51,9											
	SPT-9	10,50-10,95	26	13,2				60,0	25,4	33	17	16			SC					
	SPT-10	12,00-12,45	38	11				70,5	28,6											
	SPT-11	12,80-13,25	42	12,6				75,3	35,0											

Figure B11.Cont'n Table of Laboratory Test Results

M.E.T.U SOIL MECHANICS LABORATORY

O.D.T.Ü ZEMİN MEKANİĞİ LABORATUVARI

PROJECT/PROJE: EYMİR LAKE

1956

Sondaj Boring No	Numune Sample No	Derinlik Depth (m.)	SPT N	w_n (%)	e_o	γ_n kN/m³	G_s	Elek analizi Sieve analysis		Atterberg limitleri Atterberg Limits			Uniformluk katsayıları Uniformity numbers		USCS	Direk Kesme Deneyi Direct Shear Test(CD)		Üç Eksenli Bas.Den. Triaxial Test (UU)		Kil Yüzdesi Clay Cont. (%)
								-No 4 (%)	-No 200 (%)	LL (%)	PL (%)	PI (%)	C_u	C_c		c (kPa)	f (°)	c (kPa)	f (°)	
SU8	SPT-1	1,50-1,95	7	22,3				94,0	69,8	30	15	15			CL					
	UD-1	1,50-2,00		26			2,7	87,9	43,2	33	15	18			SC					10
	SPT-2	3,00-3,45	8	14,9				79,4	34,1	27	15	12			SC					
	SPT-3	4,50-4,95	7	15				72,8	37,3											
	UD-2	4,50-5,00		15			2,7	75,1	41,1	29	15	14			SC			31	0	12
	SPT-4	6,00-6,45	9	18,5				88,7	35,1	34	15	19			SC					
	SPT-5	7,50-7,95	6	19,8				94,5	53,0	35	15	20			CL					
	UD-3	7,50-8,00		17			2,7	78,3	37,1	33	17	16			SC			20	9	10
	UD-4	9,00-9,50																		
SA8	SPT-1	1,50-1,95	10					66,3	25,3											
	UD-1	2,50-3,00																		
	SPT-2	3,00-3,45	7					88,6	26,9	28	14	14			SC					
	UD-2	4,00-4,50																		
	SPT-3	4,50-4,95	5					73,3	26,3	28	13	15			SC					
	SPT-4	6,00-6,45	9					75,5	33,7											
	SPT-5	7,50-7,95	11					96,9	51,1	33	15	18			CL					
SB8	SPT-1	1,50-1,95	8							36	18	18								
	UD-1	2,50-3,00																		
	SPT-2	3,00-3,45	4																	
	UD-2	4,00-4,50																		
	SPT-3	4,50-4,95	12							36	18	18								
	SPT-4	6,00-6,45	5							34	14	20								
	SPT-5	7,50-7,95	11							26	14	12								

Figure B11.Cont'n Table of Laboratory Test Results

M.E.T.U SOIL MECHANICS *LABORATORY*

O.D.T.Ü ZEMİN MEKANİĞİ *LABORATUVARI* **PROJECT/PROJE:** *EYMİR LAKE*

1956

Sondaj Bering No	Numune Sample No	Derinlik Depth (m.)	SPT N	w_n (%)	e_n	γ_n kN/m³	G_s	Elek analizi Sieve analysis -No.4 (%)	-No.200 (%)	Atterberg limitleri Atterberg Limits LL (%)	PL (%)	PI (%)	Uniformluk katsayıları Uniformity numbers C_u	C_c	USCS	Direk Kesme Deneyi Direct Shear Test(CD) c (kPa)	f (°)	Üç Eksenli Bas. Den. Triaxial Test (UU) c (kPa)	f (°)	Kil Yüzdesi Clay Cont. (%)
SC8	SPT-1	1,50-1,95	7					80,3	43,1	43	22	21			SC					
	SPT-2	3,00-3,45	8					60,6	32,5	31	15	16			SC					
	SPT-3	4,50-4,95	16					83,1	19,4											
	SPT-4	6,00-6,45	9					89,7	35,2											
	SPT-5	7,50-7,95	7					71,2	30,6	33	18	15			SC					
SC10	UD-1	1,00-1,50																		
	SPT-1	1,50-1,95	6					78,2	39,9	42	22	20			SC					
	SPT-2	3,00-3,45	11					76,5	29,5											
	UD-2	4,00-4,50																		
	SPT-3	4,50-4,95	15					66,0	15,1											
	SPT-4	6,00-6,09	50/9					72,3	23,1											
	UD-3	7,00-7,50																		
	SPT-5	7,50-7,95	9					88,4	45,5	38	18	20			SC					
	SPT-6	9,00-9,45	7					86,9	51,6	38	17	21			CL					

Figure B11. Cont'n Table of Laboratory Test Results

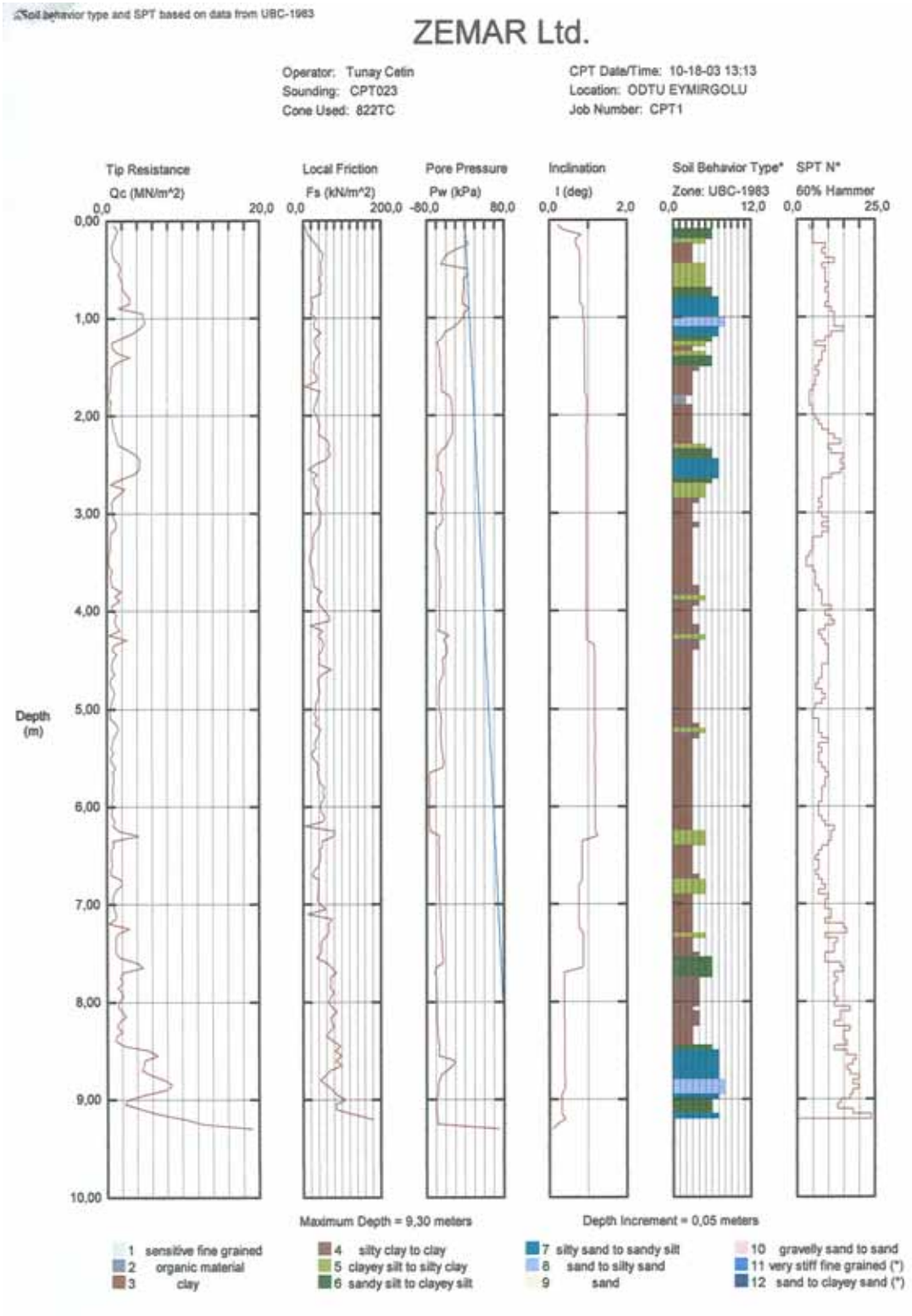

Figure B12. Documents of CPT-1

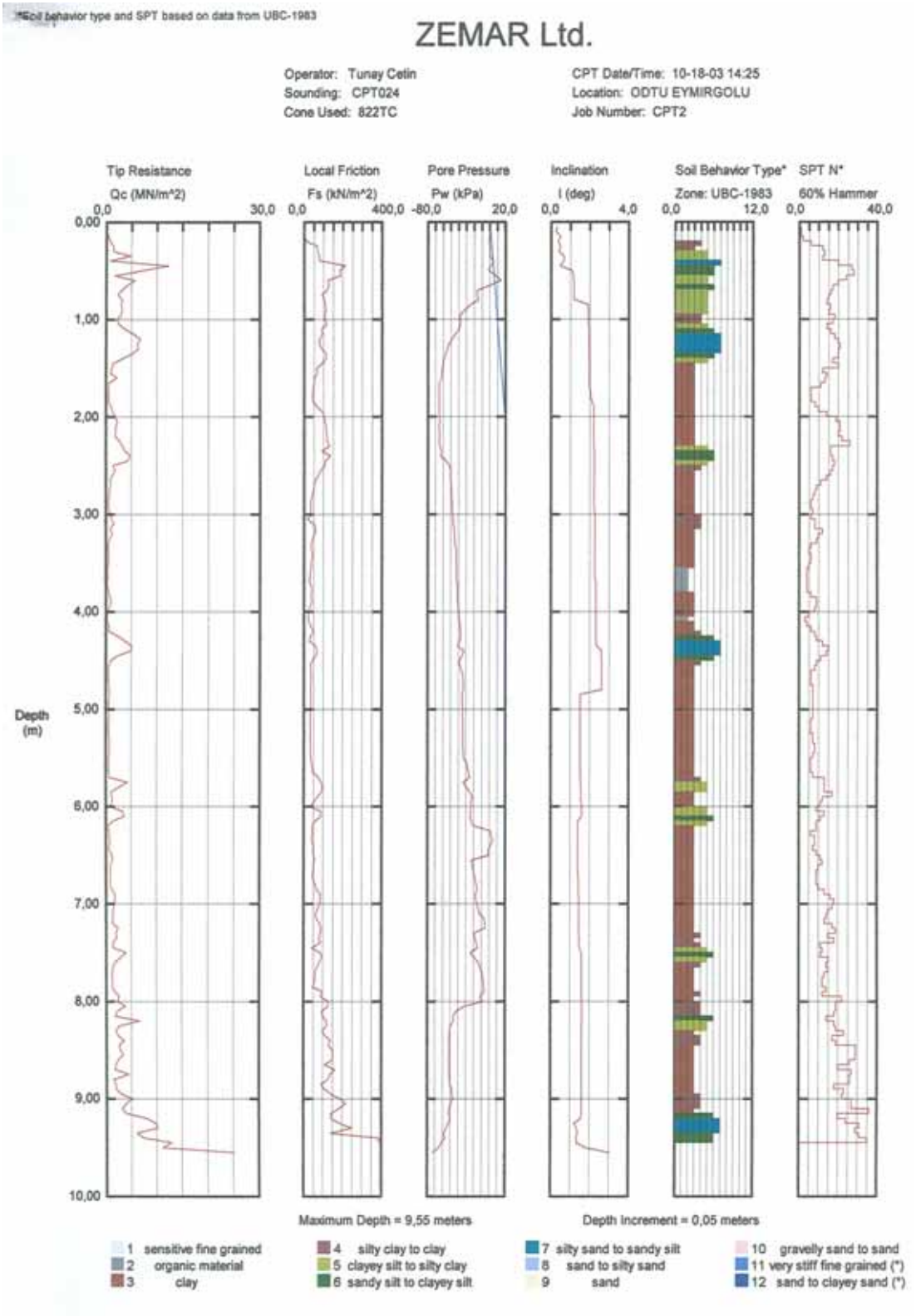

Figure B13. Documents of CPT-2

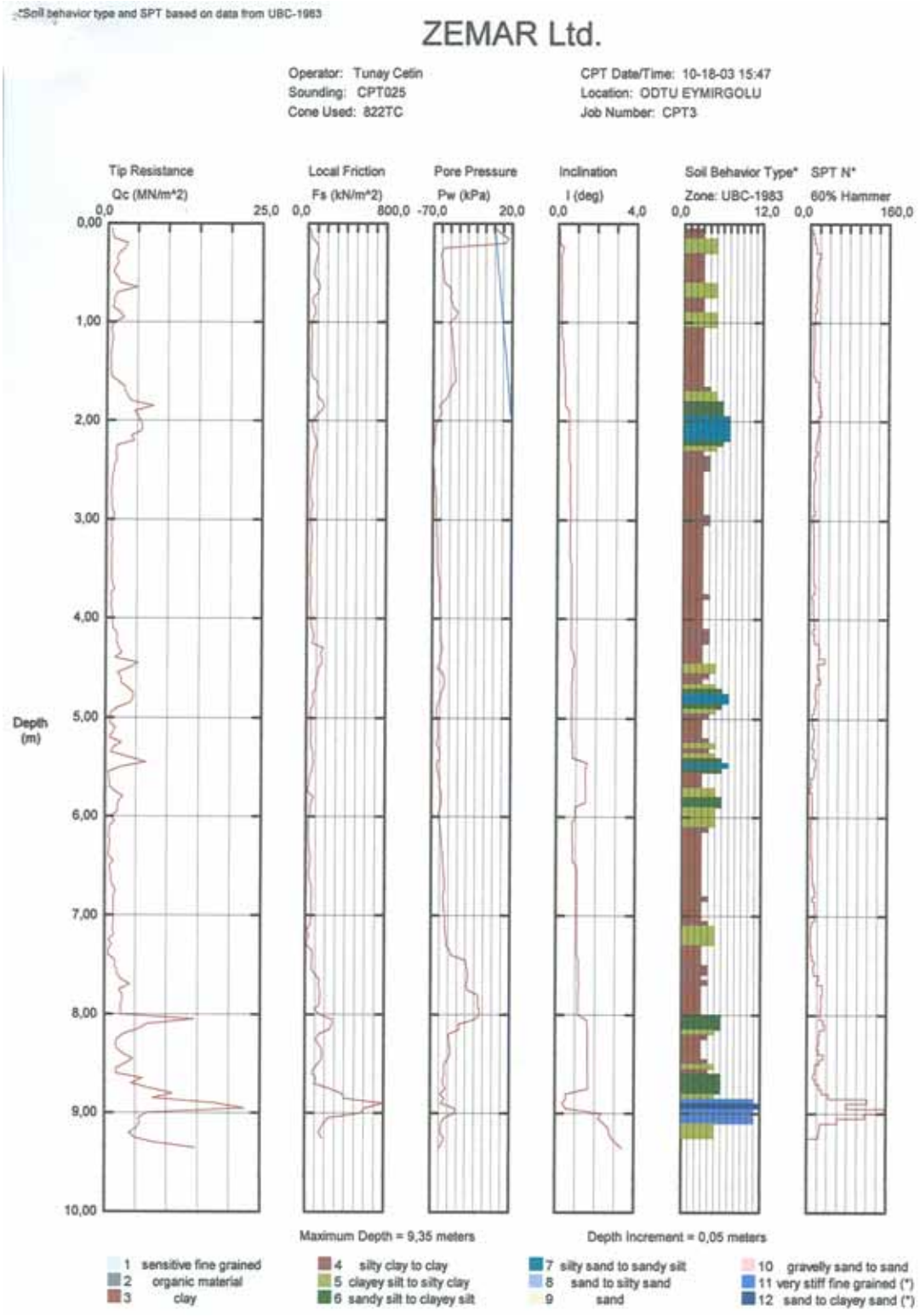

Figure B14. Documents of CPT-3

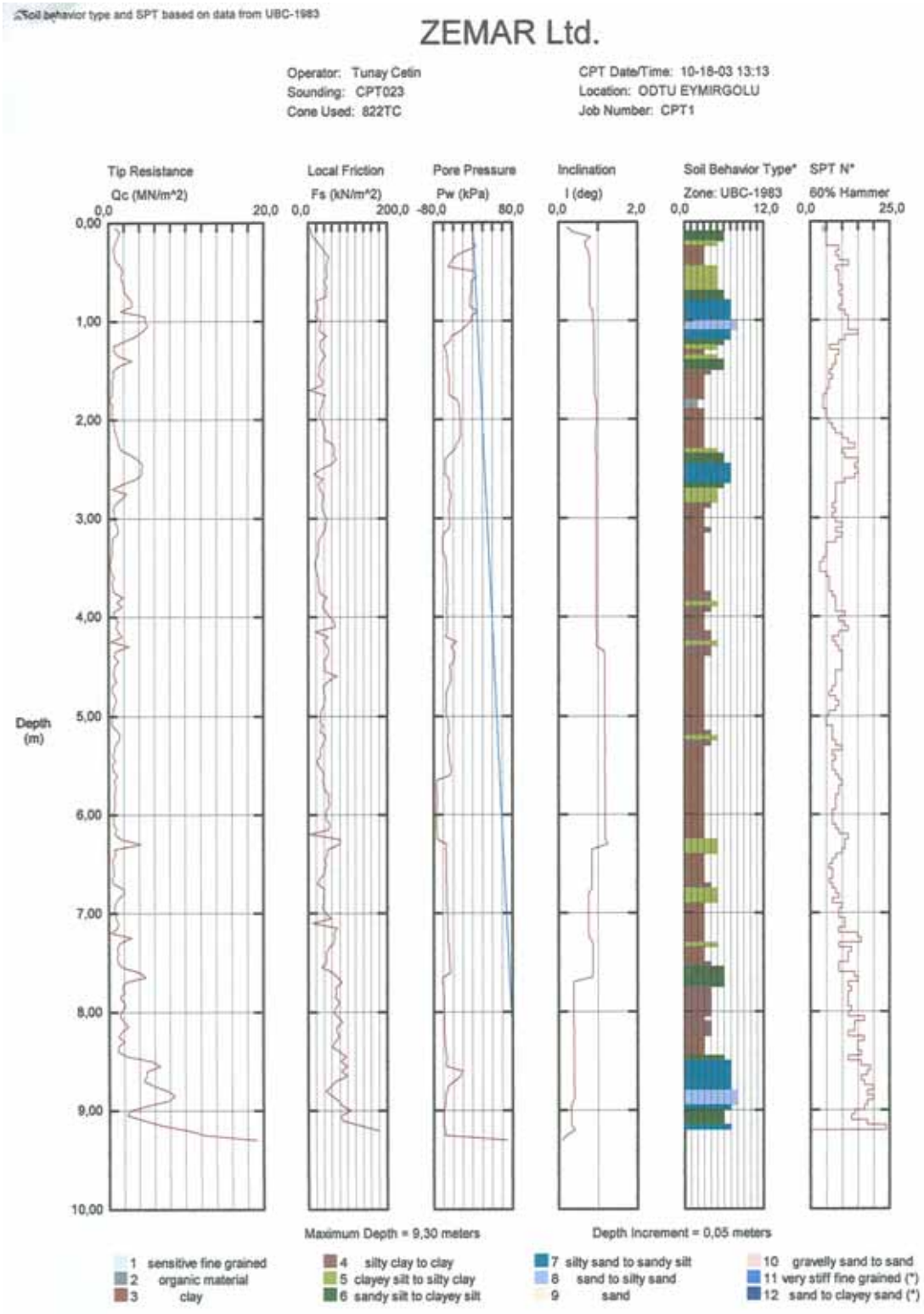

Figure B15. Documents of CPT-4

İSTANBUL TEKNİK ÜNİVERSİTESİ – İNŞAAT FAKÜLTESİ
YAPI LABORATUVARLARI YAPI MALZEMESİ GRUBU
80626 MASLAK / İSTANBUL TEL: (0212) 285 3757-58 FAX. (0212) 285 6587 TELEX: 28186 ITU-TR

Kalibrasyon Deneyi
Rapor No/Tarihi : 696 / 17.05.2000
Başvuru No/Tarih : 2048 / 17.05.2000

HİDRO-MEKANİK HİDROLİK
MAKİNA SAN. ve TİC. LTD. ŞTİ.

Tarafınızdan yapılan başvuru üzerine, 16.05.2000 tarihinde 0005216 seri no'lu hidrolik silindirin kalibrasyonu, tarafınıza ait 700 bar göstergeli pompaya bağlanarak, Amsler marka kalibrasyon aletimizle yapılmış ve sonuçları aşağıda verilmiştir.

Pompa Göstergesinden Okunan Değer (bar)	Gerçek Yük (kgf)
0	0
50	30390
100	60510
150	90630
200	120750
250	150870
300	180990
350	211110
400	241230
450	271350
500	301470
550	331590
600	361710
650	391830
700	421950

Not: Deney sırasında ortam sıcaklığı 20 °C dir.

Araş.Gör. Özkan ŞENGÜL

Prof. Dr. Mehmet UYAN

Figure C1. Calibration certificate of hydraulic jack and pump

ROCTEST TELEMAC

CALIBRATION DATA SHEET
VIBRATING WIRE PRESSURE TRANSDUCER

Model:	**TPC**
Serial number:	**78E01469**
Range:	**3000 kPa**
Temperature:	**24 °C**
Barometric pressure:	**100.94 kPa**
Cable model:	**IRC-41A**
Cable length:	**10 m**
Thermistor type:	**3 kohms**

Color code: **red & black (coil) green & white (thermistor)**

Applied pressure kPa	Reading linear unit LU	Reading frequency Hz	Full scale Error %
0.10	3204.0	1776.2	-0.24
600.10	3059.5	1735.7	0.07
1200.00	2913.9	1693.8	0.20
1799.90	2766.7	1650.5	0.14
2400.10	2619.6	1606.0	0.09
3000.00	2471.1	1559.8	-0.17
3000.00	2471.4	1559.9	-0.13
2400.00	2618.5	1605.7	-0.08
1800.00	2765.8	1650.2	0.01
1199.90	2914.2	1693.9	0.24
599.90	3059.4	1735.6	0.04
0.00	3204.5	1776.3	-0.17
		Maximum error %:	0.24

Calibration factor: CF = **-4.0903E+00** kPa / LU
CK = **-4.1541E-03** kPa / Hz²
Temperature factor: CT = **-1.6105E+00** kPa / °C

Calculated pressure:

$$\Delta P(kPa) = CF\,(L_1 - L_0) - CT\,(T_1 - T_0) - (B_1 - B_0)$$

or

$$\Delta P(kPa) = CK\,(F_1^2 - F_0^2) - CT\,(T_1 - T_0) - (B_1 - B_0)$$

L_0, L_1 = Initial (at installation) and current reading, in LU
F_0, F_1 = Initial (at installation) and current reading, in Hz
T_0, T_1 = Initial (at installation) and current temperature, in °C
B_0, B_1 = Initial (at installation) and current barometric pressure, in kPa
LU = Linear unit with K = 1.0156, position 4, MB-6T readout

Traceability no: T100B951 Procedure: PE100DRC
Filename: 090401B.xls

Calibrated by: Dorina Jugureanu D.J. Date: 9/4/01

Tel. : (1)-450-465-1113 • 1-877-ROCTEST (USA, Canada) • 33 (1) 64.06.40.80 (Europe) • www.roctest.com • www.telemac.fr

Figure C2. Calibration certificate of total pressure cell

VITA

Aslı Özkeskin was born in Ankara, Turkey on March 31, 1971. She received her B.S. degree in Civil Engineering from Middle East Technical University in June 1993. In March 1996, she awarded the degree of M.S. in Civil Engineering. She worked as a research assistant in the Geotechnical Division of the Civil Engineering Department from 1994 to 2001. Since then she works as a geotechnical engineer in private sector. Her main areas of interest are soft ground improvement techniques and deep excavations.